Future Extensions to Passive Optical Access Networks

Robert Radziwilowicz

Thesis submitted to the
Faculty of Graduate and Postdoctoral Studies
In partial fulfillment of the requirements
For the PhD degree in Electrical and Computer Engineering

School of Electrical Engineering and Computer Science
Faculty of Engineering
University of Ottawa

Acknowledgements

I would like to thank those who helped make this thesis possible.

I am most thankful to my supervisor, Dr. Trevor Hall, whose support, advice, insightful criticisms, and patient encouragement from the very beginning aided my completion of this thesis in innumerable ways.

Thanks to Erin Knight who helped significantly with her great editorial support, Zohreh Galehdar who provided moral support, and to Dominic Olivieri who provided technical support in the laboratory.

Lastly I offer my regards and thanks to all of those who supported me in any respect during the completion of this project - I am truly grateful.

Contents

Abbreviations

PON - Passive Optical Network

EPON - Ethernet Passive Optical Network

GPON - Gigabit-capable Passive Optical Network

IEEE - Institute of Electrical and Electronics Engineers

ITU - International Telecommunication Union

SOA – Semiconductor Optical Amplifier

AAPN – Agile All-Photonic Network

FPGA – Field Programmable Gate Array

PC – Personal Computer

ISDN - Integrated Services Digital Network

DSL – Digital Subscriber Line

WDM – Wavelength Division Multiplexing

CWDM – Coarse Wavelength Division Multiplexing

DWDM –Dense Wavelength Division Multiplexing

TDM – Time Division Multiplexing

WiFi – Wireless Fidelity

LAN – Local Access Network

BER – Bit Error Ratio

Abstract

Rapid changes in population distribution across Canada and the introduction of new telecommunication services to the consumer market have resulted in a number of significant challenges for existing network infrastructure. Fast growing populations in metropolitan regions require high density access networks to meet the growing need for bandwidth that results. Furthermore, new services such as high definition TV, online gaming and real-time video teleconferencing are becoming increasingly popular among consumers. These services require higher bandwidth to be available to end users. Changes in the Canadian economy will soon lead to a transition in Canadian industry from manufacturing to services and exploration of natural resources. This will create opportunities for new industrial development and growth in northern regions. Expanding industrialization towards northern Canada will require deployment of reliable telecommunication infrastructure.

The existing telecommunication infrastructure available to consumers consists mainly of Digital Subscriber Lines (DSL) that are deployed over the plain telephony network and cable TV infrastructure. However, this infrastructure does not provide sufficient capacity to satisfy future demands for reach, bandwidth and number of served customers. The combination of limited available bandwidth and limited density of DSL access network put significant constraints on expansion possibilities of existing infrastructure. The answer to this dilemma is deployment of optical fiber access networks that provide both bandwidth and scalability, thus satisfying the growing number of consumers and bandwidth. Although optical access networks have been present for over 10 years, cost of deployment and installation remains too high to implement widely enough to meet the demand of consumers.

A growing need also exists for technology capable of accommodating a smooth transition from DSL based infrastructure to an all-optical access network. This technology should be able to provide bridging functionality between copper based networks and optical networks. Costs of manufacturing, deployment and maintenance must be low enough to make this technology widely available to the consumer market. Configuration flexibility, compatibility with widely accepted standards such as Ethernet and Internet Protocol, and transparency for transmitted data will make this technology attractive for commercial access network operators.

The combination of open source software, Linux operating system and Personal Computer (PC) based hardware platform is proposed to become the foundation for low cost and flexible technology that will provide transition towards all-optical infrastructures. An innovative prototype of a low-cost optical gigabit Ethernet switch is presented and its benchmark results are discussed. Scalability of the switch and its future applications in optical networks are studied. A prototype of a software based data encapsulation system was designed and implemented in a PC based platform, and its performance was evaluated using real data that was captured in commercial LAN. Semiconductor optical amplifiers (SOA) are studied as a building block in next generation switching devices for all-optical access networks. A prototype of an SOA-based low-cost optical switching device with implemented FPGA based controlling mechanism is presented and its characteristics are discussed. SOA is also studied as an energy efficient optical amplifier that can be deployed in end user facilities.

The presented results provide proof of concept of a low cost flexible platform that can be used to

design and build network devices to facilitate the transition of existing telecommunication networks towards next generation optical access infrastructure.

Introduction

The current state of communications technology in North America relies heavily on copper cable network infrastructure in order to enable communications of all types to the population for both business and personal applications. In recent years, telecommunication companies have been slowly integrating Passive Optical Network technology into existing infrastructure to augment its capabilities and keep up with increased demands. We utilize these convergent networks daily for a huge gamut of applications ranging from voice over IP to video on demand, and the demand for a strong communications infrastructure will only continue to grow as populations multiply and cities expand. Despite this, a problem exists that the current state of communication network infrastructure has significant limits in its growth – it is not reasonable or feasible to envision major physical infrastructure developments because not only is it incredibly costly, but takes a tremendous amount of manpower and time to deploy. For this reason, a way to expand the capabilities of the existing network infrastructure must be developed and implemented in order to meet the needs of customers and society as a whole.

Existing communications networks' main obstacles can be broken down into three categories: growing numbers of new users, increased demand from existing users, and insufficient network reach. To address these three key problems, accommodate for expansion and also anticipate future trends, this thesis presents four solutions that can be implemented within current frameworks and also be compatible with the existing convergent infrastructure while maintaining low cost to implement. These solutions are as follows:

- Energy efficient optical signal amplifiers that extend reach of the network and allow greater number of connections available to end user.

- Active optical switching devices to interconnect existing network infrastructures in order to improve communication between end users.

- Optical noise filtering methods to improve the quality of transmitted signal, in turn extending network reach.

- Personal computer based architecture which provide low cost transitional technology from the existing hybrid electro-optical telecommunication infrastructure to the next generation all-optical access networks.

These four proposed solutions are not only innovative because of their relative ease of deployment compared to similar systems, and their ability to fill technological gaps, but they are also dramatically lower in cost than any other solutions being explored at present, making them especially attractive for commercial applications.

The thesis consists of eight chapters (including introduction) and a summary chapter. These chapters lead readers through the entire work that has been successfully accomplished. The detailed description and comparison of technologies and standards that are implemented in existing commercial access networks is presented in the second chapter. The third chapter explores shortfalls of commercially deployed passive optical networks. The fourth chapter presents extensions for passive optical networks that have been already developed in academic and industrial research institutions. An innovative study of the traffic distribution in commercial access network is presented in chapter five. Chapter six presents a comparison between the Agile All-Photonic Network and Passive Optical Networks. It also presents an innovative application of low cost computer architecture in devices that enhance access networks. Chapter seven explores signal amplification technologies and their shortfalls in existing optical networks. It also presents innovative applications of semiconductor optical amplifier in optical switching devices and energy efficient signal amplification devices. Chapter eight presents an innovative design of universal testing system for design and evaluation access network extensions that implements advanced signal modulation techniques. The last chapter presents a summary of the thesis, makes suggestions for how the work may be further progressed and provides a list of publications that consist of research results.

Background and literature review

This chapter presents detailed information on the status of commercial access networks and provides a list of existing wired and wireless technologies that are implemented in commercial access network infrastructures. The chapter also presents the status of Passive Optical Access Network (PON) in public telecommunication infrastructure and it explores the major differences and incompatibilities between existing PON standards that create obstacles in developing new technologies for PON improvement.

Review of commercial access networks

Since the very first packet-switching models of digital networking such as ARPANET [1] (Advanced Research Projects Agency Network), Telenet [2] or X.25 [3] were successfully developed, a growing interest in public access and hobbyist networking systems started appearing among private users. The very first access networks such as UUCP (Unix-to-Unix Copy) [4] or FidoNet [5] were only a group of disjointed separate networks administrated by a small group of enthusiasts.

An environment where number of small, unrelated access networks existed next to each other created a need to develop a protocol for internetworking based on packet-switching technologies. This protocol would be able to join different networks together into single group of sub-networks. The concept of the network could be separated from its physical implementation when a simple common network system, the Internet Protocol Suite, was defined [6].

All existing access networks can be divided into two main groups that represent the technologies that they have implemented. The first group consists of all network technologies that use open space to transmit telecommunication signals. All wireless systems such as Wireless Fidelity (WiFi) [7], Worldwide Interoperability for Microwave Access (WiMAX) [8], Local Multipoint Distribution Service (LMDS) [9] belong to this particular group including cellular telephony networks such as Global System for Mobile Communications (GSM) [10], Code Division Multiples Access (CDMA) [11] and optical free space transmission such as ARTEMIS [12].
The second group consists of networks that implement non-open medium where the transmitted signal

has limited propagation space from a geometrical perspective. Telecommunication signal in those networks is transmitted over medium such as copper cable and optical fiber. Example of wired networks are Synchronous Optical Network (SONET) [13], Synchronous Digital Hierarchy (SDH) [14] and Digital Subscriber Line (DSL) [15].

The early evolution of access networks was driven by the widespread adoption of personal computers (PCs) in homes and businesses, and this evolution was primarily focused on wired technologies. Growing access to low-cost PCs and rapid increase in the number of fields where applications were found were the main push for implementating new technologies to provide interconnection between those computers.

Today access networks have exceeded their traditional role of interconnection between stationary computers. The new access networks have removed boundaries that used to limit end users to exchange data only in specific locations. Rapidly growing popularity of mobile devices provided as strong push to develop new technologies that allow mobile users to access information from almost any geographical location. Expansion of access networks over mobile devices is not the only direction where evolution is progressing.

Changes in content of public media such as TV or radio and number of new services that were added to the public broadcast system had a significant impact on the development of a multi-service platform-independent access infrastructure where Internet, TV, telephony, radio, video on demand and online gaming created an information cloud that surrounds end users.

To better understand the importance of optical networks as one of the most promising technologies implemented in access infrastructure, a brief review of popular architectures that shaped access network infrastructure for the last 20 years is presented here.

Wired networks

Dial-Up

Dial-up access was one of the first technologies available to end users. This technology uses the facilities of the public switched telephone network (PSTN) to establish a dialled connection to an Internet service provider (ISP) via telephone lines. The computer or router located at user facilities uses an attached modem to encode and decode Internet Protocol (IP) packets and control information into and from analog audio frequency signals, respectively.

Dial-up connections require no infrastructure other than the public telephone network. Since telephone access became affordable and widely available, dial-up has become very useful for travelers. Dial-up is often the only choice available for rural or remote areas where broadband installations are not prevalent due to low population and demand. Dial-up access may also be an alternative for users on limited budgets as it is offered free by some ISPs, though broadband is increasingly available at lower prices in many countries due to market competition.

Although dial-up is a low-cost and easy-to-access service that allows for simple applications such as email or web browsing, it does not provide sufficient bandwidth to accommodate more advanced

services offered by ISPs such as video on demand or video conferencing.
Dial-up requires time for establishing a usable telephone connection (up to several seconds, depending on the location) and performs handshaking for protocol synchronization before data transfers can take place.
The theoretical maximum speed of dial-up is 56 kb/s using V.92 protocol [16], but in practice bandwidth that is available to end users does not exceed 50 kb/s. The major factors that limit speed of connection is noise in telephone lines, especially in locations with high density of deployed telephones. The modem quality also plays a role in the connection speed. Other factors such as long loops, loading coils, pair gain, electric fences (usually in rural locations), and digital loop carriers may also limit transmission speed to 20 kb/s or less. Dial-up has also a significant latency that may exceed 300ms, that makes it unsuitable for latency sensitive applications such as online gaming or real time video conferencing.
To increase transmission speed that is available to end users, a number of data compression techniques were implemented. For example V.44 [17] theoretically allows the increase in speed of data transmission six times (up to 320 kb/s), but in reality compression ratio depends strongly on content of transmitted data. Files such as JPG, MPEG, ZIP or MP3 are already compressed and further compression is difficult.

Integrated Services Digital Network (ISDN)

ISDN [18] was the next step in access network improvement. It provides a set of communications standards for simultaneous digital transmission of voice, video, data, and other network services over the traditional PSTN.
This technology offers circuit-switched connections (for voice or data), and packet-switched connections (data only), in increments of 64 kb/s. ISDN typically provides a maximum of 128 kb/s in both upstream and downstream directions. Channel bonding can achieve a greater data rate; typically 6 to 8 channels, 64 kb/s each are bonded.
Although ISDN provides simultaneous voice, video, and text transmission between individual desktop videoconferencing systems and group videoconferencing systems, it was widely criticized for it high cost of implementation and limited distance that required additional investments in signal repeaters [19].
Today ISDN still remains in use because of its low latency but due to high operational costs it is used for very narrow spectrum of applications such as high-end videoconferencing made on corporate level.
ISDN had a major market share in Europe and Japan (known as INS64) but it was much less common in North America.

Digital Subscriber Line (DSL)

DSL (originally stood for Digital Subscriber Loop) is a technology that provides digital data transmission over the wires of a local telephone network. DSL uses a higher frequency band (greater than 25 kHz) above the low frequency that is used by voice communications (5 kHz and below). On the customer premises a DSL filter is installed on each outlet for telephone to remove the high frequency band, eliminating interference with the operation of the telephone set, and enabling simultaneous use.
The bandwidth available to DSL subscribers varies from 256 kb/s to 24 Mb/s in the direction to the

customer (downstream), depending on DSL technology, line conditions, and service-level implementation.
From the perspective of the data transmission there are two types of DSL: Asynchronous DSL (ADLS) where upstream data transmission is lower than downstream and Symmetric DSL (SDSL) where both upstream and downstream data rates are equal.
Subscribers send upstream data through telephone lines to a telecommunication operator where traffic reaches a Digital Subscriber Line Access Multiplexer (DSLAM) (Figure 2). The DSLAM equipment collects the data from its many modem ports and aggregates their voice and data traffic into one complex composite "signal" via multiplexing. Depending on its device architecture and setup, a DSLAM aggregates the DSL lines over its Asynchronous Transfer Mode (ATM), Frame Relay or Internet Protocol network (IP-DSLAM). The multiplexed signal is then directed to a router (or switch) that provides access point to the Internet.

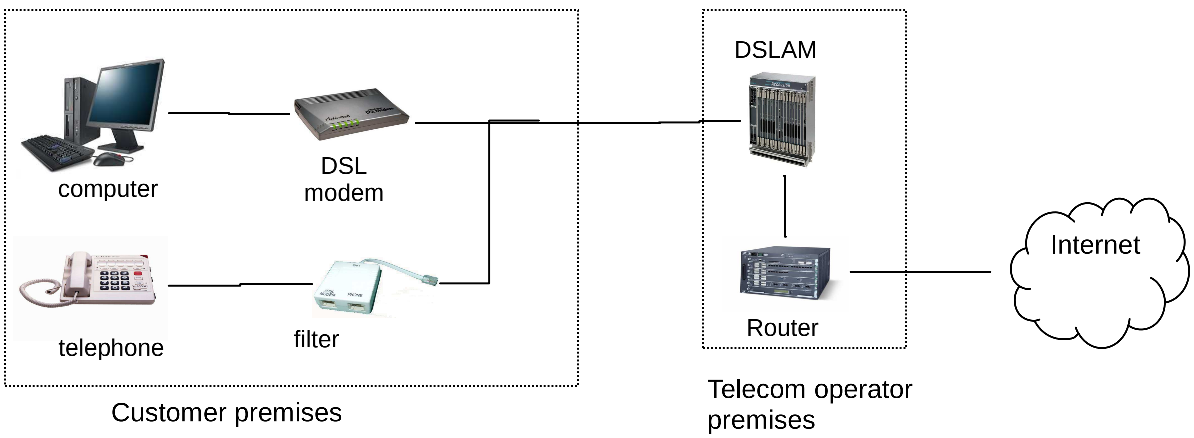

Figure 2; DSL consumer architecture

Since data is transmitted mainly through telephone lines (via a twisted pair of copper cables) the DSL bandwidth is sensitive to line attenuation, and varies between different customer locations. The greater the distance between a customer and DSLAM, the higher the signal attenuation and the lower is the bandwidth available for that particular customer. Bandwidth may vary from about 800kb/s at 5km link to about 25 Mb/s at 300 m link.
The advantage of the DSL architecture is that the customer is not required to have a land line telephone service. Those customers are offered a “dry-DSL” service (called also “naked DSL”), that is provided over the local loop, and does not require any PSTN service.
The main advantage of the DSL technology is its low-cost of deployment and maintenance. The wide spread of existing PSTN (and CATV) infrastructure allows for the mass deployment of DSL terminals that connect a large number of users to the access network.
The main disadvantage of DSL is its high sensitivity to length of the PSTN link that DSL signal is transmitted over as well as high sensitivity to quality of existing PSTN infrastructure. This leads to high differentiation of available bandwidth between different locations of customer premises.

Wireless networks

Local Multipoint Distribution Service (LMDS)

LMDS was primarily designed as a point-to-multipoint architecture for applications in digital TV broadcast. It is regulated in the standard IEEE 802.16 [20] and it operates on microwave frequencies across the 26 GHz and 29 GHz bands with maximal bit rate of 38 Mb/s. Most deployments use phase-shift-keying (PSK) modulation or straight amplitude modulation. LMDS has very limited propagation distance (about 2.5km) due to absorption of a microwave radio frequency signal by atmospheric rain, snow and ice. In point-to-point configuration it is possible to deploy an 8-km link.
LMDS did not find as many commercial applications as DSL or WiFi did. The main obstacles are short range and high cost of deployment. Many incoming new technologies such as WiMAX prevented LMDS from being widely deployed for personal users. Most of existing deployments were customized for enterprise businesses to provide limited point-to-point data transmission.

Wireless Fidelity (WiFi)

WiFi is a trademark of Wi-Fi Alliance, a trade association that promotes Wireless Local Access Network technology and certifies products if they conform to IEEE 802.11 standard [21] of interoperability. IEEE 802.11 is a set of standards defining wireless local area network (WLAN) computer communication in the 2.4 GHz, 3.6 GHz and 5 GHz frequency bands.

There are several extensions within IEEE 802.11 standard that define frequency, modulation and reach of the transmitted signal:

Version	Released	Frequency [Ghz]	Theoretical PHY Rate [Mb/s]	Practical Rate [Mb/s]
802.11	1997	2.4	2	1
802.11b	1999	2.4	11	4.4
802.11a	1999	5	54	24
802.11g	2003	2.4	54	24
802.11n	2009	2.4 , 5	600	150

Figure 3; IEEE 802.11 standards vary in frequency spectrum and throughput

- 802.11a [22] extension uses the same data link layer protocol and frame format as the original 802.11, but it has implemented orthogonal frequency-division multiplexing (OFDM) . It operates in the 5 GHz band with a maximum net data rate of 54 Mb/s, plus error correction code, which yields realistic net achievable throughput in the range of 20 Mb/s. Although this extension does not suffer from interference with vastly used 2.4 GHz frequency devices, it has a significant indoor reach limit because a large part of short wavelength signals are absorbed by walls and other solid objects.

- 802.11b [23] extension provides 11 Mb/s bandwidth and it uses 2.4 GHz band with carrier sense multiple access with collision avoidance (CSMA/CA) media access method. This extension has longer reach distance than 802.11a. Its longer wavelengths are less absorbed by solid objects than 5 GHz, therefore it is more suitable for indoor operations. Typical indoor range is 30 m at 11 Mb/s and 90m at 1 Mb/s. Unfortunately this extension suffers from interference with other devices that use 2.4 GHz signals such as bluetooth, microwave ovens, cordless telephones.

- 802.11g [24] extension was ratified in 2003 and it uses 2.4 GHz band (similar to 802.11b) but it has implemented an OFDM based transmission scheme (similar to 802.11a). It provided 54 Mb/s transmission ratio and 22 Mb/s throughput. This extension is fully backwards compatible with 802.11b therefore new g-class devices can be deployed over existing b-class infrastructure. The 802.11g similarly to 802.11b suffers from interference with other 2.4 GHz devices (cordless telephones, microwave ovens, etc...)

- 802.11n [25] is the most recent extension that implements multiple-input multiple-output (MIMO) antennas that operates in both 2.4 GHz and 5 GHz bands. MIMO is a technology that uses multiple antennas to coherently resolve more information than using a single antenna. This configuration spatially multiplexes (through Spatial Division Multiplexing, SDM) multiple independent data streams that are transferred simultaneously within one spectral channel of bandwidth. MIMO SDM can significantly increase data throughput as the number of resolved spatial data streams is increased. Each spatial stream requires a discrete antenna at both the transmitter and the receiver. In addition, MIMO technology requires a separate radio frequency chain and analog-to-digital converter for each MIMO antenna, which translates to higher implementation costs compared to non-MIMO systems. 802.11g incorporates another feature: 40MHz channels that double the channel width from 20 MHz in previous 802.11 extensions. This allows for a doubling of the data rate over a single 20 MHz channel. The 802.11n standard is backward compatible with 802.11a/b/g therefore it can be deployed as an extension for existing WiFi infrastructures.

The 802.11 standards and its extensions provides a cost effective solution for short distance access networks that can be deployed in locations where permanent wired networks are not accessible and costly to deploy. WiFi is also considered as one of the prime candidates to implement an open access public wireless network deployed over metropolitan areas [26].

Mobile telephony

Rapidly growing popularity of mobile telephony has become a main push for telephony operators to introduce new services over the existing infrastructure. Today mobile telephony provides not only voice or Short Messaging Service (SMS), but also offers video teleconferencing, web browsing, email, instant messaging (Yahoo, MSN), Multimedia Messaging Services (MMS) and use of Global Positioning System (GPS). Those additional services provided by telephony operators as value-added services (from the marketing perspective) transformed a traditional mobile voice communication network into a dynamic multipurpose mobile access network where subscribers have access to services that were available in the past only to broadband wired networks.

The Global System for Mobile Communications (GSM) network offers data transfer through General Packet Radio Service (GPRS) and Enhanced Data rates for GSM Evolution (EDGE). GPRS is a packet oriented mobile data service on the second and third generation cellular communication systems. GPRS was originally standardized by the European Telecommunications Standards Institute (ETSI) in response to the earlier Cellular Digital Packet Data (CDPD) and NTT DoCoMo's i-mode packet switched cellular technologies.

GPRS is a best-effort service (as opposed to circuit switching), where a certain quality of service (QoS) is guaranteed during the connection. In second-generation systems, GPRS provides data rates of 114 Kb/second. Second generation cellular technology combined with GPRS is sometimes described as 2.5G, that is, a technology between the second (2G) and third (3G) generations of mobile telephony. It provides moderate-speed data transfer, by using unused time division multiple access (TDMA) channels in, for example, the GSM system. GPRS was integrated into the 1997 GSM release, as well as newer releases. GPRS uses a rate adaptation algorithm that adapts the modulation and coding scheme (MCS) according to the quality of the radio channel to improve robustness of data transmission. It supports Internet Protocol (IP), Point to Point Protocol (PPP) and X.25 connections. GPRS is now maintained by the 3rd Generation Partnership Project (3GPP) [27]

EDGE was standardized by 3GPP and AT&T in the United States, and deployed in the US on GSM networks beginning in 2003. This extension delivers up to 1Mb/s data transmission (with average of 400kb/s) making it much faster than GPRS. Although EDGE is compatible with existing GSM infrastructure it has implemented more sophisticated transmission techniques than GPRS. It implements Gaussian Minimum-Shift Keying (GMSK) and it uses higher-order PSK/8 phase shift keying (8PSK) for the upper five of its nine modulation and coding schemes.

EDGE produces a 3-bit word for every change in carrier phase. This effectively triples the gross data rate offered by GSM. EDGE introduces also a new technology: Incremental Redundancy, which, instead of retransmitting disturbed packets, sends more redundancy information to be combined in the receiver. This technology increases the probability of correct decoding in the end user mobile telephone.
The Global mobile Suppliers Association (GSA) states that, as of January 2009, there were 413 GSM/EDGE networks in 177 countries, from a total of 441 mobile network operator commitments in 184 countries [28].

CDMA2000 (also known as International Mobile Telecommunications Multi-Carrier (IMT-MC)) is a mobile technology standard that was designed and approved after GSM was widely implemented. It uses Code Division Multiple Access (CDMA) channel access, to send voice, data, and signalling data between mobile phones and cellular sites. The standard was drafted by CDMA Development Group (CDG) [29] and approved by the International Telecommunication Union (ITU).
CDMA2000 implements Orthogonal Frequency Division Multiplexing (OFDM), advanced control and signalling mechanisms and improved interference management techniques. It also implements Quality of Service (QoS), and antenna techniques such as Multiple Inputs Multiple Outputs (MIMO) and beam-forming to increase data throughput rates and quality of service, while significantly improving network capacity.

CDMA2000 includes CDMA2000 1X (1X) and CDMA2000 EV-DO (EV-DO) standards. CDMA2000 1X (IS-2000) supports circuit-switched voice up to 35 simultaneous calls per sector and high-speed data of up to 153 kb/s in both directions. It was ratified by International Telecommunications Union (ITU) as an IMT-2000 standard in year 1999.
CDMA2000 EV-DO (Evolution-Data Optimized) implements new high-speed packet-switched transmission techniques that are specifically designed and optimized for a data-centric broadband network that can deliver 3 Mb/s peak data rate in a mobile environment. CDMA2000 EV-DO was ratified as an IMT-2000 standard (CDMA2000 High Rate packet Data Air Interface, IS-856) in year 2001.

Although mobile telephony infrastructure evolved into access networks, which is a robust platform for value-added services, it has its limitations when data transmission speed is concerned. The limited bandwidth does not offer the full spectrum of services available to end users in wired networks such as IPTV or Video on Demand.

Technologies described in this section do not have capabilities of handling more sophisticated online services such as HDTV, Video on Demand, and online 3D gaming. Bandwidth that can be offered to each subscriber is not sufficient to handle high demand data transfer. The following table represents a comparison between different HDTV formats according to the size of file transmitted for each audio-video channel:

Movie	File size
Standard DVD	3GB/h
Uncompressed 1280 X 720 (HDTV)	150GB/h
Uncompressed 1920 X 1080 (HDTV)	350GB/h
MPEG2 HDTV	9GB/h
MPEG4 HDTV	5GB/h

Figure 4; Transmitted file size of different HDTV formats

HDTV-720 requires bandwidth of 340 Mb/s for audio and video transmission while HDTV-1080 requires over 790 Mb/s. None of the commercially widespread public access network technologies that were described above can guarantee such bandwidth to each end user. Although MPEG2 and MPEG4 compression techniques bring HDTV closer to the end user, it can not take place without hardware audio-video decoders implemented in end user terminals.

The new audio-video services that will be offered soon through access networks will require network operators to provide subscribers with a much wider “pipeline“. The only technology that is currently available, and that has virtually unlimited transmission capacity, is optical network. The chapter below describes the most promising architecture of access network where optical transmission has been implemented to ensure that end users do have access to new bandwidth-intensive services.

History and general architecture of PONs

The PON has a long history, which can be traced back to the time when Asynchronous Transfer Mode (ATM) was a predominant technology implemented in optical networks. At that time, ATM technology was expected to be a unified solution for various types of communication networks ranging from long distance back-bone to local area networks (LANs).
However, after several years of development and deployment of ATM facilities, key issues made this technique fail to achieve its objective. ATM drawbacks included:

- Large header field which wastes network bandwidth (about 10% of each ATM frame was occupied by cell header).
- Low efficiency of the network capacity caused by need for the retransmission of an entire IP packet when the loss of a single cell occurs.
- Very complicated sublayer architecture makes the cost of ATM facilities much higher in comparison to Ethernet facilities.

Those challenging issues eventually made network providers and operators lose interest in the ATM. In the period when the ATM still dominated commercial networks, the first generation of PON was developed based on the ATM techniques. However, because of extremely high costs, Asynchronous PON (APON) [30] did not gain widespread popularity and was unable to compete with traditional DSL techniques.

After APON, the next generation PON techniques included Ethernet PON (EPON). EPON is based on low-cost Ethernet technology; therefore much cheaper than APON. In addition to EPON, there is another PON called GPON that was standardized in parallel with EPON. EPON is standardized by IEEE and GPON is standardized by ITU. Compared to EPON, GPON seems to be more powerful to support various types of upper layer frames such as ATM cell, general frames including IP packets and Ethernet frames. Subsequent to the current generation PON, the next generation PON techniques will be integrated with WDM technique to further increase the capacity.

Architecture of PONs

A PON is a network that uses optical fibre as the main medium for data transmission. This network is transparent for the data, and the transmitted signal is not taken under the electro-optical conversion at any time. The typical PON consists of three components: Optical Line Terminal (OLT), Optical Network Unit (ONU) and Remote Node (RN) (Figure 5).

The OLT is a device located in the Central Office (CO) of the network operator and it is responsible for sending and receiving data from multiple customers. The data travels to number of customers through passive splitters that are collocated with optical amplifiers. Optical amplifiers and splitters are assembled inside of the Remote Node that is deployed along the transmission line. The RN usually has a form of the all-weather resistant external module that is deployed in the field between the OLT and customers.

Each customer is connected to the PON through the Optical Network Unit that plays a role of the access node. Each ONU has its own identification number and an electro-optical converter that allows the customer to use the ONU with traditional devices such as telephone, CATV receiver or Ethernet card in a PC.

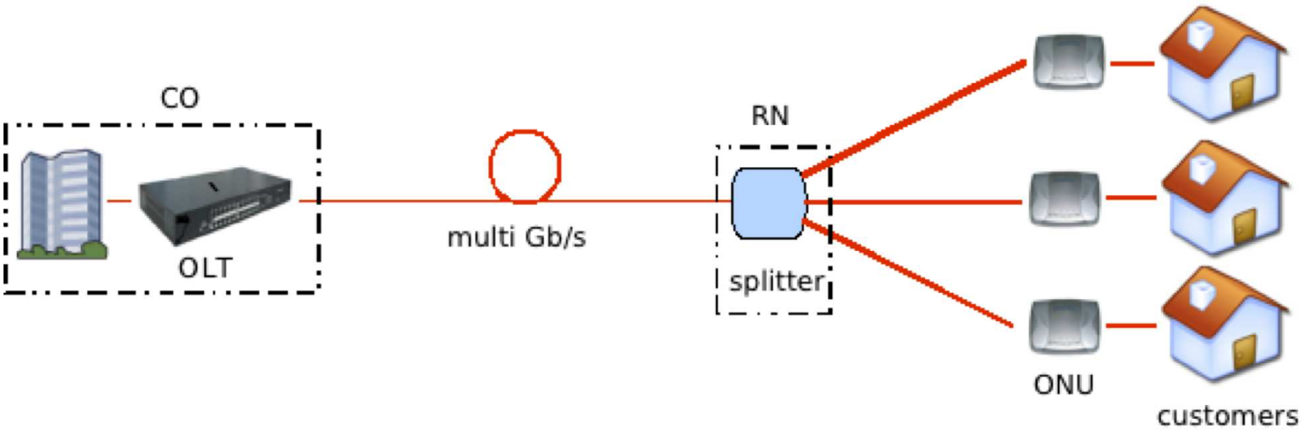

Figure 5; General Architecture of PONs

PONs implement two wavelengths to provide bidirectional transmission in the network. One wavelength (usually 1490nm) used for the traffic that is transmitted from the OLT to customers is called the downstream signal and it has a form of a continuous stream of data that is encapsulated in frames. This stream is sent to all of the customers through passive splitters but it is read only by ONUs that frames are addressed to.

From OLT to ONUs, downstream traffic transmission is easy, based on a broadcast principle to send each ONU a copy of signal, and each ONU judges whether the packet belongs to itself or others based on the MAC address in the header of each frame. If the MAC header in the frame matches the MAC address of an ONU, then this ONU will access this frame; otherwise, it simply drops the frame. Based on such a mechanism, there is no collision in downstream traffic transmission as there is only a single traffic source from OLT.

Another wavelength (usually 1310nm) is used for the traffic, called the upstream signal that is sent by the customer to the OLT. The upstream data is encapsulated at the ONU into constant length slots. Those slots are sent to the OLT according to the time schedule that is predefined by the OLT. The number of slots used by each ONU in equal time intervals depends on bandwidth that is assigned by the OLT to specific customers.

There are two ways to allocate capacity to ONUs in the upstream direction. The simplest way is based on a fixed allocation strategy; that is, each ONU is assigned a fixed time slot to transmit its traffic to OLT. Each time that traffic is transmitted, there would be no other ONUs sending traffic to OLT.

Because data traffic from users comes in bursts, there can be some traffic at times, while other times there can be a long quiet period. Thus, if there is a fixed time slot allocated for each ONU, when there is no or little traffic transmitted during the time slot, the capacity of this time slot will be wasted due to the fixed allocation. To this end, a more advanced technique is based on a dynamic allocation strategy.

That is, it is the OLT that is responsible for the capacity allocations between ONUs.

When an ONU has more traffic to transmit, it is assigned more capacity; otherwise, it is allocated less capacity. By doing this, a PON can significantly improve the upstream capacity utilization and other performance criteria such as average packet delay and throughput. To realize this, OLT specifically run a polling protocol which polls each ONU while periodically determining the amount bandwidth required for the next round of transmission. When the ONU sends data upstream to OLT, such bandwidth request information will be piggybacked on the uploaded data. The OLT gets this information, and then schedules the time for the ONU to transmit data in the second round. Once scheduled, the OLT sends a GRANT message to the ONU with detailed information. Thus, overall this is an interleaving polling process. It has been verified to achieve an efficient performance in terms of bandwidth utilization and average packet delay.

In addition, to support differential quality of service of upstream traffic data, more advanced bandwidth allocation and scheduling have been devised. One important scheduling approach is called intra-ONU scheduling [31] in which several queues are set, and each of the queues has different priorities. The frames with higher priorities are always transmitted earlier than those in lower priority queues. This can help assure QoS of higher priority services such as VoIP.

Standards of PONs

There are two main competing standardization bodies governing PONs: The Telecommunication Standardization Sector (ITU-T) that operates on behalf of International Telecommunication Union (ITU) [32] based in Geneva, Switzerland and Institute of Electrical and Electronics Engineers (IEEE) [33] based in the United States.

The standardization work of ITU dates back to 1865, with the birth of the International Telegraph Union. It became a United Nations specialized agency in 1947, and the International Telegraph and Telephone Consultative Committee (CCITT), (from the French name "Comité Consultatif International Téléphonique et Télégraphique") was created in 1956. It was renamed ITU-T in 1993.
ITU is an intergovernmental public-private partnership organization within 191 countries (Member States) and over 700 public and private sector companies as well as international and regional telecommunication entities, known as Sector Members and Associates, which undertake most of the work of the ITU.

The IEEE is a non-profit professional association incorporated under the Not-for-Profit Corporation Law of the state of New York, United States, and it has over 390,000 members in 160 countries. It was established in 1963 by the merger of the Institute of Radio Engineers (IRE, founded 1912) and the American Institute of Electrical Engineers (AIEE, founded 1884). EEE performs its standards making and maintaining functions through the IEEE Standards Association (IEEE-SA).

ITU standards

ATM Passive Optical Network (APON) standards were developed in 1998 and modified in 2000. The

APON standard is known as the ITU-T G.983 [30]. This standard defines passive networks that transmit both upstream and downstream traffic with the speed of 155 Mb/s. It implements time division multiplexing for the upstream transmission and static bandwidth allocation. This standard was the first official standardized passive optical network and it did not support CATV transmission. APON consists of 16x splitter in original version (32x in modified version) and it implements Virtual Path Identifier/Virtual Channel Identifier (VPI/VCI) that is similar to ATM network.

Although many APONs that were deployed at the end of the 1990s are still used in commercial applications, this standard is no longer applied to new deployments due to its low bandwidth and static bandwidth allocation.

The Broadband Passive Optical Network (BPON) standard was developed in 2002 under the same name, ITU-T G.983, as the older APON. This standard is a result of the natural evolution of the APON and offers downstream transmission at a rate of 622 Mb/s and upstream transmission at 155 Mb/s.

BPON provides dynamic bandwidth allocation for the upstream traffic, 64x split ratio and support for the CATV service. It was the first PON that used a standard management interface between the OLT and the ONU, enabling development of mixed-vendor networks.

Transmission direction	Bit rate [Mb/s]
Downstream	1244.16
	2488.32
Upstream	155.52
	622.08
	1244.16
	2488.32

Figure 6; GPON bitrates

Gigabit PON (GPON) standard was developed in 2004 under the name ITU-T G.984 [32]. This standard replaces the ATM model of data transmission with the new Generic Encapsulation Method (GEM). GPON provides 2.488 Gb/s downstream transmission and 1.244 Mb/s upstream transmission. It offers enhanced security features and maximum split ratio of 64x (increased to 128x after 2 years). GPON is one of the most popular standards in North America and it is the most often considered candidate for future improvements.

IEEE standards

IEEE 802.3j standard, called Ethernet PON (EPON) [34], was developed in 1993 and it defines transmission of the Ethernet frames over the optical fibre with the bit rate 10Mb/s. The Ethernet Over the Fiber standard was improved in 1998 with the introduction of standard 802.3z, called also Gigabit Ethernet PON (GEPON), that offers a bit rate of 1Gb/s.

The 802.3ae Ethernet over the fibre standard followed the GEPON standard in 2003 and increased

transmission speed to 10 Gb/s. The success of EPON and GEPON encouraged IEEE from 2001 to 2004 to develop an additional standard 802.3ah that defines implementation of the Ethernet transmission in optical Last Mile applications.
In the last five years there has been ongoing work on the new standard 802.3av (10GEPON) that provides support for DWDM. At the same time the standard 802.3aq has been developed to provide 10Gb/s Ethernet over the multi mode fibre transmission.

EPON and GEPON standards are very popular in Asia and Europe. Although the 10GEPON standard is still in the development stage and has not finalized detailed standardization, it has already attracted a large number of network vendors due to its promised support of the DWDM transmission [35].

The already established standard carries several limitations such as the number of customers that can be served by a single PON, which is usually not higher than 64, reflecting a maximal split ratio of 64x. The transmission distance without any additional amplification systems is limited to 20km. The number of wavelengths is limited to about 18 due to the implementation of the CWDM in PONs. There is also a significant lack of compatibility between IEEE and ITU standards such as different transmission speed (1 Gb/s GEPON vs. 2.488 Gb/s GPON) and different encapsulation of the transmitted data (modified Ethernet in EPON vs. GEM in GPON).

Some of the limitations carried by the IEEE and ITU standards are called “soft type” due to several solutions that were developed by device vendors. Huawei Technologies Ltd. provides APON with split ratio 64x (in comparison to standard 16x), AD-net Technology Co. offers 1 Gb/s EPON with split 64x (in comparison to standard 32x), Flexlight and Infinera offer the GPON over 130 km with the DWDM extension (in comparison to standard GPON limited to 20 km).

Differences and compatibility issues

Interconnecting access networks belonging to IEEE and ITU standards is difficult due to their multiple differences. The main difference between ITU and IEEE PONs is the way that data is encapsulated into frames before it is sent along a light path. While EPON use an encapsulation model that is derived from the Ethernet standard [36], GPON implements its own proprietary GPON Encapsulation Method (GEM) [37].

The Ethernet framing system encapsulates whole data frames with sizes ranging between 46 and 1500 bytes (no packet fragmentation is allowed), by adding an 8-byte frame preamble followed by a 14-byte long Ethernet header (including source and destination addresses), as well as frame type/size - a value smaller or equal to 1500 indicates the size of the conveyed payload; however, if the value of this field is greater than or equal to 1536, then the length/type field indicates the nature of the MAC client protocol (protocol type).

Additionally, the Ethernet transmission protocol operation requires individual data frames to be separated by IPGs, defined by the IEEE 802.3ah standard as 96-ns time intervals, equal to 12-byte transmission times for 1 Gb/s 1000BASE-X Ethernet. It is therefore straightforward to estimate that, for a data stream that has size ranging from 46 to 1500 bytes, the Ethernet framing overhead is constant and equal to *8 + 14 + 4 + 12 = 38 bytes*. Since the Ethernet layer typically carries varied length IP packets originating from subscriber applications, it must be noted that very short IPv4 data frames ranging between 21 (minimum IPv4 packet composed of a header and a single byte payload) and 45 bytes must be zero-padded to 46 bytes prior to Ethernet encapsulation.

Besides the standard Ethernet framing overhead, EPON also implements Multi-Point Control Protocol (MPCP) that is defined in the IEEE 802.3ah [33] standard. The MPCP adds to EPON the scheduling overhead that consists of control message overhead, guard band overhead, discovery overhead, and frame delineation overhead.

GPON Encapsulation Method is an extended form of ITU-T recommendation G.7041, a generic framing procedure that was originally developed for sending IP packets over SDH networks. Downstream and upstream transmission in GPON use different frame formats. The downstream frame consists of the physical control block downstream (PCBD), the ATM section and the GEM section. The downstream frame provides the common time reference for the PON and provides the common control signalling for the upstream (Figure 7).

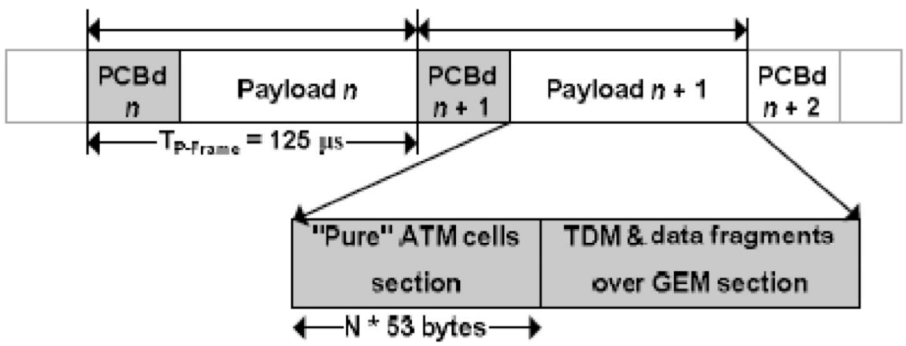

Figure 7; GPON downstream frames [38]

The frame length is 125µm for both downstream data rates. The PCBd length range is the same for both data rates and depends on the number of allocation structures per frame. If there is no data to be sent, the downstream frame is still transmitted and used for time synchronization.

Upstream transmission uses Time Division Multiplexing Access (TDMA), under control on the OLT located at the Central Office (CO), which assigns variable time length slots to each ONU for synchronized transmission of its data bursts. The upstream frame consists of multiple transmission bursts. Each upstream burst contains at a minimum the Physical Layer Overhead (PLOu). Besides the payload, it may also contain the Physical Layer Operations, Administration and Management (PLOAM), Power Levelling Sequence (PLS), and Dynamic Bandwidth Report (DBR) fields (Figure 8).

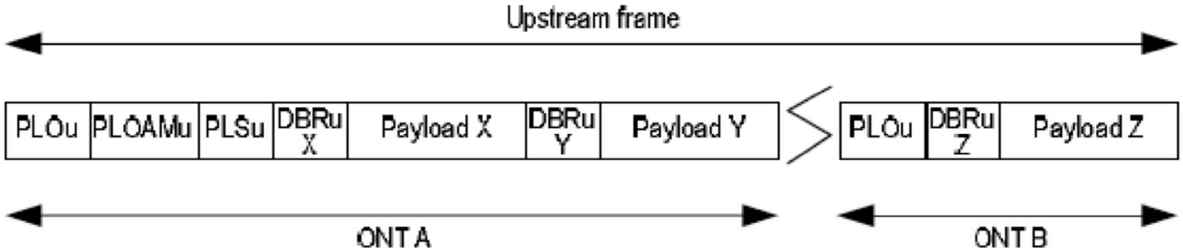

Figure 8; GPON upstream frame [38]

The upstream frame length is the same as in the downstream frame for all rates. Each frame contains a number of transmissions from one or more ONUs. During each allocation period according to the OLT control, the ONU can send from one to four types of PON overheads and user data.
GPON also has its own proprietary mechanism for Quality of Service (QoS) in upstream transmission: T-CONT. There are five types of QoS control in GPON:

- Type-1 T-CONT service is based on unsolicited periodic permits granting fixed payload allocation or catering to fixed bandwidth requirements. This is a static T-CONT type and is not serviced by Dynamic Bandwidth Allocation (DBA).
- Type-2 T-CONT is intended for variable bit rate with bounded delay and jitter requirements like video and voice over IP.
- Type- 3 T-CONT is intended for guaranteed delay. Type-4 T-CONT is for the best effort transmission.
- Type-5 T-CONT is combined for two or more of the other four types defined above and in this case the individual bandwidth reporting and assignment is done at the ONU.

In case of EPON there is no proprietary QoS mechanism. QoS is implemented on the foundation of the MPCP. Although MPCP is not concerned with any particular bandwidth allocation, it is a platform to facilitate the implementation of various allocation algorithms in EPON through its two-way messaging support. EPON relies on two Ethernet control messages (GATE and REPORT) during its regular operation. GATE messages (allocated timeslots) are transmitted by the OLT to ONU, while ONU reports its buffer status to the OLT by using REPORT messages [39].

Differences listed above are significant roadblocks in the way to interconnect or merge EPON- and PON-based access networks. Geographical differentiation between deployed PONs across the world is gradually losing its significance. Globalisation of the telecommunication business leads to accessibility a wide spectrum of communication technologies that can be chosen based on economical conditions in given macro-region. An example of region with mixed EPON and GPON deployments is China, where the national telecommunication operator (China Telecomm) is deploying EPON and GPON as replacement for existing DSL infrastructure. The components for EPON and GPON deployments are provided by Alcatel-Lucent. [40] If any circumstances would require GPON and EPON to be connected, the interconnection access point would have to require electro-optical signal converters, encapsulation systems and inter-protocol translation mechanisms. Existence of two parallel standards of PON creates difficulty in design and implementation of universal transparent devices for both types of PON. It also forces network operators to purchase equipment from a limited number of vendors since GPON and EPON devices are not inter-exchangeable.

Challenges faced by existing PONs

This chapter describes in detail a number of challenges exhibited by existing commercial network infrastructures such as limited network reach and a limited number of end users that can be connected to the access network. The chapter presents also predictions for future growth in bandwidth demand in access networks and it compares capacity and capability of commercial infrastructures to address changes in population density and geographic distribution.

The rapidly growing popularity of internet-based services increases the number of end users that are being connected to the access networks every year. For the last 10 years Internet popularity has been booming and widespread online services have accelerated the rate of Internet penetration within the population. In the United States for example, Internet penetration has exceeded 70% of population in 2009, and it is expected to reach 80% in 2011 (fig9).

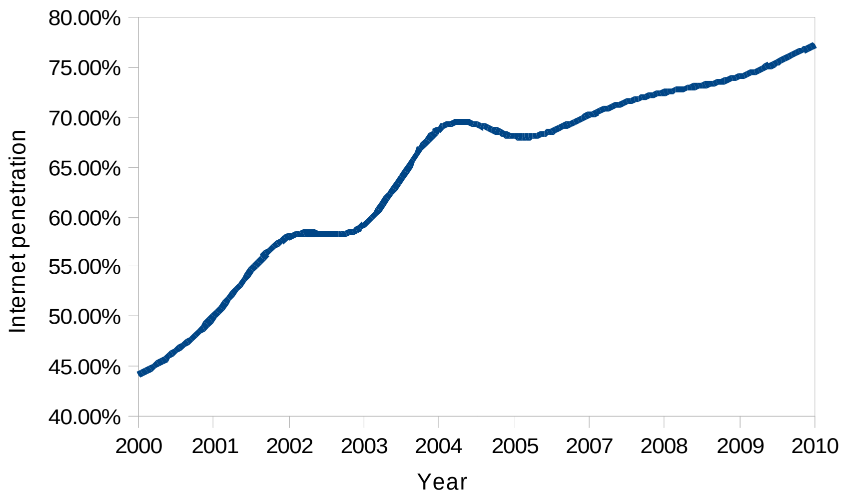

Figure 9; Internet penetration in the United States [41]

Bandwidth demand

The demand for higher bandwidth and the growing number of services offered online push existing PONs to their limits of capability. Network operators look for possible ways to improve already deployed PONs in order to satisfy high demand in the near future. There are several problems that have to be addressed to make PONs ready for new bandwidth-hungry services, a high density of interconnected end users, and extended reach distance.

One of the issues that must be addressed is the increase of bandwidth available to each customer. Novel services offered to end users such as High Definition TV (HDTV) and Video on Demand (VoD) set a new level of bandwidth consumption. A two-hour HDTV uncompressed movie requires 150 GB of data to be sent every hour (fig 10) and that translates to over 340Mb/s bit rate. This number must be multiplied if a subscriber wants to watch multiple video channels at the same time (the average household has two HD TVs).

Movie	File size
Standard DVD	3GB/h
Uncompressed 1280 X 720 (HDTV)	150GB/h
Uncompressed 1920 X 1080 (HDTV)	350GB/h
MPEG2 HDTV	9GB/h
MPEG4 HDTV	5GB/h

Figure 10; Bandwidth requirements for high definition video streaming [42]

Only optical networks can provide such a high bit rate but existing PONs cannot handle such bandwidth without sophisticated data compression technologies. MPEG2 compression allows streaming of HDTV channels over 20Mb/s link and MPEG4 further limits bit rate to 10Mb/s.

The leading markets, namely the US and Japan, had HDTV penetration in the range of 20% to 30% of households in 2006. This suggests that these two countries had more than 70% of the world's HDTV households in 2006, with worldwide estimates ranging from 25 to 50 million households. In 2010 the HDTV penetration in the US exceeded 60% [43] and the forecasts have worldwide penetration exceeding 10% of TV households in 2011. About one-third of the world's TV households presently subscribe to some type of CATV service. The estimates for the number of Internet Protocol TV (IPTV) subscribers worldwide in 2006 are about 5 million – less than 1% of TV households and about 2% of CATV households. Forecasts estimate the number of IPTV subscribers in four or five years rise from 70 to 150 million – again approaching levels near 10% of TV households [42].

This clearly suggests that HDTV and IPTV may become in the near future the most popular services (next to VoIP, online shopping and plain internet browsing) that are offered by network operators. The data on HDTV penetration into TV households suggests that there is potential demand for more than one simultaneous HDTV signal. Some households already have acquired a second HDTV set, and this percentage is only expected to increase. There is also the possibility of subscribers seeking to watch one HDTV program while receiving and recording another, either in HD or SD. Therefore total bandwidth requirements per household will be determined by summarizing all subscribed services, which will certainly be much higher than the bit rate for a single HDTV channel.

The downstream transmission is not the only service that will impact bandwidth requirement in near future. New online services that involve a higher level of subscriber interaction such as high definition online gaming, real time video conferencing or video online editing will also apply pressure on network operators to provide access to a sufficient amount of upstream bandwidth. Typical xDSL services that are offered to Canadian subscribers in metropolitan areas do not exceed 2Mb/s of upstream bandwidth and in many cases hover below 500Kb/s when the end user facility is located in a suburban area.

The next level for proposed upstream transmission is 10 Mbs/s but considering the rapid growth of online applications, this may be a very conservative estimation. Operators in Japan and Korea offer 100 Mb/s for upstream services, and higher speeds are said to be underway.

In summary, implemented modifications in data transmission technologies are required to accommodate high bandwidth services aforementioned in order for service providers to remain competitive.

Density of end users

Another problem that service providers face is how to connect a large number of new customers to the network. Every new customer is a new source of revenue for service providers but existing PONs can only serve a limited number of customers due to the limited split ratio of deployed splitters and limited optical power transmitted through those splitters. A PON split ratio varies between 32 to 128 but the typical value is 64 [44]. Assuming an average input of optical power in the PON is between 0.5 to 5 dBm [45], the average output power that reaches end user facilities, when a 128x splitter is implemented, will vary from approximately -20dBm to -16dBm. If a network provider wants to double its revenue without increasing subscription fees, then the number of end users should be at least doubled [46], and this will lead to a drop in output optical power of -23 dBm

The problem of an increasing density of end users connected to an access network is becoming significant in metropolitan areas where high residential density is induced by the popularity of condominium housing.
For example, the State of New Jersey (around 7400 square miles of land area) had a population density of approximately 1000 residents per square mile in 1980. This density had grown to 1051 in 1990 and to 1144 in year 2000, finally reaching 1195 residents per square mile in year 2010 [47]. The total population in NJ was estimated to be 9 million in 2009 with housing units in multi-unit structures (such as condominium skyscrapers) exceeding 36% of residential real estate [48].

Relatively small urban areas filled with skyscrapers that accommodate thousasnds of apartments in each building, presents a big challenge for optical network providers to ensure sufficient power of optical signal delivered to each subscriber.
This problem becomes even more crucial to address when you consider that in the future, HDTV broadcast will be the most popular consumer service offered in metropolitan areas. The Super Bowl XLV finals in 2011 attracted over 111 million viewers, which placed it in first place as the most watched television program in US history (Super Bowl XLIV drew in 106 million viewers in 2010). There are many more TV shows that skyrocket in terms of popularity among viewers: National Hockey League (NHL) Playoffs, National Basketball League (NBL) and National Association for Stock Car Auto Racing (NASCAR) among others.
Widespread popularity of TV broadcast brings an excellent opportunity for network operators to increase their revenue stream by offering those broadcasts in high definition format that is closely aligned with the growing number of large scale flat screen TV sets purchased by consumers.

The above examples suggest certainly that in the near future there will be great bandwidth demands for online services provided to a large number of consumers distributed over the existing network infrastructure. The existing network infrastructure will have to be modified not only to handle high bandwidth streaming but also to accommodate the high distribution density of consumers connected to the access infrastructure within limited geographic regions.

Higher power optical signal emitted by OLT could be a possible solution to the problem of high density of end users connected to single PON tree, but it would require additional capital and operational costs that are related to the implementation of high-power transmitters. There have been reported designs of high power super luminescent diodes (SLD) for WDM-PON applications [49]. In addition, the high power optical signal injected to telecommunication fibre may cause unwanted nonlinear optical effects that will increase link impairments and deteriorate quality of transmitted signal.

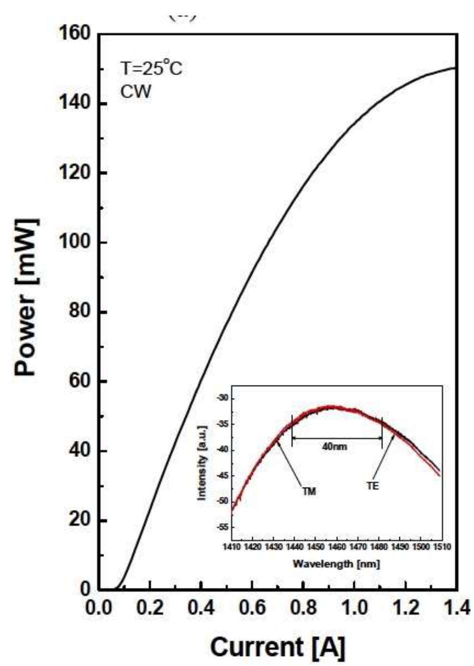

Figure 11; WDM SLD output power vs. supply current [49]

Those diodes are capable of emitting light with optical power exceeding 21 dBm, when 1.47 A supply current is provided and stable temperature of 25°C is ensured (fig 11).

Requirements for high-current supplies and stable temperature associated with implementation of high power laser transmitters will certainly have a negative impact on OLT investment costs due to the additional cooling systems that will need to be deployed in OLT facilities resulting in higher energy consumption, elevating the operational costs.

High optical power injected to the PON grid may also excite some unwanted nonlinear effects in optical fibres [50] and that may lead to additional optical noise. Under certain conditions there may appear effects of Self-Phase Modulation (SPM), Cross-Phase Modulation (XPM) and Four Wave Mixing (FWM). SPM may occur when the refractive index of a fibre contains a nonlinear dependent on intensity component, which causes the phase shift proportional to impulse intensity. SPM is observed in high bit rate (over 2 Gb/s) optical systems that use small impulses durations (less than 200-400 ps) and high transmission power.

XPM occurs in multi-wavelength optical systems such as CWDM and DWDM systems, and it exhibits (similar to SPM) a change in refractive index as light intensity increases. Since channel power levels in CWDM-DWDM systems are approximately identical, the XPM effect increments nonlinear phase shifting approximately in 2N times, where N is number of used optical channels in the fibre. XPM leads to the same distortions of impulses, as SPM, only in a greater degree. The XPM effect in a greater degree, rather than SPM, depends on dispersion in the fibre-optical line and leads to amplitude distortions from pulse jitter.

FWM is an effect of interaction of three waves with frequencies ω_1, ω_2, ω_3 when the critical power level of laser radiation meets nonlinearity of the optical fibre. This effect leads to create a fourth wavelength $\omega_4 = \omega_1 \pm \omega_2 \pm \omega_3$. It may create a false signal that can enter into working bands of channels. Number of false channels M is related to number of legitimate channels N that are used in optical systems: $M = [N^2(N-1)]/2$. Therefore a 4-channel PON may have 24 false signals, and a 16-channel WDM-PON may have 1920 false signals.

Another solution for deteriorating output power of optical signal due to high split ratio would be implementing higher sensitivity photo receivers in ONU devices. High sensitivity receivers for 1.25 Gb/s PON applications were reported in [51]. To improve receiving signal with low optical power a PIN photo detector was implemented in IEEE EPON (802.3ah) and ITU-T GPON (G984.2). Although the achieved bit error ratio (BER) was in the range of 10^{-12} when optical power was -30dBm, it increased to 10^{-6} when the optical power experienced only a small change of -1 dBm (Figure 12).

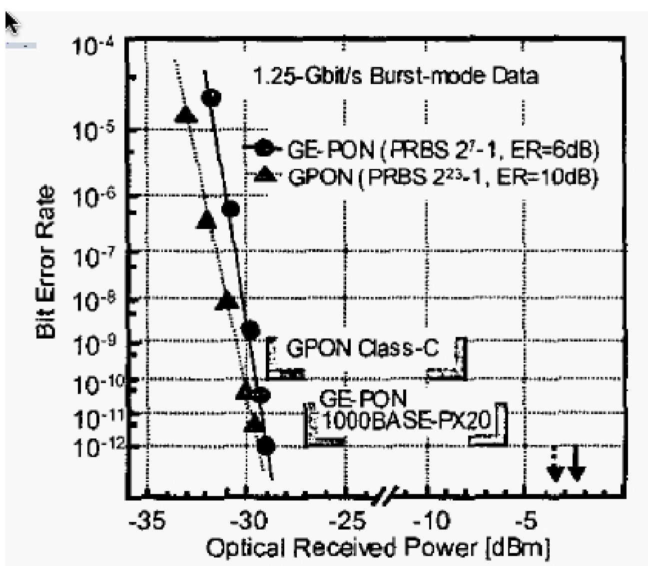

Figure 12; Changes of BER as function of received power in PIN photo receiver at 1.25Gb/s PON [51]

High sensitivity receivers for commercial 10 Gb PON (developed by NTT laboratories) were reported in [52]. The proposed PIN photo receiver achieved BER=10^{-12} in GEPON when the optical power was -19 dBm and the transmission rate was 10Gb/s. Although the error ratio appeared to be stable at the 10^{-12} level for continuous transmission as well as burst transmission, it quickly exceeded a ratio of 10^{-7} when the received optical power changed only within -2 dBm (fig 13).

An additional method can be implemented to improve extraction of data from distorted optical signal. The Forward Error Correction (FEC) is a technique used for controlling errors in data transmission over unreliable or noisy communication channels. FEC is accomplished by adding redundancy to the transmitted information using a predetermined algorithm. A redundant bit may be a complex function of many original information bits. The ITU-T (G.709) standard recommends a Reed-Solomon technique as FEC in optical gigabit communication.

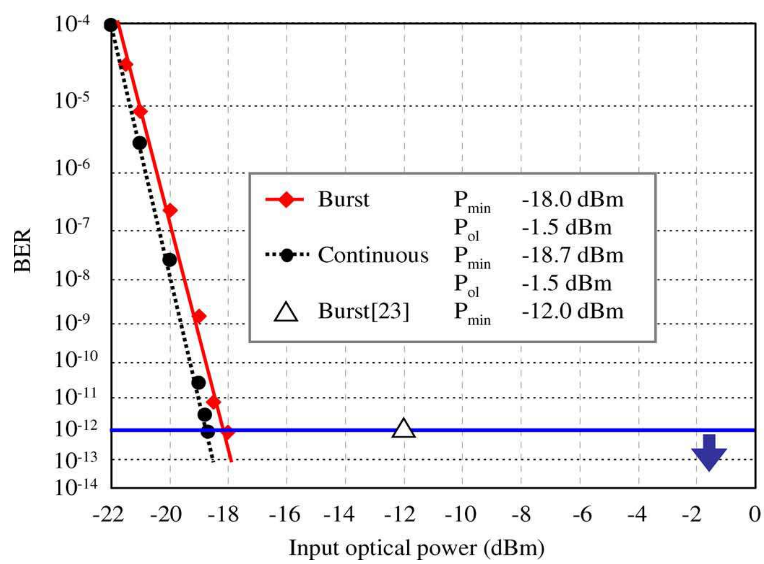

Figure 13; BER performance of PIN photo receiver at 10Gb/s PON [52]

Research results of PIN photo detectors as candidates for implementation in high sensitivity PON photo receivers indicate that this technology could be a good solution for deployment in subscriber premises if the output power of the transmitted signal is severely weakened by multiple splitters implemented in access networks.

Although high sensitivity PIN photo receivers perform well when output optical power is stable (even when low), they exhibit an increase of BER when optical power experiences a drop down for less than -2 dBm. This effect is especially visible for higher bit rates such as 10 Gb/s. It implies that increasing sensitivity of the photo receiver may be a good solution to high density of connected subscribers when a 1 Gb/s commercial network is considered. If bit rate 10 Gb/s or higher is considered, stability of photo receivers needs an improvement to handle unexpected variations in optical output power.

Another aspect of low power output signal at the consumer premises has to be considered. Network operators have been seeking possible ways of decreasing cost of end user terminals to make PONs more accessible to broader range of consumers. One of the most frequent propositions is to eliminate certain active components of ONU such as receivers and transmitters. Those two elements would be possibly replaced by one component: Reflective SOA (RSOA) [53]. This modification would simplify ONUs architecture and decrease operational costs related to the power consumption.

Although the implementation of RSOA may have a positive impact on capital and operational costs of ONU, it would require that the optical power at subscriber premises be no lower than -20 dBm [54]. If optical power drops below the accepted threshold (when split ratio at the remote node is too high) RSOA may cause a significant increase in BER.

Long reach of the network

The wide geographic reach of PONs is another issue that must be considered when network topology is planned and access infrastructure is deployed.

The booming popularity of suburban housing developments [55] ignited by high costs of dwelling and limited development space in downtown cores and near-downtown regions [56], resulted in the development of a number of low-density remote settlements filled mainly with single houses and semidetached units.

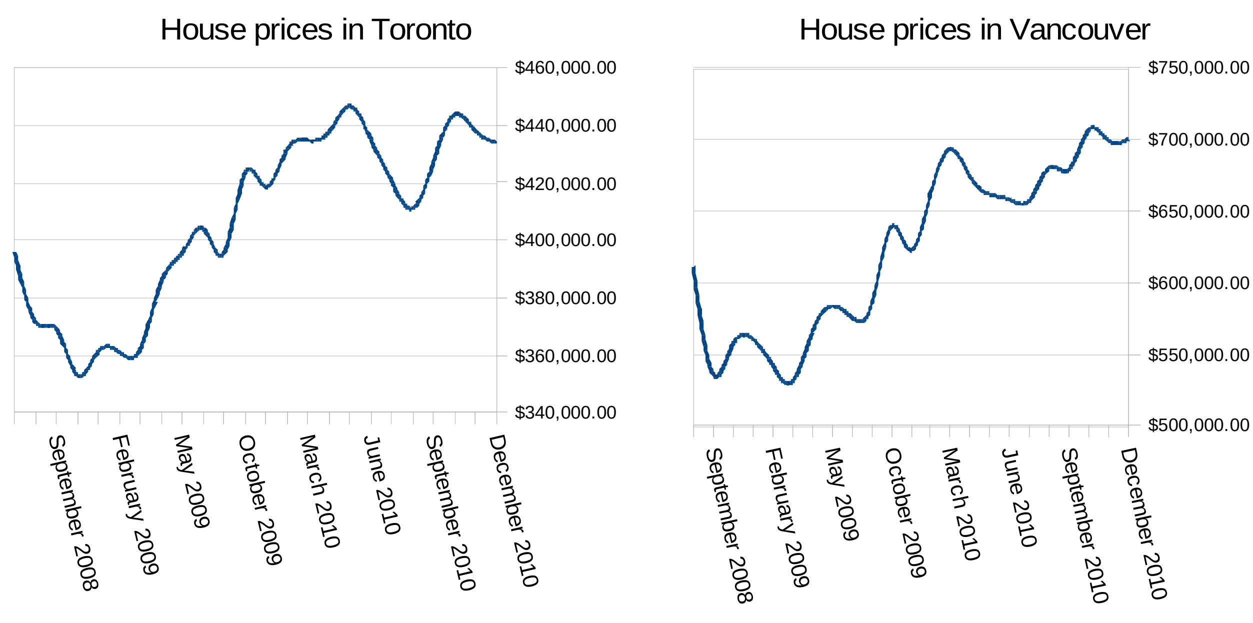

Figure 14; Change in average house price in Toronto and Vancouver [56]

Rising costs of housing in major cities (Figure 14) drove residents farther from the downtown cores to seek affordable housing in suburban locations. New settlements such as Jackson Trails, Findlay Creek, Half Moon Bay or Chaperal Town near the City of Ottawa (Ontario) require not only connecting to certain municipal infrastructure such as the electrical grid, water, sewage and public road system, but also to communications media such as telephone lines, cable TV and internet.

In the past, xDSL was a predominant solution for remote locations. Although it was inexpensive and easy to implement, it had one major drawback: low bandwidth for end users due to long distance to the DSLAM node. Modern deployment of an optical telecommunication network in remote locations faces a similar problem of considerable geographic distance between end user and the central office. Although a low-density residential area does not exhibit problems related to high splitting ratio, it draws attention to problems related to length of the optical link and all components deployed along the light path that are potential sources of optical loss.

Losses related to optical fibre, connectors, splitters and other passive components of the optical path are described and standardized by the Telecommunications Industry Association (TIA) [57] in the TIA-568 document published for the first time in 2001. This document is a set of three telecommunication standards (ANSI/TIA/EIA-568-B.1-2001, -B.2-2001, and -B.3-2001) that address commercial building cabling for telecommunication products and services. Most manufacturers and users of cabling systems in the US use it as a standard for premises cabling. The section TIA-568-B.3 of the document specifically addresses components of fibre optic infrastructure (fig 15, 16).

Fiber Type	Wavelength (nm)	Max Attenuation Coefficient (dB/km)
50/125 (OM2, OM3)	850	3.5
	1300	1.5
62.5/125 (OM1)	850	3.5
	1300	1.5
Singlemode (OS1, OS2) (Premises)	1310	1
	1550	1
Singlemode (OS1, OS2) (Outside Plant)	1310	0.5
	1550	0.5

Figure 15; Fibre Optic Performance: standard TIA-568-B.3 [57]

TIA-568-B.3 defines optical fibre loss, optical connector loss and splicer loss (0.3 dB/splice). Optical network vendors use those guidelines to estimate an optical power budget required for specific fibre network deployments.

Fiber Type	Wavelength (nm)	Loss (dB)	Optical Return Loss (dB)
Multimode	850	0.75	20
	1300	0.75	20
Singlemode	1310	0.75	26 (CATV:55)
	1550	0.75	26 (CATV:55)

Figure 16 Optical Fibre Connector Mating Loss: standard TIA-568-B.3 [57]

Also implemented is an international standard ISO-11801 [58] that is very similar to the TIA standards except that it has some slight variations from one country to the next.

A typical EPON that has a standardized 20-km reach and a minimum of two connectors (for each end point) would exhibit a loss of: *20*0.5dB+2*0.75dB=11.5dB* according to the TIA standard. This estimation is very optimistic and does not consider the standard x64 splitter and extra connectors and splices that would have to be implemented if a PON is deployed over the existing public infrastructure. The realistic scenario would have to include not only losses related to additional splitters or connectors but also losses related to fibre misalignment, dirt or stain covering fibre faces, unexpected fibre bends and all other imperfections that may occur during deployment of the telecommunication infrastructure.

As it is shown above there are a number of fundamental issues that PONs will have to face in the near future. The development and implementation of innovative technology is required to enhance existing commercial PON deployment as well as ensure that new generation PONs will be ready to face future challenges.

PON extension scenarios

This chapter presents technologies that can be potentially implemented in existing PONs to extend their reach and to improve their capacity. The chapter provides also detailed review of existing projects that address number of drawbacks in existing PONs. The chapter also compares results of already published works from the perspective of potential commercialization and their compatibility with existing telecommunication infrastructure.

As was presented in the previous chapter, issues related to the expansion of PONs can be grouped in three main categories:

- Density of end users connected to the network
- Maximal distance of the network range
- Bandwidth available to subscribers

There are a number of projects initiated in both academia and industry to address one or more problems faced by PONs. Those projects are in different stages of design and development. Some of them have already been implemented in commercial networks, some are in very advanced development stage, while others have never gone beyond the developmental stage.

To address the problem of available bandwidth and density of end users, multi wavelength technologies are very often proposed as universal solution. WDM [59] is a good candidate for extending existing PONs that have implemented only two or three wavelengths (shared in TDM fashion). To effectively take advantage of multiple wavelengths deployed in access networks, a low-cost model of wavelength assigning between end users is required as well as improved methods for sharing multiple wavelengths.

Many extension designs implement Arrayed Waveguide Grating (AWG) [60] as a key component in Wavelength Division Multiplexing (WDM) optical communications systems. AWG has the advantage of compact physical size and easy of integration with other optical components, such as lasers, amplifiers, and photodetectors. Small features of this device allow for a mass production on large wafers and therefore it enables manufacturers to maintain low production costs.

First generation extensions

One of the oldest projects that addressed the issue of high bandwidth demand per single customer was Composite Passive Optical Network (CPON) [61]. This technology implements Wavelength Dense Multiplexing (WDM) 1500 nm band in the downstream transmission and single wavelength Time Division Multiplexing (TDMA) shared in the upstream. The single wavelength receiver is used at the OLT (Figure 17).

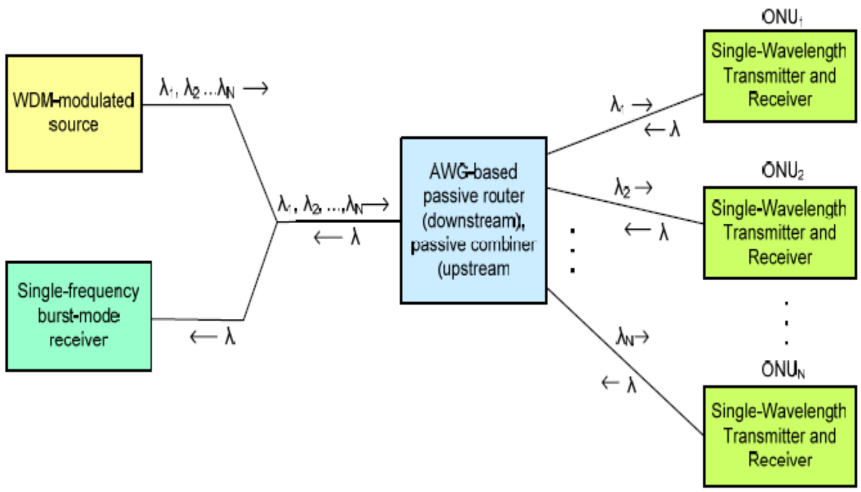

Figure 17; Composite PON [61]

Each customer has dedicated wavelength for downstream transmission. This solution provides high bandwidth to each customer but it does not guarantee good scalability especially when Coarse Wavelength Dense Multiplexing (CWDM) technology is used. A limited number of wavelengths prevent a high number of customers to be connected to the PON. CPON in its basic version finds applications in enterprise business where low customer numbers have a large bandwidth requirement. In addition to this CPON represents an early model of WDM-PON because of implemented multiwavelengtth downstream transmission.

The problem of merging multiple PONs that are already deployed in the field is addressed by the Stanford University Access Dynamic Wavelength Assignment (SUCCESS-DWA) PON architecture [62].

SUCCESS implements dynamic wavelength allocation to provide bandwidth sharing between multiple PONs. It consists of tuneable lasers (TLs) and the Array Waveguides (AWG) at the CO, while WDM filters and a burst-mode receiver are employed within the ONUs. Significant feature of all-optical multi-access network which is different from conventional point-to-point links is that the amplitude and phase of the received packets can be quite different from packet to packet due to different fiber attenuation and the chromatic dispersion caused by the variation of the transmitters' wavelengths. Burst mode receivers are suitable for those networks because they offer fast response time to improve detection of short packet or burst data. A wideband WDM filter residing between the AWG and the PON separates up- and downstream traffic. The main requirement for this model is that all wavelengths from the OLT must reach all ONUs across separate physical PONs (Figure 18). TL1 can reach PON1 through AWG channels 1,5,9,.... and PON2 through channels 2,6,10,.... etc. Each TL can reach any ONU in each PON by determining what wavelength is servicing a particular ONU. This model is scalable by adding new TL and AWG. Since each TL can access only one user at the time, the efficient scheduling algorithm is required.

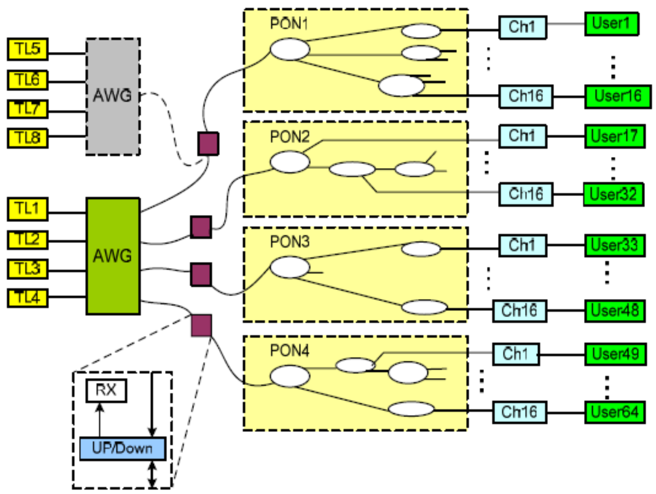

Figure 18; SUCCESS-DWA PON architecture [61]

To avoid head of line blocking, several virtual output queues are implemented. One queue can be serviced by several TLs so that an implemented arbiter prevents more than one TL from accessing one queue at a time. This model avoids collision; however, it is not fully scalable for a large number of ONUs. An incoming packet is assigned to the transmitter with the shortest queue to minimize delay. The scheduler traces the destination address of the packet at the end of queue and assigns the incoming packet to the same queue if the addresses are the same. QoS is implemented by prioritizing packets when they are assigned to the queues.

The problem of connecting a high number of customers to a single PON is addressed in the WDM Super-PON project [63]. This type of PON covers a range of over 100 km with a splitting ratio reaching 2000 with the aid of optical amplifiers (OAs). Optical amplifiers are placed in the feeder fiber (the one connecting OLT and RN) and after the RN, this solution provides sufficient power budget to the network. SPON uses two DWDM channels, one of upstream and one for downstream. The "blue" half (1525 nm – 1543 nm) of the C-band carries downstream channels while the "red" half (1547 nm–1565 nm) carries upstream channels, which are separated by low-cost red or blue filters (RBF). ONU is a colorless device that uses an electro-absorption modulator-semiconductor optical amplifier (EAM-SOA) to modulate and amplify outgoing signal.

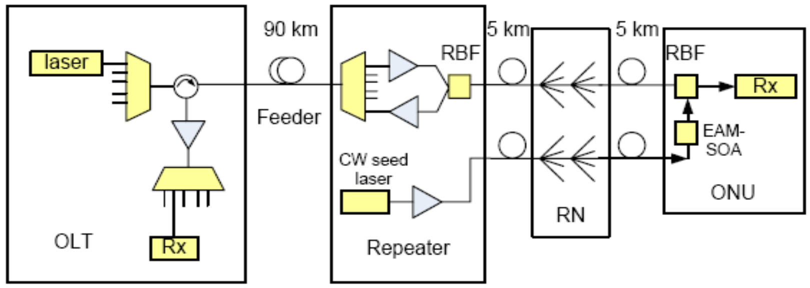

Figure19; Super-PON with colorless ONUs [61]

The remote node (called also "repeater") contains a continuous-wave (cw) seed laser followed by a booster amplifier, distributing an upstream optical source signal to each ONU within a splitter PON group. All upstream wavelengths are amplified by an EDFA preamplifier before being separated into each receiver at the OLT (Figure 19). The Super-PON model provides long-distance service and accommodates many ONUs. The remote node requires its own power source for implemented active devices such as seed laser; therefore it is not considered to be a fully passive network.

The solution for the scalability problem of PONs is presented in the Multistage AWG-WDM-PON project [64]. This architecture implements the periodic routing property of the Array Waveguide (AWG) to reuse one wavelength for more than one subscriber.

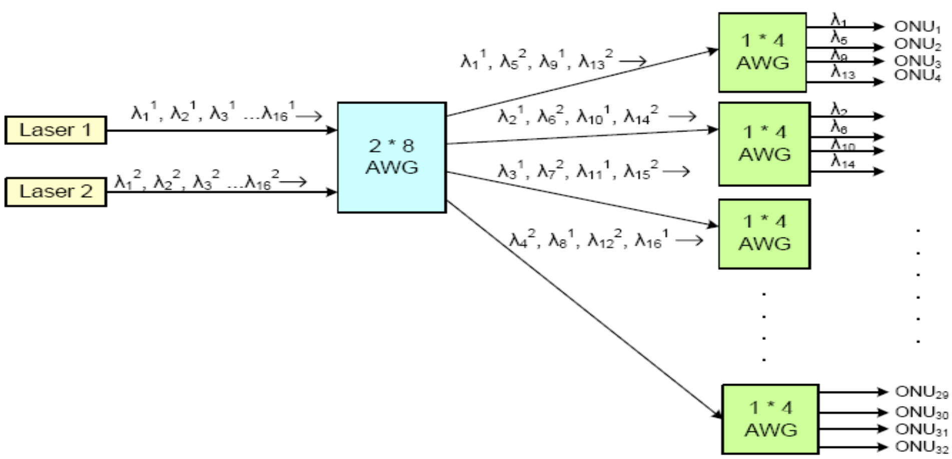

Figure 20; AWG-WDM PON [61]

This architecture provides scalability in bandwidth as well as in number of users, either by employing additional wavelengths at the OLT or by cascading multiple stages of AWGs with increasing AWG coarseness at each stage (Figure 20).

The problem of the high costs of end-user terminals is addressed in the project Remote Interrogation of Terminal Network (RITENET) [65]. The RITNET architecture eliminates the transmitter on the ONU side by modulating the downstream signal and by sending it back to the OLT. The ONU splits the light with a passive tap. The portion of the light detected by the receiver and the remainder is looped back toward the OLT through a modulator.

The signal (the same channel) from the OLT is shared for downstream and upstream transmission through time sharing fashion. In other words, both the upstream and downstream channels have to be shared by the ONUs using TDMA or dynamic bandwidth allocation.

A 2x2N AWG-based router is used to route the wavelengths. The OLT consists of a tuneable laser (its modes correspond to those of the AWG) that is capable of wavelength stepping through the ONU channels (Figure 21).

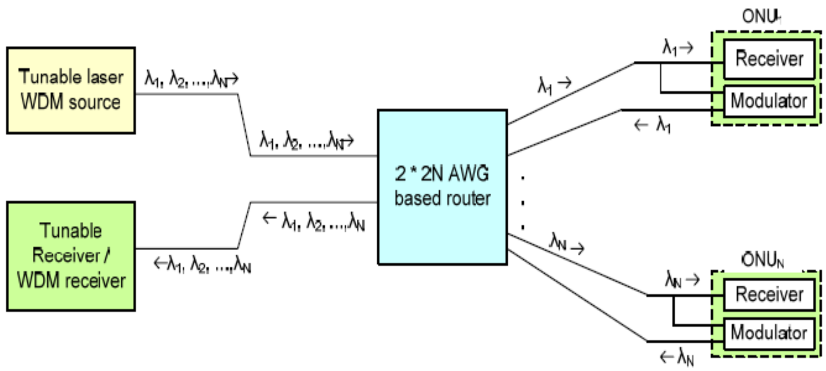

Figure 21; RITNET PON [61]

RITENET reduces end-terminal costs at the ONU, but the distance from the OLT to the ONU is much less because signal from the OLT has to travel double the distance. The number of fibers employed in this architecture is doubled, so it raises the cost of deployment and maintenance of this PON model.

Requirement of implementation a tuneable laser or an array of transmitters and receivers increases the cost of OLT, and therefore makes RITENET a more expensive architecture compared to alternative CPON and LARNET (both described later). The advantage of this model is the availability of symmetrical bandwidth in the downstream and upstream directions.

Another method of limiting costs of end-user terminal is presented in Local Access Router Network (LARNET) [66]. LARNET-PON has implemented a broad-spectrum source at the ONU, such as a low-cost light-emitting diode (LED). The spectrum of this LED is sliced by the AWG-based router into different optical bands in the upstream direction.

An advantage of using an edge-emitting LED is that each ONU can have the same device, as opposed to employing DFB lasers at each ONU, which may require the DFBs to be different. Each ONU has a broad-spectrum source that sends a signal to different ports of AWG router. Wavelength that is sliced at the output port depends on the input port that the signal reaches, and therefore a particular ONU (Figure 22).

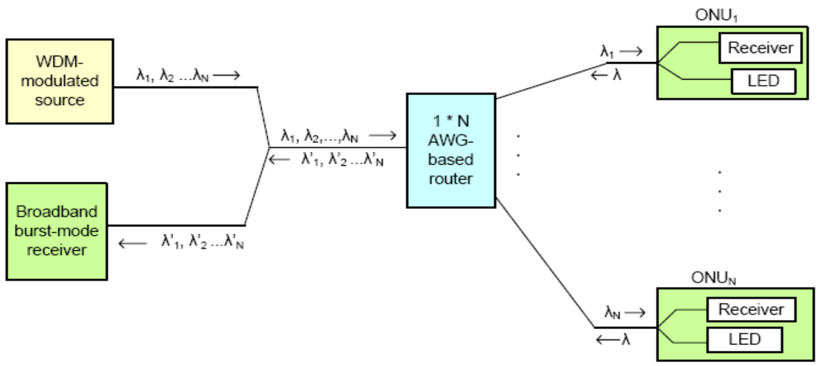

Figure 22; LARNET PON [61]

The downstream signal consisting of multiple wavelength components is generated at the OLT by a multifrequency laser (MFL). This signal is coupled into the transmission fibre through a 1300-nm and 1500-nm multiplexer. A broadband receiver is also employed at the central office, which can receive any spectral component of the edge-emitting LED. This means that OLT can receive any wavelength from any of the ONUs. Implementing single receivers at the OLT requires that the upstream channel be shared between the ONUs in the TDMA model. The limitation with this architecture is that spectrally slicing a broad-spectrum source by an AWG may lead to high power loss.

The issue of network survivability is addressed by the project "Wonder-PON" [67] proposed at the Politecnico di Torino. It consists of N nodes connected to two counter rotating WDM rings. Each ring provides W wavelengths where N>=W. One ring is used only for transmission and another one only for reception. Transmission wavelengths are switched to the reception ring at a folding point between the two rings. The way packets travel consists of two parts: during the first ring traversal, transmitted packets traverse the transmission ring until the folding point, where they are switched to the reception ring and then received during the second ring traversal. Similarly, this architecture works on a folded bus network, where each ONU has one receiver and one transmitter working on a single WDM channel (Figure 23).

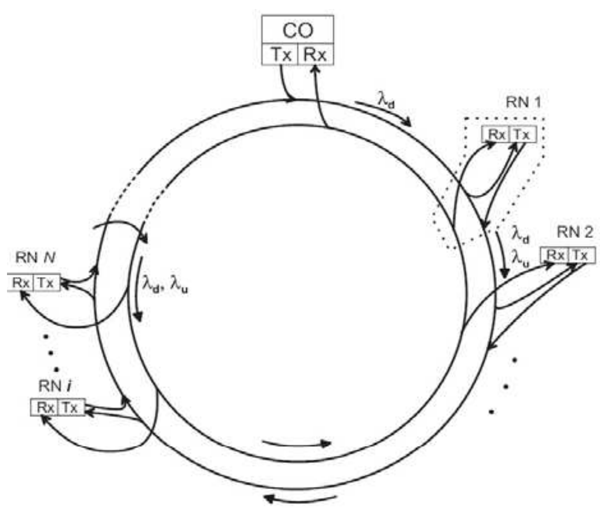

Figure 23; WONDER-PON [61]

The architecture utilizes one wavelength for upstream transmission and one wavelength for downstream transmission. Receivers at ONUs and OLT are centered only for those specific wavelengths. This model allows ONUs to exchange data without intermediate OLT if burst mode receivers are implemented and if the distributed access protocol is used. The drawback of this model is that a number of couplers attached to the ring causes major power loss. To minimize the number of splitters in the ring, ONUs can be grouped.

The WONDER network can be used as a collector of PONs, where PONs are connected to the ring through couplers. To avoid interference of upstream signals, the circulator is used instead of 2xN splitter (Figure 24).

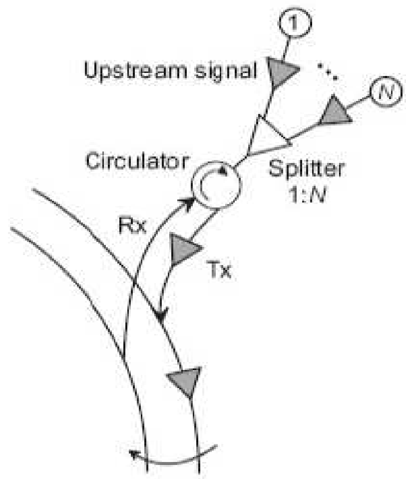

Figure 24; WONDER-PON as a collector for PONs [61]

Each logical PON will have assigned one upstream wavelength as well as one downstream wavelength. EDFA amplifiers will be implemented to deal with power loses.

The method for connecting a large number of customers to the network is proposed in the project Scalable Advanced Ring-based passive Dense Access Network Architecture (SARDANA) [68]. This project targets the performance enhancement of dense Fibre-to-the-Home networks. It implements a robust highly-scalable access PON with impairment compensation. The proposed network incorporates a novel WDM/TDM overlay which enables it to serve between 1000 and 4000 users and extend the reach to 100 km while maintaining the passive nature of the network.

The SARDANA architecture is similar to the original WONDER-PON network with the exception that the main ring consists of two independent fibres rather than folded single fibre. Multiple of PON trees are connected to main rings at Remote Nodes. Each tree PON has dedicated wavelengths for upstream and downstream. The upstream channel in each tree is shared in TDM fashion. The scalability of the model is realized by adding a new RN to the ring and assigning two additional wavelengths at the OLT to the new tree PON. Both main rings are connected to tree PONs through two stages of couplers. The first stage is 90/10 and the second stage is 50/50 coupler. This 50/50 interconnection provides protection functionality that lets the downstream signal be received by tree PONs from an east and west fibre connection as well as two paths for the upstream signal (Figure 25).

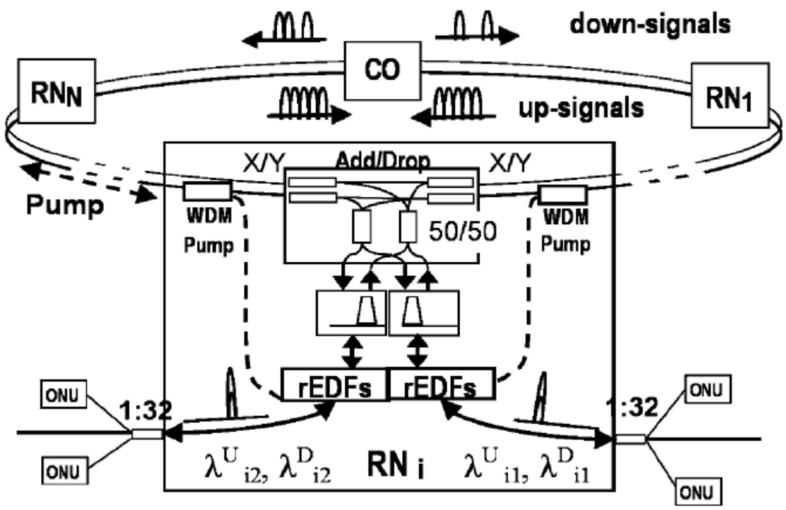

Figure 25; Remote Node architecture in SARDANA-PON [61]

Each remote node services two PON-trees with single fibres. The trees can be configured with 16-, 32-, 64 ONUs and respective bandwidth: 156 Mb/s, 78 Mb/s, 39 Mb/s per single ONU. The signal amplification is done at the RN using EDFAs that are remotely pumped by 1480 nm lasers. The experimental prototype used ASK 10 Gb/s and provided 150 Mb/s per user in half duplex mode. The tunable laser of the OLT provides an optical carrier to the ONUs for half of the time for intensity modulation (IM) upstream modulation by the RSOAs.

Using RSOAs with modulation capabilities up to 2.5 Gbits/s, the minimum guaranteed upstream bandwidth of 40 Mbits/s can be offered to each ONU. The pump power from the OLT 1480-nm lasers is reused at several RNs by injecting the remaining excess pump power of the EDF to the fibre ring to use it at the next RN, thanks to the EDF characteristics and the low losses of currently commercial 1480/1550 multiplexers (of 0.2 dB).

Optical transmission measurements have been done at 1543.73nm (ITU-T channel 42). An EDFA booster (placed after the tunable laser at the OLT) provides 10 dBm for the downstream signal. This signal propagates through 25km of standard single mode fiber (SSMF), corresponding to the distance from remote node #4 to the OLT, in case of a 100-km fibre ring. Experiments demonstrate that this access architecture can serve 1024 users and 50km, or 512 users and 100km configurations offering guaranteed downstream bandwidths of 155 Mbits/s per user. Each remote node produces passing attenuation of 1.04dB for downstream (due to twice 0.46dB, 90% passing, and 0.05 dB excess losses, 0.08dB maximum specified; plus 0.02 dB for splices) and 1.52 dB for the upstream transmission (due to extra pump-signal WDMs, 0.23 dB each, 0.3 dB maximum, and splices).

Signal and pump variable attenuators have been included to emulate other RNs at the corresponding

light paths. Downstream signals are dropped by the 90/10 and 50/50 couplers. The total dropping losses are 13.2 dB (10 dB due to 10% of dropping, 3 dB because of the 50/50 splitter, and 0.2 dB due to excess losses and splices).
Low loss 2.1 dB in thin-film 100 GHz filters defined in ITU-T standard have been used for wavelength selection at 1543.74 nm. The result of the experimental setup shown that Experiments demonstrate that this access architecture can serve 1024 users and 50 km or 512 users and 100-km configurations offering guaranteed downstream bandwidths of 155 Mbits/s per user.

The demand for high bandwidth per single customer is addressed by projects Photonic Integrated Extended Metro and Access Network (PIEMAN) [69]. PIEMAN is the project of a new all-optical communication system that will allow individual subscribers to directly access bandwidths at up to 10 Gbit/s both upstream and downstream. This architecture will integrate access and metro networks into one system.

This integration will simplify the network architecture and reduce the cost to deliver future broadband services to all residential customers. The main assumption is that access and metro portions of the network are provided by separate systems.

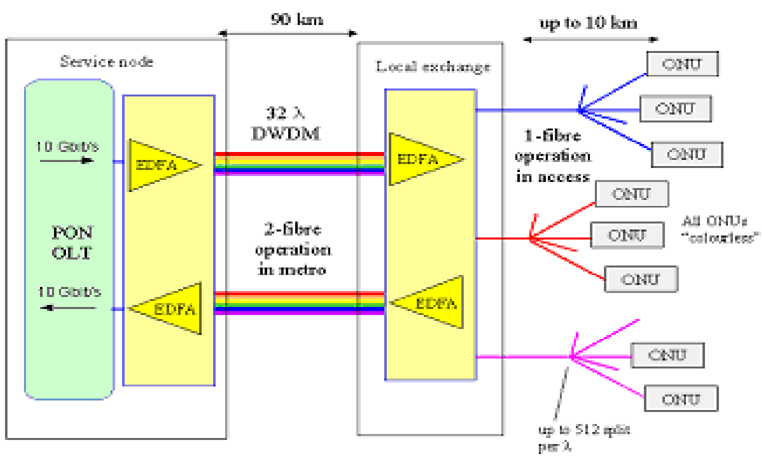

Figure 26; PIEMAN-PON architecture [61]

The project addresses the European national geographies that require a reach of 100 km from the customer to the major service node. Since deploying point-to-point fibre from each customer to the service node up to 100 km away will be expensive, so PIEMAN will use multi-wavelength, high split passive optical networks (PONs) to make efficient use of fibre. The first generations of PONs are now standardized and commercially available. The most advanced of these (GPON and GE-PON) typically offer 2.4 Gbit/s downstream and 1.2 Gbit/s upstream, shared between 32 customers (via passive optical splitters and a TDMA protocol), over a reach of up to 20 km.

Extensions comparison

The previous chapter reviewed a number of extensions that have been proposed by business and academic institutions to solve certain technical issues faced by present PONs. From a business perspective, all technical problems surrounding PONs can be grouped into classes that reflect certain aspects of network expansion. This classification helps to provide a comparison between extensions regarding to the maximal number of end-users served, distance to reach, bandwidth offered to each customer, reliability, QoS and protocol transparency. While most of the PON extensions are protocol transparent, due to their optical fibre used as the transport medium and data encapsulation methods, number of end users or max distance varies depending on technology that is implemented. Figure 27 presents comparison various projects of next generation PON architectures and their limitations.

Extension	Max. distance [km]	Number of customers served	Max bandwidth per customer [Gb/s]	Muli wavelength technology	Downstream wavelength sharing
CPON	20-25	Depends on number of wavelengths	Limited by Rx/Tx	CWDM	No
SUCCESS-DWA	25	64 (with 4 Tx in ONU)	1.25	CWDM (DWDM planned)	Yes (within single tree)
SUPER-PON	100	2000	2.4	CWDM	
MULTISTAGE AWG-PON	20	32	1.25	CWDM (DWDM tested)	TDM
RITNET	20-25	Depends on number of wavelengths	Limited by re-modulation at the ONU	CWDM	No
LARNET	20-25	Depends on number of wavelengths	0.662	CWDM	No
WONDER-PON	25 (between RNs)	16 (RNs)	10 (per wavelength)	CWDM (16)	TDM
SARDANA	100	1024	0.155	CWDM	TDM
PIEMAN	100	512 (per wavelength)	10	DWDM (32)	TDM

Figure 27; Extensions comparison

There is no one universal access network that can fit different markets to serve different demands and different expectations. Enterprise customers who have very high bandwidth demands will take advantage of the PON that offers a full wavelength (RITNET, LARNET), while personal users, that represent a much larger portion of the telecom market and that have lower bandwidth demand (daily usage of CATV, VoIP, Internet), will fit to the network model where wavelength is shared among a number of end-users. The examples of this model are PIEMAN and Multistage-AWG.

Limitations of networks presented in figure 27 have their roots in technologies implemented in the network. The most common technologies implemented in commercial PONs as well as prototypes of PONs extensions are listed in figure 28.

	Splitter WDM-PON	AWG-based PON	CWDM-PON	Cascaded AWGs
DS/US Bit Rate a[Gb/s]	1, 2.5, 4, 10 dedicated	1, 2.5, 4, 10 dedicated	1, 2.5, 4, 10 dedicated	1, 2.5, 4, 10 dedicated
Wavelengths Grid	100 (50) GHz	100 GHz, 50 GHz inter-leaved	20 nm (L-, C-, S-, and O-bands)	100 GHz, 50 GHz inter-leaved
Max. split	1:32	1:40	1:8	1:40
Max. budget [dB]	8 (1G APD)	10 (1G PIN)	13 (1G PIN)	12 (1G APD)
ONU link cost [rel.]	242 (1G per λ)	256 (1G per λ)	122 (1G per λ)	300 (1G per λ)
	Amplified DWDM	**CWDM+TDMA**	**DWDM+TDMA**	**Amplified, TDMA**
DS/US Bit Rate [Gb/s]	1, 2.5, 4, 10 dedicated	Up to ~1Gb/s (~250 Mb/s for 1:8 split and 2.5G aggregate bit rate, 90 percent efficiency)	Up to ~1Gb/s (~500 Mb/s for 1:4 split and 2.5G aggregate bit rate, 90 percent efficiency)	Up to ~1Gb/s (~250 Mb/s for 1:8 split and 2.5G aggregate bit rate, 90 percent efficiency)
Wavelengths Grid	100 (50) GHz	20 nm	100 (50) GHz	100 (50) GHz
Max. split	1:40	1:64	1:160	>1:320
Max. budget [dB]	>30, scalable	11 (1:64, 2G5 APD)	11 (1:160, 2G5 APD)	>30, scalable
ONU link cost [rel.]	280 (1G per λ, PIN, 1 active node, plus booster and pre-amp in OLT)	132 (2.5G per l)	234 (2.5G per λ)	198 (2.5G per λ, PIN, 1 active node, plus booster and pre-amp in OLT)

Figure 28; Comparison of the PONs technologies [70]

Value added services such as Quality of Service (QoS) or guaranteed delay are most often implemented as a software solution that is embedded in scheduling algorithms at the OLT as long as the service provide communication between nodes is in the same PON access tree. More difficult situation is faced when QoS is implemented to the communication between nodes that are located in different PONs connected by a large backbone network. Some PON standards have implemented certain elements of the QoS such as EPON with its Logical Link Control Identification (LLID) [71]. The main reason for introducing LLID is because PON systems do not support a multicast upstream transmission.

This effect is related to the problem of guaranteed delay – this value is a variation QoS constraint that is caused by the difference between communication layers of access network and backbone network [71]. Some of PON extensions provide their own solutions for QoS such as SUCCESS-DWA with its Service Level Agreement (SLA). This particular SLA implementation consists of two priorities of downstream traffic: high priority (HP) and best effort (BE) [72]. This implementation is derived directly from traditional models of virtual output queues (VOQ) assigned to tuneable lasers at the OLT.

It is clear that HDTV and real-time gaming will be soon be major players among service provided to end users and will occupy a large portion of the available bandwidth. New generation PONs will face a demand that easily reaches 1 Gb/s by the year 2015. The current or even next-generation GE-PON/G-PON will have difficulty of guaranteeing QoS for applications which require such huge bandwidth and real-time [73]. Since WDM technology is not yet fully standardized (although next generation of 10GE-PON supposed to support WDM), number of projects has been launched to investigate more advanced access networks with implemented QoS.

Second generation extensions

Most of the projects that were presented above proposed PON extensions that were based on a multi wavelength transmission scheme. The dynamic wavelength assignment and TDM were dominating research subjects for designing and developing new PON enhancement.

Recent achievements in developing multi gigabit network processors [74] and innovative technologies that pushed bit the rate of optical transmitters to 10 Gb/s [75] could trigger a large number of research projects. This research would be able to address issues of implementing 10-Gb/s transmission in PONs. Unfortunately, recent breakdowns in the global economy [76] and visible ineffectiveness of applied government stimulus plans for economical recovery [77] caused a significant slowdown in research and development activities related to new technologies. The telecommunications industry has joined other industries in applying investment cuts and in postponing the introduction of new technologies.

Another factor that plays important role in slowing down implementation of new and expensive technologies is financial hangover that telecommunication business has been suffering for lat 10 years. The premature upgrade of European wireless telephony from 2G to 3G in late 90s and early 2000 required huge investments that had little chance of being balanced due to overestimated revenues. The early introduction of innovative mobile services for consumers has dragged wireless telephony carriers into significant debt that pushed telecomm businesses on the edge of bankruptcy [78]. The European telecom industry has spent over $230 billion USD into upgrading to 3 G. In the result France Telecom has increased its debt to a $55 billion, similarly Deutsche Telekom owes $50 billion, and British Telecom has debt exceeding $43 billion.

Remembering the failure of European early 3G, the telecomm industry is cautious in approaching any new technologies or innovative network enhancements that would have to be accompanied with significant investment costs. Stagnation in a world economy forced the telecommunication industry to look for budget cuts and to limit investments strictly to those that are absolutely necessary to sustain their business models. Research and development was one of the fields that suffered the most. Even if research did provide positive results and prototype devices were successfully tested, telecomm operators very often chose not to implement the new technologies in commercial deployed networks due to additional investment costs and uncertainty of estimated revenues.

Although interest in 10G PON has not decreased significantly during last 5 years, and IEEE published final 10GE-PON recommendations [79], the research effort has shifted from systems that implement relatively expensive 10Gb/s bit rate technologies to systems that offer alternative paths for PON enhancement.

New research projects that aim to design new generation PON extensions focus strongly on implementing WDM in PONs and merging it with existing TDM schemes. Research efforts will result in WDM-PONs and hybrid WDM-TDM PONs that will be able to offer bandwidth that is comparable to 10G-PON.

The first fully mature DWDM-PON that was ready for commercializing WDM-PON was designed by

Korea Telecomm in April 2008 [59]. The network was deployed in Kwangju city in Korea and it connected 320 subscribers. Commercial success of this project encouraged academic and industrial research centers to increase research efforts in the area of WDM implementation in PONs.

WDM-PON architecture

WDM-PON is defined as a PON system in which each ONU uses a different wavelength, i.e., a unique wavelength, in each direction to communicate with the OLT. Figure 29 presents a typical WDM-PON configuration. ONU_k (k=1 to n) emits the upstream signal with wavelength λ_{uk} and receives the downstream signal with wavelength λ_{dk}.

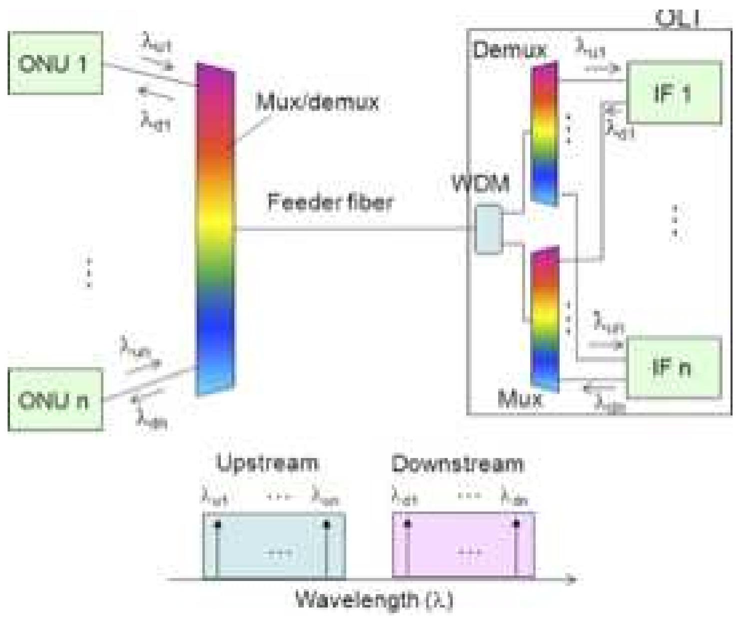

Figure 29; Architecture of WDM-PON [80]

To achieve the wavelength multiplexing of upstream signals from λ_{u1} to λ_{un} as well as the wavelength demultiplexing of downstream signals from λ_{d1} to λ_{dn} , a wavelength splitter/router is typically used as the optical branching device instead of the power splitter used in TDM-based PON systems. The OLT consists of *n* interface cards (IF_1 to IF_n). The most unique feature of this architecture is that point-to-point communication is facilitated between IF k and ONU k logically. Therefore, this type of WDM-PON system is sometimes called the "virtual point-to-point" system.

WDM/TDM PON static architecture

Static WDM/TDM-PON is a PON system in which several wavelengths can be used in each direction to realize communication between the OLT and a number of ONUs. Each wavelength can be shared by several ONUs, and the wavelength(s) assigned to an ONU remains unchanged from installation until disconnection. The optical branching device is typically wavelength filter/router, or a combination of a power splitter and a wavelength filter/router.

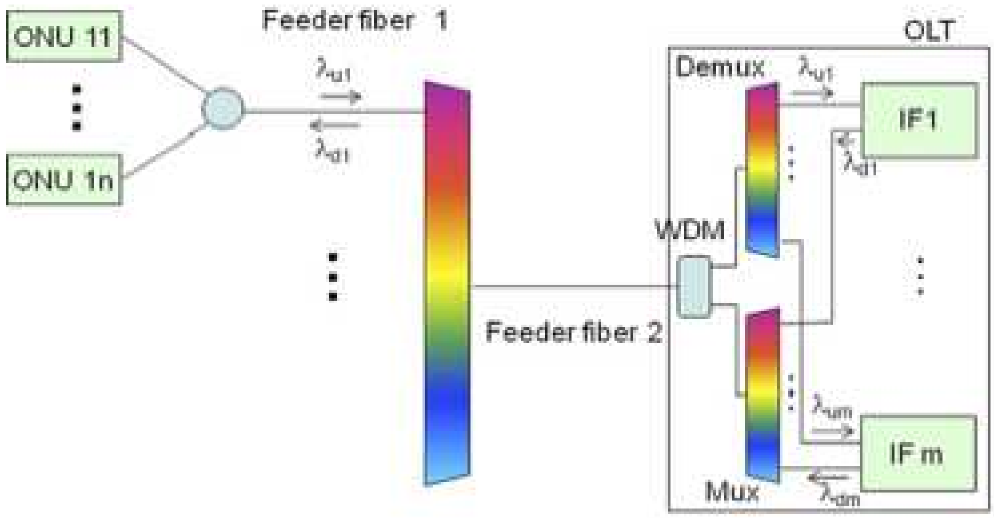

Figure 30; Architecture of static WDM-PON [80]

Figure 2 presents the generic architecture for the static WDM/TDM-PON system. ONU_{j1} to ONU_{jn} (j=1 to m) access the same interface card (IF_j) in the OLT by using the same wavelength: λ_{uj} and λ_{dj} for upstream and downstream, respectively. Namely, *m* is the number of TDM-PONs stacked/overlain by WDM. Therefore, there are *m* interface cards (IF_1 to IF_m) in the OLT side.

The static WDM/TDM-PON architecture becomes very effective when the network has to be extended in section *feeder fibre 2* (Figure 30). If that section is extended then fibre cost, which increases with the reach, can be shared among the high number of ONUs. Node consolidation using long-reach optical access systems is an effective way for network operators to decrease the operational expenditure (OPEX) if the provided system capital expenditure (CAPEX) is sufficiently low. In this approach, *feeder fibre 1* (Figure 14) constitutes the section between the subscriber's home and the nearest remote node (RN), and *feeder fibre 2* the section between the network operators central office (CO) and a RN. The distances typical of the former and the latter sections are 10 km to 20 km and 40 km to 80 km, respectively.

WDM/TDM PON dynamic architecture

Dynamic WDM/TDM-PON is a PON system in which several wavelengths can be used in each direction to establish communication between the OLT and a number of ONUs, each wavelength can be shared by several ONUs, and ONU wavelength assignment can be dynamically changed during communication/operation [81].

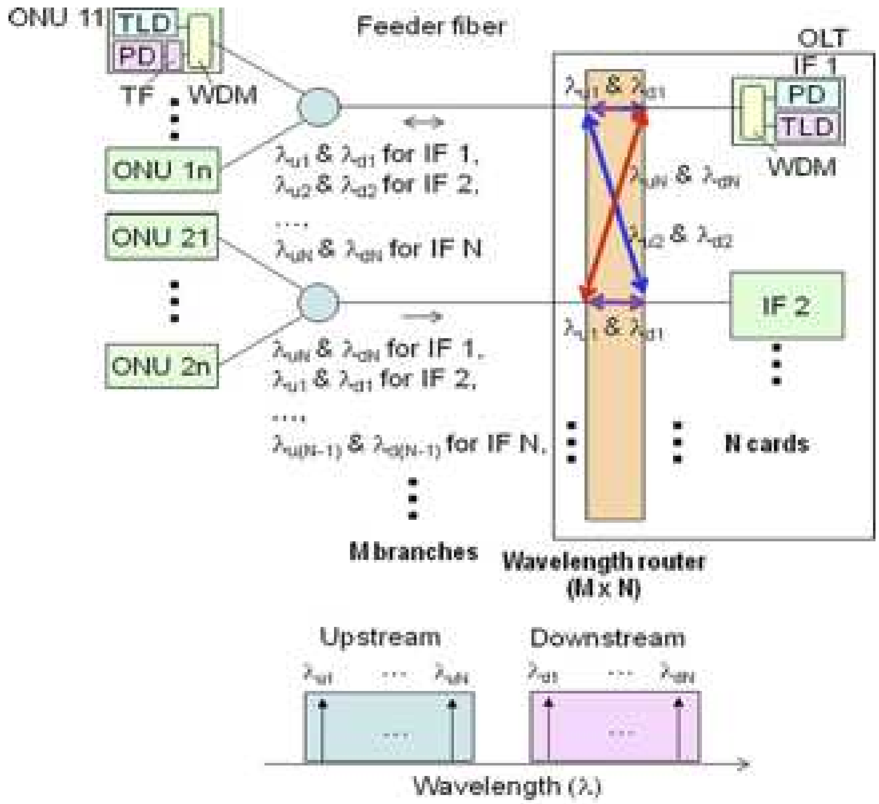

Figure 31; Architecture of dynamic WDM/TDM-PON [80]

Figure 32 presents an example of dynamic WDM/TDM-PON architecture. The system comprises ONU_{11} to ONU_{Mn}, IF_1 to IF_N in OLT, *M* power splitters, and an *M*-by-*N* passive wavelength router. ONU_{jk} accesses port *j* of the wavelength router via power splitter *j* (j = 1 to M, k = 1 to n). *M* is the number of power-splitter branches, *N* is the number of IF cards, and *n* is the number of ports of every power splitter. This system allows each ONU to access every IF by using a wavelength tuneable laser diode (TLD) as the transmitter: ONU_{1k} can access IF 1, 2, . . . *0* by using λ_{u1} , λ_{u2} , . . , λ_{uN} , respectively.

Arrayed waveguide gratings (AWGs) can be used as the wavelength router; they offer cyclic wavelength-transfer, so ONU *2k*, *3k*, . . . , *Mk* can access all IFs by using the appropriate wavelength among λ_{u1} , λ_{u2} , . . , λ_{uN} as well. The same criteria can be adopted for downstream signals: λ_{uk} and λ_{dk} are always used as a pair as shown in the figure (k = 1 to N), so that each ONU always receives its downstream signal from the IF card that to which the ONU sends its upstream signal. In this case, a tuneable filter (TF) is necessary at the ONU for wavelength selection.

Dynamic wavelength re-assignment permits each ONU to access an uncongested IF (and the network behind the IF) when congestion occurs, and that provides load balancing among IF cards. It also allows each ONU to access a live/healthy IF (and the network behind the IF) when failure occurs and that provides network resilience. It also implements some power-saving functionality: number of IF cards may be turned off when the total traffic is low.

Technologies that enables WDM-PON

Perhaps one of the most natural ways of implementing the WDM feature in PONs would be to employ a different laser locked to a specific wavelength in each ONU. Unfortunately, this method would certainly increase operational costs of PONs. Alternative, a cost-effective method would be to deploy colourless ONUs that can serve any received wavelength at any time. There are number of technologies that are considered as good candidates for colourless ONU: injection locking [82], wavelength seeding [83], remote modulation [84], wavelength tuning [85] and spectrum slicing [86].

Injection locking scheme

Wavelength-locked Fabry–Perot laser diode (F-P LD) with an external injection of the spectrum-sliced amplified spontaneous emission (ASE) is frequently proposed as a candidate for injection locking devices in PONs. The injected ASE forces the F-P LD to operate as a quasi-single mode, and the noise intensity and the mode partition noise of the F-P LD are suppressed [87]. In addition to this, the wavelength-locked F-P LD is very attractive because of its cost effectiveness and colour-free operation–awavelength-independent operation. Since the wavelength-locked F-P LD was proposed as a low cost source for WDM-PON, experimental results and the system demonstrations have been announced [88]. The example of a system with implemented injection locking technology is presented in Figure 32.

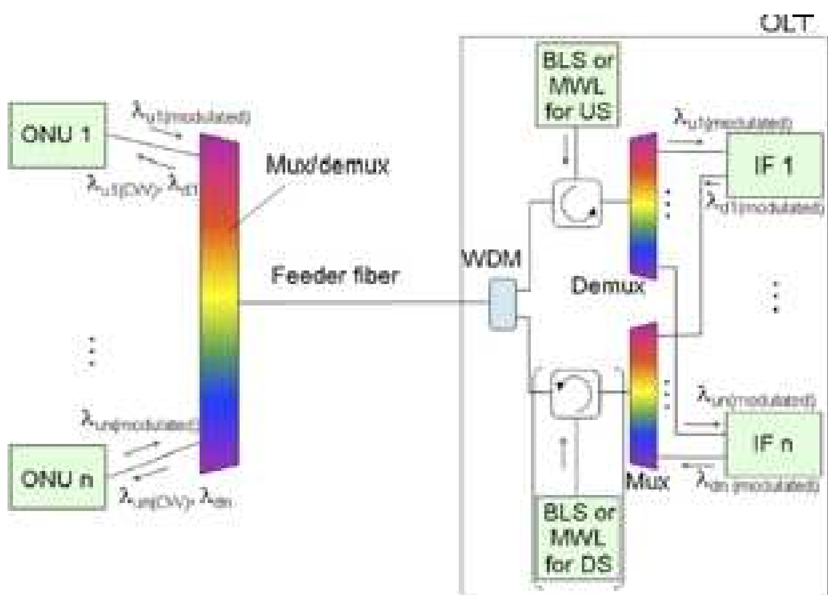

Figure 32; WDM-PON architecture with injection locking mechanism [80]

In this particular architecture a Fabry–Perot laser diode (FP-LD) is used as the transmitter of each ONU. The sliced light wave is injected into the FP-LD, so that the laser wavelength is locked to the wavelength of the injected light wave. By directly modulating the FP-LD, each ONU can send an upstream signal with an appropriate wavelength, $\lambda_{uk(modulated)}$ (Figure 32), which dispenses with the need for ONU-specific LDs.

A recently proposed WDM-PON architecture with implemented injection locking mechanisms was published in October 2010 [89]. The proposed architecture consists of side-mode injection-locked Antireflection coated Fabry–Perot Laser Amplifier (AR-FPLA) that has a 25-channel locking capacity with a corresponding wavelength locking range of 30nm.

The experimental PON prototype consisted of a standard FPLD with an integrated optical isolator that was employed as the master laser for injection-locking the AR-FPLA with a longitudinal mode spacing of 0.6 nm. The front-facet reflectivity of the AR-FPLA was coated as low as 1%, and the rear-facet reflectivity was increasing to 99%. Such a highly asymmetric coating allowed the efficient injection of ASE, which also reduced undesirable backward reflection at front-facet. The experimental PON architecture is presented in Figure 33.

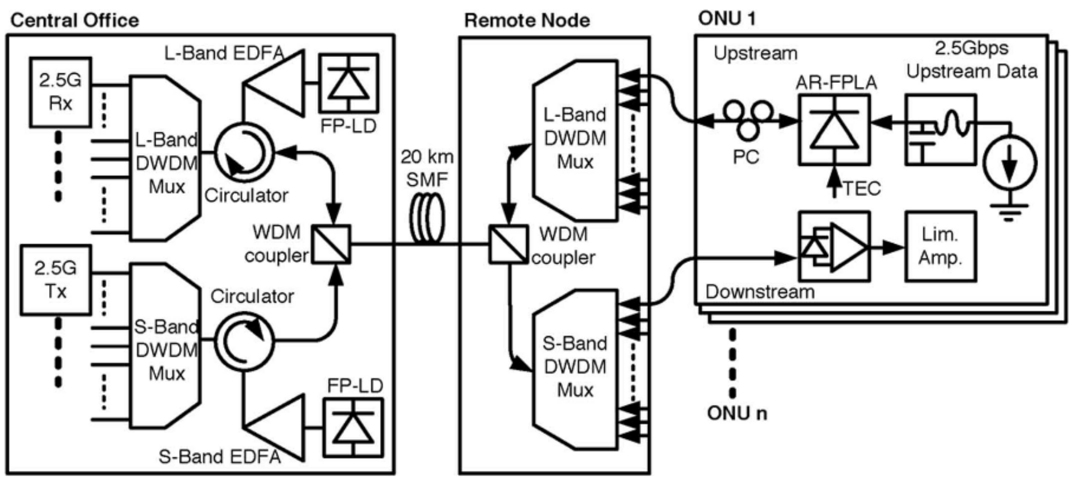

Figure 33; WDM-PON prototype with injection locking mechanism [89]

To facilitate the injection-locking scheme, the design and fabrication procedures of the AR-FPLA were modified from a conventional FPLD without significantly increasing the production cost. The threshold current of the AR-FPLA was 13 mA. A long-term test of the AR-FPLAs biased at 80 mA and 85°C with output power of 5 mW for 4500 hours was done for the stable operation of 40 devices used in testing the PON prototype.

The prototype PON consisted of ONUs that had transmitters connected to polarization controllers (PC). PCs were adjusted to maximize the efficiency of injection from the master FPLD. Before being injected into each AR-FPLA at the ONU end, the master FPLD output was channelized by a DWDM multiplexer built-in with the DWDM-PON and amplified by a EDFA (SDO, OAS-1000) with a maximum output power of dBm, which consequently caused a reduction on threshold current of the slave AR-FPLA.

The external injection-locking condition was easily achieved by matching the slave AR-FPLA wavelength with the incoming master signal via a slight temperature and current detuning. The side-mode injection-locked AR-FPLA acted like a single-mode source with high side-mode suppression ratio (SMSR), which was directly modulated by a 2.5 Gb/s PRBS for a transmission performance diagnosis.

The FPLD used in the PON prototype had a long-cavity to shrink its longitudinal mode spacing to 0.6 nm, and to make it close the channel spacing of 50 GHz set by the AWG-based DWDM. The FPLD emitted a number of modes before passing through the DWDM. DWDM filtered those modes into a single-mode spectrum for injection-lock AR-FPLA.

The reported experimental results (Figure 34) show BER varying between 10^{-9} and 10^{-12} for different longitudinal modes and eye diagram opening with and without applied injection.

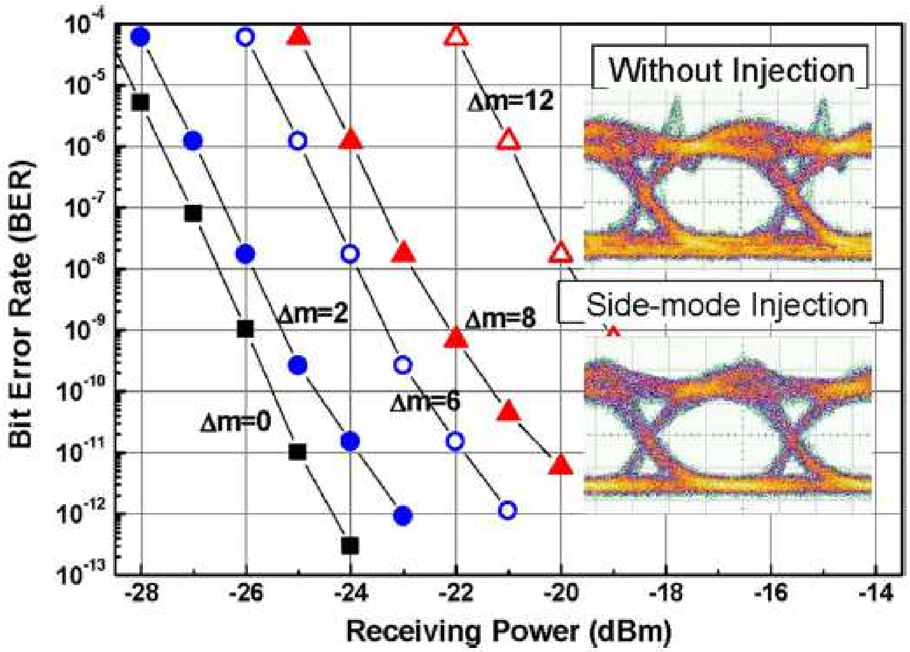

Figure 34; BER analysis of wavelength injection locked 1% AR-FPLA at different longitudinal modes [89]

There is reported power penalty for detecting the data-stream with BER of less than 10^{-12}. This effect was caused by the relaxation on the oscillation and the increasing bandwidth of the AR-FPLA after injection-locking. Alternatively, if the farthest side-mode (the 12th modes away from the central mode) of the AR-FPLA is injection-locked, the receiving sensitivity at BER of 10^{-12} dramatically degrades to -17 dBm with a power penalty of 7 dB, which is mainly attributed to the reduced SNR of the side-mode injection-locked AR-FPLA.

If this type ONUs are deployed over the commercial WDM-PON system then 17 modes of the AR-FPLA can be used to achieve a data communication with BER less than 10^{-9} at receiving power of larger than -22 dBm at 2.5 Gb/s. At same BER criterion, there are at least 25 side modes applicable for data transmission with their maximum receiving sensitivity degrading to -19 dBm.

Wavelength seeding scheme

WDM-PON architecture with wavelength seeding scheme is very similar to the one presented in figure 16 except a reflective semiconductor optical amplifier (RSOA) is used as the transmitter for each ONU. The sliced light wave is fed into the RSOA, so that the light wave is amplified and modulated by the upstream signal, and sent back to the MUX/DMUX over the same fibre. The same scheme can be optionally applied to downstream signals by adding Broadband Light Source (BLS) or Multiwavelength Light Source (MWL) to the downstream circuit; this yields colorless IF cards.

As the first commercial prototype of WDM-PON with 32-wavelength, 16 ONUs and wavelength seeding components were presented by the France Telecomm in 2006 [83]. The principle of this design is presented in figure 35.

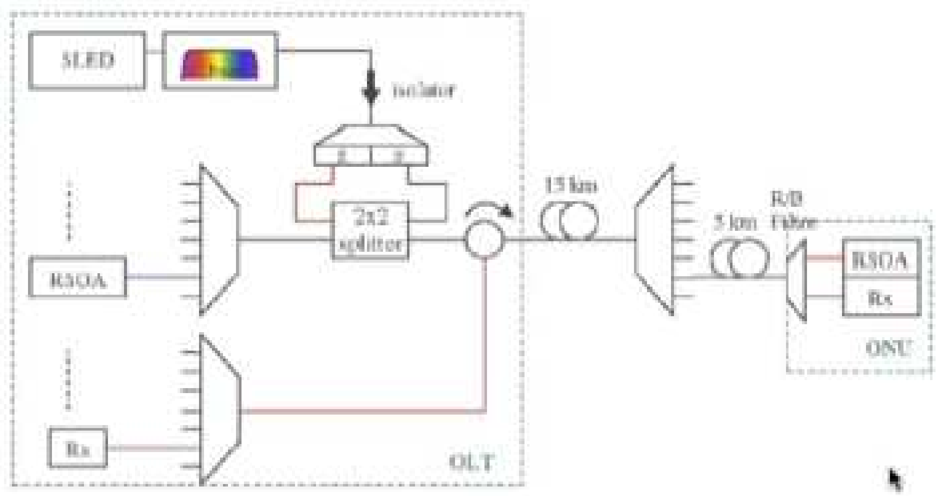

Figure 35; Architecture of wavelength slicing WDM-PON prototype [83]

The broadband source is a spectrum sliced superluminescent diode (SLED) emitting unpolarised and incoherent light over the 50nm optical bandwidth. There is also a bandpass filter implemented to limit the spectrum to the C band. The red/blue filter (Figure 36) separates the optical spectrum into two parts. The blue part, which corresponds to the short wavelengths, is used for the downstream signals and the red part for the upstream signals. A 2x2 optical splitter is used to insert the two optical spectra in opposite directions in the feeder link. An optical isolator is added to avoid injection of light back in the SLED. Both spectra are sliced by AWG, at the OLT for downstream signals and at the remote node for upstream signals.

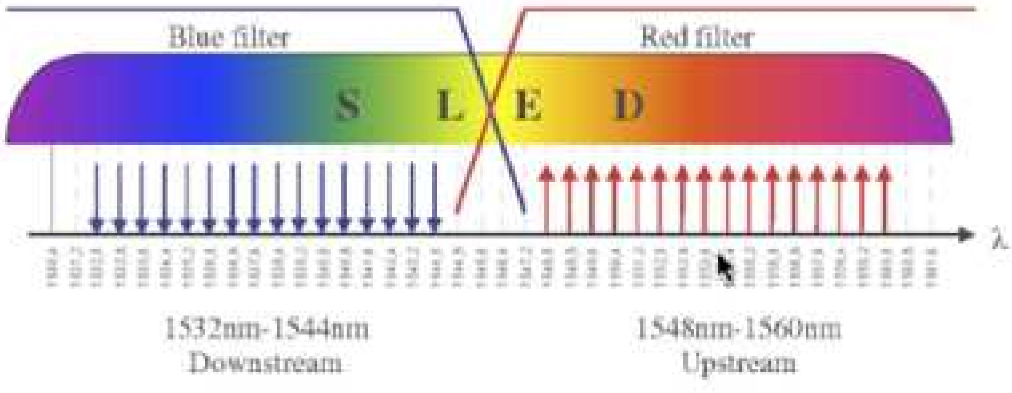

Figure 36; Implementation or red/blue filter in WDM-PON [83]

In the ONU a red/blue filter separates up and downstream wavelengths. The red signal is modulated by an R-SOA with upstream data, amplified and reflected in the input fibre. The downstream signal is detected by a photodiode. The SLED and R-SOA spectra are centered at 1550 nm and cover the C band. The red/blue filter provides 32 available wavelengths: 16 in the red part and 16 in the green part. The RSOA can operate with any of these wavelengths so it can be implemented in ONU as well as in OLT. It can also be modulated at 1.25 GHz and it has gain around 18 dB. Since RSOA was polarization-independent, polarization- independent AWG was used also. The prototype had spacing at 100 GHz to ensure enough wavelengths, and AWG had Gaussian-shaped filters spacing with 0.4 nm optical bandwidth.

The output optical power of SLED was 16 dBm at 500 mA current supply. Spectral density in C band was -17.5 dB/0.1nm. The optical power provided to RSOA was -20 dBm at the OLT and -25 dBm at ONU. This difference is caused by optical losses in 20 km optical fibre between OLT and ONU. The prototype achieved BER=10^{-10} for both upstream and downstream transmission when RSOA was provided with 4 Vpp modulation and 60 mA bias current.

Remote modulation scheme

The remote modulation scheme employs an optical modulator as the transmitter in each ONU to realize the colourless ONUs. Each ONU receives a continuous light wave with a unique center wavelength, modulates it, and sends it as the upstream signal. An optical amplifier may be employed to amplify the light wave before or after modulation. The upstream and downstream signals can be allocated in different wavelength bands; a wavelength divider is used to divide these two bands and so to separate the downstream signal to the photodiode and the continuous light wave (to be used for upstream transmission) in this case.

An alternative option is to reuse the downstream wavelength for upstream: a power divider is used instead of the wavelength divider in this case. Several ideas for the reuse of the downstream wavelength have been reported, such as the erasure of intensity modulation by SOA [90], and the use of phase modulation for downstream transmission [91].

Commercial prototype of 5 Gb/s WDM-PON with implemented remote modulation through RSOA was presented by the France Telecomm in 2007 [92]. The choice of RSOA as the modulating device was driven by number of RSOAs features such as:

- ON/OFF switching time is in the nanosecond range
- wide optical bandwidth (more than 60 nm) which can be centred in the range of 1200-1550 nm,
- low noise figure (NF) around 6 dB

The implemented RSOA consisted of a buried ridge stripe (BRS) of InGaAsP into InP, with one cleaved facet, the mirror, and one anti-reflection coated facet. In order to optimize the optical power which reduces carrier lifetime, while keeping the chip dimensions as low as possible, an optical confinement of 80 % was chosen. The fibre-to-fibre gain and noise figure (NF) versus optical input power are shown on figure 37 for a driving current of 73mA and a 4 Vpp (16 dBm) signal modulation. At 20°C, the saturation input power reached -20 dBm.

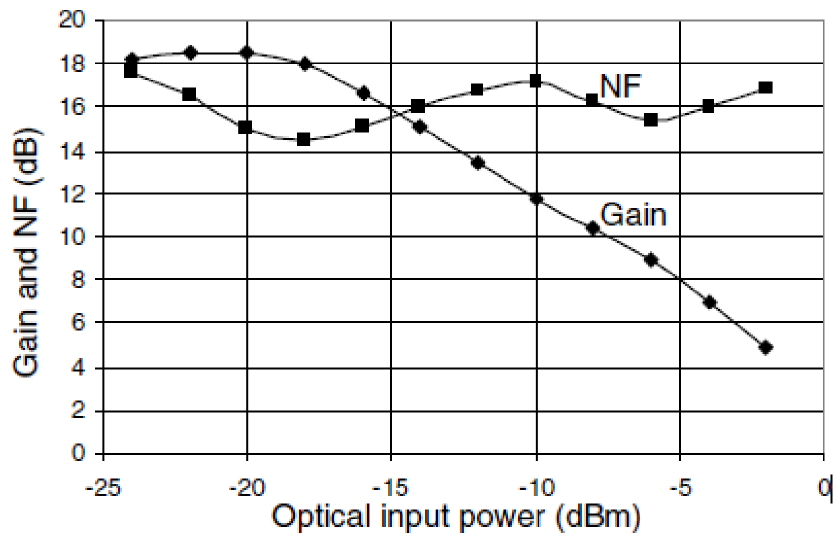

Figure 37; RSOA gain in WDM-PON [92]

Due to the high confinement factor, NF was about 16 dB [61]. The polarisation-dependent gain was around 1 dB. The RSOA modulation speed limitation was dominated by the RC time-constant due to the BRS structure in the absence of relaxation oscillation resonance [93]. The RSOA electro-optic response is shown in figure 38 with 100 mA driving current at 1508 nm in function of different optical input powers. The 3 dB electrical bandwidth was about 2 GHz.

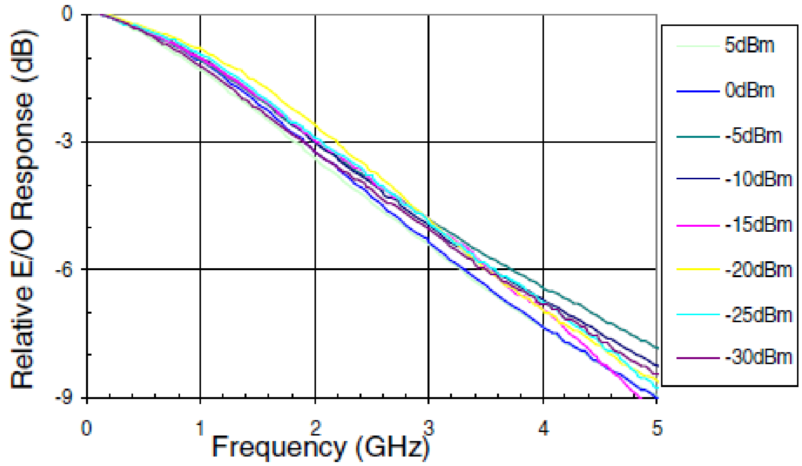

Figure 38; RSOA E/O response gain at 1508nm [92]

The PON prototype schematic is presented in figure 40. The upstream transmission is realized with a continuous wave (CW) light that is distributed from the CO to each ONU, modulated, amplified, and sent back to the CO. The evaluation of RSOA performance was carried out at 2.5 Gb/s and 5 Gbit/s.

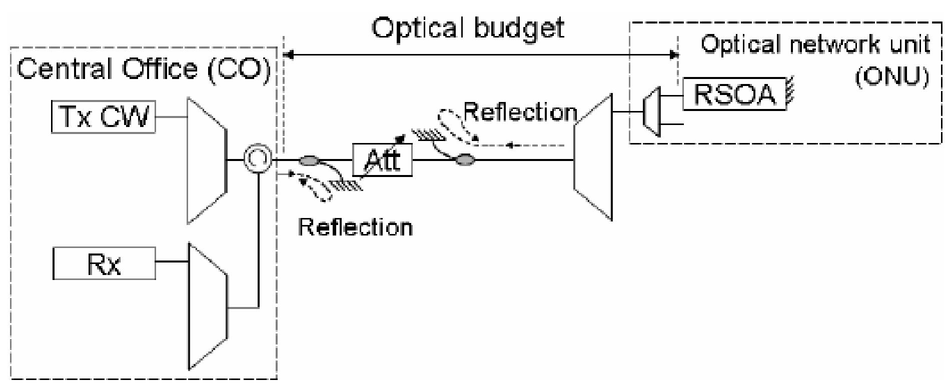

Figure 40; WDM-PON prototype with implemented remote modulation scheme [92]

The prototype took the effect of Rayleigh into account [93]. Because 5 Gb/s clock data recovery modules were not available at that time, and because jitter at the reception due to propagation through the fibre link would prevented efficient synchronisation, an optical attenuator was necessary to simulate the fibre link. Two reflectors were used to simulate Rayleigh backscattering in order to evaluate the upstream transmission penalties in a bidirectional scheme.

The reflected power was set to -32 dB, which corresponds to Rayleigh back-reflection for more than 20 km of standard single mode fibre (SMF). The RSOA was modulated with 27-1 pseudorandom binary sequences (PRBS) (similar to signal with 8B/10B coding) at 2.5 Gb/s and 5 Gb/s with 73 mA driving current and 4Vpp modulation amplitude. A Gaussian shaped AWG with 100 GHz channel spacing and

0.4 nm passband at -3 dB was also implemented in the prototype. Experimental results of 2.5 Gb/s BER measurements are presented at figure 41 with a 20 dB optical power budget. Figure 42 presents 5 Gb/s BER with 15 dB optical power budget.

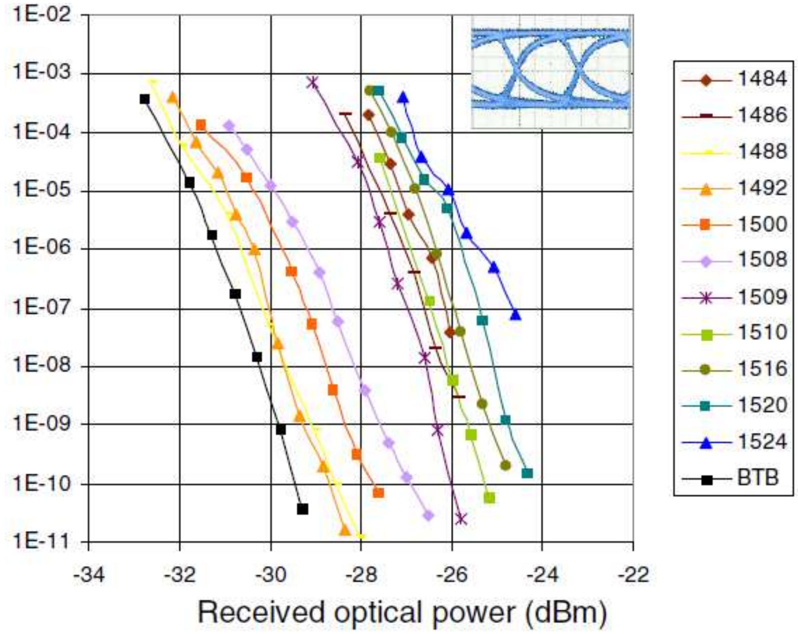

Figure 41; RSOA BER curves at 2.5 Gb/s when input optical power was -20 dBm [92]

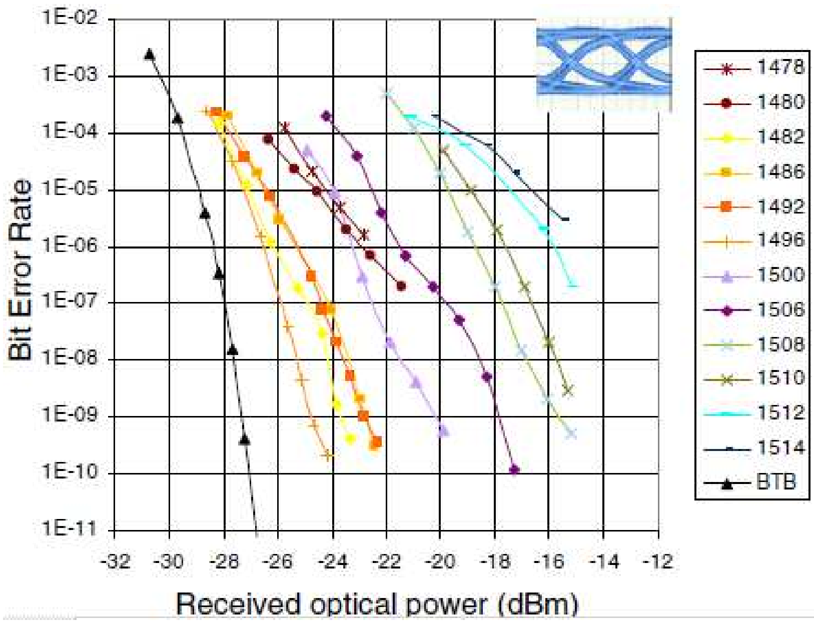

Figure 42; RSOA BER curves at 5 Gb/s when input optical power was -15 dBm [92]

The above experimental results show that 2.5 Gbit/s transmission was possible over a BER of 10^{-9} between 1488 nm and 1520 nm (32 nm bandwidth). The 5 Gbit/s transmission was possible between 1482 nm and 1510 nm (28 nm bandwidth). The sensitivity degradations at 10^{-9} BER of these two bit rates are shown in figure 43.

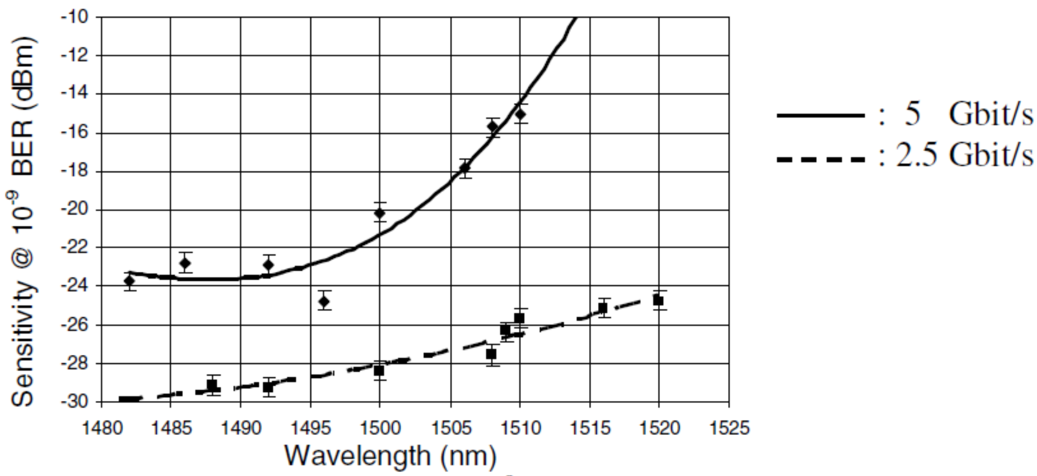

Figure 43; Optical receiver sensitivity at 10^{-9} BER [92]

The visible degradation was explained by the small extinction ratios of 5.7 dB and 3.7 dB at the different bit rates, by interference with Rayleigh backscattered light at reception and also by the evolution of the NF with the wavelength.

Wavelength tuning scheme

Employing a wavelength tunable laser in each ONU is one of the simplest ways to implement the colorless ONU. The key challenge is to realize a wavelength-tunable ONU that has reasonable cost for access network applications. There are number of research results published about possible ways of implementing low-cost wavelength-tunable devices; [94], [85]. The wavelength-tunable sources have already become popular in optical transmission systems for core networks. For example, a wavelength-tunable transponder yields a unified transponder inventory for several wavelength channels. To make those sources available for application in access networks further progress in cost reduction has to be achieved.

Interesting prototype of wavelength-tunable L-band DWDM-SFP transceiver was published in 2008 by NTT Corporation [94]. The transceiver was deployed together with the commercial PON over the same “Class B+” optical distribution network (ODN) that has a loss budget of 28 dB (Figure 44).

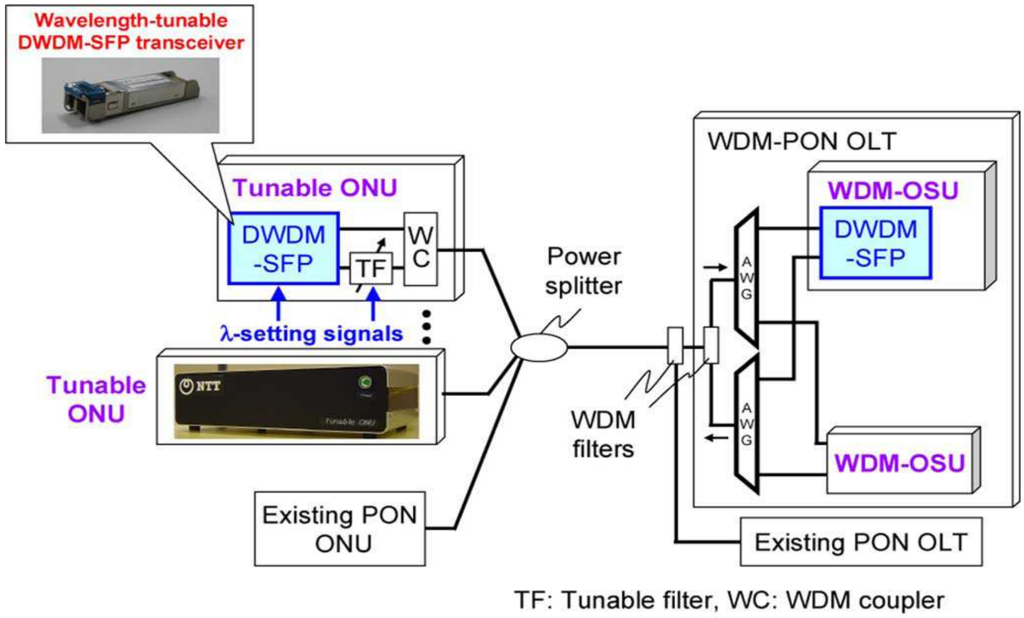

Figure 44; Colorless WDM-PON coexisting with commercial PON [94]

The commercial PON and the WDM-PON prototype were overlaid on the same ODN via a power splitter. The WDM-PON OLT consists of a WDM filter, arrayed waveguide gratings (AWGs), and multiple WDM optical subscriber units (WDM-OSUs), each of which communicates with each tunable ONU by assigning two specific wavelengths for the downstream and upstream. The deployed optical network unit (ONU), consisted of the prototype of wavelength-tunable DWDM-SFP transceiver, a tunable filter (TF) that selects a preassigned downstream signal, and a WDM coupler (WC) that divides/combines the upstream and downstream signals. The wavelength of the DWDM-SFP transceiver and the center passband of the tunable filter (TF) could be changed due to implementation of wavelength-setting signals. Storing a wavelength assignment table in the ONU could provide automatic wavelength setting. The wavelength assignment indicates combinations of corresponding downstream and upstream wavelengths.

Figure 45 show wavelength allocation that enables coexistence of the existing PON and colorless WDM-PON. The ITU-T G.983.3 standard defines the wavelength allocation that is implemented in B-PON, GE-PON, and G-PON**.** According to G.983.3, the upstream wavelengths of the existing PON systems vary from 1260 nm to 1360nm and downstream wavelengths vary from 1480 nm to 1500nm. Wavelengths that are provided for video transmission range from 1550 nm to 1560 nm. Therefore, the coexistence-type colorless WDM-PON uses the future-band defined in G.983.3 with DWDM technologies in order to utilize effectively a limited wavelength bandwidth and achieve the colorless ONU with a comparatively narrow tuning range. This wavelength band configuration ensures that there is no significant degradation due to the crosstalk between the existing PON and the WDM-PON.

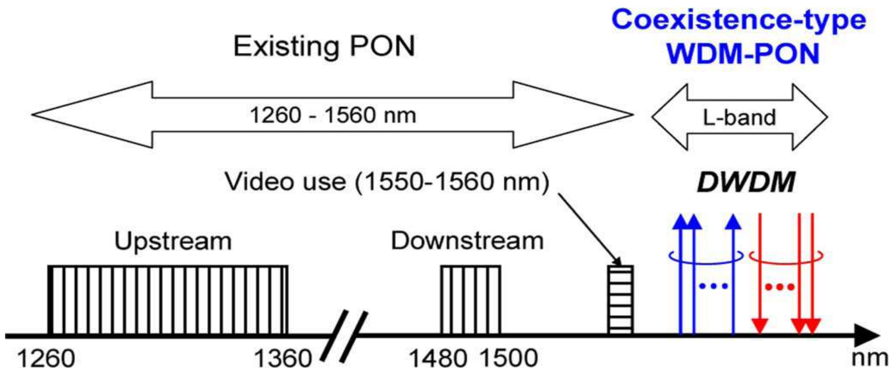

Figure 45; Wavelength allocation of coexistence-type colorless WDM-PON [94]

The main component of the prototype wavelength-tunable DWDM-SFP transceiver is a distributed feedback laser diode (DFB-LD) and an avalanche photodiode (APD). The prototype architecture is very similar to conventional DWDM-SFP transceiver, except the emission wavelength can be modified by externally changing the temperature of the DFB-LD. The temperature variation between 15°C and 50°C provides wavelength change across 350 GHz over the temperature change of 15°C–50°C.

Although this method does provide wavelength tuning it is not suitable for systems that require fast changes. The 350 GHz change takes 10seconds and it consumes 1.4W of power. The prototyped ONU achieved wavelength tuning range at 25°C in range of 1591.26nm to 1594.22 nm. This results in eight-channel tunability with 50 GHz of inter-channel spacing (Figure 46).

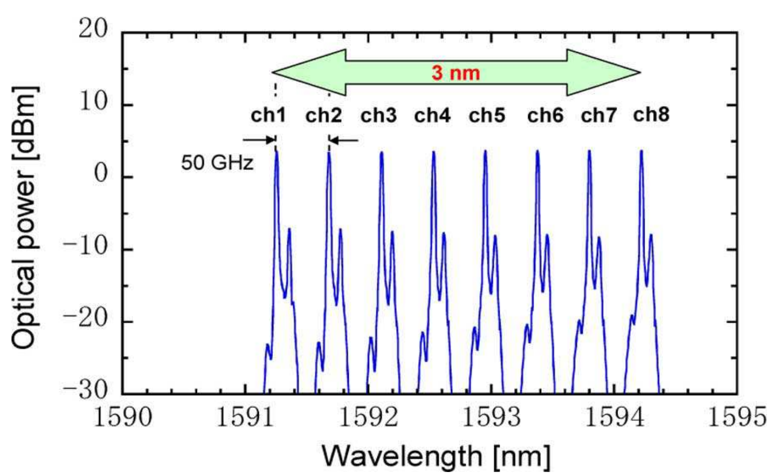

Figure 46; Tunability capabilities of prototype ONU at 25°C

The proposed prototype has wide spread variation of output optical power across relatively narrow optical spectrum. The highest peak of optical power (+5 dBm) was observed at 1591.25 nm while 1591.20 nm and 1591.31 nm and 1591.40 nm experienced minimum of -25 dBm and -20 dBm respectively (Figure 47).

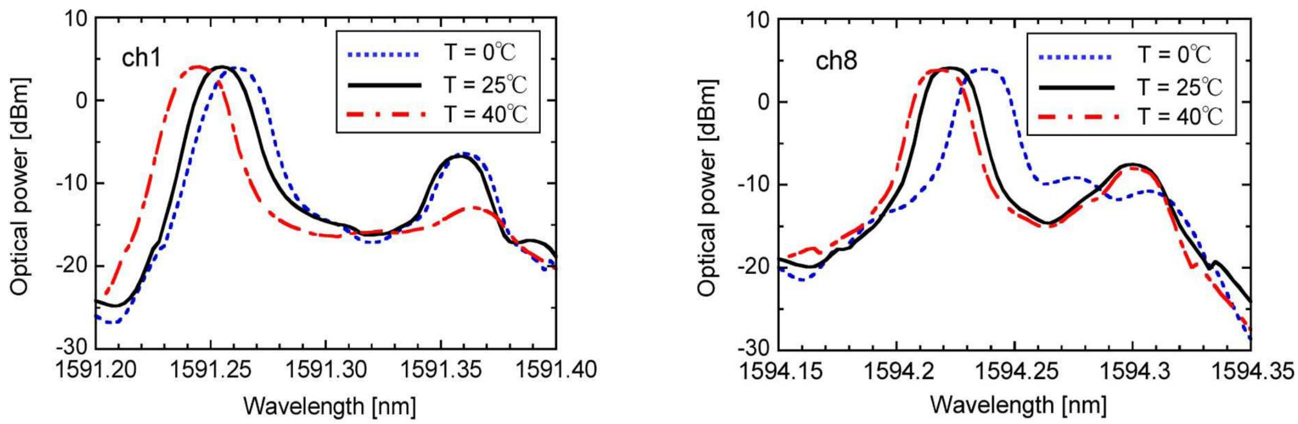

Figure 47; Output optical power across optical spectrum at the channel 1 and 8 [94]

Similar shape of power characteristics was observed at channel 8. In addition to this, the observed peaks of optical power experienced shift towards shorter wavelengths when temperature increased form 0°C to 40°C. The bit-error rate (BER) was examined for eight upstream signals at the channel spacing of 50 GHz and three chosen temperatures. The applied bit rate was 1.25 Gb/s and a pseudo random bit sequence (PRBS) was 2^7-1.

Neither significant dependence between wavelength and BER nor big dependence between temperature and BER were observed. There was a slight improvement of BER when temperature increased. BER in range of 10^{-12} was achieved when total received was greater then -32.1 dBm in all channels in the temperature range of 0°C to 40°C. The deviations in the optical output power from the tunable ONU prototype were below 0.02 nm in the temperature 0°C and 0.2 dB in the temperature 40°C.

The described prototype of 3nm wavelength-tunable DWDM-SFP transceiver is applicable in 1.25 Gb/s in the temperature range of 0°C to 40°C, which sufficiently meets the Class B+ ODN loss budget requirement of 28 dB.

Spectrum slicing scheme

Typical WDM-PON configuration with the implemented spectrum-slicing technology consists of super luminescent diode (SLD) or another source of lightwave with a broad optical spectrum. All ONUs deployed n PON do have the same SLD so all of the emit the same spectra.. The upstream lightwave is modulated with data and sent to the OLT via mux/demuxes. The optical spectrum that is sent from each ONU is sliced by the first mux/demux at different central wavelengths, and all upstream signals are thus WDM multiplexed in the feeder fiber. The example configuration of such architecture is presented on figure 48.

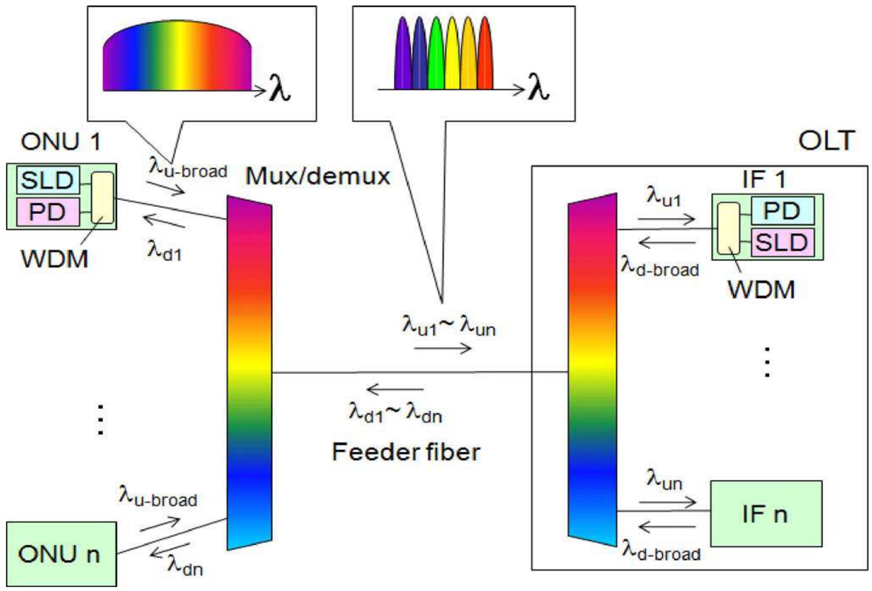

Figure 48; Example architecture of WDM-PON with spectrum-slicing technology [80]

According to [86] the signal-to-noise ratio (SNR) of the signal-signal beat noise is proportional to the ratio of the data rate to sliced bandwidth. Therefore, the sliced bandwidth must be increased to realize the high-speed operation. This will effect in decreasing the number of available channels if the light source has a fixed bandwidth. If the sliced bandwidth is increased then the fiber-dispersion penalty is higher. To counter balance this negative effect a forward error correction (FEC) may be applied in PON prototype.

There have been published number of research results, such as [95], indicating that use of FEC is an effective tool to increases the loss budget and the spectrum efficiency. According to that publication a 10Gb/s transmission was possible over 20km of dispersion-shifted fiber (DSF) in DWDM PON system with 200 GHz of the channel spacing. In addition to that, publication [96] presented that SOA can effectively reduce the intensity noise induced by the spectrum slicing in a WDM-PON with this scheme.

Spectrum efficiency and loss budget are not the only issues targeted in WDM-PON with implemented spectrum slicing techniques. Spectrum-sliced PONs that have implemented spectral filtering through multiplexers and demultiplexers suffer from increase in excess intensity noise (EIN). The increased EIN restricts data bandwidth when the spontaneous beat noise becomes dominant in the optical receiver. There were papers published in the past that proposed implementation of saturated SOA to counter balance EIN [97], unfortunately experimental results proved later that the optical spectrum of a gain-saturated SOA amplified spectrum-sliced ASE not only undergoes spectral distortion but is also broadened due to nonlinearities of the SOA.

Similar problems were reported by in a spectrum sliced WDM-PON with implemented C-band BLS and injection seeded RSOA. Although RSOA was considered as an effective EIN suppressor there was observed a significant increase of EIN due to distorted spectrum of a gain-saturated RSOA after it was filtered by mux/demux. Increased EIN deteriorated the signal-to-noise ratio (SNR) of the received signal.

There were published results of research [98] that suggest a new configuration of WDM-PON with spectrum sliced scheme. The new WDM-PON prototype had Gaussian passband AWG at the optical line terminal (OLT) replaced by a flat-top passband arrayed waveguide grating (AWG). This replacement was considered as a temporary solution since use of flat-top passband AWGs at the OLT and the remote node (RN) did not sufficiently reduce the EIN in the WDM-PON link.

In October 2010 there was published new interesting work on implementing pre-spectrum-sliced seed light (PS-SL) in WDM-PON with spectrum slicing scheme [99]. The goal of this work was to reduce the multiple spectral filtering effects at the multiplexer in OLT and the in remote node (RN). To achieve that goal the optical bandwidth per channel of the PS-SL was designed to be narrower than the optical passband of the implemented AWG.. This method led to effective suppression of EIN, although the spectrum of the R-SOA amplified signal was distorted. Consequently, error-free transmission was achieved for the 100 GHz spectrum sliced 1.25 Gb/s WDM-PON over a 20 km single mode fiber (SMF).

Figure 49 presents schematic diagram of proposed PS-SL configuration that consists of a bandpass filter (BPF), a gain-flattening filter (GFF), and a mirror (reflectivity is 99%), with a double-stage erbium-doped fiber amplifier (EDFA).

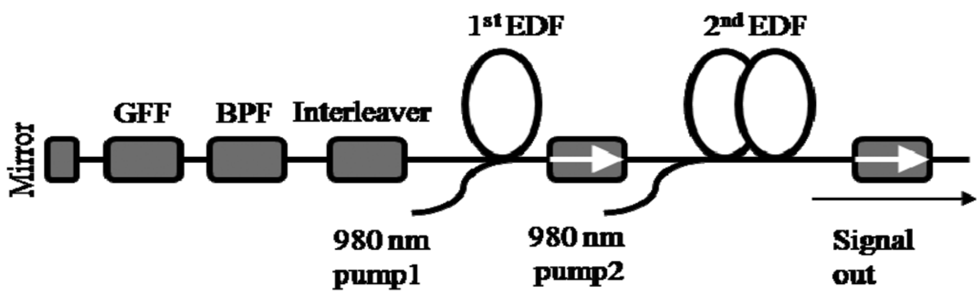

Figure 49; PS-SL configuration for WDM-PON [99]

The general idea of the proposed PS-SL is to reduce spectral filtering through applying an AWG with passband that is wider then the optical bandwidth of the signal. The PS-SL was build using a commercial off-the-shelf optical interleaver with a periodic, 100-GHz channel spacing and 40 GHz passband per channel. After spectral filtering through the interleaver, the spectrum sliced narrow-bandwidth backward ASE was injected into the BPF and the GFF. The transmission spectra of both BPF and GFF were designed to produce a flat output spectrum in the operating wavelength band from 1535.04 nm to 1559.79 nm. The reflected ASE from the mirror was acting as an input signal to the first-stage EDFA. To achieve optical output power greater then 21 dBm two 980 nm pump laser diodes of 180 mW and 280 mW were used.

The prototype of WDM-PON with implemented flat-top passband AWGs with 100-GHz channel spacing at the OLT and the RN is presented in figure 50.

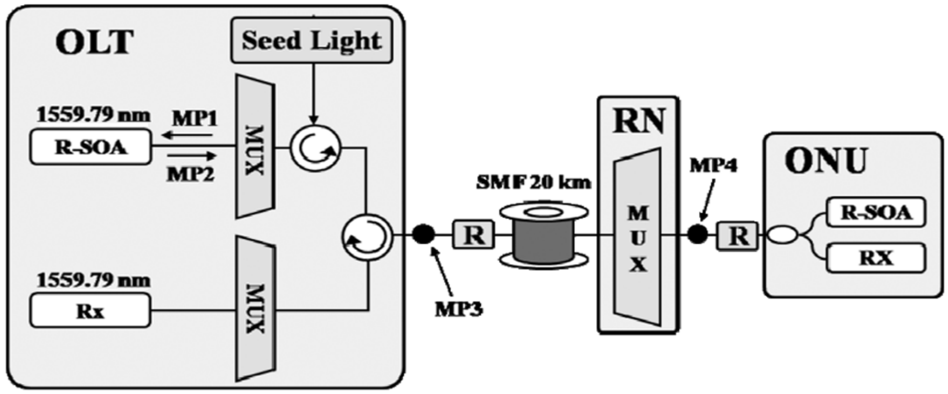

Figure 50; Prototype WDM-PON with flat-top passband AWG [99]

The RSOA transmitter should be operated in the deep saturated region to suppress EIN, therefore the injection power to the RSOA was maintained at around 3 dBm at the OLT. The gain of RSOA was 10 dBm and the total insertion loss of the AWG and optical circulators was 7 dB. The 0 dBm of downstream signal was used as an input to a 20 km SMF through the multiplexer at OLT. After the 20 km transmission, the downstream signal was demultiplexed by the AWG at the remote node (RN) and inserted into an optical network unit (ONU) transceiver. The ONU transceiver consisted of a 50:50 optical power splitter, an RSOA based transmitter, and a p-i-n photodiode receiver. Feed-forward current injection (FFCI) was utilized to eliminate downstream data on the upstream signal to the ONU transceiver.

The PON prototype has been tested in four different measurements points (MP) for changes in spectrum of the transmitted optical signal. The comparison between measured spectra in different points is presented on figure 51. The marked points indicate the spectrum-sliced ASE (MP1), and the output spectrum of the RSOA (MP2), the multiplexer in OLT (MP3), and the RN (MP4). To keep the consistent experimental condition, the injection power was always adjusted to -3 dBm in all cases. The output spectrum of the RSOA was spectrally broadened and asymmetrically shaped due to nonlinearities of gain-saturated RSOA. Spectral broadening of the RSOA amplified spectrum-sliced ASE was caused by intensity fluctuations of the spectrum-sliced ASE. Intensity fluctuations of the spectrum-sliced ASE resulted in carrier density fluctuations in the RSOA, which modulated the phase of the signal.

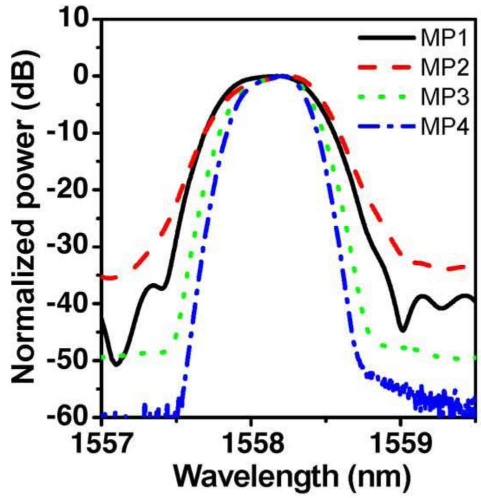

Figure 51; Changes of the optical spectrum in prototype WDM-PON [99]

Multiple spectral filtering steps at the multiplexer in the OLT and the RN caused variations in the spectral components between the output spectra of the RSOA (MP2) and the RN (MP4). Consequently, the EIN was increased by multiple spectral filtering steps, which reduces optical frequency components in the signal, and was visible in the optical eye diagrams (Figure 52).

a) 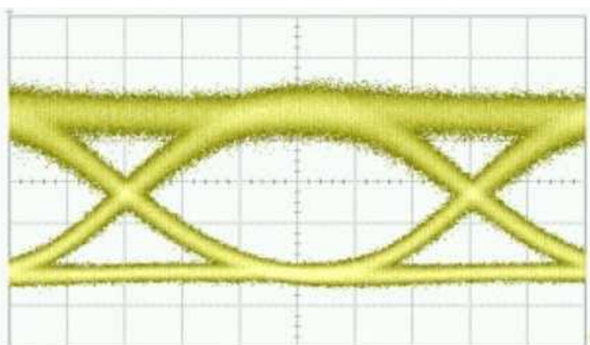 b) 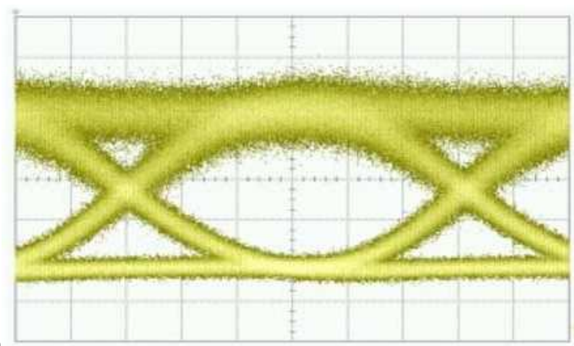

Figure 52; Impact of EIN on eye diagram. Back-to-back configuration (a) and after 20km transmission and the RN (b) [99]

PON prototype was also tested for BER and power penalty. The results of BER after 20-km transmission and the RN, along with the BER for the back-to-back configuration are presented in figure 53. Error floor was observed in the case of BLS seeding. However, in all cases of PS-SL seeding, the BER curves were well behaved with no indication of error floors.

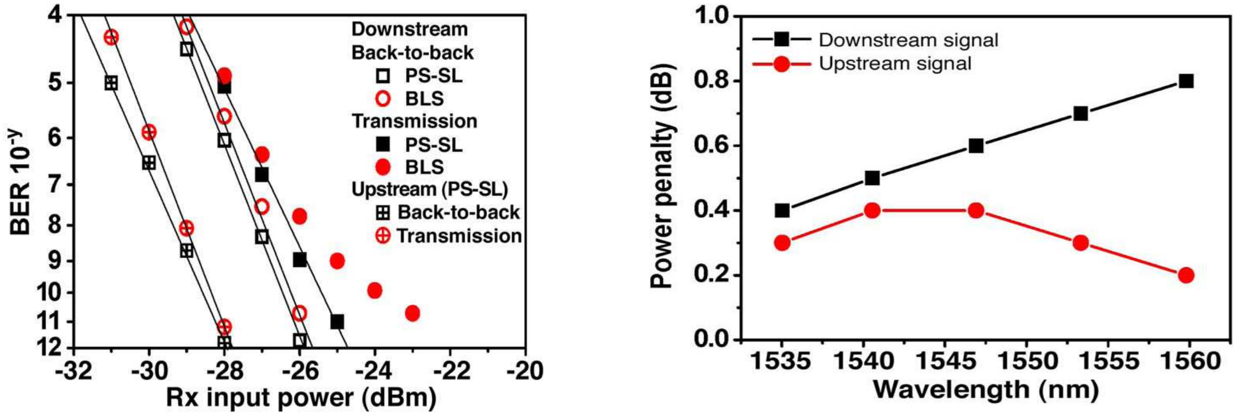

Figure 53; BER performance and power penalties at channels: 1, 8, 16, 24, 32 after 20-km transmission and the RN [99]

Success of this particular PON prototype proved that by using narrow-bandwidth PS-SL used with flat-top passband AWG the SNR degradation due to spectral filtering is efficiently suppressed in a spectrum-sliced WDM-PON.

Multiplexing and demultiplexing components

Another important component for the WDM-PON development are optical multiplexing and demultiplexing components. Mux/demux devices are usually deployed outdoors in remoter nodes in locations near by end user facilities. Remote node is usually exposed to temperature fluctuations, humidity and other harsh conditions of environment for example: temperatures in Canada can vary from -35°C in Winter to +30°C in Summer and humidity can vary from 10% to 80% therefore remote node and its internal components should have much higher tolerance for external environmental conditions than any indoor equipment.

Ideally multiplexing device should be completely passive because placing an active device outdoors greatly increases operational costs, and sometimes it is difficult to supply power to the device. To satisfy environmental condition requirements, athermal arrayed waveguide gratings [100] and thin-film-based WDM filters can be implemented in WDM-PON applications. The athermal AWG prototype built by NTT Corporation exhibits stable wavelength center in temperature range -5°C to 65°C (Figure 54).

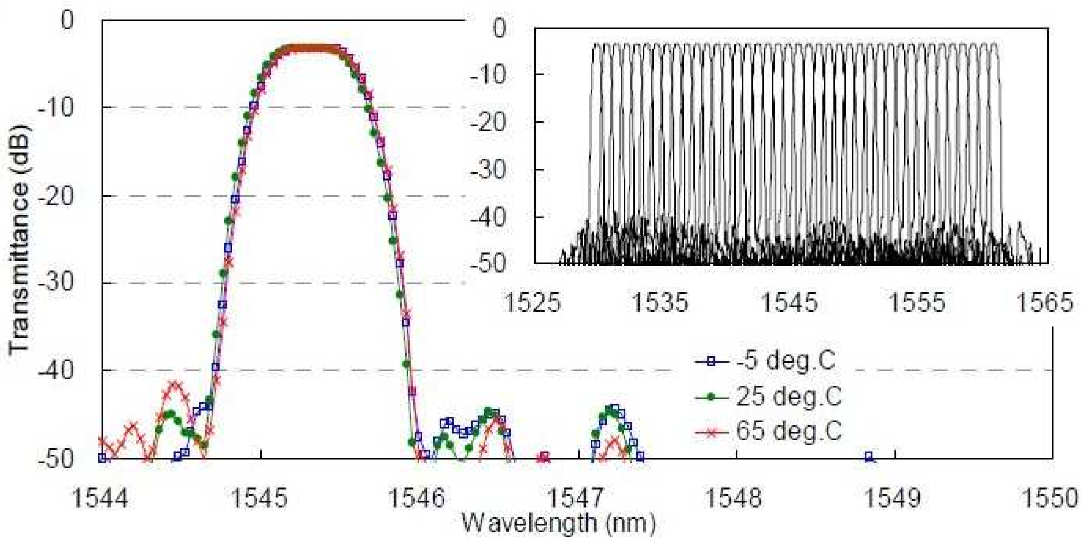

Figure 54; Athermal AWG: transmission spectra at center channel (measured at different temperatures) and all 40 channels measured at 25°C [100]

Although this prototype is a very promising device, more work is required to obtain AWG that can work in lower temperatures to make it suitable for Canadian Winter conditions. There is no requirement to use either an optical coupler/splitter or an optical switch between ONUs and OLT for path protection [101] because AWG provides wavelength-routing functionality.

10G WDM-PON architecture

Although work on standardization of 10G-EPON was completed by the IEEE802.3av Task Force in 2009 there is already growing interest in this standard. Because of high costs of components required for 10G-PON, very limited number of successful commercial deployments has been reported. Significant capital investments have been provided by telecommunication industry towards deployment of EPON and GPON infrastructure during last three to ten years therefore replacement of existing infrastructure with new 10G-PON may not be economically justified.

Amount of capital investment required to implement 10G-PON is a soft spot of this technology therefore an increasing interest in deploying in future 10G-PON over the existing PON infrastructure is observed. To achieve that new generation 10G-PON has to be down-compatible with already existing commercial PONs and WDM-PONs that have data rate below 10 Gb/s.

The first successful prototype of 10G-EPON that is compatible with commercial 1G EPON was reported by Mitsubishi Electric Corporation at the NFOEC conference in 2010 [102]. The prototype consisted of dual-rate burst-mode transceivers that ensured the new prototype is compatible with both 10G-EPON and 1G-EPON infrastructure. The implemented 10G/1G dual-rate burst-mode transceiver incorporated a dual-rate burst-mode optical receiver and 82GS/s sampling CDR to fully compliant with IEEE802.3av 10G-EPON standards. In addition, the burst-mode receiver (compatible with 10.3 Gb/s and 1.25 Gb/s) had sensitivity -35.6 dBm at the BER 10^{-12}.

The configuration of a 10G/1G dual-rate burst-mode 3R receiver for 10G-EPON OLT prototype is presented in figure 55. The dual-rate burst-mode 3R receiver consisted of a burst-mode optical receiver and an 82.5 GS/s sampling CDR. The received 10.3 Gb/s and 1.25 Gb/s burst optical packets had different power levels and arbitrary phases, so the packet powers were normalized by amplifying each at an appropriate gain and regenerating them at the proper threshold level in a burst-mode optical receiver. IN addition, 82.5 GS/s sampling CDR retimed the regenerated packets from the burst-mode optical receiver, which still had arbitrary phases, to align the phases of the packets.

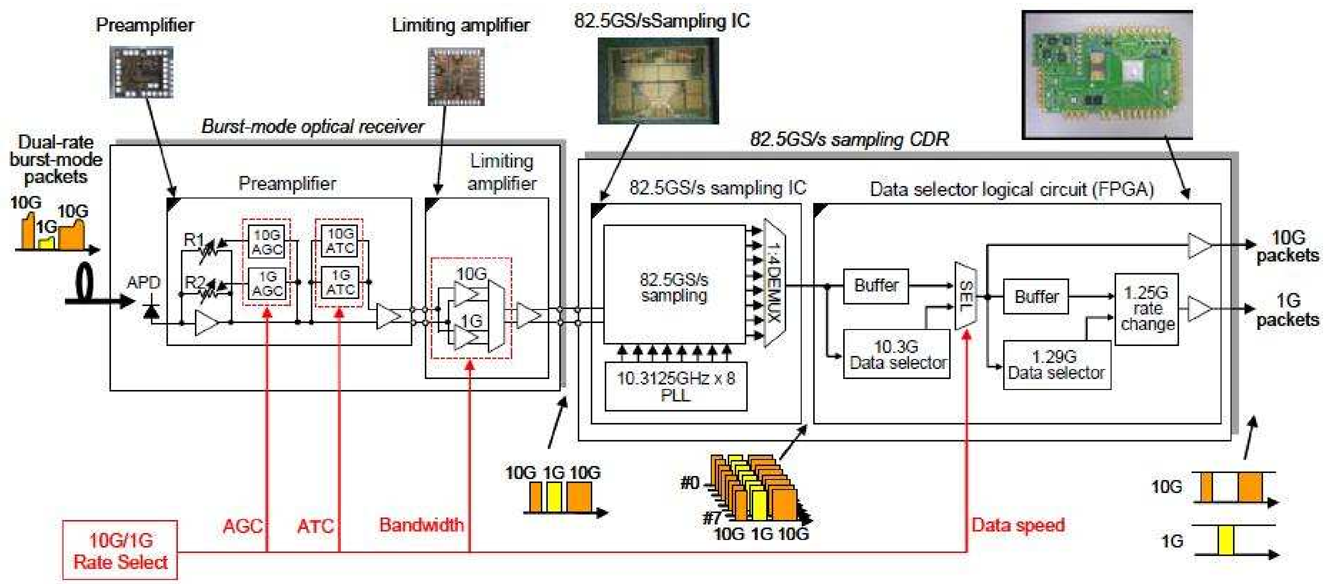

Figure 55; Prototype of the 10G/1G dual-rate burst-mode receiver [102]

To achieve the receiver sensitivity specified in IEEE802.3av standard the burst-mode optical receiver employed a dual-rate APD-preamplifier and a dual-rate limiting amplifier, which could switch both of their gain and bandwidth optimized for 10.3 Gb/s and 1.25 Gb/s packets. Preamplifier and the limiting amplifier (photos shown in figure 35) were fabricated in 0.13 μm SiGe BiCMOS process technology.

The multiplication factor of APD was set to eight. Its maximum transimpedance gains were as following: 66dBΩ at frequency 6.4 GHz for 10G operation and 86 dBΩ with frequency 0.95 GHz for 1G operation. The preamplifier for APD had implemented an Automatic Gain Control (AGC) and an Automatic Threshold Control (ATC) function to achieve the wide burst dynamic range, which enabled it to vary its gain continuously to compensate both the received powers and the unspecified transient responses of the burst packets from both of 10G-EPON ONUs and GE-PON ONUs. In addition, the AGC and ATC response time were measured as 800ns for 10.3 Gb/s and 400ns for 1.25 Gb/s operation, therefore they did fulfill requirement of receiver settling time specified in IEEE802.3av.

To evaluate BER of the dual rate receiver in the prototype PON, 10G-EPON ONU burst-mode transmitters and GE-PON ONU burst-mode transmitters were used, which satisfy requirements of the IEEE802.3av standard. The BER 10^{-12} was achieved at 1.25 Gb/s operation with -35 dBm received optical power and 10 Gb/s with -25 dBm received optical power (Figure 56).

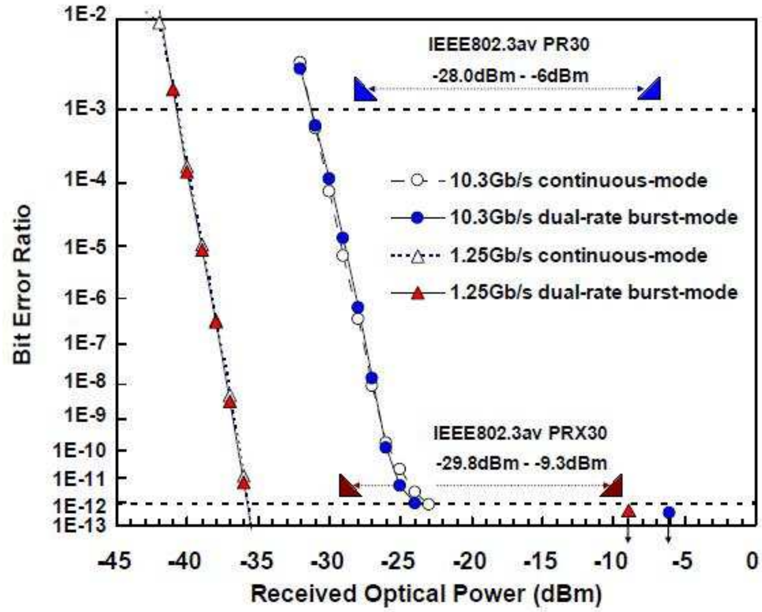

Figure 56; BER of the dual rate receiver prototype [102]

The dual rate burst receiver was integrated with 1G and 10G transmitters on XFP-E size package that was mounted on 82.5 GS/s sampling CDR FPGA development board (Figure 57).

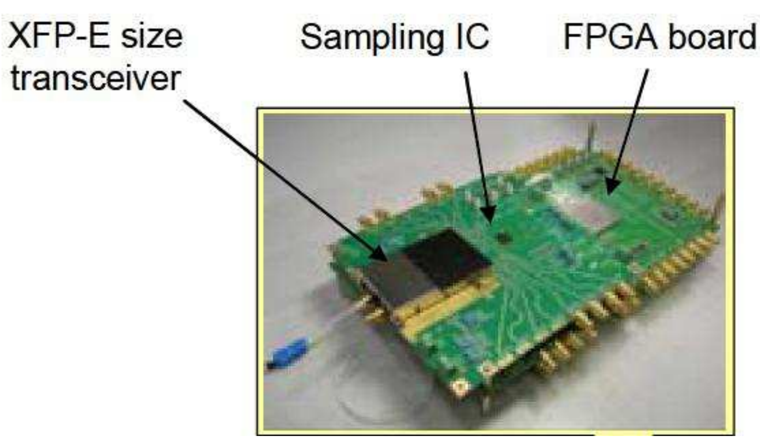

Figure 57; Dual-range transceiver prototype [102]

Light sources were cooled 10G EA-LD with the wavelength of 1577.2 nm and optical power +3.6 dBm and an uncooled 1G DFB-LD with the wavelength of 1491.2nm and optical power +5.3 dBm. For ONU side, two 10G-ONUs, a 1G-ONU, and a multiple LLID 1G-ONU which emulated virtual 29 uplink were used. SMF of 20km and 10km were inserted into one 10G ONU and one 1G ONU branch, respectively (fig 58).

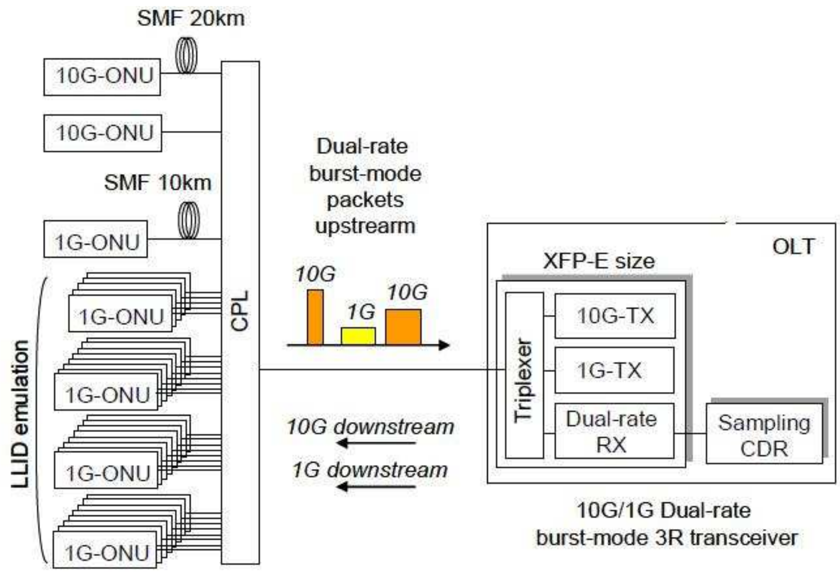

Figure 58; Dual-range PON prototype [102]

The prototype system throughput was tested by Ethernet random frames at 10 Gb/s and 1 Gb/s upstream. The observed throughputs were 218.8 Mbps with synctime of 1200 ns and FEC overhead (10 G) and 24.3 Mbps with synctime of 800 ns (1G). When downstream transmission was evaluated, 10 Gb/s and 1 Gb/s downstream throughputs were 8.56Gbps with FEC fields and 982 Mbps were recorded respectively. The observed loss budget was 33.5 dB for 10G-EPON and GE-PON was successfully achieved without Ethernet frame loss.

This successful prototype presented by Mitsubishi Corp. shows a possible path where development of 10G-PON may follow to ensure new generation PON will be compatible with existing 1G PON infrastructures and therefore capital expenses of deployment will be significantly limited.

Traffic distribution analysis in access network

This chapter presents a study of the traffic distribution in commercial access networks. The study is innovative because it incorporates observation of real-time data flow in commercial infrastructure rather than only simulating the traffic flow behavior based on theoretical models. In addition the innovative element of this study is using commercial Ethernet LAN infrastructure that consist approximately 200 end-user workstations. Although Ethernet LAN has different architecture than PON, it can be used to model bi-directional traffic flow that will be generated in near future by consumers in access networks with deployed new services such as video teleconferencing or online gaming. To perform traffic observation software based traffic analyzer was built. This analyzer has innovative design because it is a low cost flexible device built on PC based platform that supports both optical Ethernet and copper Ethernet interfaces. The analyzer implemented software that monitors the traffic flow and performs real-time analysis of IP packets and Ethernet frames based on custom predefined characteristics such as packets (frames) length, type, destination and source address, content, frequency of appearance and type of the communication protocol. The study results aided the understanding of the nature of the traffic flow in commercial local access networks.

Traffic characteristics have to be studied in detail to better understand how network devices should be designed, how well they will be utilized and what will be the most probable network throughput. There are a number of works published about theoretical modeling of the Internet traffic flow such as [103], [104] and a number of methods for the traffic simulation were proposed, for example [105] and [106]. The most common parameters that are considered when a model of the IP traffic is developed are: packets inter-arrival time, IP addresses carried by packets, transport protocols distribution, frame sizes, destination and source port numbers and carrier link utilization.

One of the simplest approaches of finding the inter-arrival process of the network is to check if the packets arrival per second in the network can be described by a regular Poisson process. Research suggests that although some of the complexities in data traffic can not be explained by Poisson when looked at separately, the aggregated traffic might still be Poisson distributed. If the traffic is indeed distributed in a Poisson manner, the inter-arrival times will be independent of each other. It can be verified if this is the case, by finding and plotting the autocorrelation of inter-arrival times. If they are indeed independent, the autocorrelation value should be close to zero. This way it is possible to check if the observed inter-arrival times on the network is independent, and compare it to the generated traffic.

IP addresses distribution and its dynamics can also be used to model the network traffic. This method requires the assumption that the number of IP addresses in a network increases over time, as packets from new IP addresses arrive and depart. The numbers of IP addresses going through the link during a certain time period can then be compared to how much traffic there is at that specific time period. This information can then be used to model the network traffic flow. The cumulative development of new IPs from the start of the trace can be plotted as a function of time. This can be done both for the observed and the generated traffic, and the results can be compared.

Network traffic can also be modeled through the study of packet types that are received or generated. The packets can be classified into three classes: *TCP*, *UDP* and *Other*. Intuitively, the protocol of a previous packet influences the probability of the protocol for the next packet. A simple way to model this behavior is by predicting the probability of the next packet given the current packet. This method requires the assumption that there is a correlation between the packets.

Another approach to model the network traffic is to study the distribution of Ethernet packets size. Since Ethernet is a dominate technology in access networks, its characteristics can be used to model the traffic characteristics. Discrete probability distribution of Ethernet frames can be created by retrieving the frame size of each packet and grouping the observations together. The minimum size of an Ethernet frame is 64 bytes and maximum size is 1518 bytes, therefore the frame sizes can be grouped into different groups according to size. The probability of a packet belonging to one group can then be easily found by looping through the list of all frames, and assigning their frame size to one of the groups. The number of frames in a group should to be normalized with the total number of frames to find the probability. The distribution of observed and generated frame sizes can be plotted in a histogram and compared.

One of lesser known methods of network traffic modeling is to observe specific port numbers that indicate the type of sent and received packets. The port numbers are used to identify the applications which generate the flows and therefore the content of the traffic. In most cases, port numbers can be grouped into four sets: *Well known* (ports: 0-1023), *Registered* (ports: 1024-49151), *Dynamic* (ports: 49152-65535) or *Other* (a non IP packet). The number of packets that come to certain port is counted during a specified period of time. With the knowledge of the source and destination ports of each packet in the trace, a probability distribution can be estimated. In addition, based on whether the last packet is *Well-known*, *Registered*, *Dynamic* or other, the probabilities for the next packet can be calculated.

Network traffic can also be modeled through career link utilization. To model the utilization parameter, information about the number of frames in a link over a certain period of time and the frame sizes are required. The usual approach is to use the number of frames per second parameter and a frame size parameter. With the distributions of these two parameters, the utilization of the network is evaluated. By multiplying the average size of a frame with the number of frames per second will give the amount of data (in bytes) sent per second and the percentage of the available bandwidth it consumed

Although there are a number of methods proposed to model and simulate traffic flow in access networks there has been little work done on the analysis of real traffic that is being captured in a live network over a longer period of time. Theoretical simulations and traffic modeling may not guarantee a full view of the data flow in an access network. Therefore, study of real traffic flow in a live network is recommended.

To analyze and better understand the real nature of traffic transmitted in a typical access network infrastructure and furthermore to evaluate challenges faced by PONs regarding the structure of the traffic flow, a traffic monitoring system was designed, built and deployed in Ethernet LAN. The monitoring LAN chosen was the 100 Mb/s on-campus Ethernet network at the University of Ottawa. This network is a good example of a heavy loaded communication infrastructure that transports traffic for number of different services.

The custom network node was designed and built to be able to monitor and analyze the traffic flow in real time without affecting the analyzed flow in any way. The foundation for the node design was a personal computer (PC) with an Intel Pentium VI processor and 1 GB RAM. This computer was equipped with a fast Ethernet interface that supports up to 1 Gb/s data rate and a 100 GB hard drive to provide enough space to store the captured information about monitored traffic. The recorded information was later used to perform post-processing data analysis that did not require any real-time monitoring activities.

The software engine of the node was a Linux Mandrake 2009 operating system with a significantly modified kernel. The kernel modifications included the removal of unused libraries to decrease the overall size of the kernel and its memory footprint in addition to improving its processing speed. The modified kernel was recompiled with specific options to ensure its optimization for the Intel processor that was used in the node. Further modifications consisted of disabling network services and system services that were not critical for the system functionality (such as FTP service, web service, printing service, etc…).

The monitoring node had a modular architecture that offered high flexibility in configuration, which allows it to be easily optimized for monitoring any type of traffic that flows in Ethernet LAN if equipped in Ethernet NIC or any other network type and if equipped with appropriate network interface such as ATM, FDDI or SAN. The detailed architecture of the node is presented in figure 59

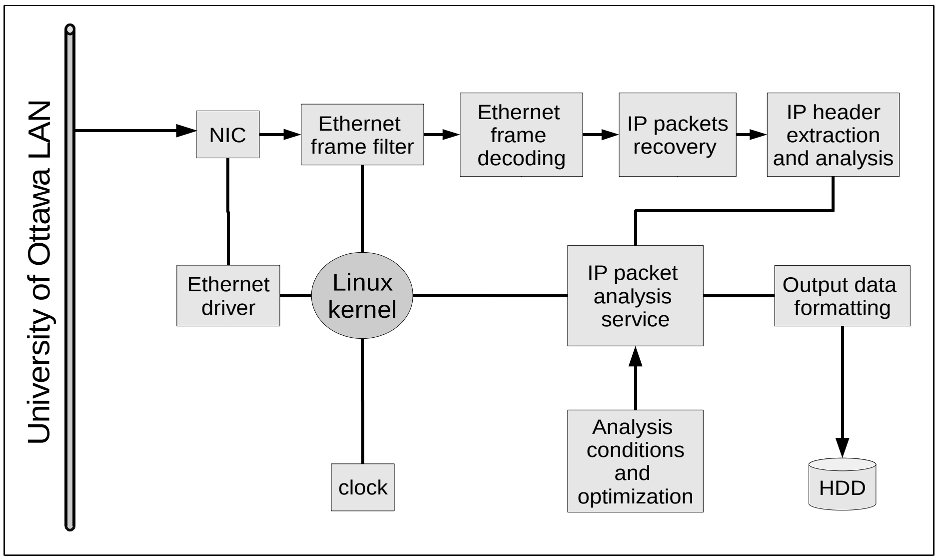

Figure 59: Architecture of the monitoring node

The monitoring node was connected to LAN at the School for Electrical Engineering and Computer Science (University of Ottawa campus) through the network interface card (NIC). Collected Ethernet frames were filtered by the Ethernet frame filter to reject erroneous frames. The frames were then decoded and IP packets were extracted. The custom built IP packet processing service performed analysis of packet type and header content. Detailed information about each packet such as: type, size, content, time stamp, source and destination addresses were collected (by the *Ethereal* tool) and saved in a table format on the hard drive (HDD). The node had also implemented services for real time monitoring system components such as network interface load, cpu load, HDD load and memory usage.

The process of network monitoring was run during a week day and lasted twelve hours. The total number of analyzed packets was approximately four million. Figure 60 shows the packet size statistics of the traffic captured by the monitoring node. The graph does not include locally broadcasted ARP packets, which were filtered out by the Linux. It can be easily observed that most of the Internet traffic is transported in packets sizes between 55 bytes and 700 bytes with a high density of packets between 60 bytes and 380 bytes. Only a small number of packets are larger than 750 bytes and almost no packets are larger than 1100 bytes (the packet size axis was cut at 1100 bytes for clarity).

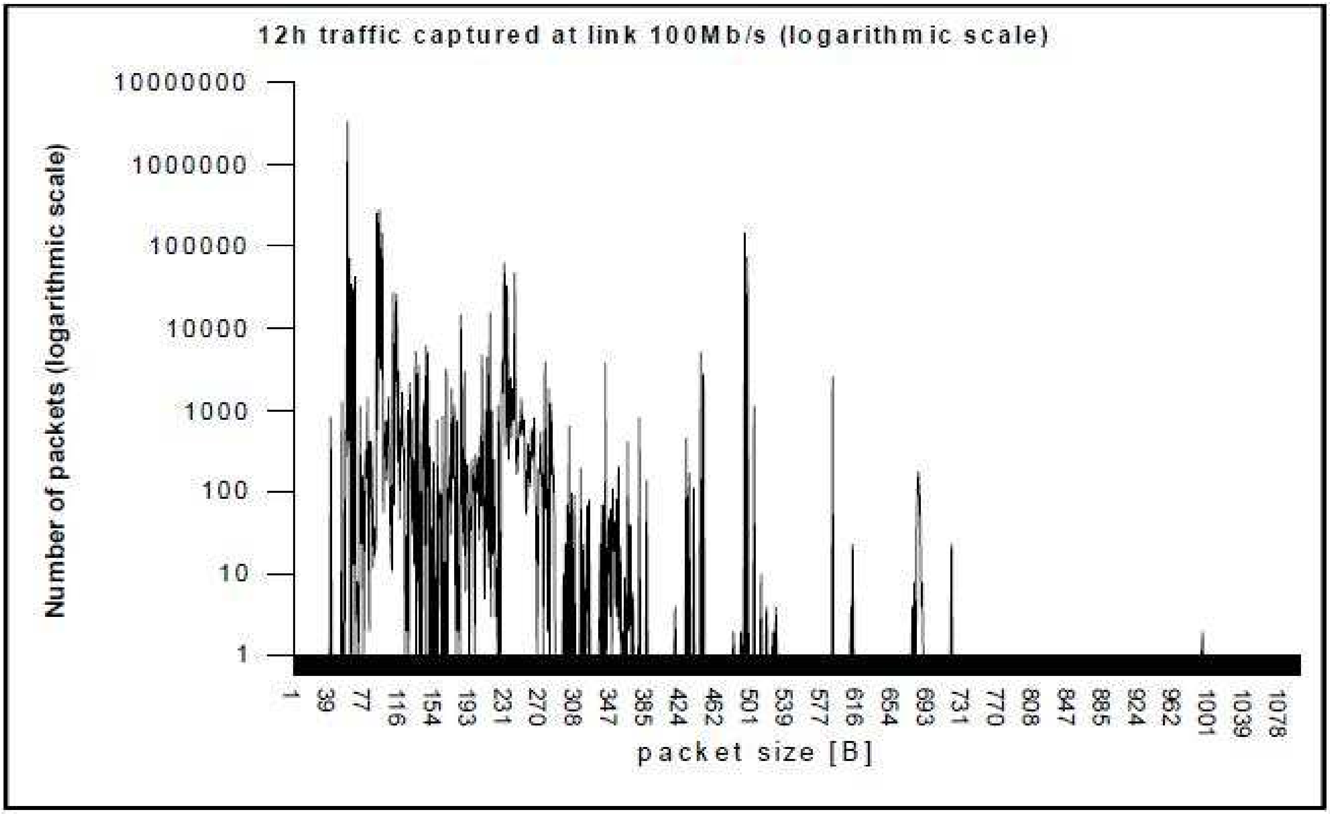

Figure 60: Traffic statistics over period of 12h in 100Mb/s LAN

One of the ways to improve the performance of existing PON infrastructure is to improve the utilization of the existing bandwidth with minimal costs of capital expenses required to implement modifications. As previously mentioned, ITU GPON standard does allow for packet fragmentation while IEEE EPON standard does not implement packet fragmentation [107] therefore GPON would certainly be able to better utilize space in the PON frame.

Unfortunately things become more complicated when GPON and EPON frame encapsulation methods are compared. GPON employs the GPON Encapsulation Method (GEM) [108] to enable packet fragmentation. This method uses a complicated algorithm to delineate variable-size GEM segments and reconstruct the packets at the receiving device. EPON standard implements the Ethernet framing format, which carries variable-length packets without fragmentation. This method is easier to implement, as it has a lower cost of implementation (when compared to GPON) and its operational costs are also lower, mainly because Ethernet frame format is well known and it has been widely used for many years in Ethernet copper LAN infrastructure; 10Mb, 100Mb and 1Gb.

Since EPON is built on very strong foundation of existing Ethernet technologies, it is usually preferred by network vendors over the GPON which requires expensive GEM encapsulation methods.

A possible method of improving utilization of bandwidth in existing PON infrastructure would be to apply modifications in encapsulation techniques to make them suitable for packet fragmentation but at the same time keeping those techniques within the well known frame of Ethernet technology. Such modification would certainly require relatively inexpensive changes in encapsulation algorithms on a both sides of the PON link: in ONU and in OLT.

Studies of different encapsulation methods in access networks are presented in chapter 6 and proposition of inexpensive modifications to the ONUs and OLT are presented with regards to information collected on real traffic flow in Ethernet LAN.

Modification of the encapsulation model in access network

This chapter proposes applying in PON a similar architecture to the one implemented in the Agile All-Photnic Network (AAPN). The similarities between PON and AAPN are explored and potential advantages of those similarities are described. The software based data encapsulating system was designed and implemented in a low cost PC-based platform that incorporates a number of technologies used before in AAPN. The encapsulating systems had implemented multiple buffers for input and output queues that stores incoming and outgoing traffic. The system also implemented traffic aggregation and slot assembling functionality that was optimized for commercially available low cost computer processors.

The chapter presents also results of the node benchmark tests and evaluates potential application of low cost off-the-shelf components in network devices. The encapsulation system was taken under the stress test to evaluate its performance under traffic load that was identical to the traffic observed and studied in chapter 5.

The chapter also presents an innovative prototype of an ‘optical’ switch that is built from off-the-shelf PC-based components and it offers full compatibility with IP, Ethernet IEEE 802.3 and MPLS. The performance evaluation of the switch working with 1 Gb/s optical network infrastructure is presented and available paths for upgrade of the switch to 10 Gb/s are described. The possible methods of upgrading the switch to 40 Gb/s and beyond are also discussed and potential drawbacks of this architecture are listed

A possible way to improve the performance of existing PONs without significant capital investments is to simplify the data encapsulation techniques in both ONU and OLT. In this way, implementing cheaper and less complex processing devices in PONs becomes feasible and the overall cost of the device will become lower.

Before any changes in the encapsulation model can be proposed, several PONs characteristics should be reviewed to understand the strengths and weaknesses of the existing PON infrastructure. The following features will be reviewed here: frame structure in PON, burst-mode characteristics of the transmitted traffic, agility of the network and its transparency for transmitted data.

Data encapsulation in PON

How the data is encapsulated into frames or time slots in PON is one of the factors that decide the efficiency of the optical link utilization and the operational cost of the optical infrastructure. Although IEEE and ITU standards of PON implement different methods of data encapsulation, they both require data segmentation in upstream and downstream links since IP packets have different lengths.

Both BPON and GPON architectures were conceived by the FSAN group, which is driven by major incumbent telecommunications operators. Most of the operators are heavily invested in providing legacy TDM services. Accordingly, both BPON and GPON are optimized for TDM traffic and rely on framing structures with very strict timing and synchronization requirements. In BPON, an upstream frame consists of 53 time slots, where each time slot is comprised of one ATM cell and 3 bytes of overhead. When two consecutive times slots are given to different ONUs, these 3 bytes, or approximately 154ns of the overhead, should be sufficient to shut down the laser in the first ONU, turn it on in the second ONU, and perform gain adjustment and clock synchronization at the OLT.

Similarly, very strict timing is specified for GPON, where only 16 bit (less than 13ns) are allocated for the laser-on and laser-off times at 1.244 Gb/s line rate. Such short intervals require more expensive, higher-speed laser drivers at the ONU. A very tight bound of 44 bit times (less than 36ns) is allotted for the gain control and clock recovery.

To reduce the range of necessary gain adjustment, BPON and GPON perform a power-leveling operation in which the OLT instructs individual ONUs to adjust their transmitting power, so that the level of signals received at the OLT from different ONUs are approximately equal.

In EPON, the main emphasis was placed on preserving the architectural model of Ethernet. No explicit framing structure exists in EPON; the Ethernet frames are transmitted in bursts with a standard inter-frame spacing. The burst sizes and physical layer overhead are large in EPON. For example, the maximum Automatic Gain Control (AGC) interval is set to 400ns [107], which provides enough time to the OLT to adjust gain without ONUs performing the power-leveling operation. As a result, ONUs do not require any protocol and circuitry to adjust the laser power. Also, the laser-on and laser-off times are capped at 512ns, a significantly higher boundary (?) than that of GPON. The relaxed physical overhead values are just a few of many cost-cutting steps taken by EPON.

Another cost-cutting step of EPON is the preservation of the Ethernet framing format, which carries variable-length packets without fragmentation. In contrast, both BPON and GPON break the packets into multiple fragments. BPON uses ATM Adaptation Layer 5 **(**AAL5)[109] to break a packet into cells at the transmitting end and to reassemble multiple cell payloads into a complete packet at the receiving end. GPON employs the GPON Encapsulation Method (GEM) [108] to enable packet fragmentation. This method uses a complicated algorithm to delineate variable-size GEM segments and reconstruct the packets at the receiving device.

In the previous chapter (5) a study of real traffic statistics was presented. The results of the study revealed that a great majority of internet traffic is carried by packets with a size between 55 bytes and 700 bytes. Knowledge about characteristics of the Internet traffic can be very helpful in the design and evaluation of PON improvements that are related to data encapsulation methods.

The standard EPON frame structure is presented in figure 61. The downstream traffic is segmented into fixed interval frames, which each carry multiple variable-length packets. Each packet is formatted according to IEEE 802.3 standard and it consists of header and error detection field. Clocking information, in the form of a synchronization marker, is included at the beginning of each frame. The synchronization marker is a 1-byte code that is transmitted every 2 ms in order to synchronize the ONUs with the OLT.

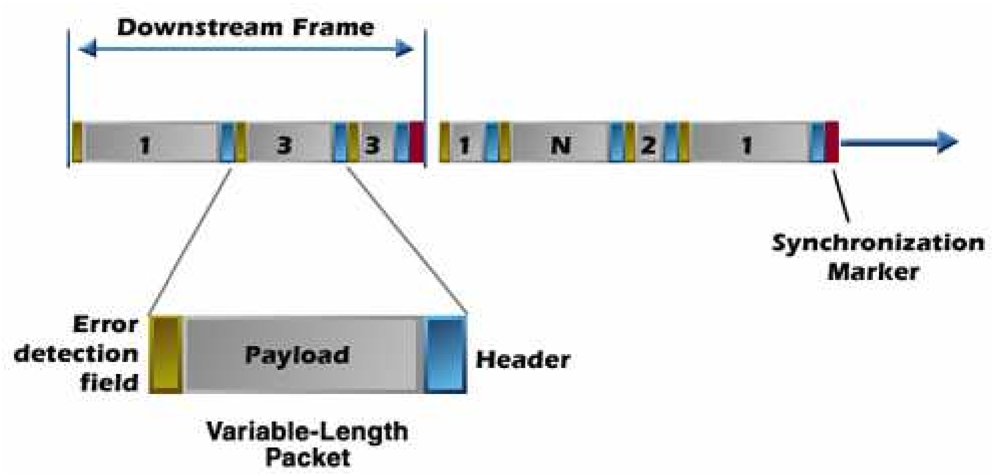

Figure 61: Downstream EPON frame

The EPON upstream traffic is multiplexed in time domain onto a common optical fiber in order to avoid collisions between the upstream traffic from each ONU (Figure 62). The upstream traffic is segmented into frames and each frame is further segmented into ONU-specific time-slots. The upstream frames are formed by continuous transmission intervals of 2ms. A frame header identifies the start of each upstream frame.

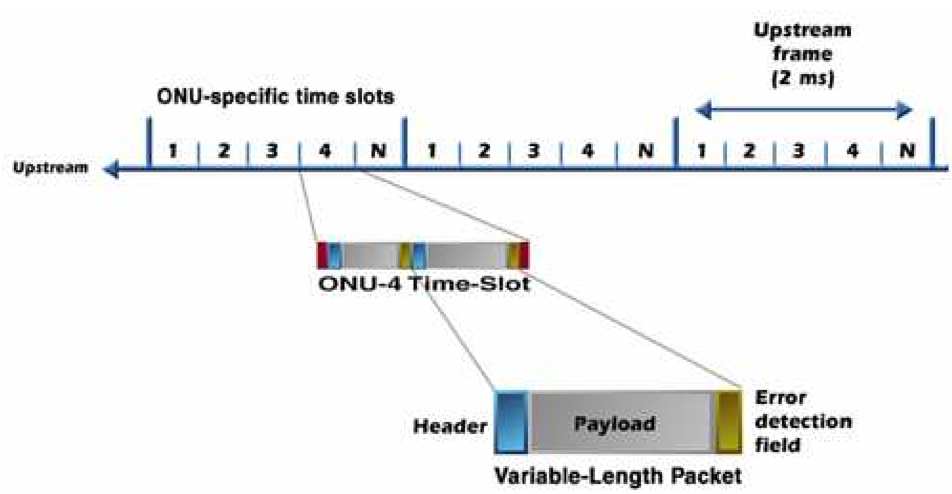

Figure 62: Upstream EPON frame

The ONU-specific time slots are transmission intervals within each upstream frame that are dedicated to the transmission of variable-length packets (up to 1518 bytes in length) from specific ONUs. Each ONU has a dedicated time-slot within each upstream frame. For example, each upstream frame is divided into N time slots, with each time slot corresponding to its respective ONU, 1 through N.

The TDM controller for each ONU, in conjunction with timing information from the OLT, controls the upstream transmission timing of the variable-length packets within the dedicated time-slots. Figure 2 shows an expanded view of a ONU-specific time slot (dedicated to ONU-4) that includes two variable-length packets and time-slot overhead. The time-slot overhead includes a guard band, timing indicators and signal power indicators. When there is no traffic to transmit from the ONU a time-slot may be filled with an idle signal.

As shown above, downstream traffic has the form of Ethernet broadcast where destination ONUs pick their packets based on the header information. Upstream transmission has much higher level of complexity because the EPON allows for variable length Ethernet packets and packets fragmentation. The EPON frame has a constant length but since the number and length of the packets is variable and each packet may come from different ONU, the effectiveness in scheduling algorithms and bandwidth allocation to each ONU becomes an issue.

Burst-mode characteristic of the traffic in PON

Another important note on PON encapsulation is the fact that both EPON and GPON transmitters can be considered as burst-mode devices. The main difference between burst-mode receiver and standard receiver is that bust-mode receiver is typically DC-coupled and the threshold setting of the receiver circuitry must adapt to the amplitude of the received signal in a very short time. Secondly, clock and phase recovery by a burst-mode receiver must be performed very quickly in nanosecond timescale. In PON the OLT transmitter works in continuous mode since downstream transmission is broadcasted to all ONUs while its receiver is burst mode. In contrast, ONU needs burst mode transmitter and continuous mode receiver.

The burst-mode transmitter prototype for 10G EPON was presented by Mitsubishi Electric Corporation in July 2010 [110]. It had the form of a standard XFP plug-in module that integrated the following components: Bi-Directional optical module (BIDI),

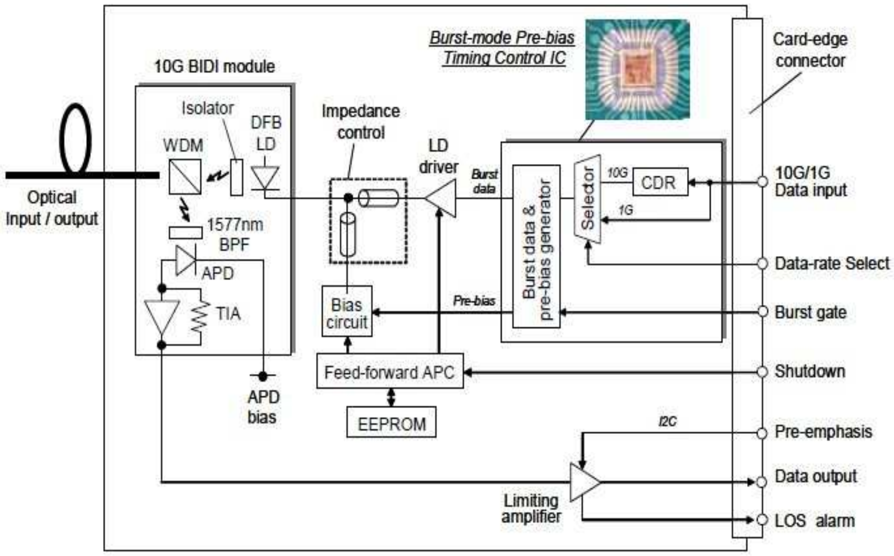

Figure 63: Burst mode transceiver for 10G EPON [110]

DC-coupled burst-mode transmitter circuit and a receiver circuit. The BIDI module consisted of a high output power DFB-LD with the wavelength of 1270 nm, a high-sensitive APD-TIA, a WDM filter, and a 1577 nm optical band-pass filter (BPF) (Figure 63). The device had the power consumption 2.8 W.

The waveforms representing time that are required by the transceiver to turn-on and turn-off the laser are presented in figure 64. The turn-on time takes 10 ns and it does not exhibit dependency on temperature. However the turn-off time varies from 3 ns to 7 ns, depending on the temperature.

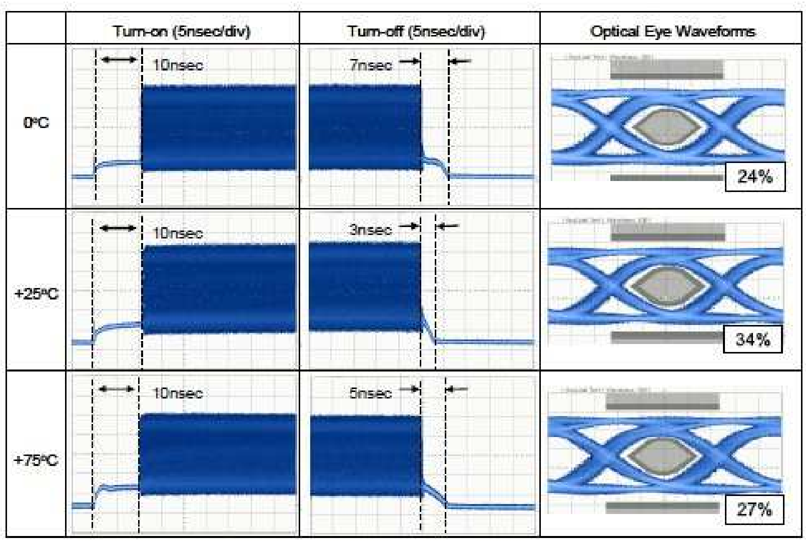

Figure 64: Measured LD turn-on/off waveforms [110]

The burst-mode receiver prototype for 10G EPON was presented by Hitachi Corporation in September 2010 [111]. The developed prototype is compatible with the standard IEEE802.3av1, which defines the maximum receiver settling time as 800 ns and the maximum CDR synchronization time as 400 ns, which means the total maximum overhead length should be 1200 ns. The receiver consisted of an avalanche photodiode (APD), a transimpedance amplifier (TIA), and a limiting amplifier (LA) (Figure 65). The receiver was connected to a serializer/deserializer (SerDes) which was connected to a MAC Logic circuit.

The receiver required a burst-reset signal to initialize its condition. AC coupling was used in both the TIA-LA and LA-SerDes connections. The TIA-IC had a gain switching function and the ATC had a boost function, which enabled it to achieve a wide dynamic range and a fast receiver settling time. The LA-IC had a differential stabilization circuit and a function that detected loss of signal (LOS).

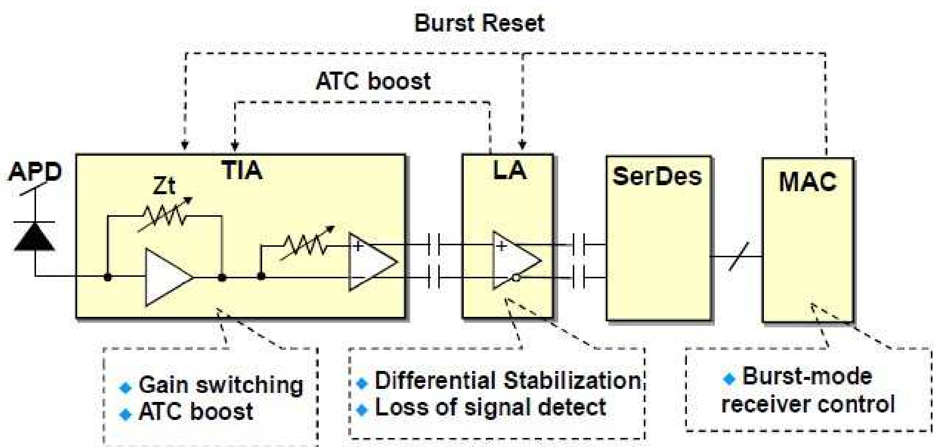

Figure 65: Burst-mode receiver prototype designed by Hitachi Corp. [111]

The MAC Logic circuit is constructed using FPGA. It has a burst-mode receiver control function, which sends a burst-reset signal to the burst-mode receiver. The role of the ATC boost was to quickly synchronize with the input signals. It converts a single-ended signal into a differential signal. In the initial phase, the ATC circuit's time constant is set to a small number in order to respond faster to the rising edge of a signal, whereas if the input signal is detected in the LA, the time constant is set to a large number to settle its amplitude. The prototype receiver achieved a BER of 10^{-12} at the signal sensitivity of -27 dBm and a wavelength 1303 nm.

Agility of the PON to dynamically allocate bandwidth

The third important characteristic of PON is the agility which specifies an ability to rapidly adapt bandwidth allocation as traffic demand varies. A common issue of the standard IEEE 802.3ah (EPON standard) is the Dynamic Bandwidth Allocation (DBA) algorithm. DBA schemes have been considered as a way of handling bandwidth and Quality of Service (QoS) requirements in EPON. Most of the existing DBA models are based in a centralized algorithm that runs at the OLT and allocates transmission windows to every active ONU.

One of the oldest bandwidth allocation protocols designed for EPON is Interleaved Polling with Adaptive Cycle Time (IPACT) [112]. The IPACT protocol is where the OLT distributes the bandwidth on-the-fly according to each ONU's request and without considering the effect of other ONUs on that distribution. This algorithm uses an interleaved polling approach where the next ONU is polled before the transmission from the previous one has arrived. Another algorithm designed for PON was presented in [113]. This method provides a uniform distribution of slots over the cycle according to the class of service (CoS). It guarantees delay and bandwidth but it is not very efficient and requires a complex calculation. A third method of bandwidth allocation was proposed [114]. This other approach implements the calculation of a fair bandwidth distribution by taking into account all the ONUs' requirements in the network. In this case, a waiting period is required after each cycle of transmission in order to acquire all the information from the rest of the ONUs, which may lead to more delays.

The problem of delay in bandwidth allocation mechanisms was addressed in [115]. The model is called Bandwidth Guarantee Delay Sensitive Dynamic Bandwidth Allocation (BGDS-DBA) and it calculates bandwidth based on a combination of three variables: guaranteed bandwidth according to the service level agreement (SLA) with the subscriber, the period between two consecutive ONU bandwidth windows, and the time when the last report from the ONU is received by the OLT. This method allows each ONU to accommodate traffic with a different class of service (CoS).

Changes in bandwidth allocation and scheduling algorithms did not experience dramatic changes since the first EPON was deployed. Most of the changes in DBA were applied as evolutionary improvements that address certain drawbacks in existing technologies and algorithms.

Transparency of the PON for the transmitted data

Since PON is a network that is unaware of type and content of transmitted data it is virtually transparent to end users. IP packets are encapsulated into variable-length Ethernet packets and those packets are then encapsulated into constant length EPON frames, also called time slots in the case of TDM-PON. All the encapsulation procedures, as well as incoming frames extraction processes, are performed without end user awareness. It also does not involve any end user applications such as web browsers, file transfer programs, Video on Demand client software or VoIP software.

This transparency feature is very important from the perspective of developing new deployments of PON. The proposition for implementing PON as an all-optical extension of metro WDM infrastructure was published in [116]. The proposed architecture allows PON to be not only an extension of Metro Area Network (MAN) but also it can work as a sub-network within its own network domain (Figure 66).

In this architecture the central office is a general hub that interconnects M PONs. Each PON has N_i ONUs which is equal to the splitting ratio N_i of the passive coupler. The value M is largely determined by the configuration of the CO while N_i has a physical limitation because of the power budget limitation. The power budget determines the allowable losses on the path between a source and destination for a given transmitter power and receiver sensitivity. Typical commercial PONs use N_i =

32 or N_i = 64 as the maximum splitting ratio which gives a power loss of $10log(N_i)$dB plus excess losses. Considering the typical distances in urban regions, the distribution fiber has a length of 1 km and a feeder fiber a length of 4 km. Separated fibers are used for upstream and downstream transmission, and the operating bit rate is 155.52 Mbps (STM-1).

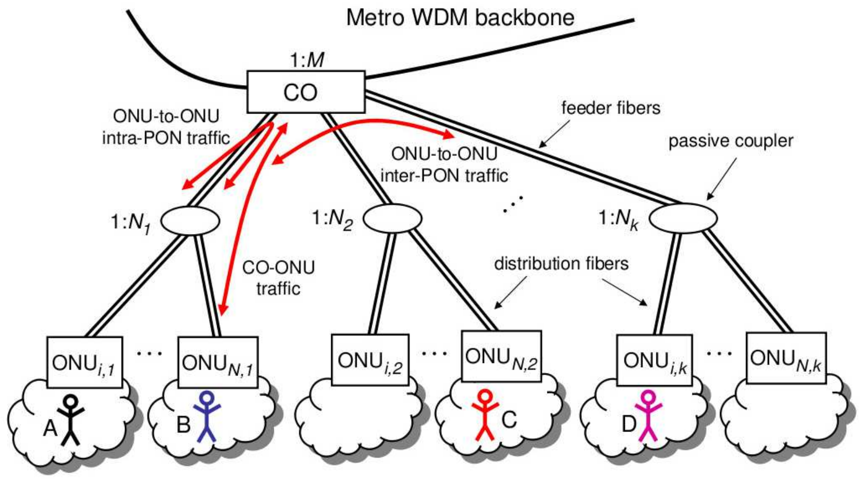

Figure 66: PON implemented as an extension of WDM-MAN [116]

Architectures like this one show the great potential of PONs transparent data transmission. It opens up new opportunities for PON to be implemented as an extension of existing optical network infrastructure regardless of the data being transmitted.

The description provided in the above discussion confirmed that PON does have a number of similarities to the AAPN network. It is agile, transparent, all-optical and transmits data in the form of frames (or time slots). In addition, the data flow can be presented as a burst-mode transmission. Considering this fact, PON can be represented as a particular example of the Agile All-Photonic Network.

Agile-All Photonic Network (AAPN) with the burst-aggregated traffic

AAPN overview

To better understand the importance of the similarities between PON and Agile All-Photonic Network (AAPN) a more thorough discussion on AAPN is required. An AAPN is a wavelength division multiplexed network that consists of several overlaid stars that are formed by edge nodes that aggregate traffic, interconnected by buffer-less optical core nodes that perform fast switching in order to provide bandwidth allocation in sub-wavelength granularities [117] (Figure 67).

Most proposals for photonic networks envisage a mesh topology, which distributes the load over many switches. However, in the AAPN, the photonic core switches have an enormous capacity, which permits a simpler star topology that has been proven to favorably compare with mesh architectures [118]. The AAPN is mainly characterized by its agility; that is, the ability to rapidly adapt bandwidth allocation as the traffic demand varies.

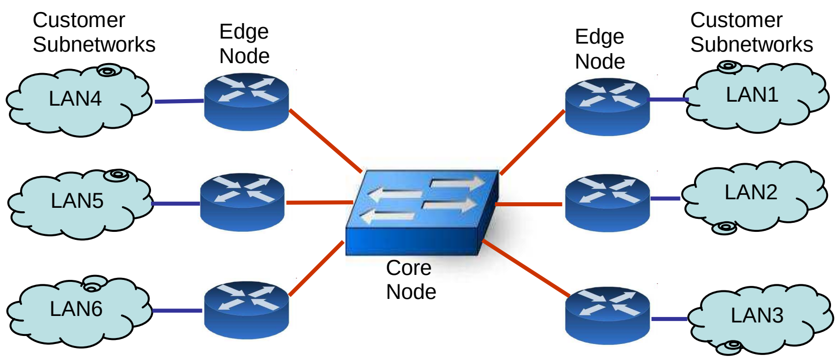

Figure 67: AAPN in a basic (single core node) configuration

One important feature of AAPNs is that most of the control and routing mechanisms reside at the edge nodes, which play the role of points of presence (POP) for customer networks. The fully optical data transmission between edge nodes and the transparency of the core nodes make the AAPN core unaware of data content, which allows different types of subnetworks (IP, ATM, FR, X.25, etc.) to be connected to the POP. Since there are a limited number of optical ports in the core node, the AAPN may use a selector to effectively expand the port count by allowing the connection of more than one edge node to one port of the core node (Figure 68).

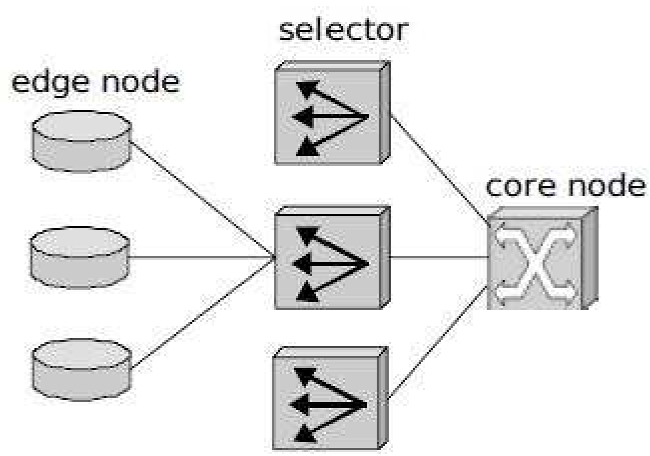

Figure 68: Implementation of selectors in AAPN [119]

Although ideally the core node would switch individual packets to give the finest possible bandwidth granularity, this would require a switching time on the order of nanoseconds, which is very difficult to achieve with today's technology. A more realistic scenario is to aggregate several packets with the same destination address (the same destination edge node) into larger units to allow an increase of the switching time on the order of microseconds, which is already available with today’s technology for small port counts and is being intensively researched for large port counts.

The AAPN is designed to work in one of two possible modes: Time Division Multiplexing (TDM) or Optical Burst Switching (OBS). In the TDM mode, data is transmitted in the form of fixed size units called “slots”. In the OBS mode, data is transmitted in very large units called bursts, which can be either a constant or variable size. Both modes require the edge node to aggregate and encapsulate the variable sized packets from surrounding subnetworks into slots/bursts that will contain packets from the same flow. A flow in this context is defined as the traffic that has the same source and destination edge nodes.

In the OBS mode, the core switch is configured in response to requests by burst headers issued in advance of the arrival of a burst payload or by reservation requests signalled by edge nodes in advance of the transmission of the burst. In the TDM mode, a periodic sequence of core switch configurations is calculated to adapt it to traffic demands as reported by the edge nodes. The core node controller is responsible for assigning bandwidth to the different flows after a request has been received from them, which is based on the traffic measured at the edge node or even predicted with a suitable algorithm.

Once the bandwidth for each flow has been calculated, the core node controller sends, to each edge node, the respective schedule; i.e., the information about the number and position in time of the assigned slots. The core node controller is also responsible for changing the configuration of the core optical space switches for every slot in order to provide the bandwidth calculated and to effectively send the slots to their correct destinations (i.e., switching the light paths every slot). Several bandwidth allocation methods for AAPN have been investigated in [120] and [121].

The main feature of the AAPN is its transparency to any customer subnetwork connected to an edge node. It plays a similar role to that of traditional backbone networks such as ATM or Frame Relay and can be seen as a single, transparent switch; which may be conveniently MPLS enabled or otherwise.

Role of Edge Nodes

The role of the edge node is to provide the ability to interface the customer subnetworks to the optical domain of the AAPN core. It is therefore a hybrid electro-optical system that performs traffic encapsulation into bursts or TDM slots, traffic buffering and monitoring, signaling and issuing of bandwidth requests among other functions.

A data packet arriving from outside the AAPN domain will first be interrogated to determine its correct destination edge node. It will then be assembled in a slot or burst together with other packets that are destined for the same node. Once assembled, the slot waits for transmission enqueued in a buffer that corresponds to the destination edge node, which is called flow buffer. From the flow buffer, it will be read and then sent to the core on the assigned wavelength and time slot (wavelength, frame and position in the frame in the case of TDM-AAPN).

A data slot/burst arriving from the AAPN core will first be deserialized and then sent to a flow buffer to wait to be disassembled into its constituent packets. The packets will then be sent to the attached router so they can reach their destination subnetwork. If the edge node is to perform the tasks of the router as well, then the packets must be interrogated to identify each packet's destination subnetwork and enqueued for transmission in the corresponding buffer to be sent out in accordance with that subnetwork's protocols.

Traffic aggregation requires efficient buffers and flexible queuing methods as well as a flexible rule for mapping customer addresses into buffers. In addition, the AAPN is expected to be fully compatible with MPLS subnetworks and this characteristic places an additional requirement on the edge node design as it will also be responsible for proper label recognition.

The AAPN protocols will be used to exchange information among the edge nodes about the customer networks connected to AAPN POPs. A look-up table is built to map the addresses of incoming packets onto the appropriate buffers.

Data aggregation and encapsulation

When a packet arrives from a customer subnetwork, it will be processed by a preprocessing unit (software or hardware) in order to be routed to the correct destination edge node based on its destination IP address and directed to the appropriate flow buffer. The MPLS label can be used instead if the AAPN works as part of an MPLS domain. The look-up table is dynamically updated at each edge node when changes in the network topology occur; for example when customer subnetworks are attached to or detached from an edge node or when the domain address of one of the customer subnetworks changes. The exchange of information about these changes is performed by signaling mechanisms.

If the AAPN edge node is attached to a router, exact look-up and the task of assigning MPLS labels to IP addresses is off-loaded to the router (or the routers in the subnetworks) and the edge node may be considered as a 'linecard' that interfaces the router to the photonic network.

When OBS is used, the burst assembly mechanism can be timer-based, threshold-based, or a composite of both [122]. In a timer-based burst assembly approach, a burst is created and sent into the optical network at periodic time intervals; hence the network may have variable burst lengths, which may be undesirable (too short or too long, depending on the offered load). In a threshold-based approach, a limit is placed on the length of each burst and thus the network will have fixed size bursts, but the aggregation delay experienced by the packets may be too long if the arrival rate is low. The composite method combines both approaches, with the timer optimally set to the largest value commensurate with the tolerable delay. The vast majority of bursts are then of a maximal (fixed) length.

When TDM is used, the incoming traffic is aggregated into fixed size units called envelopes or slots, which are equal in size to the time slots. The performance objective of the TDM-AAPN is to have 10 μs time slots, which corresponds to 100 kb envelopes for a 10 Gb/s link. A simple way to build the slots consists of aggregating an integer number of variable-size packets without performing packet division.

This method is fast and relatively easy to maintain but it does not fully utilize all the available bandwidth, because each slot may be left with some empty space. Besides, the slot size must be set equal to the maximum possible packet size, which may be too large.

A second method would consist of segmenting variable length packets into fixed length cells, then the cells are packed into slots. Cells should be just longer than the smallest possible packet size. The slot may now be an integer multiple of the cell size which can be smaller than the longest length packet. Bandwidth may still be inefficiently utilized due to voids within cells.

A third possible method would divide incoming packets. Variable length packets are packed into slots and they may cross slot boundaries without introducing voids. Effectively, variable length packets are transported 'natively' (unchanged), with the slot acting as a 'block size'. This method is more complex. It introduces a slight additional processing delay and more complex buffering requirements, especially at the destination edge node, but it significantly improves the bandwidth utilization and therefore decreases the overall delay.

To prevent excessive delay for packets from low rate flows, provisions must be made to time-out the slot aggregation process. In this case, if the arrival rate of the packets is low the edge node may not have enough data to fill-up a slot before a time-out occurs, so slots may leave the edge node with large empty spaces. All methods will then have the drawback of inefficient bandwidth utilization for low input loads.

Control information for the packet aggregation/deaggregation protocols will be sent within the same slot. Each slot of data, a 'data slot', has its own header with information about the number and size of encapsulated packets, which will be used to properly unpack the envelopes and reassemble packets at the destination edge node.

The envelope that represents a single data slot consists of a header and a group of encapsulated packets. The first bits of a slot must be a pre-amble to enable burst mode receivers to lock onto the bit sequence, i.e., slot/packet level synchronization to slotted time (bit level synchronization will not be used). The first bit of the header (Figure 69) is a single flag bit 'ctrl.flag' that differentiates data slots from control slots. The source and destination nodes fields follow with their corresponding numbers. If an AAPN consists of, for example, 128 edge nodes then two fields, 7b-long, are required to identify the edge nodes. The next field is the slot identification number.

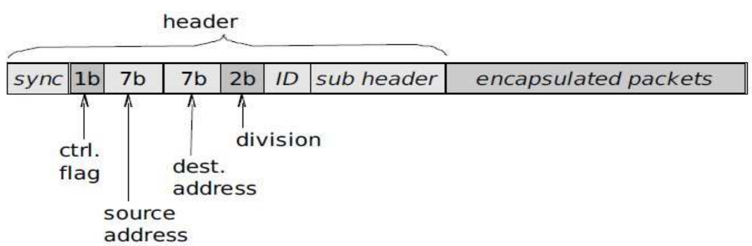

Figure 69: Time slot structure in the AAPN [119]

The division field indicates if the slot carries any divided packets. Two bits would be enough since there are four possibilities: "no divided packets", "first packet is divided", "last packet is divided" and "both packets are divided". This field will be used by the destination edge node for extraction of the encapsulated packets to determine which packets should be kept in cache memory for reassembling.

The information about the number and sizes of the encapsulated packets will be stored in a subheader field, which will be the last element of the header in the slot. This information can be encoded in the form of a group of numbers that will define the positions of the boundaries between packets. If a slot carries M encapsulated packets then the positions of the M-1 boundaries have to be stored. The maximum size of the header is dictated by the worst possible scenario of the encapsulation procedure: when all the encapsulated packets are of the smallest possible length (24B header + 1b of data in the case of IP traffic).

Quality of Service implementation

There may be two approaches to QoS provision: provision by the core controller and provision by the edge node. In the former approach it is the bandwidth allocation algorithm that deals with this issue. The method would most probably involve the use of separate buffers for the various levels of QoS for each flow. The edge node would only be concerned with the number of levels being used so that the correct total number of buffers can be implemented. Traffic requests/allocations would therefore consider not only the flow, but also the QoS level. Bandwidth is requested for the triplets source-destination-QoS level.

To provide QoS at the edge node independently from the bandwidth allocation methods, the incoming packets from different subnetworks could be directed to temporary buffers separated not only by destination edge node but also by QoS level. The slots would already be built with the appropriate percentage of packets from different classes according to the QoS rule (e.g. 50% from gold class, 30% from silver and 20% from bronze). The bandwidth allocation method would proceed normally, without any additional consideration for QoS. However, packet division and header information would be significantly more complex with this method of encapsulation.

Scheduling

Once the incoming packets are aggregated and stored in their respective flow buffers, the edge node has to perform the appropriate scheduling of slots (or bursts) to send the data to the core en route to the destination edge nodes.

The scheduling Processing Unit (PU) receives the scheduling information from the core controller and then reads the slots/bursts from the buffers (via the multiplexer) in the order preset by the global bandwidth allocation method. In the TDM mode, the number of slots read from the same buffer for each frame depends on the bandwidth assigned to the corresponding traffic flow.

Receiving frames by the edge node

The first task in the receiving module is to deserialize the 10 Gb/s incoming data stream to obtain several lower rate data streams that can be processed by slower processing units in parallel. A 1:8 deserializer can be used, with its outputs being 1.25 Gb/s (it is also possible to use it in the 1:16 configuration [123]). The lower rate streams can then be examined to separate the control slots from the data slots and to send the data slots to their appropriate flow buffers (organized by source edge node in figure 70). Control slots are directed to the appropriate processor in charge of maintaining look-up tables, schedulers, etc.

Data slots are sent to PUs for packet extraction and reassembly using the information in the slot header. The memory needed in the processing unit for packet extraction and reassembly could be implemented as additional external cache memory (similar to a SPARC64 CPU architecture with 2 MB external cache) and its depth will depend on whether or not the bandwidth allocation algorithm guarantees that there will be no mis-sequencing of slots. Note that an individual star guarantees in-sequence delivery of slots even when flow level load balancing is used across its wavelengths.

When the allocation method in used it does not guarantee in-sequence delivery (bandwidth allocation algorithms that act over several stars), the extraction/reassembly buffers will have to be deeper in order to accommodate for more than one packet fragment waiting to be completed. If a suitable load balancing technique is used, it is possible to bind the buffers depth.

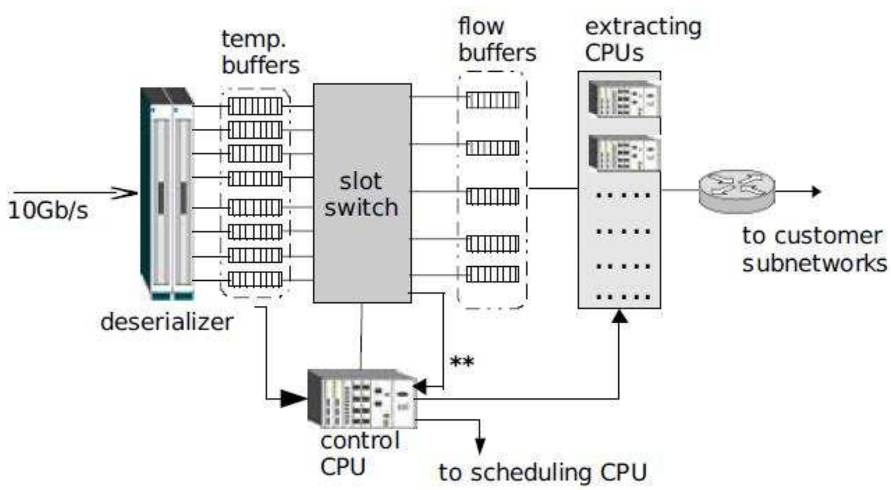

Figure 70: Packets extraction in the AAPN [119]

The extracted packets are sent from the PUs to the output buffers that correspond to their destination subnetwork via an internal packet switch. If the AAPN edge node works as a line card attached to a router, then the buffering of the packets according to their destination subnetworks is a task for the attached router and not the AAPN line card.

Signalling processes

Control information exchanged between the edge nodes and the core node can consist of several types, including bandwidth requests, bandwidth allocation and network topology changes (but not slot aggregation information, which will be included in the header of the same slot).

It is possible to have the control information contained within the data slots. However, this would introduce unnecessary complications in the processing of arriving slots. The use of separate control slots (as opposed to data slots) to carry this information is a more straightforward approach. The control slots would be the same size as the data slots and must have a high priority to be transmitted and processed upon arrival.

The theoretical architecture of the AAPN has the edge nodes and the core nodes as completely separate entities. In practice, however, an edge node will be collocated with the core node in such a way that the control slots with bandwidth requests will be destined to this edge node, which will serve as the core controller (using either the same PU or a second one if necessary to simplify the software and/or divide the processing burden).

There are two possible implementations for signalling the control slots. The first method is out-of-band signalling (Figure 71) which involves a separate wavelength channel dedicated only to the transmission of control slots. The links consist of two separate sub-links: the data channels consisting of several wavelengths that transmit only data, and a control channel for control information only.

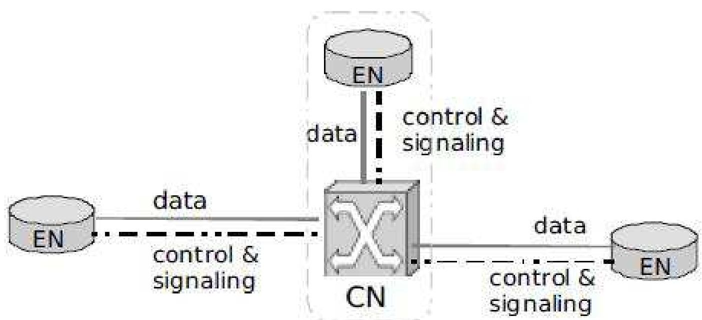

Figure 71: Out-of-band signalling in the AAPN [119]

The second signalling method is in-band signalling, which consists of sending both data and control slots on the same wavelength(s).

Signalling consists mainly of bandwidth requests, bandwidth allocation and network topology changes. In a TDM-AAPN, regarding bandwidth request/allocation (the bulk of signalling data), only one control slot will be sent from the edge node to the core node and one will be received in every frame. Considering this, the out-of-band signalling option would be wasteful and therefore is unlikely to be used.

Traffic flow monitoring

It is necessary to monitor in real-time the traffic that arrives at the edge node from customer subnetworks. The statistics of the traffic arriving from outside the AAPN will be used to calculate the bandwidth requests that will be sent to the core controller.

Traffic monitoring at each edge node will be a hybrid of hardware-software functionality. It is necessary to have counters for each of the flow buffers, which will register the number of slots that arrive at the buffer. These counters will be read in regular time intervals, followed by the resetting of the counter. Traffic statistics calculations will be performed based on the information read and in the simplest case it will only add the numbers read from the counters. The bandwidth allocation method in use may also require knowledge of the length of the buffers at any time in order to account for backlogs in the queues. Alternatively, counters registering the number of slots departing may also be used for this purpose.

Both measurements (arrivals and queue lengths) are usually provided by the memory management. For buffer implementation with the QDRII memory, the length of each queue will be measured automatically if the appropriate software is loaded on the memory controller (a custom Field Programmable Gate Array, FPGA board).

Prototype of data encapsulation system for PON

Based on the characteristics of PON and AAPN listed in previous chapters, a number of features that are identical (or similar) in both networks can be provided. The similarities play a key role in transferring certain AAPN technologies and models into PON infrastructure in the form of extensions and modifications.

AAPN and PON are both transparent networks for the transmitted data. Therefore they are not aware of the protocol that is implemented in customer subnetworks. In addition, both AAPN and PON can interconnect subnetworks that have different native protocols. This is possible when Edge Node (ONU) is equipped with the appropriate interface for connecting to customer subnetworks.

AAPN and PON are both agile networks from the perspective of dynamic bandwidth allocation. Both AAPN and PON have implemented technologies that allow edge nodes (ONUs) to create requests for bandwidth assignment.

Both network infrastructures have implemented technologies for data encapsulation. Packets received from customer LAN are encapsulated into native slots (Ethernet frames) and the transmitted along the optical path. Edge Nodes (ONUs) are responsible for data aggregation followed by the encapsulation process. Additionally, they are responsible for encoding of incoming slot/frame and customer data extraction.

Both network infrastructures have traffic flow that can be represented as burst-type transmission, where the entire link between the specific EN and CN (specific ONU and OLT) is dedicated to the data transmission within a defined time interval.

Considering the number of similarities between both infrastructures, there is a new suggested approach for design and implementation of hardware and software for ONU and OLT that can significantly reduce their costs of manufacturing and maintenance. The low cost technologies that were originally proposed for AAPN can also be accommodated in EPON infrastructure.

Since EPON transmits 2 ms long bursts that accommodate approximately 250 kB of data at 1 Gb/s, it is possible to implement a low-cost hardware that was designed for generic personal computer (PC) as an engine that performs the tasks of burst aggregation (traffic aggregation, queuing, encapsulation, etc…). To evaluate this proposal an innovative EPON prototype was designed and built. The prototype was based entirely on low-cost PC components and its software application was written in C, compiled in two different optimization models and runs in the Linux operating system.

Benchmark of the cost-efficient encapsulation system

Since it is desirable to use off-the-shelf technology (i.e. commercially available) as much as possible to lower the costs, several tests have been performed to evaluate the capabilities of current technology in the market. In particular, commercial multi-CPU units could be used to perform parallel slot aggregation/deaggregation. To estimate the viability of this option, two types of tests implemented in C language were performed. The first test is a benchmark that measures the maximum speed for writing and reading sequences of bytes from multiple buffers in the RAM. The second test is a software implementation of the scheduler that emulates traffic aggregation and slot assembling in the Edge Node. Both tests were performed on several PCs with different memory and CPU configurations, namely:

- Intel Celeron 1.7GHz (128KB cache)
  Memory: 256MB RAM (SDRAM) 100MHz bus.
  OS: Mandrake Linux 10.2 (kernel: 2.6.11_6mdk).
  Compilers: Intel C v9.0, GNU C v3.4.3

- Intel Pentium 4 2.8GHz (512KB cache)
  Memory: 768RAM (SDRAM) 133MHz bus.
  OS: Mandrake Linux 10.1 (kernel: 2.6.9 + MPLS v1.946).
  Compilers: Intel C v9.0, GNU C v3.4.1

- Intel Pentium 4-HT (dual core) 2.8GHz (512KB cache)
  Memory: 2GB RAM (DDR) 133MHz bus.
  OS: Mandrake Linux 10.2 (kernel: 2.6.11-smp).
  Compilers: Intel C v9.0, GNU C v3.4.3

All PCs have an implemented Linux operating system to ensure efficient memory management. All system services that were not required for performing benchmark processes were disabled to unload CPU from unnecessary tasks.

Read from/write to multiple buffers

The benchmark test consisted of writing to/reading from 64 buffers of 100 kB, 300 kB or 500 kB in length. The length of the buffers was chosen to evaluate system performance for aggregation of bursts with lengths smaller, bigger and similar to those implemented in EPON.

To ensure the benchmark reflects the conditions of the real IP traffic load, buffers had assigned groups of IP addresses extracted from packets that were captured from the commercial LAN. The buffers were filed according to size and destination address of the earlier captured packets.

The test measured the total time taken to fill or empty the buffers. The results are presented on figures 72 and 73.

Hardware	64x100kB		64x300kB		64x500kB	
	Write [Gb/s]	Read [Gb/s]	Write [Gb/s]	Read [Gb/s]	Write [Gb/s]	Read [Gb/s]
Celeron / iCC	1.4	5.96	1.36	5.96	1.22	6.11
Celeron/ GCC	0.5	1.16	0.49	1.15	0.45	0.75
Pentium4 / iCC	2.8	9.54	**2.8**	10.22	2.74	9.54
Pentium4 / GCC	0.87	1.91	**0.86**	1.96	0.86	1.92
Pentium4 HT / iCC	2.98	7.95	2.92	8.94	**3.1**	**9.17**
Pentium4 HT / GCC	0.57	1.16	0.38	0.66	0.48	0.95

Figure 72: Memory access speed benchmark test (iCC: Intel C, GCC: GNU C)

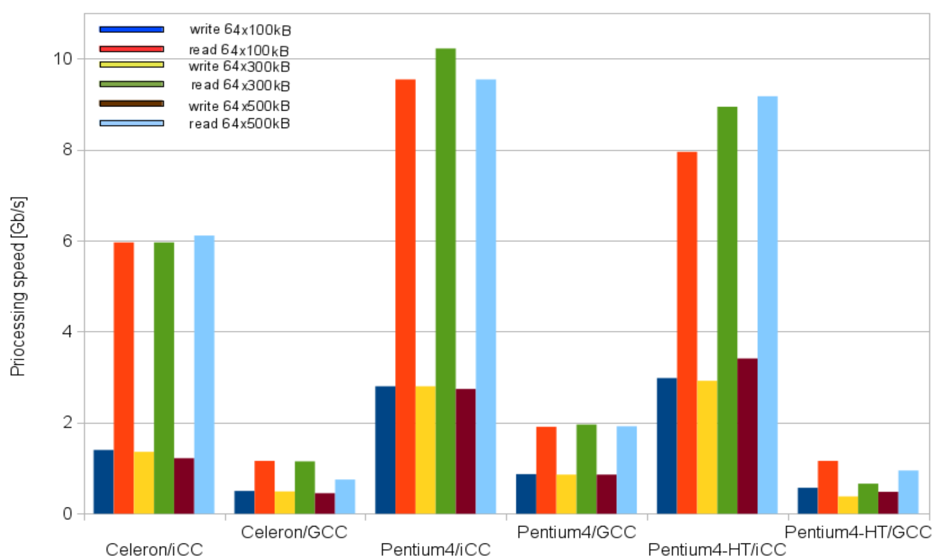

Figure 73: Memory access benchmarks comparison (iCC: Intel C, GCC: GNU C)

When standard software implementation is deployed over the hardware platform the speed of writing to buffers is about 500 Mb/s and reading from buffers reaches 1 Gb/s. This result indicates that this particular low cost hardware-software configuration can possibly serve as ONUs with five Ethernet ports (100 Mb/s each) connected to customer LANs, and a 1 Gb/s optical trunk that connects ONU to the OLT. This configuration reflects the performance of commercial ONU supplied with 1G EPON.

The recompilation of the software application for the particular type of used CPU significantly improves the use of embedded cache memory in addition to speeding up the data transfer between the CPU and RAM. After this modification, the speed of writing to buffers exceeds 2.9Gb/s and reading from buffers exceeds 10Gb/s. This result indicates that a well optimized combination of software and low-cost hardware is suitable for implementation in ONU with one 10Gb optical trunk to OLT and three 1Gb Ethernet ports (electrical or optical) connected to customer LANs.

The performance of a low cost system has been proven to be sufficient to be considered as a valid candidate for implementation in ONUs for 1 Gb EPON. The implementation off the shelf technologies that were originally designed for low-cost personal computers may significantly decrease retail cost of the ONU. In the year 2010, the average cost of the ONU with three Ethernet ports (100 Mb/s each) and one 1 Gb/s optical EPON port was $370 USD. This cost may be potentially decreased to about $200 USD if PC-based components are used to build the ONU. In addition, such architecture would offer an additional advantage of improved configuration flexibility thanks to software based implemented algorithms for traffic aggregation, encapsulation and scheduling.

The benchmark test results also show that the single core Pentium4 CPU performs slightly more efficiently than the dual core Pentium4-HT. This is the result of the lack of synchronization between both cores in the HT CPU, since the binary code was not optimized for parallel computing. This, however, can be easily fixed when the next prototype is designed.

Traffic aggregation and slot assembling

The previous chapter presented a study on low-cost PC-based architecture limitations related to memory access required for successful data aggregation and data buffering. To provide more detailed knowledge about performance of the proposed hybrid hardware-software architecture, additional study of data aggregation and encapsulation was performed.

The additional emulation was designed and implemented to evaluate the system performance under the full load of traffic flow processing. Emulation of the encapsulation process consisted of 32 input queues and 32 assembly buffers 12500 bytes long (a 100 kb time slot in AAPN). Two models were used; the first model consists of a CPU performing all the tasks: receiving incoming IP packets, directing packets to the appropriate input buffer according to its destination, transferring packets from input buffers to assembly buffers and encapsulating packets into slots. The second model consists of a CPU performing only 2 tasks: transferring packets from input buffers to assembly buffers and slot assembling.

The traffic used was a group of 5.5 million IP packets captured from the LAN at the University of Ottawa campus. The information about packet headers was saved on hard disk and then used for packet generation in the emulation.

Hardware	Full load [Mb/s]	2 tasks only [Mb/s]
Celeron / GCC	119.5	129.9
Celeron / iCC	680.7	947.2
Pentium4 / GCC	196.1	211.22
Pentium4 / iCC	1191.8	2093.24
Pentium4 HT / GCC	194.4	214.25
Pentium4 HT / iCC	981.83	2065.29

Figure 74: Emulation of the encapsulation process (iCC: Intel C, GCC: GNU C)

The emulation results presented in figure 74 indicate that the proposed low-cost hardware and software combination exceeds 1.1 Gb/s of traffic processing speed under full load, and exceeds 2 Gb/s under partial load.

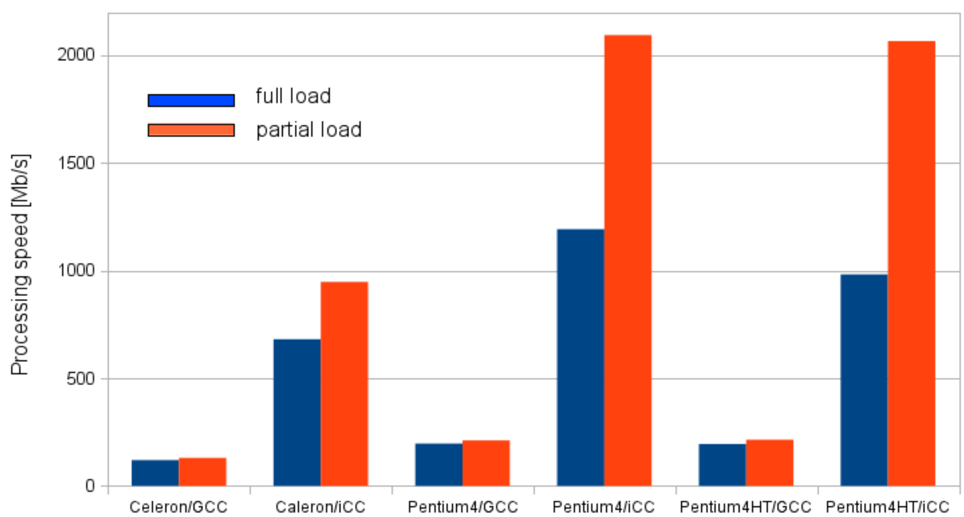

Figure 75: Performance comparison of the system under full and partial load (iCC: Intel C, GCC: GNU C).

Figure 75 confirms the advantage of the hardware dedicated binary code over the generic universal code. It shows as well that the CPU responsible only for slot assembling and bandwidth monitoring performs almost twice as fast than the fully loaded one for the Pentium4 / iCC combination. This result indicates the great advantage of having the main board of the Edge Node with a separate CPU working as the input scheduler designed for receiving the traffic and directing it to the appropriate input buffers.

The emulation test results proves that low-cost combination of multipurpose hardware (PC components) and a well optimized software application is capable of performing tasks such as traffic aggregation, encapsulation and queuing, that were usually implemented in more expensive dedicated hardware platforms in ONUs. The processing performance that was achieved with this prototype is comparable to commercial gigabit network processors such as NPA CPU manufactured by EZ Chip Corp. [124]

The results are also promising from the perspective of designing new OLT architectures. In the year 2010 an average cost of OLT with two EPON gigabit ports was in the range of $10000 USD (example price quotation obtained from Enablence Corp in 2009). The device had implemented expensive hardware (similar to those used in multi-gigabit routers) that was responsible for all computing tasks that are required to serve EPON trees. Implementing a combination of multipurpose CPUs, DDR3 RAM [125] and software application (optimized for this particular hardware configuration) would be a good candidate for new low-cost OLT.

Multi-CPU architectures had been the subject of many studies in the past, mostly due to their potential applications in scientific computational tasks. Due to the high cost of multi-CPU systems and the fact that most of the user-level protocols were developed on single-CPU platforms, parallel processing systems did not find their way to commercial network devices.

A significant reduction of design and manufacturing costs of multi-CPU systems allowed for wide range applications in network devices. In [126] they described, analyzed, designed, implemented, and evaluated a parallel version of a user-level protocol layer on the two-CPU Alteon Gigabit Ethernet NIC implemented in Pentium-III PC with Linux operating system. This prototype network node achieved a total processing bandwidth of 964 Mb/s.

Although this particular prototype was a significant success considering the achieved bandwidth, the whole system was still strongly dependent on dedicated network CPUs rather than generic multipurpose CPUs. The network CPU was a 388-pin ASIC that consisted of two MIPS microprocessors running at 88 MHz, an internal memory bus with interface to external SRAM, a 64-bit, 66 MHz PCI interface, and an interface to an external MAC.

While the traffic processing tasks were performed almost solely by Ethernet dedicated CPUs in [126], the prototype presented in this chapter performed all traffic processing tasks in the low-cost generic CPU, which makes it an innovative approach. The single multipurpose CPU exceeded 1.1Gb/s under the full load, and it also proved that the performance would certainly be improved if dual CPU hardware configuration was applied with software that truly supports multi-tasking processing. Such configuration could possibly reduce the cost of OLT to the range of $5000 USD.

In addition, it is highly possible to further reduce the costs of design and manufacturing OLTs and ONUs due to new technologies that have been recently developed. In February 2011, the subsidiary of the Intel Corporation in Haifa (Israel) published a prototype of an innovative multi-CPU chip manufactured in 32 nm technology [127]. The presented chip consists of four processing cores, a DDR3 memory controller and an 8 MB cache. In addition, it can be manufactured in a small size BGA package for low-power devices. Technologies such this one are very promising candidates for significant reduction of the costs related to manufacturing and design new generation of OLTs and ONUs.

Implementation of improved ONU data encapsulation prototype with off-the-shelf components

The prototype of ONU evaluated in the previous chapter exhibits performance that is sufficient for implementation in a 1 Gb EPON and at the same time it points to a direction for cost efficient design of new generation ONUs and OLTs.

To evaluate low-cost architecture of ONU that supports processing bandwidth above 2 Gb/s, a new hardware configuration is proposed. Memory access is still one of the key issues to be solved when using off-the-shelf technology to provide multi-gigabit processing bandwidth. QDRII memory with 1 Gb/s data rate is a promising option but is not yet widely commercialized and is still expensive. DDRII memory with 533 Mb/s data rate could be used instead [128].

Parallel processing in a multi-CPU main board should be used in the Edge Node, especially for the encapsulation/extraction processes. There are several types of multi-CPU main boards designed for AMD and Intel CPUs that are in mass production. Most vendors offer dual-CPU boards.

One possible configuration for an improved ONU prototype could be:

- Main board: Tyan Thunder K8QW(S4881) [129]. This min board supports 4 processors with 64 bit dual core architecture in the basic configuration. The extended configuration allows the use of 8 CPUs by applying the M4881 add-on processor board. It has one PCI64-133MHz slot and two PCI64-100MHz slots that can be used by optical gigabit interfaces, as well as embedded dual Gigabit Ethernet LAN ports that can be used for remote monitoring and maintenance. It is equipped with 16 DDR DIMM slots, grouped in 4 slots per CPU. This feature enables association of groups of memory with CPUs.
- CPU: AMD Opteron [130]. This CPU has 64 bit dual core architecture and an embedded memory controller that supports up to 8 registered DIMMs. This feature allows all the CPUs on board to access in parallel their own groups of memory. Opteron has also implemented the HyperTransport technology [131] that allows up to 25 Gb/s aggregated data transfer in both directions between the CPU and I/O devices in 16 virtual channels. Other important features are the 1MB L2 cache memory that can be used for faster queues of packets/slots, and the 64 KB L1 cache that can be used for high speed aggregation of packets into slots.
- Memory: 2 GB 400 MHz DDR ECC Registered CL3 (3-3-3) DIMM Dual Rank (KVR400D4R3A/2G) [132]. This memory has a maximum data rate of 400 MHz with a throughput of 3200 MB/s. There can be up to 8 GB of memory per CPU using these DDR modules.

Using the above components there can be up to 8 parallel processes for the various tasks of the edge node and the maximum extended configuration is capable of maintaining 16 parallel processes. The load of each CPU can be balanced by software. Another issue to be solved in this configuration is the realization of the 10 Gb/s output stream (slots sent to the core). Even using a dedicated 64 bit CPU for slot scheduling and a PCI64-133MHz interface for data transmission between the CPU and the optical transmitter, the maximum data rate is only 8.5 Gb/s. Nevertheless, the quickly growing demand for high data transfer between CPU and I/O devices in new applications should force vendors to implement a 166MHz PCI64, which will offer a 10.5 Gb/s data rate.

The hardware implementation that bridges optical transmission and software is a very challenging task, with the main issues being the need to process fast data streams (10 Gb/s) and the fast memory access required to buffer packets and slots at this speed. Parallel processing of packets and slots will be required to avoid the use of very costly devices.

Regarding traffic encapsulation and extraction, it is essential to make the most effective utilization of bandwidth. Efficient and short slot headers with information about the number and the boundaries between packets in the slot are necessary to achieve this.

The new QDRII technology is a promising solution for fast buffers implementation given its very short access time, but this is still a new technology not widely commercialized. This implementation requires FPGA boards with embedded memory controllers. The advantage of this technology is the available programmable logic that can easily maintain several virtual queues in one physical memory chip and already performs several functions for traffic monitoring. However, the main drawback is that the memory embedded on the board is not easy to upgrade and very costly to do so (changes in physical configuration very often require replacing the FPGA board altogether).

The results of the ONU prototype evaluation gives us a measure of the capabilities of off-the-shelf CPUs to perform the encapsulation of real IP traffic and the scheduling of slots. A single Pentium 4 working at 2.8 GHz with a 133 MHz system bus is able to handle up to 2 Gb/s streams. The use of several CPUs with several parallel processes allows higher bit rates to be processed. The results also emphasize the importance that the source code should be compiled using a native compiler designed for the particular type of CPU. A software implementation on commercial CPUs in standard C language has the advantage of being easily optimized and being portable when the hardware is upgraded. Something to keep in mind, however, is that some producers of CPUs provide their own functions for certain operations like memory access or optimization of cache memory utilization; those functions will therefore have to be changed if the CPU is upgraded.

Bandwidth use in burst mode ONU

The previous chapters shown that off the shelf components implemented in desktop PCs can be considered candidates to build low-cost ONU and, after some improvements, also OLT. The processing power of CPUs that are used in consumer market products is certainly sufficient to support 1 Gb EPON and 10 Gb EPON.

Technical capabilities of PC-based ONU prototype that works in burst mode transmission are proven and the next issue that has to be addressed in a low-cost burst mode ONU is how efficient the available bandwidth is used.

One of the techniques that are implemented in AAPN is the Optical Burst Switching (OBS) as a method of traffic aggregation and transmission across the network. OBS is a technique where several IP packets with the same destination and other common attributes such as Quality of Service (QoS) parameters are assembled into a burst and forwarded through a buffer less network as a one entity [133]. The idea is to use no buffering at the intermediate nodes and to send the header and the associated payload on two different wavelength channels with the header being sent slightly ahead in time.

Since similar techniques of burst aggregation are used in both: AAPN Edge Node (EN) and PON ONU, analysis of traffic encapsulation in OBS-AAPN are very useful to understand efficiency of the encapsulation process in the ONU. The traffic aggregation and encapsulation process has direct impact on efficiency of the bandwidth use in the proposed low-cost ONU prototype.

One important design issue in an Optical Burst Switched Network is the burst aggregation method. The burst assembly mechanism can be timer-based or threshold-based [134]. In a timer-based burst assembly approach, a burst is created and sent into the optical network at periodic time intervals; hence the network may have variable length input bursts. The major drawback of this approach is that the scheme might produce undesirable burst lengths at different loads. In a threshold-based approach, a limit is placed on the length each burst; hence the network will have fixed size-input bursts [134].

The problem of this approach is that it does not give any guarantee on the assembly delay that the packets will experience during the burst aggregation process. The objective of this chapter is to evaluate in the context of OBS networks and TDM-PON networks a third approach that combines the timer-based and threshold-based approach into a single composite burst assembly mechanism to address the aforementioned deficiencies.

The practical implementation of this composite burst aggregation method is introduced as "encapsulation" of the incoming streams of variable length packets into constant length units called "envelopes". In those networks based on the time domain switching model, the envelope represents the length of a single timeslot and consists only of traffic with the same destination. The traffic encapsulation is presented as a practical emulation of the composite burst aggregation method with- and without IP packet fragmentation. The emulation of the traffic aggregation is performed using real IP packets captured from typical everyday Internet traffic and measurements of the average bandwidth utilization are performed.

In an OBS network, if the burst size is too large then it will occupy the network resources for a long period of time and block the transmission of other bursts. On the other hand, if the load on the input line is too low, then gathering enough packets to make a burst of certain predefined length may take an unacceptably long time. Therefore, a limit has to be placed both on the maximum burst size and the waiting time of the packets in the burst assembly mechanism. To perform all these functions properly, a composite burst assembly mechanism can work as follows:

1. A logical queue is associated with each destination at the edges of the burst switch network.
2. A timer is started whenever a packet arrives in an empty queue.

3. A burst is created and queued for transmission either when the elapsed time equals the burst completion time limit (which could be adaptive to the traffic conditions) or when the size of the queue reaches the maximum data burst size.
4. After the burst is queued for transmission, the timer is reset and only restarted by the arrival of the next packet with the same destination.

Contention for output ports at the core switch can result in burst drops and hence the relevant performance parameters are the blocking probability and the waiting time. It is possible to eliminate blocking by reserving resources at the expense of increased waiting time but a consideration of this is outside the scope of this paper.

Analytical model for Poisson arrivals

The thorough analytical model of the burst aggregation method was published in [122]. The analysis was done in the context of IP packet arrivals that were represented by Poisson process. The analytical model of burst aggregation with Poisson arrivals was numerically evaluated by Matlab code. The mean arrival rate was set to 50000 sec. The maximum burst length was 32 packets and the time out was 0.7 ms. Figure 76 show the probability distribution of the delay experienced by a packet (averaged over burst locations) considering only the length-out and time-out approach, respectively with a sampling interval equal to 13.3 цs.

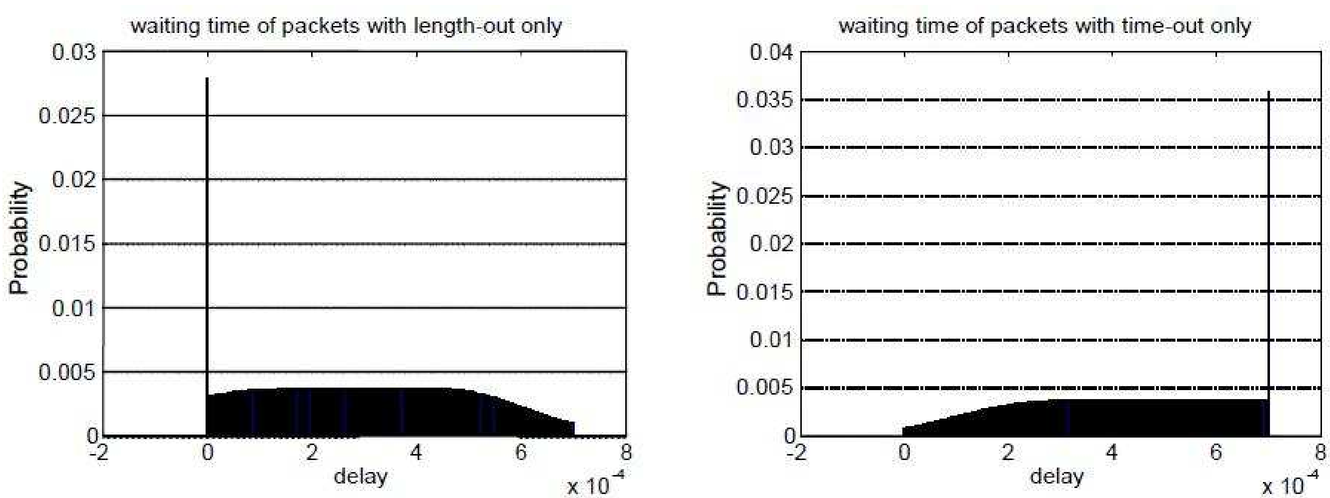

Figure 76; Probability distribution of the delay experienced by a packet [122]

Figure 77 shows the probability distribution of the delay experienced by a packet (averaged over burst locations) combining both the length-out and time-out mechanisms into a single composite burst assembly mechanism. It can be seen that the approximate equations provide a good qualitative description of the exact distributions.

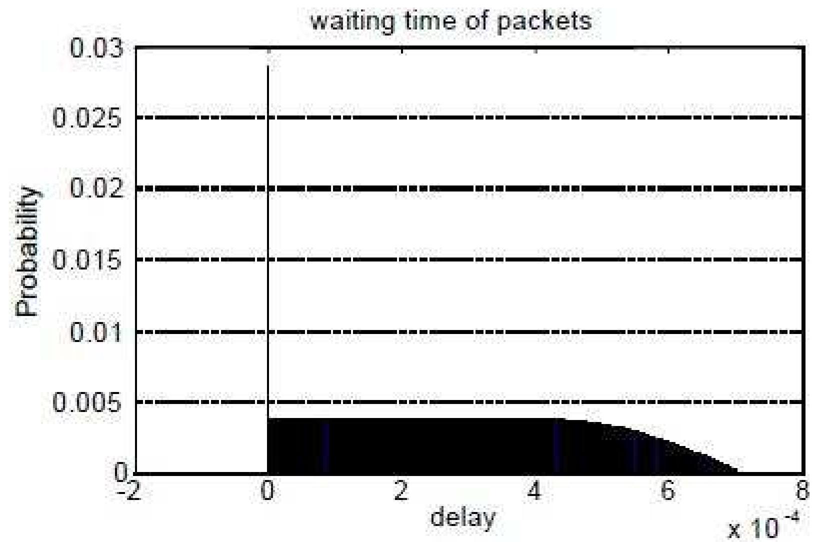

Figure 77; Probability distribution of the delay experienced by a packet considering the composite burst assembly mechanism with a sampling interval equal to 13.3цs [122].

The results of the analytical model and Matlab calculations were confronted with network simulation that was built using commercial tool OPNET Modeler. The example OBS access network consisting of 12 users, 12 edge nodes (ONUs) and 1 core node (OLT) was implemented using OPNET Modeler and the analytical model was used to verify its accuracy. In this simulation, bursts were created and queued for transmission when either the size of the bursts reached its maximum size or the time-out occurred. All the available sources generated Poisson traffic and the transmission speed was 10 Gb/s. The packet size was fixed to 1500 bytes. The maximum burst length was set to 32 packets and the time-out was 0.7 ms. Figure 78 shows the numerical and OPNET density functions together, where it is shown that there is a good agreement between the analytical result and the simulation result for the composite burst assembly mechanism.

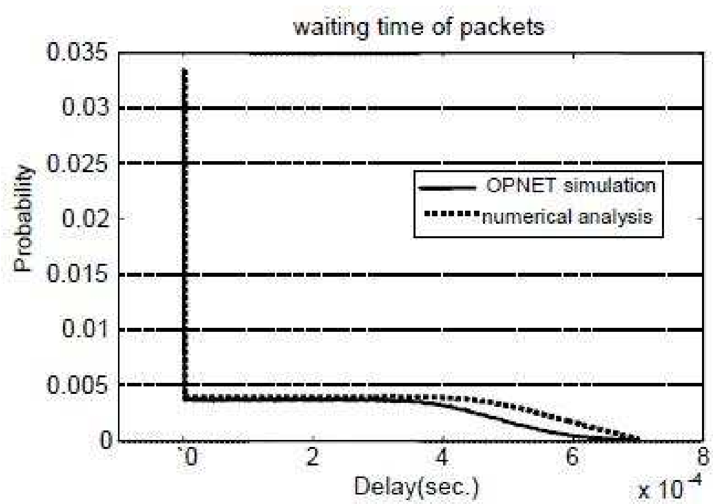

Figure 78; Comparison between the numerical analysis and the OPNET simulation result [122]

The difference between the analytical model and the simulation result arises from the assumption in the analytical model that the inter-arrival times and packet lengths are independent. In the OPNET simulation, each source contains a built-in transmission buffer that queues the generated packets when there is a transmission overlap (i.e., when the interarrival time is shorter than the last packet size), which yields a slightly different arrivals process.

The blocking probability of the composite burst assembly algorithm was also observed and compared with the length-out and time-out approach. The maximum burst size was set to 6396000 bits (533 packets) and the time-out was fixed to 10ms. Figure 79 shows the simulation result at different loads. The observed blocking probability for the length-out only mechanism is systematically lower than the blocking probability for the time-out only mechanism. This is because the time-out only mechanism results in variable length bursts and therefore there are more bursts generated for the same throughput compared to the case of fixed maximum length bursts. The greater number of bursts for the time-out only mechanism is directly responsible for the increased blocking probability. In the composite case and for large burst maximum lengths there is a sharp transition between the essentially time-out mechanism only and the length-out mechanism when $\lambda T = B_{max}$ where λ is the mean packet arrival rate, B_{max} is the maximum burst length in packets (assumed fixed size) and T is the time-out.

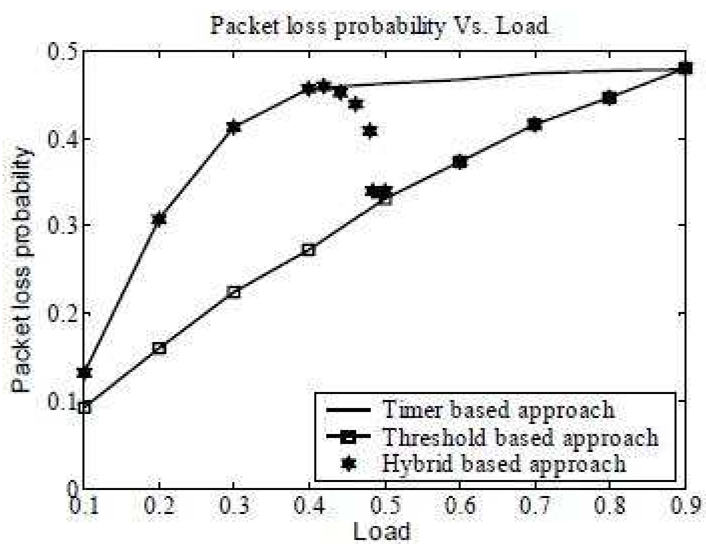

Figure 79; Blocking probability for the different burst aggregation approaches [122]

For the parameters given, the transition between the higher time-out only mechanism limit and the lower length-out only mechanism limit will be started at 40% load and it will be completed at ~50% load. In practice, the parameters would be set in such a way that this transition occurs at much lower loads and hence the higher blocking probabilities associated with the timeout mechanism (timer-based approach) would not be observable.

Encapsulation method

In a TDM-AAPN the incoming traffic to the Edge Node (similarly to ONU in EPON) is aggregated in fixed-size bursts, called "envelopes", which are equal in size to the time slots using the same procedure as used for burst aggregation described in previous section albeit with different parameters. In an OBS-AAPN core switch, resources are released immediately following the end of the burst. In TDM-AAPN, resources are only released at the end of a timeslot and hence the relevant performance parameters are the efficiency of bandwidth utilization and the waiting time. There are two main methods of performing the encapsulation. The first method consists of aggregating an integer number of variable-size packets without performing packet segmentation (Figure 80a). Although this method is fast and relatively easy to maintain, it does not fully utilize all the available bandwidth, because each envelope may be left with some empty space.

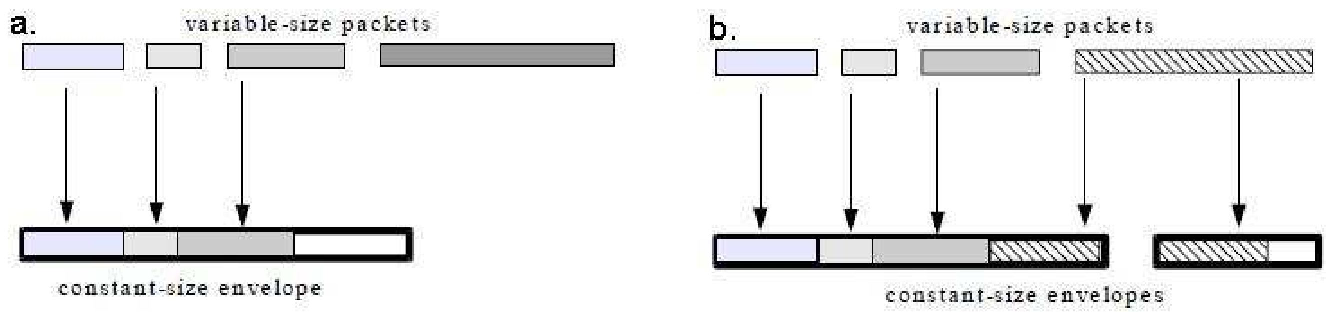

Figure 80; Encapsulation model without (a) and with packet segmentation (b)

The second method permits the segmentation of incoming packets. The envelope is filled with an integer number of packets and the space left is filled with the first part of the next packet in the flow (Figure 80b). The second part of the segmented packet is inserted at the beginning of the next envelope. This method is more complex and introduces a slight additional processing delay, but it significantly improves the efficiency of bandwidth utilization and therefore decreases the overall delay.

Both solutions require information about the encapsulated packets in each timeslot (their number and size) to provide a way of extracting packets from the envelope at the destination EN (ONU). This additional information can be transmitted in the form of a header added to each envelope or as a signal in a dedicated control link. The first solution is relatively easy to implement and to maintain but it reduces the size of the payload in the envelope, so less data can be transmitted. The second solution does not reduce the size of the payload in envelopes but it requires additional synchronization between incoming envelopes filled with packets and their corresponding control signals.

Encapsulation emulation

To evaluate efficiency of bandwidth use in low-cost ONU prototype that was operating in burst aggregation mode, PC-based prototype of the ONU was designed and built similarly to the prototype presented in the chapter 6.6.1. The prototype ONU had the following configuration:

- Hardware: Intel Pentium IV 2.8 GHz + 512 MB RAM
- Operating System: Linux Mandrake 10.0
- Kernel: 2.6.3_7mdk with implemented Multi Protocol Labeling System (MPLS) v1.9

The encapsulation system was a fully software solution written in C under the Linux Operating System (Figure 21). The system was built from three modules. The first module is a scheduler responsible for destination address recognition, and for assigning the incoming packets to the appropriate queues. The second module consists of 128 buffers that represent the output queues in the EN of the AAPN network. The buffers can also represent addresses of 128 ONUs in PON tree, or addresses of 128 subnetworks that PON tree has access to through the OLT. The third module implements buffer serving and timer initialization to ensure that no buffer waits longer than the given time-out. This time limit prevents buffers from waiting too long when there is a low load of packets with the same destination.

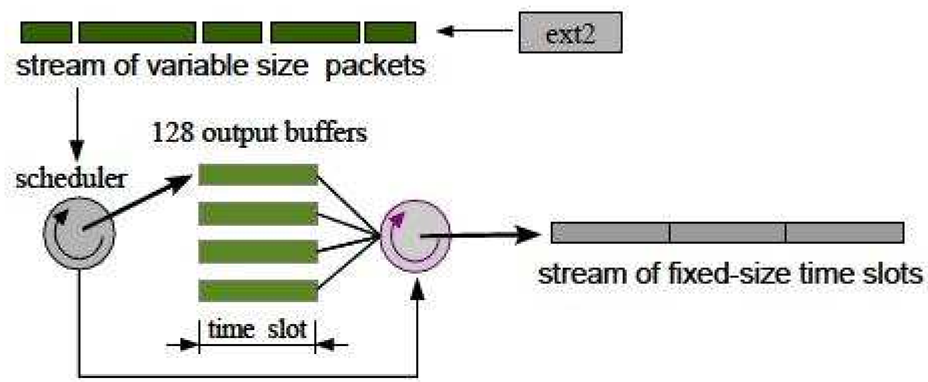

Figure 81; Traffic encapsulation system

The source of the traffic was 11 mln variable size IP packets that had been captured in LAN at the University of Ottawa during week days and saved in *ext2* file system. The purpose of using real traffic for encapsulation testing was to ensure the test environment reflected as much as possible real conditions of traffic load in commercial networks. This approach was innovative because it considered distributions of packets size and their types rather than their arrival times (as it used to be implemented in past). At the first stage of processing, the file with the captured packets was taken under a first quick scanning procedure to recognize the IP addresses (and MPLS labels). The recognized addresses were gathered into groups, and each group was assigned to one output buffer (Figure 81). The next stage consisted of streaming all the captured packets to a scheduler that directed them to the appropriate buffers (one for each destination ONU/subnetwork).

Two encapsulation models were implemented. The first preliminary model consisted of a simple streaming of packets that were then encapsulated in streams of bursts without considering destination addresses and without segmentation of packets (Figure 82). This model was used to easily check with an experimental method if the average size of the empty space in the time slots is stable at a certain traffic load, and how it varies with increasing traffic load. The size of the buffers was chosen as 100000 b, which represents a 10 µs time slot in a 10 Gb/s link. There were no time-outs implemented in this model so the buffers were served (i.e., the envelope released) when the size of the next packet assigned to the buffer did not fit the space left in the given time slot.

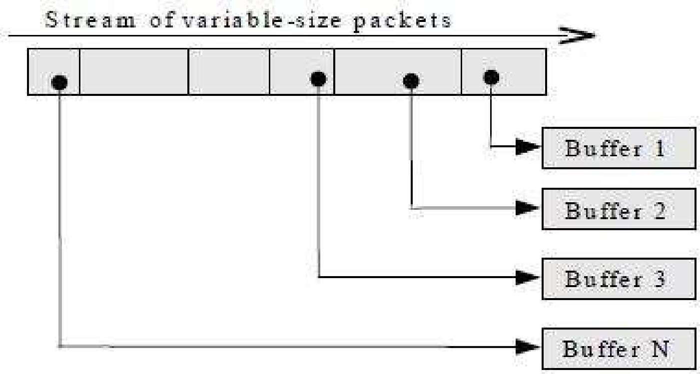

Figure 82; Simple traffic streaming

The second model consisted of the encapsulation procedure with full scheduling; IP/MPLS address recognition, and timers (Figure 83). It was implemented with- and without packet segmentation. A timer was associated with each buffer, which indicated the last time the given buffer was served. The timer information was compared to the real time by the scheduler at regular time intervals. When the difference between the timer and the real time reached the time-out given in milliseconds, the given buffer was served, no matter whether it was full with packets or not.

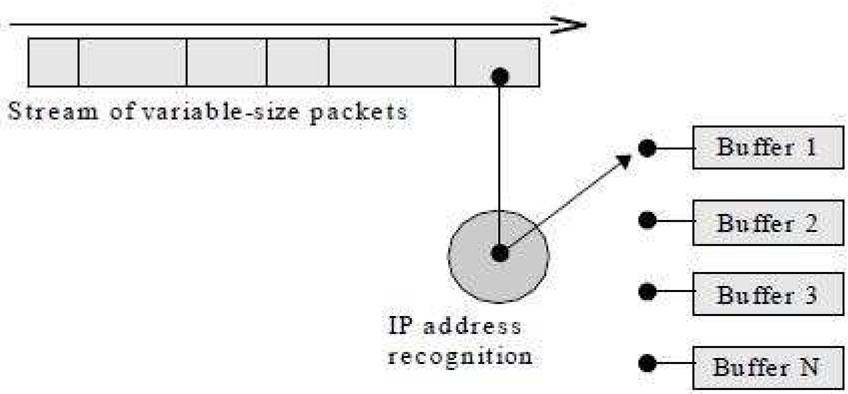

Figure 83; Encapsulation with packet scheduling

The second model gives a more detailed view of bandwidth utilization depending on the time slot size (the maximum burst length) and the time limit for aggregation (the time-out). Because the emulation of the full encapsulation procedure with scheduling and time stamping was performed using a Pentium-IV machine with a speed of 300 Mb/s, the
size of the buffers were chosen as variable from 4 kb to 30 kb, which represent time slots sized 13.3 µs

to 100 μs in a 300 Mb/s link. The time-out was also chosen as a variable between 10 ms and 70 ms to be able to study the impact it has on bandwidth utilization.

The results obtained with the simple packet streaming model without address recognition and without packet segmentation are presented in Figure 84. The encapsulation was performed for a 100 kb envelope and the average speed of the encapsulation procedure was 1822.74 Mb/s (1.78 Gb/s).

Traffic load [MB]	Number of packets	Total empty space [kB]	Average empty space [%]
17.41	63316	206.45	3.13
19.03	169976	611.54	1.16
89.13	958858	706.3	0.77
171.17	1892152	1225.36	0.69
178.44	1917716	1411.95	0.77
342.43	3781268	2489.68	0.71
515.95	5508952	4138.55	0.78
678.58	7372045	5452.85	0.77
859.14	9234669	6769.56	0.77
1030.98	11080952	8109.99	0.76

Figure 84; Results of the simple packets streaming

The above results show that for low traffic load (which is very rare in real networks) there is over 3% of unused space in each envelope, which gives approximately 54.7 Mb/s of wasted bandwidth in a 1.78 Gb/s link. For higher loads the average amount of empty spaces was stable at the level of 0.77% (Figure 85). Considering 1.78 Gb/s of the theoretical output link, this amount of unused space in envelopes results in an unused bandwidth of 14.03 Mb/s.

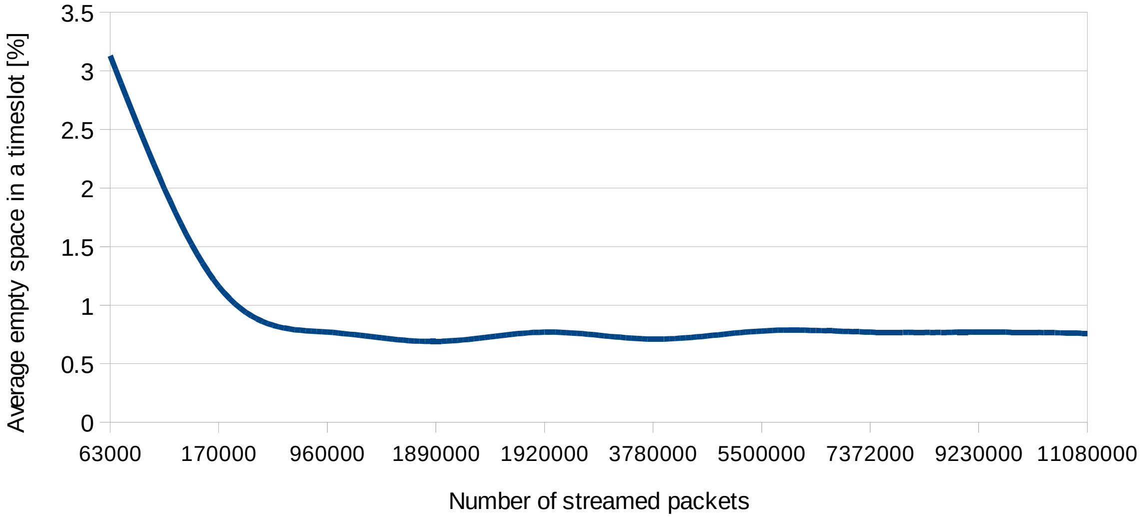

Figure 85; Stabilization of the unused space size in a timeslots

The bandwidth utilization measurements from the full encapsulation procedure performed on real Internet traffic without packet segmentation are presented in figure 86 (envelope and time slot are the same entity expressed in different units; bits and microseconds, respectively). The table shows the relation between the percentage of the underutilized bandwidth, the maximum size of the envelopes and the time-out. It shows that in the case of encapsulation without segmentation, for the shortest time slot the under-utilized bandwidth is relatively stable with the average value of 36.5%, which gives 109.5Mb/s of wasted bandwidth in a 300Mb/s link. With increasing maximum sizes for the time slot, the wasted bandwidth varies non-monotonically.

Figure 87 compares stabilization of the unused space in timeslots for different lengths of the timeslot. It is visible that for shorter timeslots (16 μs and 33 μs) the size unused space becomes stable when timeout reaches 20ms and it does not change much even when timeout is significantly increased. This comparison indicates also that shorter time slots provides better encapsulation efficiency for shorter timeouts, but as soon as timeout exceeds 15 ms the performance of longer timeslots significantly outperform shorter timeslots when the timeout increases.

Envelope	Time-out [ms]							Time slot
[b]	10	20	30	40	50	60	70	[μs]
4000	37.43%	36.61%	36.47%	36.35%	36.29%	36.25%	36.23%	13.3
5000	11.18%	10.10%	9.89%	9.74%	9.65%	9.60%	9.58%	16.7
10000	12.55%	10.21%	9.72%	9.33%	9.12%	9.00%	8.93%	33.3
15000	12.38%	8.85%	8.10%	7.50%	7.15%	6.92%	6.79%	50
20000	12.86%	8.24%	7.20%	6.40%	5.88%	5.59%	5.36%	66.7
25000	15.36%	9.45%	8.00%	6.93%	6.32%	5.97%	5.61%	83.3
30000	17.59%	10.60%	8.91%	7.69%	6.89%	6.42%	5.68%	100

Figure 86; Measured unused bandwidth for full scheduling (no segmentation)

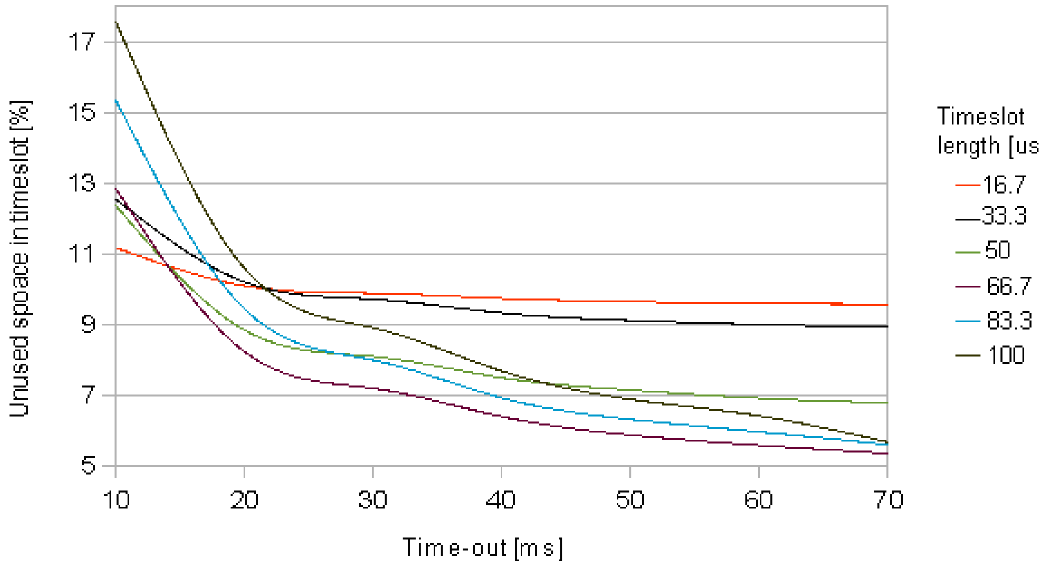

Figure 87; Stabilization of the unused space size in a timeslots (no segmentation)

The amount of underutilized bandwidth reaches the lowest values for time slots of length 50µs and 66.7µs for all values of time-out. For a constant length time slot, the amount of unused bandwidth reaches a minimum for the very large time-out of 70 ms, which will result in long buffering delays.

The results of the encapsulation procedure performed on real Internet traffic with packet segmentation are presented in figure 88, where it is shown that the relation between underutilized bandwidth, maximum envelope/burst length and timeout represents a monotonic function. For every size of time slot, the wasted bandwidth decreases as the time-out increases. It is also easy to notice that the amount of wasted bandwidth increases with increasing maximum time slot length for constant values of time-out; the smallest percentage of unused bandwidth is reached for short time slots and long time-outs.

Envelope	Time-out [ms]							Time slot
[b]	10	20	30	40	50	60	70	[µs]
4000	2.04%	0.86%	0.65%	0.50%	0.41%	0.37%	0.35%	13.3
5000	2.51%	1.06%	0.82%	0.64%	0.53%	0.48%	0.44%	16.7
10000	4.95%	2.36%	1.83%	1.46%	1.18%	1.07%	1.00%	33.3
15000	7.58%	3.71%	2.97%	2.36%	1.97%	1.78%	1.65%	50
20000	10.04%	5.23%	4.15%	3.33%	2.80%	2.55%	2.30%	66.7
25000	12.92%	6.77%	5.40%	4.35%	3.70%	3.34%	3.09%	83.3
30000	15.64%	8.33%	6.61%	5.40%	4.54%	4.18%	3.80%	100

Figure 88; Unused bandwidth during full scheduling (packet segmentation)

The data on bandwidth utilisation was collected experimentally by measuring empty spaces in slots released by the scheduling mechanism for different scheduling models, different length of slot and different timeouts.

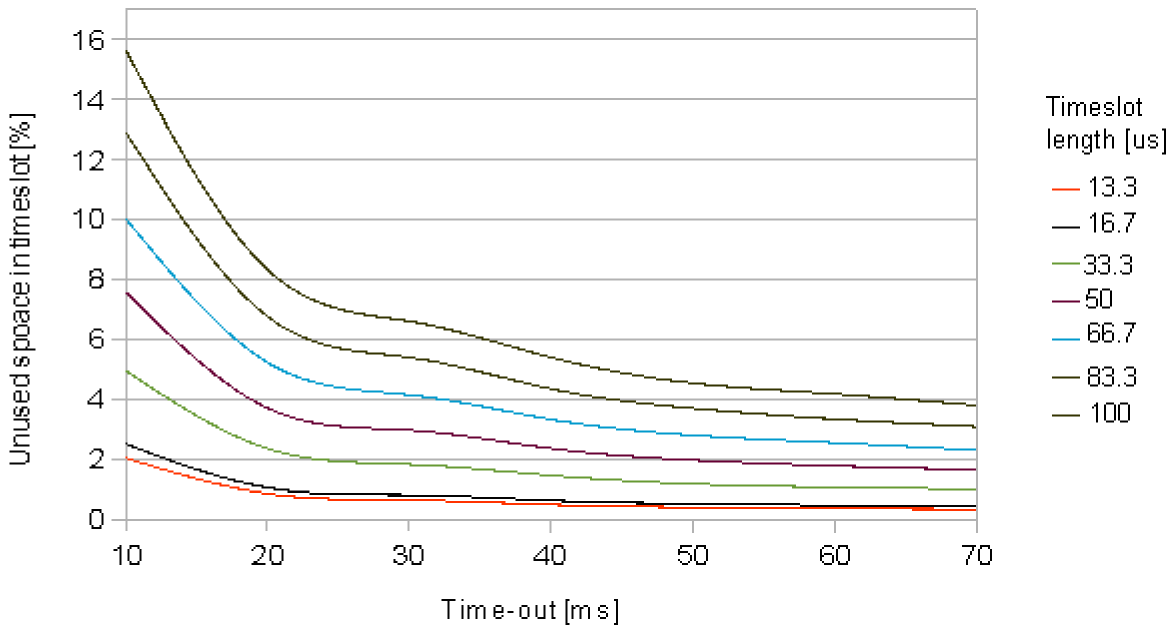

Figure 89; Stabilization of the unused space size in a timeslots (packet segmentation)

Figure 89 compares changes in encapsulation performance for different lengths of the timeslot. The comparison shows a significant difference in amount of unused spaces in timeslots for shorter timeouts. The encapsulation performance increases rapidly for all lengths of timeslot when timeout increases from 10 ms to 20 ms. The performance improvement is mediocre when timeout is in range 20ms-40ms for timeouts longer than 40ms the unused space in timeslots decays very slowly and the differences in wasted bandwidth between different lengths of timeslot does not exceed 1%.

The emulation results obtained for the simple packet streaming model without scheduling confirm the assumption that the amount of wasted bandwidth is relatively stable during the encapsulation procedure when real Internet traffic is considered. For encapsulation without packet segmentation, the size of the envelope must be at least equal to the largest packet size in the network; otherwise these packets cannot be carried (or must be fragmented after all). Emulation results show that the bandwidth utilization is a non-monotonic function of time slot size that first decreases but then starts increasing again for the larger sizes of time slots. This indicates that this method is inefficient when the full range of IP packet sizes is present in the network (the maximum possible IP packet size is 64 kB, which is larger than the basic 100 kb=12.5 kB time slot but was not present in the used LAN traffic) and therefore segmentation will be necessary.

The emulation results for encapsulation with packet segmentation clearly present bandwidth utilization as a monotonic function of time slot size and time-out value. The decreasing amount of unused bandwidth when the time slot size decreases for a constant time-out value suggests that the inter-arrival times were long compared to the time-out (traffic load was low), hence bandwidth utilization can be improved by using shorter time slots. In the case of longer time slots the traffic was not enough to fill up large envelopes in a short time, which is the reason why high bandwidth waste, 15%, has been observed. In this case the bandwidth utilization can be improved only by using larger time-out values, but the improvement will not be significant (3.8% for the 15 kb envelope with 70 ms time-out compared to 0.35% for 4 kb envelope with identical time-out) and the delays would be longer.

Low-cost optical switching node prototypes for PON

Passive optical networks by definition should consist of only passive optical components deployed along optical line between OLT and ONUs. The real conditions where commercial PON infrastructure is deployed and maintained required often implementation of active devices such as optical amplifiers. One of passive components deployed in PON is optical splitter. This device has form of standalone box that is deployed in the field near end user premises. Splitters are rated usually 32 or 64 ports in commercially deployed networks and each arm of the splitter introduce additional loss to the transmitted optical signal. AAPN architecture consists of similar device called selector [119].

Although selector plays in AAPN a similar role to what splitter does in PON, there is an important difference between those devices. Selector is an active device that is remotely controlled and monitored by the control node that is usually collocated with a core node, and splitter is a passive uncontrolled device. Replacing passive splitter by the active optical switching device in PON may bring number of benefits to network infrastructure. Active device can be remotely controlled and monitored, active switch can prevent a data transmission from/to malfunctioning ONU. Implementation of active switch may also introduce a change in the way how downstream data is transmitted In case of passive splitter downstream traffic is broadcasted to all ONUs therefore it is responsibility of each ONU to pick-up its own data from the data stream. Implementing optical switch in PON for downstream traffic would release ONUs form task of examining every incoming timeslot for its destination address.

There was published number of works related to implementing optical switching devices in access networks. In [135] an FPGA based control processor for Optical Burst Mode 3x3 switch is presented. The processor has embedded burst control packet (BCP) process and mechanisms for wavelength switching. The control processor is implemented in Verilog and deployed in Xilinx’s Virtex4 FPGA that runs with 200 MHz clock and serves traffic flow of 1 Gb/s. The scheduling time is about 50ns and the whole processing time of a BCP in core node is about 180 ns. Although this work presents a significant progress in development new technologies that are related switch controlling and scheduling it does not address architecture optical switch fabric.

In [136] proposal of core optical 10 G/s packet switch is presented. The proposed architecture consists of Array Waveguides (AWG) as optical routing components and FPGA system as a control unit. The wavelength modular packet switch architecture is presented on figure 90. Extracting optical header and determining output port is done by a number of switching sub-components placed in parallel and an advanced control mechanism.

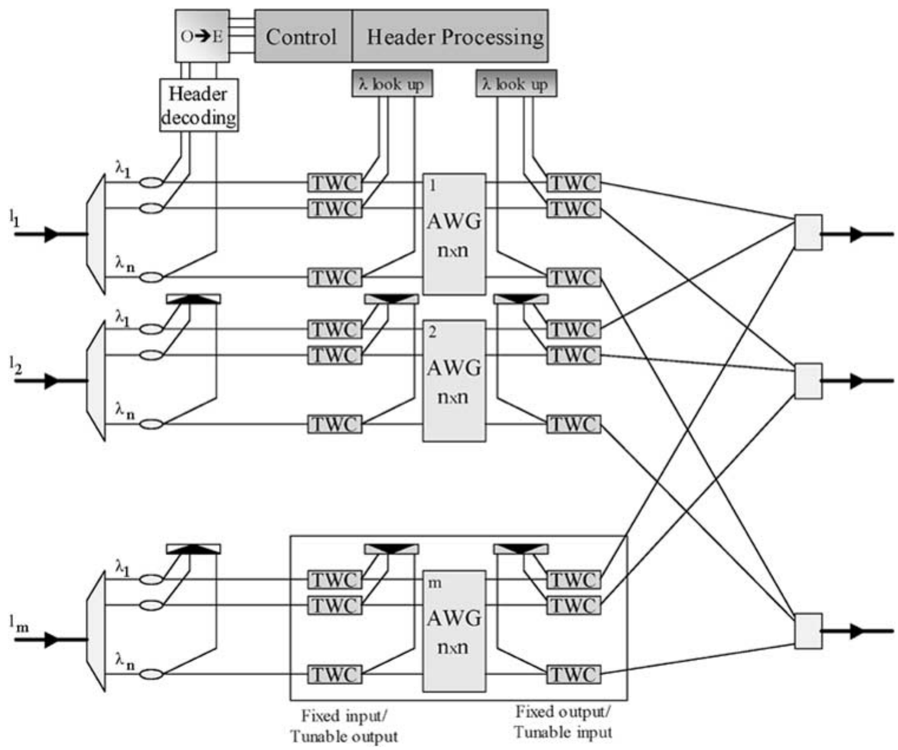

Figure 90;. Optical packets switch architecture. (*TWC*: tunable wavelength converter) [137]

Each switching sub-components receive arriving packets on the same wavelength channel and supports switching to any output port at any wavelength. Space switching of the packets inside the switching element is achieved based on wavelength conversion and selection through an arrayed waveguide grating (AWG). Directing packets to the designated output port is achieved by converting each packet to an appropriate wavelength, thus, establishing a path to the required output port according to the routing properties of the AWG.. Therefore, the conversion wavelength controls the switch path. A second stage of converters is deployed at the output of each switching element, in order to reconvert the packets to wavelengths compatible to the network or/and resolve contention.

Data processing such as address recognition, wavelength tuning for the converter, and new header generation, is performed electronically, but header extraction is achieved all optically using DPSK-based scheme. Additionally, the use of electronics for the control is compatible with the implementation of the higher layer MPLS control-plane mechanism. The control mechanism is implemented in FPGA Xilings Virtex-II Pro. After the header is extracted, the decoded optical signal is converted to the correct input levels for the FPGA. In order to support asynchronous packet transmission, the use of preamble bits at the beginning of the header is required for the FPGA to lock to the phase of the incoming bit stream and identify the start of the information. During the locking procedure, the header bits may be shifted by a maximum of 1-bit header duration (Figure 91).

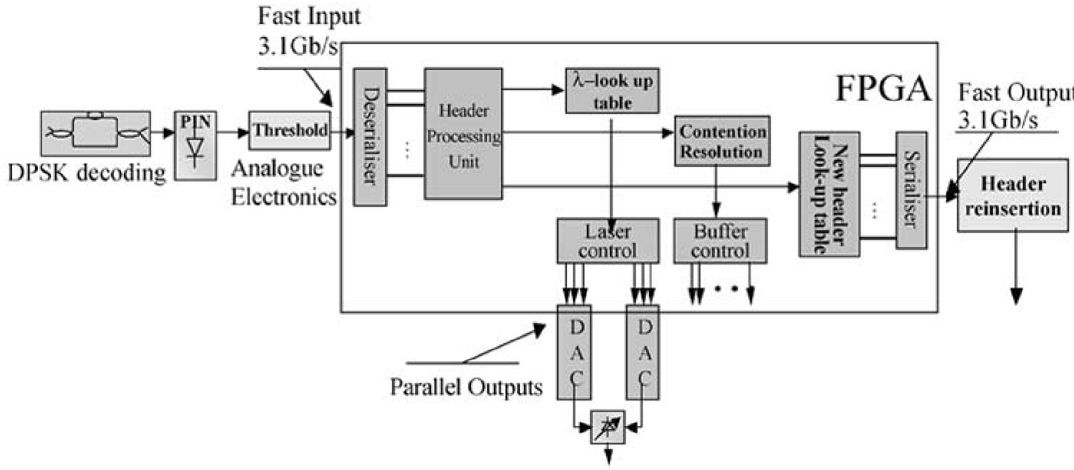

Figure 91; Switch control mechanism implemented in FPGA [136]

The wavelength conversion is realized by a grating-assisted co-directional coupler with sampled grating reflector (GCSR)-type laser. It is a four-section laser diode where one section is used to control the gain and three tuning sections, namely coupler, reflector, and phase are low current inputs used for coarse, fine, and ultrafine tuning, respectively. Accurate wavelength tuning is achieved by injecting currents only into the reflector and coupler sections of the laser, while the phase section is fixed. Tuning currents can vary between 0 and 20 mA and it consists of 1024 different values, which offer a fine resolution for the wavelength tuning. The prototype of the optical switch with the control unit is presented on figure 92.

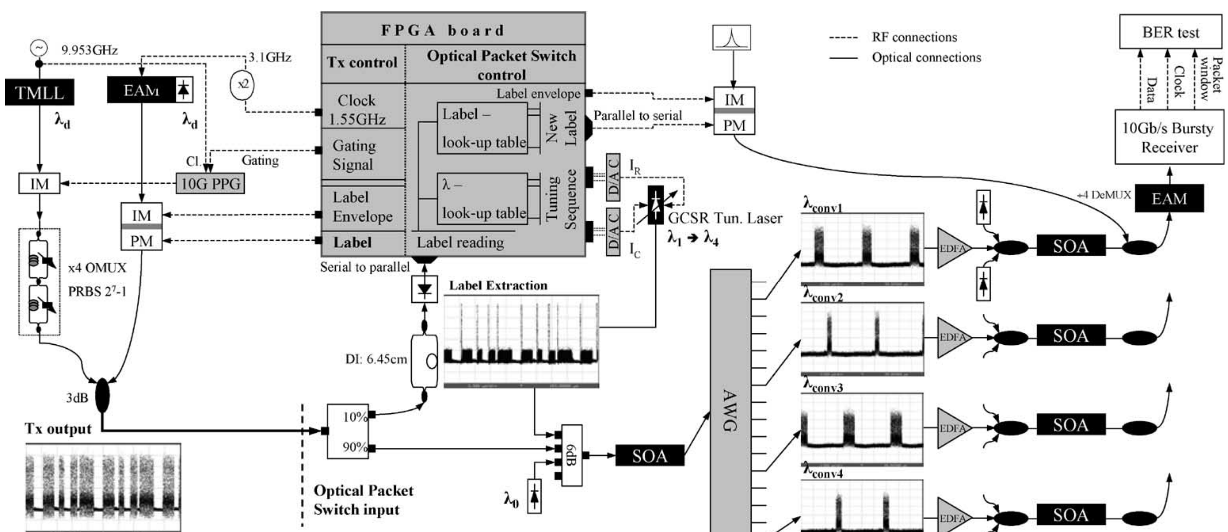

Figure 92; Prototype of the optical switch [136]

The prototype is fed with four asynchronous optical packets with different lengths and distances between them, which are repeated. The payloads are transmitted at 9Gbit/s and consist of 2^7-1 PRBS, while a unique 40-bit header at 3.1Gbit/s is assigned 20ns in front of each payload. The payloads and the header are generated at λ_d (1562.8 nm). At the input of the optical packet switch, a tap coupler separates a 10% copy of the incoming signal for DPSK header decoding through a passive 1-bit delayed interferometer (DI). The extracted headers are converted to electronic using a 6 GHz photodiode and then they are directed to the control part of the FPGA.

Application implemented in FPGA processes the header bits in parallel in order to identify a 10-bit unique pattern inside each header. The identified patterns in headers are compared with the "wavelength" and "new label" look-up tables to prepare appropriate tuning sequence for the wavelength converter and assignment of the new label, respectively. Each tuning sequence (a pair of 10 bits in parallel) is converted to the two current values for the reflector and coupler sections of the tunable laser, which in turn tune the laser to the appropriate control wavelength. The introduced processing delay for the label due to the electronics is 42 ns.

Although above design address issues of switch fabric architecture and switch control module it's very early stage of prototyping does not consider cost of production in larger scale. The proposed architecture offers switching four 10 Gb/s data streams and it ensures scalability by adding internal switching components. Unfortunately the relatively high complexity of the early stage design does not qualify it as a promising candidate for commercial applications.

The prototype the optical 4x4 switch fabric component was presented in [137]. The switching component was build in the form of 16 interconnected optical switch cells integrated on InP substrates. Each single cell involves two passive waveguides crossing each other at a 90◦ angle. The passive waveguides are made of wider band gap material and have low loss at the operating wavelength of 1550 nm. Each cross waveguide point consists of two active vertical couplers (AVC) (Figure 93). The active couplers have feature of either significant loss or gain to the optical signal concerned, and that the gain/loss and refractive index can be modulated by current injection.

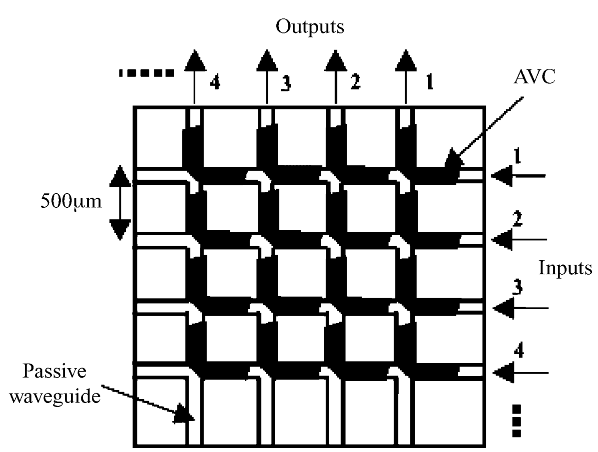

Figure 93; Architecture of the optical 4x4 switch [137]

A total internal reflection (TIR) mirror cuts vertically through the active waveguides and diagonally across the waveguides intersection, allowing the 90◦ redirection of the optical signal. The switching is done through by simultaneous refractive index and gain/absorption modulation. The prototype has physical dimensions 2.5mm x 2.5mm and works with switching current 250 mA and 1.5 V signal (Figure 94).

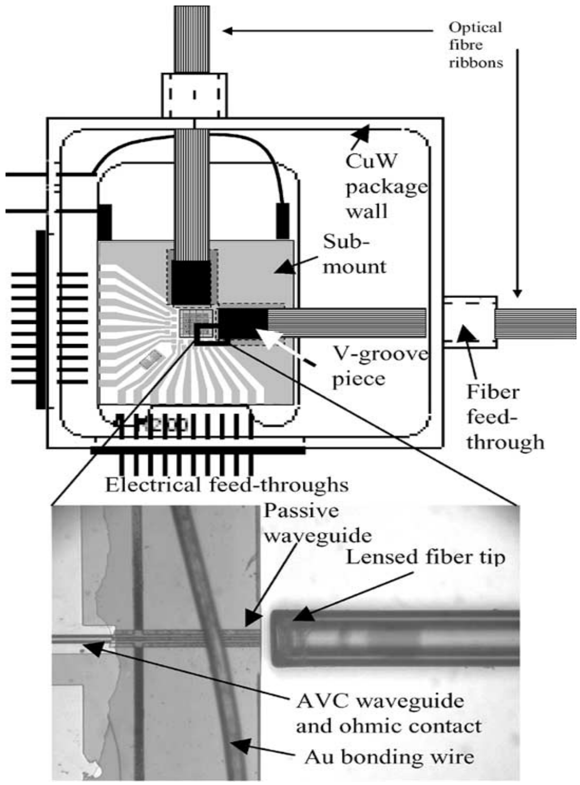

Figure 94; Packaging of the switch prototype [137]

The device was successfully operating with switching frequency 1 MHz when 2W TEC component was applied to the device. The designed component has very small physical size and that qualifies it to be integrated with other photonic components. Although small size of the component and simplicity of switching control make it very attractive candidate for commercialization it does need to have addressed problem of cooling when switch is scaled up to larger number of ports, for example 256x256. The temperature monitoring of each switching component is a key issue that has to be addressed to ensure reliability of the system in a long term operation.

There are more works related to optical switching and routing architectures such as [138], [139], [140], [141]. The reported research projects focused mainly on only one aspect of the optical switching such as control mechanisms, electro-optical signal conversion, low scale optical switch fabric, switching algorithms or temperature monitoring. Very few projects were accomplished to address all aspects of the switch design and development and therefore very few fully functional prototypes have been developed.

Great majority of the prototypes that qualify for commercialization implement electro-optical signal conversion where receiving and transmitting data is done in optical domain while packet header analysis and internal routing between ports is performed in an electrical domain. The hybrid electro-optical architecture is also often implemented in optical switching devices that are already commercially available, but due to their high manufacturing cost they are mainly deployed in enterprise network infrastructures.

Gigabit optical Ethernet switch

An innovative prototype of the low-cost 2x2 optical switch was designed, built and tested at the Centre for Research in Photonics at the University of Ottawa. Number of constrains were considered during design process to ensure that final product is not only compatible with existing optical technologies implemented in optical access network but also it can be built using existing widely available components.

The following constrains were included in optical switch design:

- Compatibility with existing fiber optic gigabit Ethernet standard IEEE 802.3z [142]. The clause 38 of this standard defines optical infrastructure that operates at 1 Gb/s in O-band (1260-1360 nm) over the single mode fiber.
- Compatibility with existing copper gigabit Ethernet standards
- The system has to be manufactured with a very limited budget (not exceeding $2000 US)
- Device has to be built from widely available off-the-shelf components that require minimal (or none) modifications
- The final product has to have form of key-ready system that can be immediately deployed in existing access network
- Maintenance of the system should be simple and it should not require any sophisticated training
- The system has to be upgradeable to higher speed of 10 Gb/s according to the standard IEEE 802.3ae [143].
- The optical switch has to be capable of communicating with O-band (1260–1360 nm), E-band (1360–1460 nm), S-band (1460–1530 nm) and C-band (1530-1565 nm) devices.
- The switch should have embedded technology that allows for remote monitoring and configuring

The PC platform was chosen to be the hardware foundation for the system. This is flexible and multi purpose hardware framework that allows for building low-budget systems. The hardware platform that was used in prototype was:

  - Motherboard: Asus P2B-F with five PCI 32 bit interfaces that operates at 66 MHz clock
  - One 100Mb Ethernet port for remote monitoring and configuration
  - Processor Intel Pentium II 266 MHz with 512 KB cache memory
  - RAM: SDRAM 256 MB

The configuration implements processor that is significantly underpowered when compared to average standards in consumer computing products such as Intel Core 2 Duo 2GHz. This drawback had to be accepted due to the requirement of main board to have multiple minimum five PCI interfaces.

The optical interfaces were implemented using four 64bit PCI Ethernet extension cards with transceiver Optoway TRS-7110-EM (Figure 95). The transceiver emits 1.25 Gb/s signal on 1310nm wavelength with output power -3dBm and detects wavelengths 1100 nm-1600 nm with sensitivity from -21 dBm to -9 dBm. The maximum transmission distance for this card is 10 km.

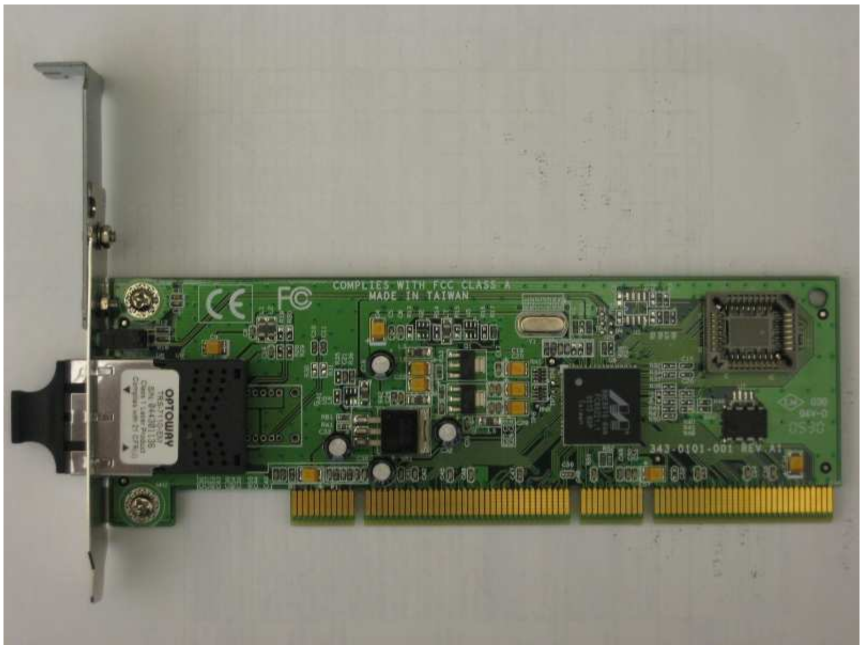

Figure 95; 1.25Gb/s optical Ethernet card with 64bit PCI interface

The gigabit Ethernet cards were down-compatible with 32bit PCI interface and they had SC optical dual-connector for two SMF fibers.

The operating system chosen for the switch was Linux Mandrake 10.1with modified kernel. The kernel modifications were implemented to remove unused functionality from the core of the system and therefore to make it lighter on memory usage and more responsive. Kernel had also embedded functionality that allows packets forwarding, routing and filtering based on content of MPLS, Ethernet and IP headers.

The switch had implemented software tools for the real time monitoring number of characteristics such as: traffic load in optical input and output ports, memory use, processor load, system processes activity, speed of traffic processing and internal routing. The switch was capable of sending and receiving control and monitoring signal in in-band and out-band model. In the out-band model the control signal can be transmitted through dedicated 100 Mb Ethernet port that is not involved in switching or routing process. In the in-band model the control signal can be transmitted through any of the optical ports and Ethernet frames that carry control data are automatically redirected to process hat is responsible for configuration and monitoring tasks.

The switch functionality has been implemented in the form of software applications to ensure its flexibility and easy upgrade. The optical Ethernet frames are examined upon arrival for the content of the header. The decision is takes if the frame consists of a regular data or a control information. If control information is detected the packet content is forwarded to the configuration module that is responsible for general switch configuration. If plain data is detected the frame is forwarded to the routing module that is responsible for appropriate forwarding the frame to the output port based on content of the destination address field. The internal routing table can be static (created manually by the network operator) or dynamic (created and modified on-the-fly based on information about addresses reported by subnetworks/nodes connected to the switch ports.

The switch can operate in any of the three predefined modes (or their combination) depending on the addressing scheme implemented in the network where switch in deployed:

- Raw Ethernet - In this mode switch is not aware of content in the data field content in the frame except when frames carry control data in in-band fashion. The addresses of ports are Ethernet only and internal routing table consists of Ethernet addresses only.

- IP over Ethernet - In this mode switch examines content of Ethernet frames and analyzes IP headers of packets encapsulated in frames. The internal routing is performed based on IP packets addresses (subnet addresses).

- MPLS over Ethernet - In this mode Ethernet packet is examined for the content of MPLS [144] labels and internal routing is performed according to MPLS labels.

To evaluate performance of the PC-based switch an experimental optical network was built and configured as shown on figure 96. The optical switch, called also core node, (CN) was connected to four client workstations through 20 meters long single mode fiber and it was also connected to monitoring and control node through copper Ethernet. Each edge node workstation (EN) was equipped with optical Ethernet interface identical to the interfaces that were implemented in the switch (Figure 96) and one copper Ethernet interface for connection with the monitoring node.

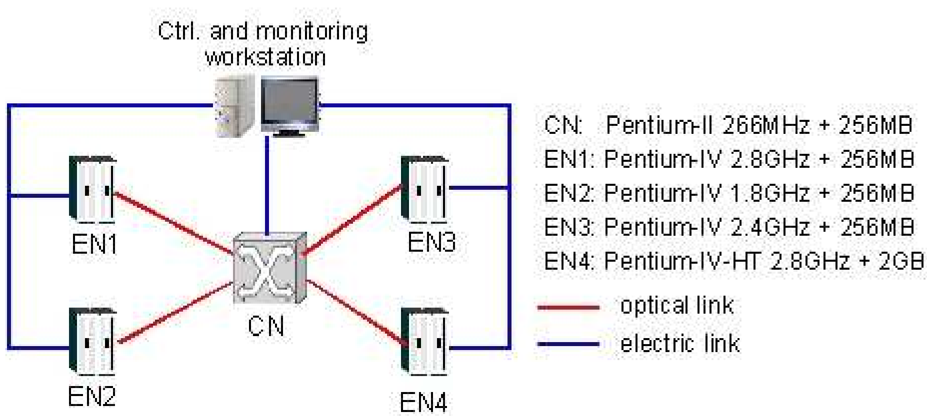

Figure 96; Test network built to test the switch performance evaluation

To estimate the CPU load a benchmark was performed by switching several logical links established between edge nodes. The data was transmitted in a fashion: "everyone to everyone", where each source was transmitting data to two destinations and each destination was receiving data from two sources. There were 23 logical channels deployed over 4 physical links. The source of the traffic was data collected from real LAN described in chapter 5.

There were performed two types of measurements in test network: total CPU load in the switch and total data rate of the traffic flowing through each port in each direction. The measurements provided information about the benchmark that can be achieved with this particular configuration of the switch and combination of software and hardware.

The results of the benchmark test are presented in figure 97. When standard MTU 1500B Ethernet frame is applied the CPU in the switch exhibits 36% of processing load and 184Mb/s data rate per port. When MTU 9000B frame (large Ethernet frames introduced in IEEE 802.3 to reduce CPU utilization) is applied the CPU total load drops down to 16% and observed data rate per port increases to 224 Mb/s.

Ethernet frame size	CPU load	Data rate per port (one direction)
1500B	36%	184 Mb/s
9000B	16%	224 Mb/s

Figure 97; Optical switch benchmark test results

Considering that each port was receiving and transmitting traffic then total throughput per one port was rated at 368 Mb/s for 1500 B frames and 448 Mb/s for 9000 B frames.

The obtained results indicates that PC-based low cost optical switch that has implemented an outdated low-budget processing unit can handle edge nodes (ONUs) with data rate exceeding 220Mb/s of downstream and upstream transmission. This data rate is over twenty times higher than data rate offered by existing commercial xDSL infrastructure. This is a very good result considering limited budget and resources that were available to build this prototype.

There are number of modifications that can be introduced to the optical switch to improve overall performance. Those modifications do not require significant financial investment but they can bring the prototype that can be a good candidate for commercialization.

Data rate transfer between optical ports and processing unit

The data inside of the switch was transmitted 32bit PCI bus that worked with 66MHz clock. This bus can transmit total 2112 Mb/s (66 MHz x 32bit) of the aggregated data between all components of the system that are connected to the bus. The total capacity of the bus is shared by number of components in the switch such as: memory, USB controller, processor, PCI extension cards, hard drive controller and graphical processor unit (GPU). Since PCI bus is shared by so many system components there is a limited bandwidth available to optical interfaces for the internal data transmission. This particular hardware configuration had approximate 896 Mb/s (4x224 Mb/s) of bandwidth occupied by optical ports for data transfer and that represents about 42% of total PCI bandwidth.

The solution for this problem can be implementing a higher clock rate to the PCI bus. By increasing clock to 133 MHz there can be a significant total bandwidth increase to 4256 Mb/s (133MHz x 32bit) and bandwidth available to optical interfaces will be increase to 1.7 Gb/s if the 42% factor is applied. This in result will provide each optical port with bandwidth of approximately 446 Mb/ for each direction of the data transfer.

Internal bandwidth available to optical interfaces
The PCI bus that was used in the prototype had data width of 32bit but extension cards with optical interfaces were designed to work with PCI 64bit bus. The downgrading data width to 32bit forced optical interfaces to work in a bottle neck conditions. Implementing 64bit PCI interfaces will increase total internal bandwidth to 4224 Mb/s if 66 MHz clock is applied, and 8512 Mb/s if 133MHz clock is applied. This solution can increase bandwidth available for optical interfaces to approximately 3.5Gb/s if 42% factor is considered. This would provide 893 Mb/s of available internal bandwidth to each optical interface.

Central processing unit (CPU)
Although speed of the main processor is not as critical for the switch performance as the bandwidth of the internal bus, its impact on overall sped of switching can not be totally neglected. Since almost all the switching functionality has been implemented in the form of the software, there has to be an appropriate CPU provided to the system to ensure that all software tasks are performed as efficient as possible.

Interrupt requests (IRQ)
An interrupt request (IRQ) value is an assigned location where the computer can expect a particular device to interrupt it when the device sends the computer signals about its operation. IRQ is generated by hardware device and it forces CPU to stop is primary tasks to provide service to the device that generated the IRQ. In certain circumstances too many generated IRQs may significantly slow down CPU therefore it is generally recommended to disable IRQ that are assigned to unused devices such as USB, RS232, Bluetooth, keyboard, mouse, floppy disk.

The presented switch prototype successfully proved concept of the low-cost active switching device that not only is compatible with existing optical Ethernet technologies but also can be built using widely available of-the-shelf components. The switch is transparent for the transmitted data therefore can work in a stealth mode where network is not aware of its presence. It can work as router or switch as well as it can provide content routing services where traffic is routed/switched based on the content of the optical packets. The switch prototype presents also an innovative concept of hybrid electro-optical node that provides bridge functionality between interconnected PON trees.

The electro-optical signal conversion is a fundamental technology that switch is build on. Although this conversion does introduce certain delay to the traffic processing it allows for number of operations to be performed on packets headers or their content such as content routing, MPLS forwarding, firewall and traffic filtering.

The switch prototype presents innovative approach to design and developing low cost network devices that introduces affordable form of combination optical and electrical network interfaces. In addition it offers great flexibility of supporting Data Link Layer (Ethernet) and Network Layer (IP) and hybridization both layers (MPLS). It also offers implementation additional functionality such as packets and frames filtering, and content switching. Although there are commercial products that offer electrical and optical interfaces, they have number of limitations such as:

- number of optical interfaces is limited to two
- switching functionality is limited to Ethernet frames
- content routing is not available
- gigabit optical ports are used mainly as trunk link that interconnects sub-networks (bridging functionality) therefore device work as Ethernet multiplexer rather than regular switch

The example of the commercial device that provides electro-optical Ethernet switching functionality is TC3845 that is built by TC Communications Inc. The device comes with four 100Mb copper Ethernet ports and two 1G optical Ethernet ports (SFP). Cost of the device exceeds $3500 and the device only supports Ethernet frames.

The switch prototype has certain disadvantage of high power consumption (approximately 300W) that exceeds power consumption in off-the-shelf commercial devices (100W), but this aspect can be addressed when new generation energy efficient components are implemented.

Migration to 10Gb/s

Although optical switch presented in previous section does provide low-cost switching and routing functionality within gigabit optical access networks (including PON) its basic configuration does not support optical 10Gb Ethernet. To ensure the switch supports 10 Gb/s optical transmission there have to be introduced significant changes in hardware configuration.

<u>Optical Ethernet interface</u>
To ensure 10 Gb/s compatibility the appropriate optical interface cards has to be implemented. New generation of PCI-X and PCI-E extension cards come equipped with optical 10 Gb transceivers. Example of the 10 Gb optical interface is presented in figure 38. It is a dual-port optical interface build on 64bit PCI-Express extension card Intel SR 82599.

Figure 98; 10 Gb/s optical extension card (Intel SR 82599)

The 10 Gb/s extension cards come in variety of configurations with up to four optical ports. Ports are often implemented in the form of SFP or XFP plug-in components therefore they provide flexibility of choosing wavelength and optical output power.

Internal communication bus

Since capacity of basic PCI bus can not provide bandwidth sufficient for 10 Gb internal routing there has to be implemented an alternative technology with wider bandwidth and/or higher clock rate. There are two good candidates to fulfill this requirement: PCI-X [145] and PCI-E buses.

PCI-X is a 64bit communication bus rated with clocks from 66MHz up to 533MHz that allows for data transfer up to 34Gb/s. Since PCI-X 2.0 standard has some limitation related to data transfer speed of operation there are allowed only specific configuration of the hardware. For the clock speeds of: 66MHz there are allowed up to four expansion cards, clock speed of 100Mhz allows for two expansion cards, and clock speed of 133MHz, 266MHz, 533MHz allows only for one expansion card. To ensure that PCI-X can support 10 Gb/s data rate a configuration with 266MHz or 533MHz will be appropriate (one card with multiple SFP interfaces).

PCI-Express [146] (PCI-E) is a 64bit communication bus that offers total bandwidth of 64 Gb/s in version 1.0. The PCI-Express is favored over the PCI-X by hardware manufacturers because it can be implemented in serial configuration (instead of old parallel configuration used n PCI-X) that allows for much higher clock rates.

Central processing unit

When data rate of 10Gb/s is considered a higher processing speed is demanded from CPU to handle the traffic flow. Good candidate for low-cost processing unit for 10Gb/s data flow is AMD Opteron. This CPU has 64 bit dual core architecture and an embedded memory controller that supports up to 8 registered memeory modules (DIMMs). Opteron has impemented also the HyperTransport technology [130] that allows up to 25 Gb/s aggregated data transfer in both directions between the CPU and I/O devices in 16 virtual channels. Other important features are the 1MB L2 cache memory that can be used for fast queues of packets / slots, and the 64KB L1 cache that can be used for high speed aggregation of packets into slots.

Migration to 40Gb/s and beyond

Optical Ethernet interface
To ensure that optical switch satisfies data rate 40 Gb/s and higher a new type of extension card with optical interface has to be implemented. The new commercially available interfaces are implemented in PCI-Express 2.0 cards with 40 Gb/s XFP plug-in transceivers (Figure 99).

Figure 99; 40Gb/s optical PCI-Express 2.0 extension card (ConnectX-2)

Internal communication bus
Ultra fast communication bus is required in PC-based optical switch to ensure it can handle processing and internal routing frames that arrives in 40 Gb/s data rate. Good candidate is PCI-Express 2.0. This bus offers data transmission up to 64 Gb/s in 16 parallel lanes. Another commercially available bus technology is PCI-X 3.0-1066 that supports 40 Gb/s data transfer.

If switch is deployed in a network where data rate reaches 100 Gb/s then the PCI-Express 3.0 bus will be required. This particular bus offers 128 Gb/s aggregated data rate in 16 parallel lines. The newest bus technology that will be present soon in commercial computing devices is PCI-X 3.0-2133. This particular bus technology should exceed 160 Gb/s of data rate but it is still in a research and prototyping stage.

Central processing unit
When data rate reaches 100 Gb/s a high end processor unit is required to handle efficient processing of traffic flow. The promising candidate is Intel i7 Extreme Edition [147]. This CPU runs with 3.7 GHz internal clock and it offers approximate 200 Gb/s of data transfer to/from external devices.

The market of consumer computing devices is dynamically changing and constantly brings new technologies that offer overwhelming computing power. This is an excellent source for wide range of components that can be used to build next generation prototypes of low-cost network devices that will be able to satisfy requirements related to multi gigabit optical access networks without expensive and complex all-optical packet processing.

Certain drawback of developing hybrid multi gigabit electro-optical switching devices is significant increase of energy consumption when throughput is increased. 40 Gb/s electro-optical switch build ion PC platform would require approximately 400 W of power supply to satisfy the processing unit. Although power consumption is a challenging issue, low cost hybrid technology is a promising candidate for transition from old all-electrical switching to the future energy efficient all-optical switching technologies.

Optical amplifiers in PON

This chapter presents a study of innovative application commercial grade Semiconductor Optical Amplifier (SOA) that was implemented in three different configurations in OC-48 PON: power booster (located at the beginning of the optical line), inline amplifier (at the half way of the optical link) and preamplifier (located before photo receiver). To ensure that test system reflects natural conditions of commercial infrastructure a section of the public telecommunication network in the City of Ottawa was used as optical line for amplifier evaluation and this also reflects an innovative approach to test bed systems design and configuration. Comparison of SOAs performance in different configurations is presented and drawbacks of each configuration are evaluated. The chapter presents also implementation of DWDM technology to improve SOA performance and increase capacity of PON.

The chapter provides also a study of innovative applications of SOA as an optical switching component. The prototype of a SOA-based optical switching device was built, its performance is evaluated and its signal response is characterized. Certain effects that were observed in SOA signal response had not been published before. The chapter describes observed effects and proposes their possible explanation.

The chapter reports also an innovative energy efficient controller for the SOA based switch. The controller is built using low cost FPGA components and consists of a software application for generating 81 parallel signals for 9x9 switch reconfiguration. The controller supports 47Gb/s data rate with the frame-by-frame optical switching mode. The performance of the switch is evaluated and available methods of further decreasing its physical dimensions and improving its energy consumption are also presented.

As it was pointed out in previous chapters, optical telecommunication networks suffer from a number of drawbacks that require certain modifications and upgrades to ensure the network is ready for expansion. The main issue to be dealt with when the optical network infrastructure is designed and deployed is signal loss. The signal loss can be caused not only by the length of the optical fiber but also by interconnections, splitters, splices, fiber adapters and fiber line imperfections such as damages and excessive bending of the fiber.

General characteristics of commercial solutions

There are two models in which the optical signal is amplified in telecommunication infrastructure. The first model involves implementation of a device called a *repeater* [148] [149] that implements electro-optical signal conversion. In this scheme, an incoming optical signal is detected by the photoreceiver and the information it carries is decoded into an electrical digital signal. The electrical signal is taken under the process of noise filtration and then it feeds the device for optical modulation in the optical transmitter (Figure 100).

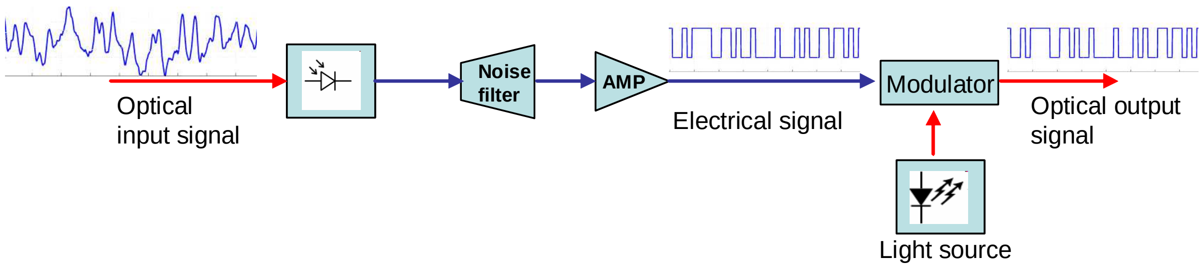

Figure 100: General architecture of the optical repeater

This model provides certain flexibility in configuration and maintenance because it allows for modular design of the repeater where each element can be easy replaced in case of failure. The drawback of this model is requiring a dedicated power supply for each component: photo receiver, noise filter, amplifier, light source and optical modulator.

This model of signal amplification also carries another drawback which is that the repeater can only support a limited data rate. The data rate of the incoming optical signal must match the data rate of the electrical circuit to ensure sufficient performance of the amplification system. The sensitivity of the photo receiver should be at a maximum at the wavelength of the incoming optical signal. Increasing the data rate in the optical line or changing the wavelength usually requires significant modification of the repeater which will increase the operational costs of the device.

Another issue that should not be neglected is a delay introduced by the opto-electrical and electro-optical signal conversion implemented in the repeater. This delay may be critical for the transmission of data such as real time audio/video.

A different model of signal amplification implements an all-optical approach that does not require any electro-optical or opto-electrical signal conversion. This model provides a gain medium that is transferred to a high energy state by a pump laser and then releases the energy in the form of radiation that has a wavelength equal to the wavelength of the telecommunication signal. The commercial devices that implement this model are: the fibre Raman amplifier (FRA) [166], erbium doped fibre amplifier (EDFA) [166], erbium doped waveguide amplifier (EDWA) [166] and praseodymium doped fibre amplifier (PDFA).

Fibre Raman Amplifier

Fibre Raman Amplifier (FRA) uses glass fibre as the gain medium. The optical signal amplification is a direct result of the non-resonant and inelastic process called stimulated Raman scattering (SRS). Energy is transferred to the telecommunication signal from a shorter wavelength pump via the glass molecules that are excited causing them to vibrate. FRA has a lower gain per unit length when compared to EDFA and therefore it requires longer fibre spans than EDFA to provide a similar performance. The FRA guides light at both the pump and signal wavelengths and it is normally a single mode to ensure the best overlap of all traveling waves. The highest gains are achieved by using fibres with small effective areas and low losses. Raman pumping can be co-directional, contra-directional or bi-directional with respect to the signal. To minimize the transfer of relative intensity noise (RIN) from the pump laser to the signal, a contra-directional launching is often preferred. Moreover, backward pumping averages out any polarization-dependent gain.

One of the biggest advantages of FRA over the EDFA is that FRA does not require special dopants embedded in the optical fibre. The common type of telecommunication fibre or dispersion compensation fibre can be implemented as an amplifying medium. In addition, Raman scattering is inelastic and it occurs as a shift to a band of lower frequencies (i.e. longer wavelengths) from the pump. Therefore, the gain can be provided at almost any wavelength by appropriate selection of the pump laser. In SiGe (silica-germania) fibres, the peak shift is about 13.2 THz from the pump and it has a full width at half the maximum bandwidth of about 7 THz. A single channel gain in the telecommunications C-band (from 1530 nm to 1565 nm) requires the pump to have a shorter wavelength by about 100 nm. Similarly, by using pump lasers with suitable wavelengths and powers, Raman amplification can be obtained in any part of the S-band (from 1460 nm to 1530 nm) or L-band (from 1565 nm to 1625 nm).

Commercial FRAs are usually sold in the form of a standard 1U size slide-in module that is compatible with telecommunication racks. Figure 101 presents an example of a commercial amplifier FA-RAMAN-3-15 that is made by Passcomm Corporation. The amplifier operates in the wavelength range of 1530-1562 nm and its optical gain is 15 dB. It can work within an optical input power range of -40dBm to +5 dBm, and the maximal optical output power is 700 mW at a noise figure of less than -1 dB.

Figure 101: Optical Raman amplifier FA-RAMAN-3-15

Erbium Doped Fibre Amplifier

Erbium Doped Fibre Amplifier (EDFA) [150] is built from a single mode optical fibre with a core that has been doped with trivalent Erbium ion Er^{3+}. The amount of the dopant is usually in the range of a few hundred parts per million. The gain is provided through a stimulated emission, similar to a laser. The dopant ions act as a three-level energy system in which the main participants are the $^{4}I_{15/2}$ ground state, the $^{4}I_{13/2}$ first excited level and the $^{4}I_{11/2}$ second excited level [151]. The net gain is obtained by pumping to achieve a population inversion in $^{4}I_{13/2}$ with respect to $^{4}I_{15/2}$. The $^{4}I_{13/2}$ level has a long lifetime in the range of 10 ms (in silicate fibre), which enables high population inversions with low pump powers. Upon achieving inversion, the stimulated emission exceeds absorption and so the signal at the wavelength corresponding to the energy difference between $^{4}I_{13/2}$ and $^{4}I_{15/2}$ is amplified. The $^{4}I_{13/2}$ - $^{4}I_{15/2}$ energy differences correspond to wavelengths around 1550 nm and those wavelengths experience signal amplification.

Figure 102 presents an example of a commercial EDFA amplifiers built by Nuphoton Technologies Corporation. It provides an amplification of 27 dB at a noise figure of 5.5 dB and it works with telecommunication L-band and C-band. The unit is shipped as a standard 1U size module to be mounted in a telecommunication rack.

Figure 102: Optical EDFA amplifier NP2000PR

Erbium Doped Waveguide Amplifier

Erbium Doped Waveguide Amplifier (EDWA) [151] [152] operates mainly on the same principles as EDFA. The main difference between EDWA and EDFA is that EDWA has the form of a planar glass waveguide offering potentially lower production costs and the prospect of integration with other components, such as splitters and multiplexers. The host glass for the Er^{3+} ions is selected to enhance the pump absorption and gain profile. Germano-silicate and phospho-silicate are common choices. In glasses that permit it, the increased refractive index required to define the waveguide can be achieved by doping with metal ions.

The main issue in the EDWA design is providing sufficient gain within a small form factor structure. The three main methods are:

- Using Er3+ doping levels that are an order of magnitude higher than in EDFAs to increase the useful pump absorption.
- Fabricating waveguides with a high refractive index difference *Δn*.
- Designing the waveguides as folded spiral structures to maximize their overall length.

High *Δn* waveguides can have a smaller bend radii which enables greater folding, but they have higher fibre coupling losses and this creates great difficulties in designing the interface to compensate for those loses. The high density of Er^{3+} ions enhances the pump absorption and therefore increases the population inversion, but it can cause an ion-ion interaction that reduces the population inversion. Most commercial EDWAs operate only in the C-band. Their main applications are in metropolitan and access networks where the number and power of the channels are relatively low [153] [154].

Although EDFA and FRA amplifiers have proven their high effectiveness in commercial telecommunication applications and their wide availability place them in a top position among optical communication devices, they do have number of drawbacks that give network operators a strong push to seek new, more efficient solutions for optical signal transmission.

Power consumption issues

EDFA amplifiers are equipped with optical pump lasers that are the only external source of energy for the process of signal amplification. The pump laser is usually implemented in the form of a Fabry-Perot or FBG stabilized laser that is hermetically sealed in a butterfly package (Figure 103). The laser operates in a wavelength 980 nm or 1480 nm and the output power is in the range of 300 mW. The laser requires a power supply for its lasing operation but it also needs a second power supply for its built-in thermo-electric cooler (TEC). Since the pump laser is an active photonic device it does require its own electronic driver circuit which monitors and controls the functionality of the laser. This driver requires its own power supply. The total power consumption of the EDFA is a total sum of the power consumed by all the internal components implemented in the amplifier.

Figure 103: EDFA pump laser diode made by Qphotonics Corp.

Because EDFA requires multiple power supplies to run all of its internal components its power consumption very often exceeds 20W at 4A. The commercial telecommunication EDFA Cisco OptoStar 64667C (Figure 104) requires 25W of power supply at 5A to achieve 24 dB amplification of the 1550 nm signal.

Figure 104: Cisco EDFA OptoStar 64667C

Integration with other photonic components

EDFAs and FRAs consist of long sections of optical fibre to ensure sufficient amplification of the optical signal. Since optical fibre has very limited bending capabilities, the amplifier requires a fairly large enclosure to accommodate the long spool of fibre, pump laser, electronic control and monitoring electrical circuits. Because of their significant size, EDFAs and FRAs are difficult to integrate with other photonic components. A typical commercial EDFA that is offered as a subcomponent for a larger optical system has an enclosure with dimensions of 250 mm (L) x 150 mm (W) x 30 mm (H).

Figure 105: EDFA module built by Opto-Link Corp.

Figure 105 presents an example of an EDFA manufactured as a subcomponent of a larger optical system. The device offers 15dBm of optical output power at 1550 nm. The enclosure is equipped with a standard 20-pin Samtec interface to connect the power supplies for the pump laser, driver circuit, power/gain control and monitoring system.

Semiconductor Optical Amplifier (SOA)

Semiconductor Optical Amplifiers (SOAs) are amplifiers which use a semiconductor to provide the gain medium. In SOAs, the population inversion, upon which the gain depends, is between the broad energy bands of the semi conductor material. Indium gallium arsenide phosphide (InGaAsP) crystals are used in which the required energy band-gap is created by the appropriate adjustment of the material composition within the device's active layer. SOAs are excited by direct current injection and they are fabricated as single transverse mode waveguides to maximize their power confinement.

General characteristic of commercial grade SOA

The good example of the commercial grade SOA is device OPB1010NCFA produced by Kamelian Corporation which is available as a stand-alone device with pigtailed input and output fibers. The device has the form of the butterfly package with a number of electrical connectors to provide power supply and to monitor and adjust the temperature of the device (Figure 106).

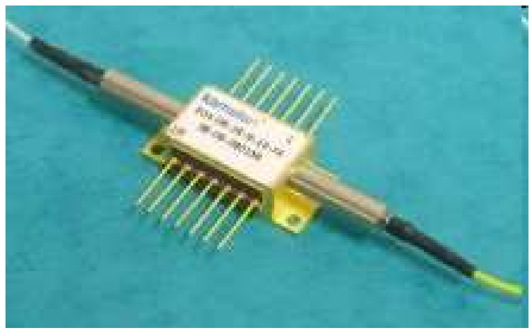

Figure 106: Commercial grade Kamelian SOA

SOA amplifiers have a similar structure to Fabry–Perot laser diodes except for the anti-reflection design elements which are located at the end-faces. SOA designs include anti-reflective coatings, tilted waveguides and window regions which can reduce end-face reflection to less than 0.001%. Since this creates a loss of power from the cavity which is greater than the gain, it prevents the amplifier from acting as a laser. SOA amplifiers are often used in telecommunication systems in the form of fibre-pigtailed components that operate at optical wavelengths between 0.85 µm and 1.6 µm and generate gains of up to 30 dB (Figure 107).

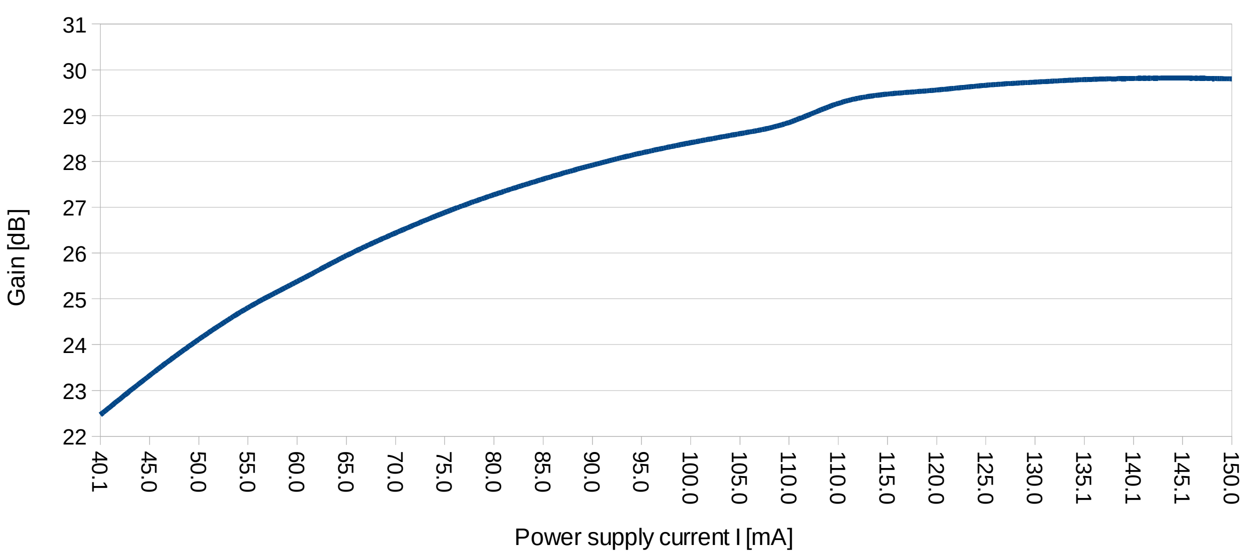

Figure 107: Optical gain of OPB1010NCFA SOA at 1550 nm

The first important characteristic that SOA exhibits is an optical gain. Commercial grade SOAs can achieve gain from 22 dB at 40 mA of power supply up to 30 dB at 140 mA power supply. The maximal gain is limited by the saturation effect that usually depends on a combination of the current supply, optical input power and temperature. Figure 107 presents measurement results of the commercial grade SOA OPB1010NCFA manufactured by Kamelian Corporation. The measured gain (at wavelength 1550 nm) reaches the saturation level at power supply around 150mA and temperature 30°C.

SOA, similar to a laser diode, requires an electronic driver that regulates the supply current as well as monitors and adjusts the device temperature. Proper temperature regulation plays an important role in achieving optimum working conditions where SOAs provide high gain at very low current supply and at the same time maintain a safe margin from the saturation conditions.

Figure 108 presents changes in SOA temperature and the gain in relation to changes in the supply current. This figure also presents the effect of gain change when the device temperature is adjusted through the cooling current. When the optical gain reached 30 dB at a supply current of 155 mA and a temperature of 20°C, the cooling current was increased from 200 mA to 260 mA. In this way, temperature of the SOA dropped down to 13°C and the gain increased to 32 dB. The gain also reaches 28 dB at a supply current 110 mA. At this point the cooling current was adjusted to decrease temperature from 19°C to 17°C and this event caused the optical gain change.

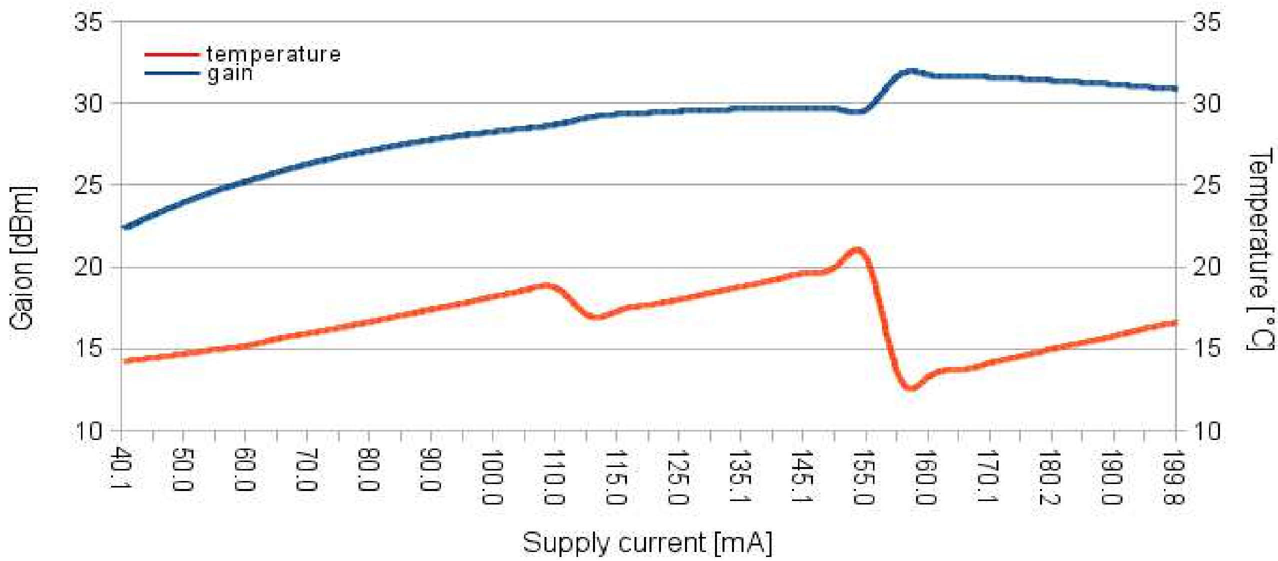

Figure 108: Optical gain (at 1550 nm) vs. temperature in OPB1010NCFA SOA

This result suggests that although SOAs do exhibit some dependency between optical gain and temperature, this dependency is not critical to SOA operation and it does not require a sophisticated and expensive cooling system. As long as SOA operation is kept away from its saturation conditions the required power consumption can be maintained on a low level.

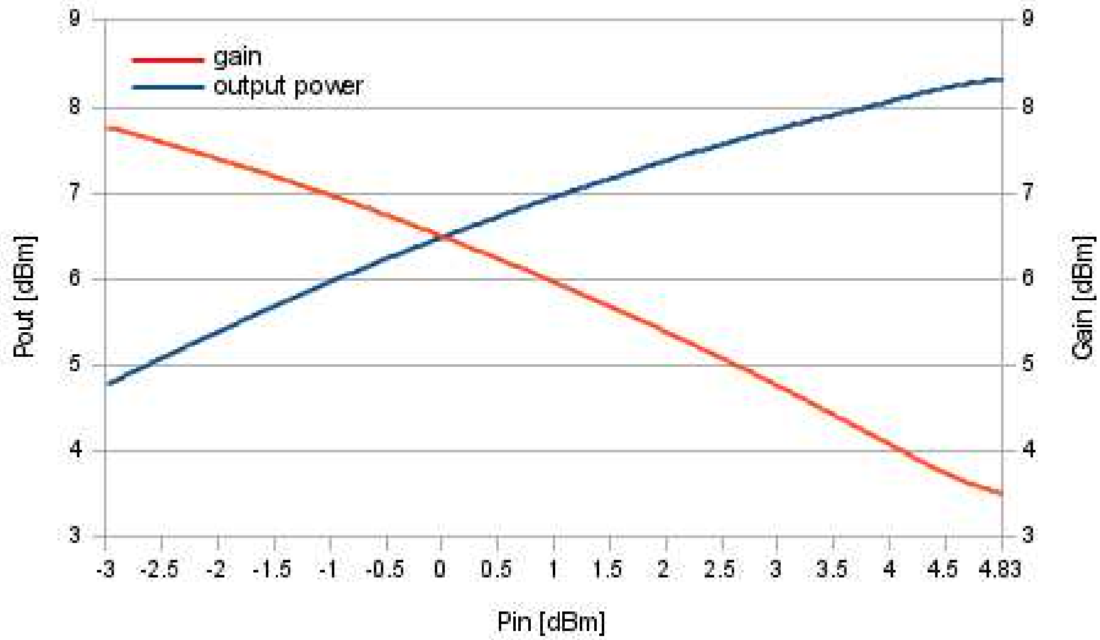

Figure 109: Gain vs. optical input power in OPB1010NCFA SOA

Another interesting characteristic exhibited by SOAs is a near linear dependency between optical gain and optical input power for a constant supply current. Figure 109 presents measurements of gain vs. optical input power at a supply current of 50 mA. The near linear characteristic of gain as a function of input power allows for easy prediction on how the amplifier will behave when the optical input power fluctuates. This feature makes it easier to design drivers that can automatically adjust the SOA supply current to ensure that the optical output power is kept stable.

Problems related to application of SOA in commercial network infrastructure

Although SOAs seem to be a very competitive alternative to existing EDFA technologies, they do possess certain drawbacks that require attention. Existing SOA devices do not offer equal amplification for both polarizations of the optical signal. Although intensive work has been done to achieve the polarization independent configuration of Reflective SOA (RSOA) [155], more research is required to ensure polarization independent characteristics of SOAs. In addition, manufacturing processes for SOA prototypes differ significantly from manufacturing processes for commercial large volume production. Therefore positive results of prototype tests do not guarantee identical results in mass produced devices.

Another important issue which must be addressed in SOA design is the patterning effect. A standard application of SOA is as an amplification unit used for post amplification, inline amplification, and pre-amplification purposes. In an ideal situation the profile of the output optical signal should be an amplified replica of the input optical signal. In reality, however, the combination of the optical input power and specific pattern of input data can cause heavy saturation of the SOA. Since SOAs have a finite recovery time, a specific pattern of high-power optical input data can be injected into the SOA; this way the amplifier will not have enough time to recover from the saturation state. This means that binary content variations of input data signal may result in an amplified output signal that is not uniform, leading to performance degradation.

One of the proposed solutions for reducing the pattern effect consists of direct amplification of the digitally coded pulses. It is based on the fact that the strong gain saturation (responsible for the pattern effect) is also responsible for self-phase modulation (SPM) and subsequent spectral broadening of the data carrier to longer wavelengths [156]. The successful prototype of the pattern effect suppression system was presented in [157]. The prototype had implemented the spectral elimination technique with a birefringent fibre loop (BFL).

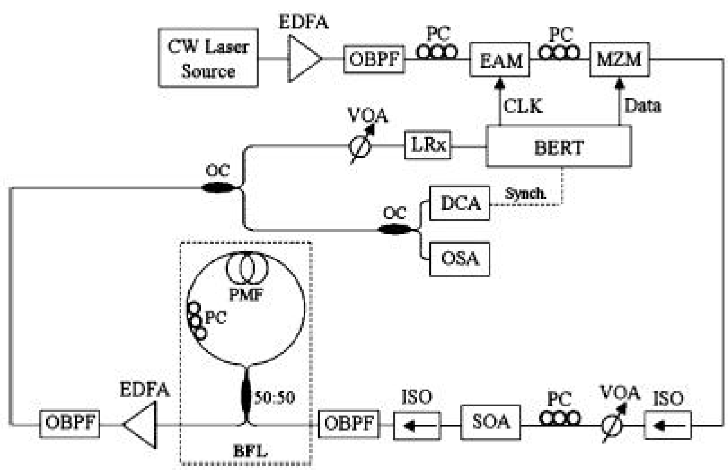

Figure 110: Prototype of the pattern effect cancellation system for SOA [157]

This method was used to compensate for the pattern effect on a 10 Gb/s return-to-zero (RZ) pseudorandom binary sequence (PRBS) amplified by an SOA. The prototype of the system is presented in figure 110. It consists of a 1550-nm tunable laser source that is amplified by an EDFA and subsequently modulated by an electroabsorption modulator (EAM) and a LiNbO Mach–Zehnder modulator (MZM). The MZM is driven by the internally synchronized clock (CLK) and data output of a BERT. The signal is amplified by an SOA (Kamelian, model OPA-20-N-C-FA) with a small-signal gain of 23 dB that drops by 3 dB when the input power is 7 dBm. The SOA had a gain polarization dependence of 0.5 dB, and a gain recovery time of about 75 ps at 1550 nm. The prototype successfully achieved a significant reduction of pattern effect (Figure 111).

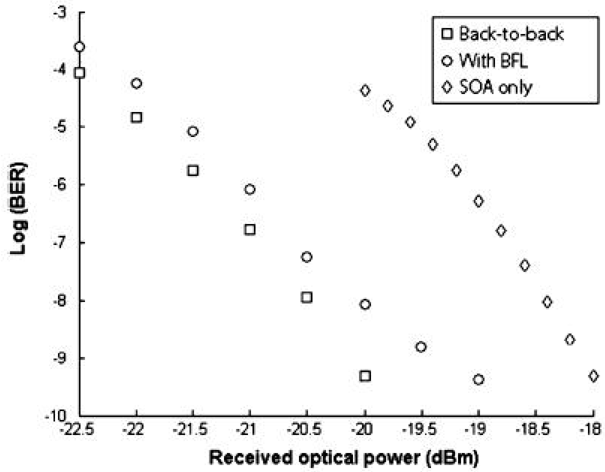

Figure 111: Results of pattern effect cancellation in the prototype system [157]

Another important issue that must be addressed is the spontaneous amplification emission (ASE). Since SOA is built in a similar way to the laser, it does have light emitting capabilities when no optical input power is present. Figure 112 presents the optical output power of radiation emitted by commercial grade Kamelien SOA for a broad range of values of injection current with no optical power input present.

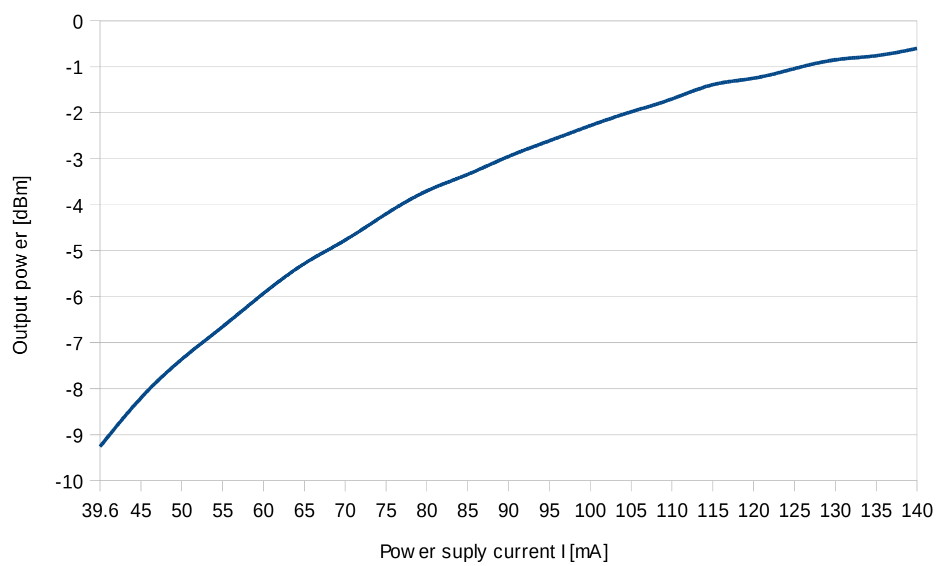

Figure 112: Total optical output power versus injection current when optical input power is not present (Kamelian OPB1010NCFA SOA)

It is obvious that the output power is significantly rising from –9.5 dBm to over -1 dBm when the current rises from 39 mA to 140 mA. Although the output power seems to be very high, it is not associated with any particular wavelength but it is distributed across broad range of spectrum. Figure 113 presents the captured optical spectrum of the signal that is emitted by Kamelian SOA when supply current is 100 mA.

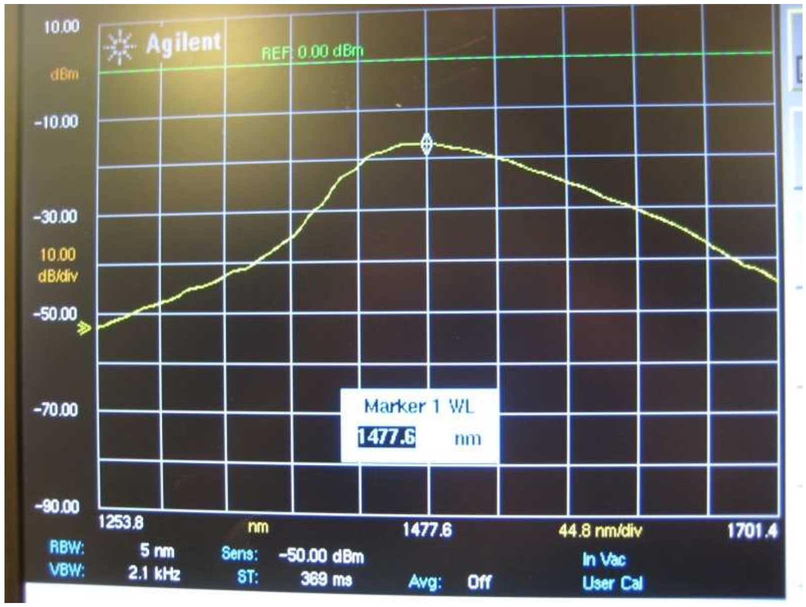

Figure 113: Spectrum of the optical signal emitted by Kamelian SOA at 100 mA with no input optical power present.

The picture of the emitted spectrum indicates that the SOA spontaneously emits a range of wavelengths at approximately 1300 nm to 1700 nm. This emission may introduce unwanted noise to the optical system and create difficulties in proper signal detection after transmission over the long distance link. A possible solution to this problem is to implement AWG filters that are located after the optical amplifier. In this way, only the original wavelength emitted by source will pass through before being amplified by the SOA.

Implementation of SOA as optical switch and modulator

In section 6.6.4 there was presented a low-cost prototype of the gigabit optical switch that was built from widely available off-the-shelf components. Although that particular optical switch has proved to be capable of handling 1Gb/s Ethernet traffic and has shown great potential of being upgraded to 10Gb/s, it was a hybrid electro-optical architecture that requires the incoming signal to be processed in an electrical domain.

There is a limited number of technologies that do not require the electro-optical conversion of the signal to perform switching tasks. These technologies include optical microelectromechanical systems (MEMS-based switching), thermal optical switching, electro-optic switching, and acousto-optic switching technologies [158].

Optical MEMS are hybrid devices that have optical, electrical, and mechanical functionalities at the same time. They are fabricated using batch process techniques derived from microelectronic fabrication [159]. The most important characteristic of MEMS is low crosstalk, wavelength insensitivity, polarization insensitivity, and high scalability. There are two main subgroups of MEMS-based optical switches: the free-space switching group that has implemented mirrors [160] or membranes and the waveguide switching group that has implemented planar moving waveguides.

Another type of optical switching devices is the thermal optical switch that is based on the waveguide thermo-optic effect or the thermal phenomena of materials. The big advantage of these types of switches is their polarization-insensitive operation and switching speed which is in the range of a millisecond. Switches based on waveguide thermo-optic effect are called thermo-optic switches (TOSW) and can use well-established planar lightwave circuit (PLC) technology [161]. TOSW devices are divided into two basic types: digital optical switches (DOSs) and interferometric switches. The thermal effects of materials can be used in thermo optic switching devices, such as thermo-capillarity optical switches [162], and thermo optic switches that implement coated microsphere resonators [163].

A third type of switching devices are electro-optical switches that perform switching functions by using electro-optic effects that offer faster switching time than thermo-optical effects. The main materials used in electro-optical switches are $LiNbO_3$ [164] , liquid crystals [165], electroholographic (EH) materials [166], and Bragg gratings [167]. The LiNbO3 switch is based on the large electro-optic coefficient of $LiNbO_3$. The most important application of this crystal is a 2×2 directional coupler. Its interference coupling ratio is regulated by changing the refractive index of the material in the coupling area [168]. The big disadvantage of using $LiNbO_3$ in a coupler is the high insertion loss and high crosstalk. Another electro-optic material that can be used in switching devices is lead zirconium titanate, doped with a lanthanum (PLZT). PLZT [169] is a material with a higher electrooptic coefficient than $LiNbO_3$ therefore is can be used in a digital optical switch (DOS). Optical switching can also be achieved by implementing liquid crystals (LC). These devices control the polarization of the light by the electo-optic effect. The electro-optic coefficient in LC is much higher than in $LiNbO_3$, which makes LC a very efficient electro-optic material.

All-optical switches belong to a relatively new group of devices that realize switching functions through the intensity-dependent fast nonlinear optic effect in optical waveguides. The nonlinear effects that can be used to perform optical switching are: two-photon absorption, self phase modulation (SPM) induced by light wave self action, four wave mixing (FWM) induced by the Kerr effect, and cross phase modulation (XPM).

There is number of parameters that define the performance of optical switching devices across all the described technologies above. The first parameter is the insertion loss defined as the optical power loss when optical signals pass through the optical switch, consisting of coupling loss, waveguide propagation loss, and excess loss. Insertion loss limits the scalability of optical switches and increases the system cost.

Another parameter is the switching speed. This parameter is defined as the time period from the moment the command is given to the switch to change its state to the moment the insertion loss of the switched path achieves more than 90 percent of its final value [160]. When the range of switching time is considered there are three groups of commercial switching applications:

- multimillisecond switching time for protection application
- nanosecond switching time for packet switching application

- picosecond switching time for bit-level optical time-division multiplexing (OTDM) application

The third important parameter is the crosstalk. This parameter is described as the ratio of the power leaked to the wrong output and the power correct output and it is used to measure the signal interference between channels. Low crosstalk and high extinction ratio indicate small signal interference or high signal quality. Typically, the crosstalk value is around 40dB.

The fourth component of optical switching performance is polarization sensitivity. It is used to measure polarization dependence. The high polarization sensitivity has a negative impact on transmission reliability, and it requires constant monitoring and the application of dynamic compensation techniques. Another parameter is the bit rate and protocol transparency. This parameter has a direct impact on the flexibility in configuring network where the switch in deployed. The last parameters to be listed are the wavelength dependencies, which determines if the switch can perform switching at each wavelength independently or if it switches the optical signal regardless of the wavelength.

Physical characteristics of switching technologies that are implemented in optical devices have a direct impact on the cost of production, implementation and maintenance. These characteristics also play a decisive role in making the switch capable of fulfilling certain requirements related to the network infrastructure such as: ability to multicast, physical dimensions of the switch, scalability, non-blocking ability (the flexibility to route or reroute any input channel to any unoccupied output channel), repeatability (the length of all the paths across the switching fabric should be identical), power consumption and temperature conditions.

The publication [158] provides a detailed list of existing commercial switching technologies as well as presenting a thorough comparison of those technologies from the perspective of insertion loss, switching speed, crosstalk, polarization dependency, wavelength dependency and transparency for telecommunication optical windows. The system level abilities of switches are also compared with respect to multicasting functionality, physical device dimensions, scalability and non-blocking switching. The insertion loss varies from about 0.5 dB for the MEMS based switch to nearly 10dB for the liquid crystal based switch. The switching speed varies from 120 ps for the semiconductor space switch based on MMI couplers [170] to over 100 ms for the thermo-optical switch with embedded coated microsphere resonators [163].

Semiconductor optical amplifiers (SOA) belong to the group of electro-optical devices that switches between ON/OFF states by imposing changes in the bias current. SOAs offer the capability of all-optical switching while the electrical domain is required to only provide proper configuring, controlling and monitoring of the switching device and a proper power supply.

The SOA switching time is in the range of 200 ps and its input loss reaches 0dB. Implementing SOA as an optical switch is not a totally new idea and it was published in the early 1990s in the form of theoretical modeling and simulation. An example of 4x4 optical switches that implement a matrix of integrated SOAs was discussed in [171]. The proposed switching device was based on a three-stage optical switch with SOA gates. The work analyzes the gain saturation under both unidirectional (isolators inserted) and bidirectional (no isolators) propagation of spontaneous emission noise, and it evaluates the noise figure penalty associated with the absence of isolators.

The problem of crosstalk in a SAO-based switch was presented in work [172]. The switch prototype was built based on a packaged 4 X 4 SOA gate switch matrix in InGaAsP/InP. To distinguish cross talk from amplified spontaneous emission, a lock-in technique was employed for the experiments. The fiber delay lines for the co-propagating signals are multiples of 300 meters, which exceed the transmitter coherence length by far. In this way all signals become mutually phase uncorrelated and the three cross talk signals were combined incoherently, as would typically be the case in a real network. The switch was examined in 84 different switching configurations with an input power of -10 dBm to all four switch inputs. The observed mean cross talk was -30.7 dB with a variance of 6.0 dB.

In recent years there has been an observed increase of interest in SOA implementation as optical switches due to significant progress in technologies for manufacturing integrated semiconductor devices. The innovative integrated 4x4 SOA-based optical switch with low insertion loss was presented in [173]. The prototype switch had an active region which incorporated a 5 Quantum Well AlGaInAs structure which was grown on an InP substrate using MBE. The SOA gate structures in the cross-point are ridge waveguides and they are interconnected with beam splitters formed with tapered waveguides and deep etched mirrors to form a broadcast-and-select non-blocking tree architecture as shown in Figure 114.

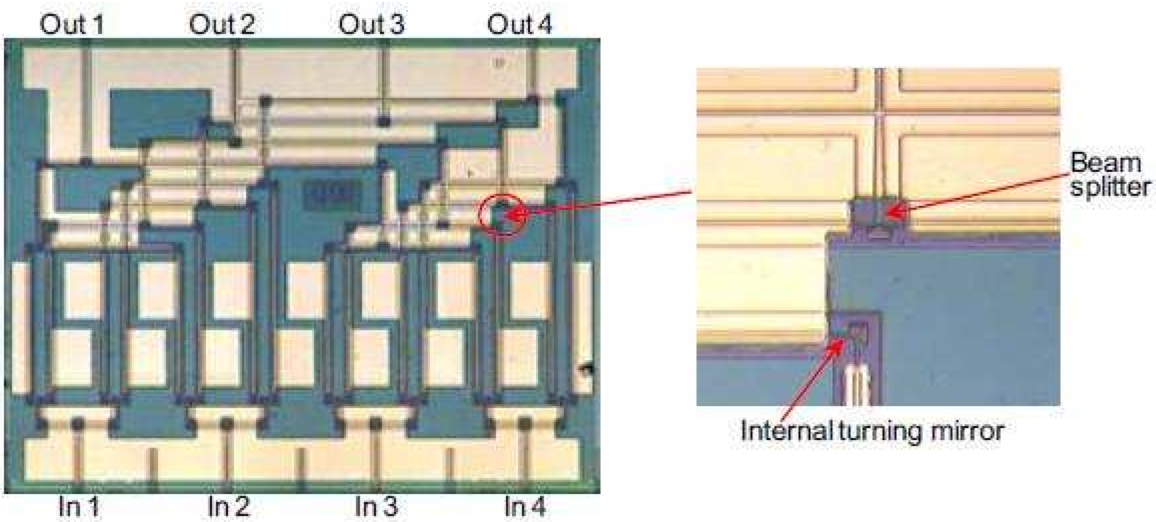

Figure 114: Prototype of 4x4 integrated SOA-based switch fabric [173]

The input and output SOA waveguides were each biased in common to provide gain blocks to overcome coupling, splitting and waveguide losses, while the middle gating SOAs were each biased individually. The lengths of the paths through the switch vary from 1.55 mm (path 1-1 and 4-4) to 2.8 mm (path 1-4 and 4-1). The chip had a very compact footprint of 2.04 mm × 1.54 mm, 10 dB fibre-to-fibre gain at 1550 nm and a 3 dB gain bandwidth of around 30 nm was observed. The switch input and output SOAs were biased at 150 mA and 320 mA, respectively. The middle gating SOAs for the seven paths were biased between 35 mA to 70 mA to achieve an unsaturated fibre-to-fibre gain of 0dB, with a coupling loss of 3 dB per facet. The transmission tests were done using eight de-correlated PRBS 10 Gbit/s channels, at wavelengths between 1548.5 nm to 1554.2 nm with 0.8 nm channel spacing. The observed BER was 10^{-9} with a power penalty below 2 dB.

Although there are number of projects that address the problems of design in SOA-based optical switching devices, they usually focus on the development of new switch fabrics with integrated multiple SOA components rather than taking advantage of existing SOA technologies. Most of successful switch fabric prototypes were designed and fabricated in recent years and they are still in the early stage of prototyping and testing which does not forecast any upcoming commercialization process and mass production in the near future.

In this project there is a focus on evaluating the existing SOA technologies that are already commercially available and incorporating those technologies into low cost and energy efficient devices that can be deployed in existing optical network infrastructures.

The commercial SOA that was available for research was Kamelian model OPB1010NCFA packaged in a butterfly enclosure with embedded cooling module (Figure 115). The package had pigtailed optical single mode fibers (SMF) in input and output ports, terminated with standard FC connectors.

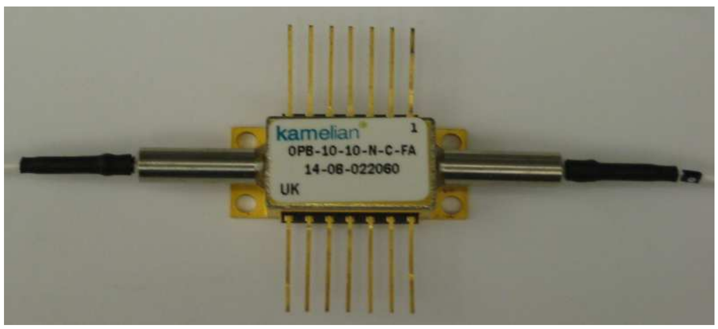

Figure 115: Commercial SOA model OPB1010NCFA

The figure 116 presents detailed dimensions of the SOA, distribution electrical in- and output ports and their functionality. The device was rated with 250 mA of maximum current supply.

pin	Description
1	TEC +
2	Thermistor
3	NC
4	NC
5	Thermistor
6	NC
7	NC
8	NC
9	NC
10	SOA Anode (+)
11	SOA Cathode (–)
12	NC
13	Case GND
14	TEC -

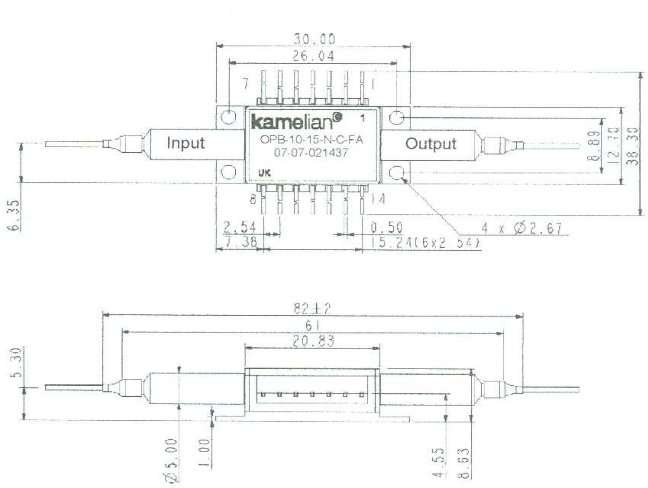

Figure 116: Detailed schematics of the Kamelian SOA

The SOA was mounted on the universal lased diode (LD) butterfly socket Thorlabs ML14S2 equipped with two 9-pin communication ports for LD driver and TEC driver (Figure 117a).

a) b)

Figure 117: Butterfly socket Thorlabs LM14S2 (a), temperature controller WTC3243 (b)

The commercial SOA required an effective temperature monitoring system. To ensure the temperature was monitored accurately and in a real time fashion, a custom temperature controller was built based on the commercially available WTC3243 Thermoelectric Temperature Controller (Figure 117b) designed by Wavelength Electronics Inc [174]. The device sensitivity is 0.01ºC. The temperature controller was connected directly to the SOA controller.

At the time when the benchmark test was performed there was no commercial driver available for SOA based devices in the laboratory. The custom driver device for SOA was designed and built to meet the following requirements:

- built from widely available low-cost electronic components
- ability to deliver supply current to SOA
- ability to deliver cooling current to TEC
- provide interface to connect to the temperature monitoring device
- provide interface for standard TTL signal to perform on/off modulating
- provide protection in case of accidental current and voltage fluctuations

The SOA driver had implemented single-chip Analog Devices ADM1611 switch in 16-Lead Thin Shrink Small Outline Package (TSSOP). Because the chip had a very small size it was difficult to integrate it manually with the other electrical components of the driver. To convert it to a universal exchangeable module, the chip was surface mounted on a TSSOP16-to-DIP16 adapter (Figure 118).

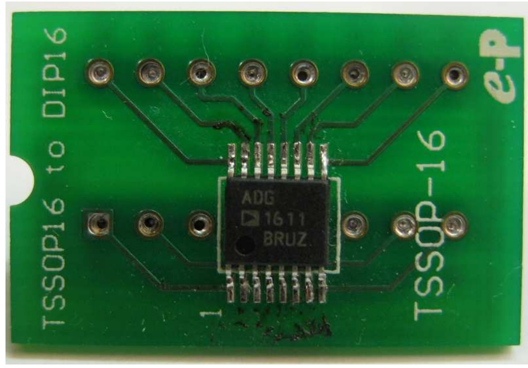

Figure 118: ADM1611 switch surface mounted on DIP16 adapter

The SOA driver had the form of a single-board prototype system with dedicated terminal ports to connect to power supplies with a SOA current and a cooling current. The board also implemented potentiometers for manual tuning values of the SOA and cooling currents (Figure 119). The supply currents were provided by the DC power supply Tektronix PS280.

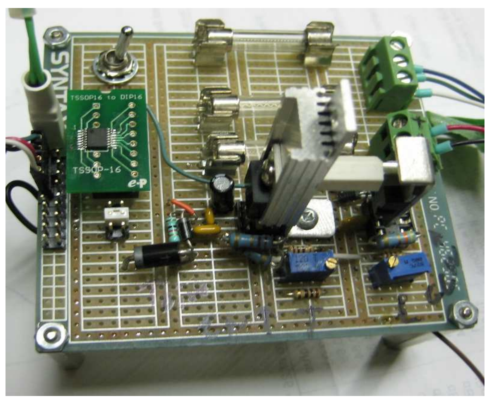

Figure 119: Custom designed low-cost driver for SOA

The benchmark tests of the SOA working as a switching device were performed using the digital scope Agilent DSOX91604A. The source of the modulating signal was the function synthesizer and generator Hewlett Packard HP3325A (Figure 120).

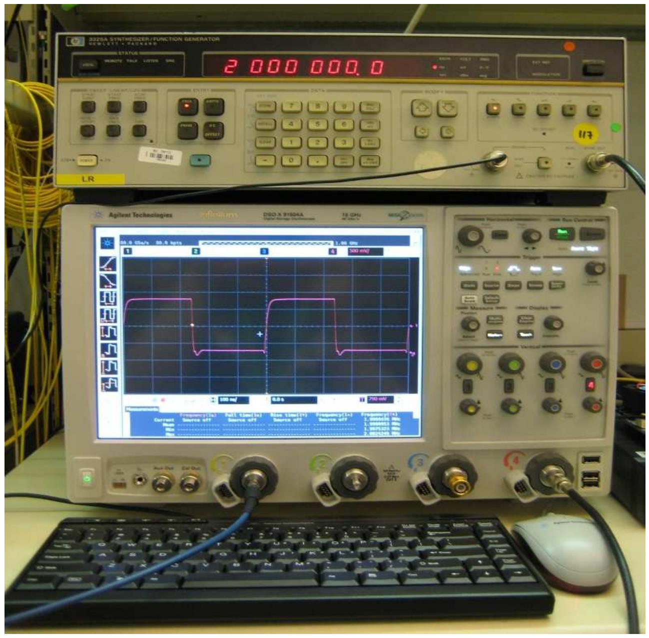

Figure 120: DSOX91604A and HP3325A used in SOA benchmark tests

The source of the optical signal was the JDSU laser diode, 1550.32 nm with 0dBm output power. The output optical signal was directed to the fast photoreceiver New Focus 1592 (Figure 121). This receiver has InGaAs photodetectors and its bandwidth is 3.5 GHz, its rise time is in the range of 115 ps and its sensitivity is 950 nm-1630 nm [175].

a) **b)**

Figure 121: JDSU laser diode (a), New Focus 1592 photoreceiver (b)

Figure 59 presents the experimental setup for the benchmark test of the SOA. The driver was fed with a square shape modulating signal with a LO level at 0V and a HI level at 1V. The SOA current supply was set to 100 mA and the temperature of the device was stabilized at 13°C with cooling current of 120 mA (Figure 122).

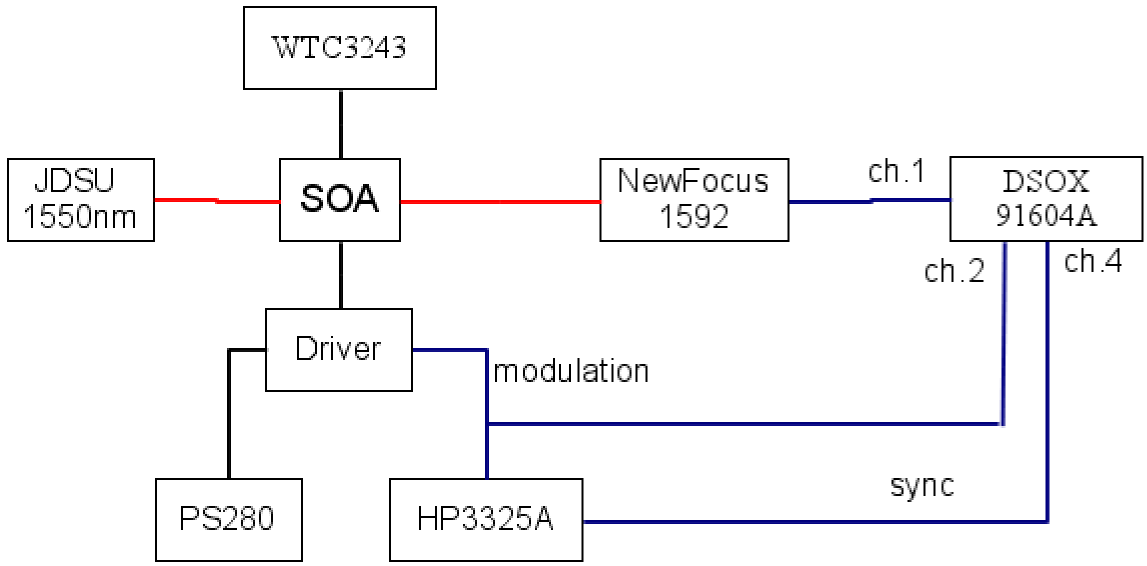

Figure 122: Experimental hardware setup for the benchmark test

The benchmark was performed as follows:

- Current supply for SOA was set to 100 mA
- Frequency of the output (modulating) signal from the function generator was gradually increased starting from 400 kHz (the photo receiver was designed for high frequency optical signal and it did not provide a good response for frequencies lower than 400 kHz)
- The response signal from the SOA was compared in real time to the original modulating signal on the scope
- The length of the LO and HI start of the response signal was recorded
- Any delay between modulation signal and response signal was recorded

The highest observed modulating frequency that allowed the SOA to have an undistorted signal response was 2.31 MHz. The measured response signal had a 224 ns length at HI state and 208 ns at LO state. The time of the falling edge was 17 ns and the time of the rising edge was 29 ns. The observed delay between the modulating signal and response signal was in the range of 222 ns for the falling edge and 202 ns for the rising edge (Figure 123).

When the modulating frequency was increased beyond 2.32 MHz, the LO state of the response signal was heavily distorted by an additional peak of approximately 60 ns width in its half maximum (FWHM). Figure 124 presents the SOA response at 2.4 MHz with visible distortion at the LO state of the response signal.

Figure 123: SOA response signal (upper) and 2.3 MHz modulating signal (lower)

Figure 124: Distorted SOA response signal (upper) at 2.4 MHz modulating signal (lower)

A significant difference was observed in the lengths of the LO and HI states of the optical signal at the SOA output port (Figure 125). This difference was not constant and changed across a spectrum of applied frequencies. The HI state had a longer length than the LO state in a range of frequencies between 400 kHz to 1.6 MHz. Both states became equal around 1.605 MHz. The LO state was longer than the HI in a range between 1.61 MHz to 2.3 MHz. The way SOA responses to different modulation frequency exhibit feature of finite gain recovery time that is the main reason for visible asymmetry in length of state HI and state LO.

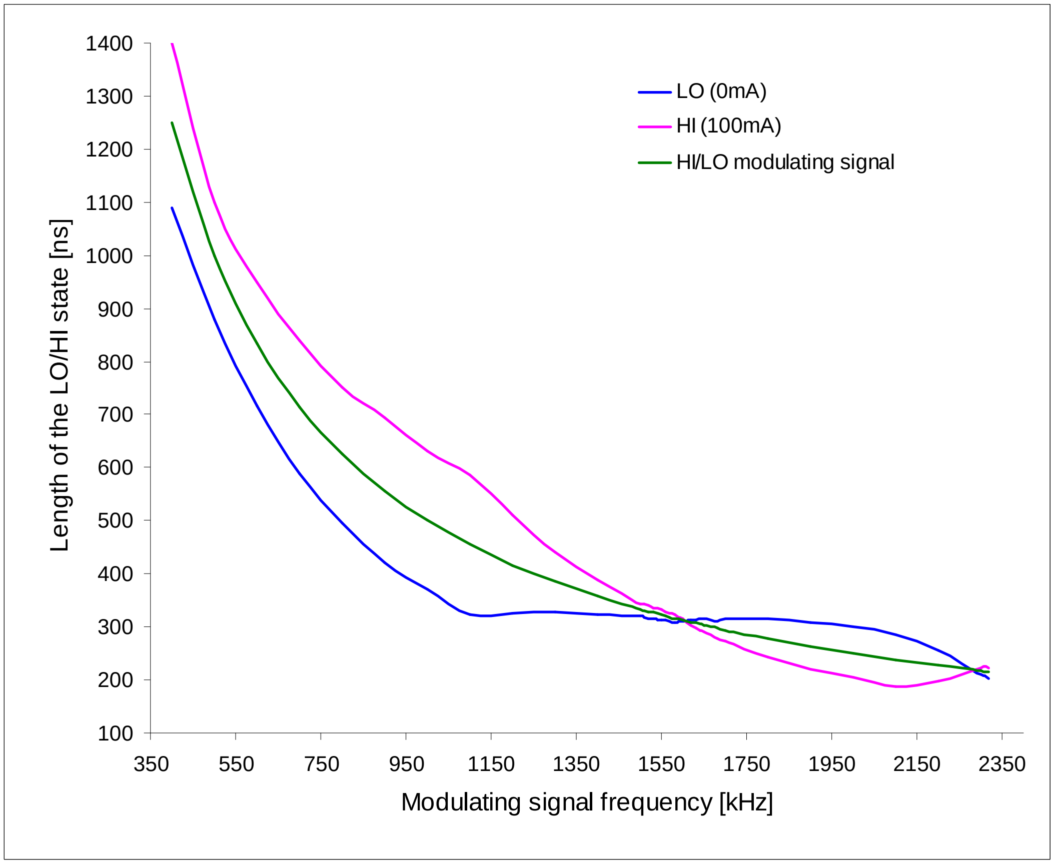

Figure 125: Changes in the length of the LO state (0 mA) and HI state (100 mA) in the SOA response signal across modulating frequencies

The phenomena of asymmetric time intervals where the LO and HI states have different lengths may be caused by the SOA driver or the SOA itself. To evaluate if this phenomenon is caused by the driver additional measurements were preformed. The output port of the driver was connected to the scope through the probe, modulating signal, and the driver output signal was compared across a spectrum of the applied frequencies (Figure 126). The test did not reveal any extraordinary distortion of the driver output signal. Although the monitored driver signal exhibited some irregularities caused by imperfections in the driver electric circuit, its shape and timing were well aligned with the original modulating signal.

Figure 126: Comparison of the 1 MHz modulating signal (bottom), driver signal (middle) and SOA response signal (top).

The results of the driver signal test indicates that the SOA was the source of the response signal distortion rather than the electrical circuit of the driver. The benchmark was repeated with identical experimental configuration except that the current supply for the SOA was lowered 40 mA. The modulating signal had a frequency in a range from 300 Hz to 3.3 MHz. Above 3.3 MHz the response signal of the SOA was significantly distorted.

The results of the benchmark test are presented in figure 127. The results show that lowering the value of the current supply allows for an extension to the frequency range where the SOA provides an undistorted signal response. In the frequency range of 300 kHz to 650 kHz the observed response signal was near symmetric and the difference between the HI and LO states did not exceed 10 ns. At frequencies of 700 kHz to 1.1 MHz there is a visible difference in the length of HI and LO states but this difference does not exceed 50 ns.

Although asymmetry in the response signal varied across the frequency spectrum, there were an observed number of certain frequency values where the response signal became symmetric. Those frequencies are approximately: 400 kHz, 550 kHz, 1.05 MHz, 2.305 MHz, 2.325 MHz, 2.550 MHz and 2.8 MHz.

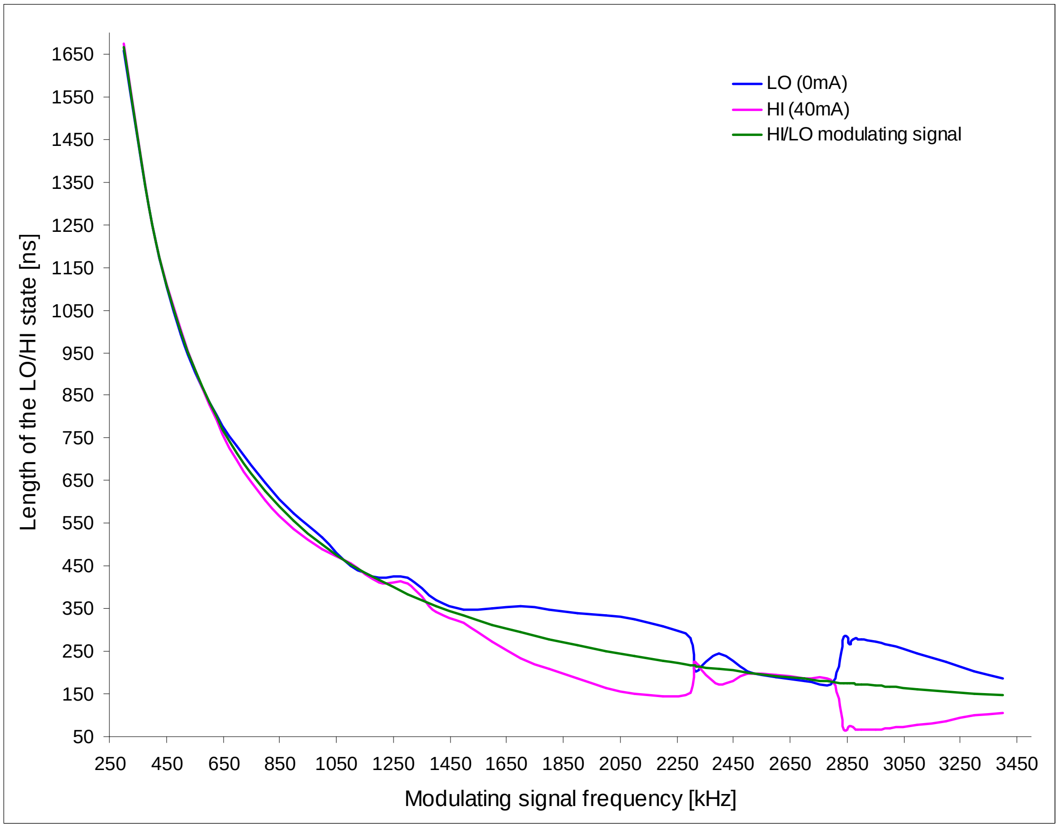

Figure 127: Changes in length of the LO (0 mA) and HI (40 mA) states in the SOA response signal across modulating frequencies.

The benchmark results indicate that this particular SOA has capabilities of signal modulation in the range of 2.8 Gb/s in ON/OFF keying and a return to zero fashion (RZ). This may place the SOA as a good candidate only for low speed access networks that do not exceed 3Gb/s data rate.

The observed asymmetry in the SOA response signal may be caused by the effect of finite gain recovery time in the SOA device. Applying high frequency modulation does not allow SOA to return fast enough from state HI to state LO. Figure 65 presents the measured characteristics of this particular device. There is a visible nonlinear pattern in the range of 5 mV to 500 mV where the supply current exhibits a strong fluctuation. When the modulating signal is applied, the SOA is forced to work with a rapidly changing supply voltage and those changes are followed by nonlinear changes of the supply current. The first benchmark was operating in a range of 0 mA to 100 mA and the second benchmark was operating in a range of 0 mA to 40 mA.

When both ranges are compared with figure 128, it is visible that they both fall into the highly nonlinear region. A possible solution to avoid the nonlinear fluctuations that disturb the symmetry of the response signal would be to apply a static bias to the SOA current. If the supply current is up-shifted about 120 mA, the SOA is moved towards the linear part of the characteristics. If this happens there must be an implemented modification to the SOA driver to allow the amplifier to work with a 120 mA current when the modulating signal is at LO state and a 200 mA current when the modulation signal is at HI state.

The significant drawback of this solution is that the supply current is associated with the HI state of the modulating signal which may have a value near the saturation level of the SOA. If that happens the SOA may become very fragile with possible patterning effects.

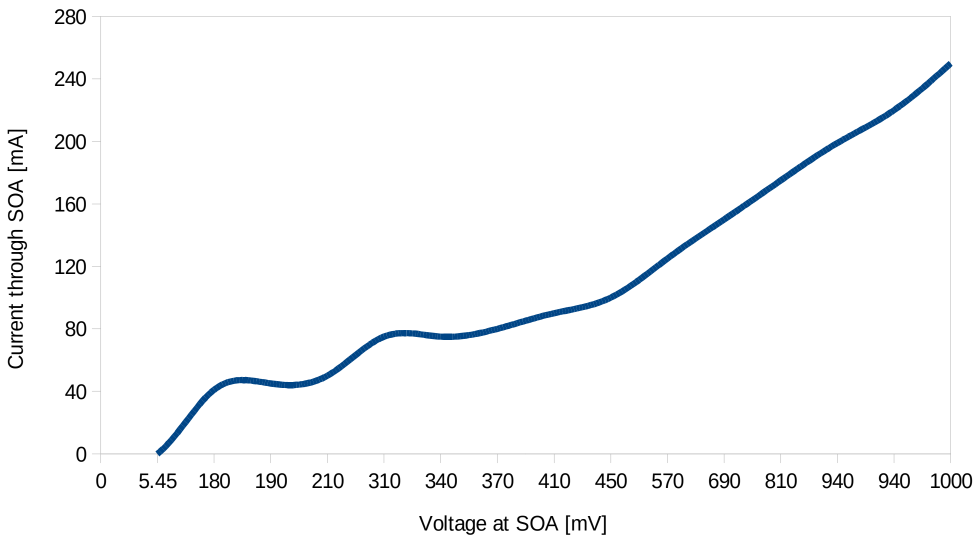

Figure 128: Measured nonlinear characteristic of the SOA (TEC=130 mA)

Although the observed frequency limitation is a significant obstacle in implementing SOA as a modulating device in a multi-gigabit optical network, the benchmark results position SOA as a promising candidate for high speed all-optical switching devices. To evaluate the potential performance of the SOA-based switch, a representation of PON Ethernet frame in the time domain must be done (Figure 129). The standard Ethernet frame is 1518B in length without a 7-byte preamble and a 1-byte start frame delimiter (SFD) or 1526B length if the preamble and SFD are included [176]. Since the payload field in the frame can be variable, the Ethernet frame can vary from 72B to 1526B. The full size Ethernet frame can be represented as a transmission time interval from about 12 ms at 1 Gb/s to 122 µs at 100 Gb/s.

	Representation in time domain		
Ethernet frame [B]	**1Gb/s**	**10Gb/s**	**100Gb/s**
1526 (preamble + SFD)	12.2 ms	1.22 ms	122 µs
72 (preamble + SFD)	575 µs	57.5 µs	5.75 µs
1518	12.1 ms	1.21 ms	121 µs
64	510 µs	51 µs	5.1 µs

Figure 129: Representation of the Ethernet frame in the time domain

Ethernet frame representation in the time domain was compared with results of the SOA switch benchmark test. If the HI state of the response signal is considered as the state when the SOA is letting traffic flow through, then the minimal size time slot length allowed to be transmitted through switch varies from 66 ns to 1.675 μs. If the frame-by-frame switching scheme is implemented and the full size frames are transmitted, those timeslots represent 184.96 Gb/s and 7.228 Gb/s, respectively. This indicates that the SOA is capable of performing frame-by-frame switching in a network infrastructure with a data rate of 184 Gb/s. This result not only exceeds all existing commercial 40G optical switching systems, but also ensures that a SOA-based all-optical switch can support future networks that may exceed 150 Gb/s.

FPGA controller for SOA-based optical switch

In the previous chapter a commercially available SOA amplifier was implemented as an all-optical switching device that features low power consumption and the ability to support optical networks with a data rate exceeding 150Gb/s. Although the SOA in a standalone butterfly package has significantly larger physical dimensions than the SOA integrated in switch fabric, it can be successfully implemented in an optical switch assembled in a 1U- or 2U-size enclosure that is compatible with standard telecommunication racks.

Figure 130 presents an example configuration of the 2x2 all-optical switch based on SOA amplifiers. The connections between the fibers are realized by splitters 1x2 with a splitting ratio of 50/50. If the switch has a higher density (above 2x2) then splitting ratios should be adjusted according to the gain of implemented SOAs.

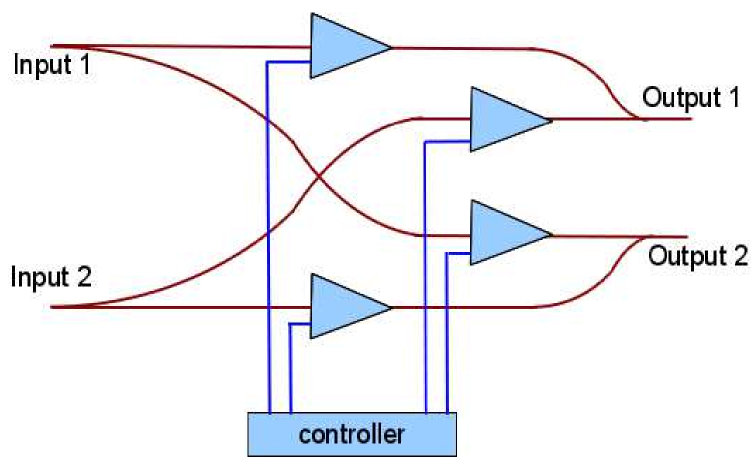

Figure 130: Example of a 2x2 all-optical switch with implemented SOAs

Every optical switch requires a controlling mechanism that ensures timely reconfiguration of the switch according to the traffic flow. The switch configuring mechanism is usually implemented in the form of an electronic controller that is collocated within the switch fabric in the same enclosure.

A prototype of a low-cost universal controller for the all-optical switch has been designed, built and tested. Before any work on the controller design began, a number of requirements and constrains were listed to ensure the controller prototype would meet the requirements related to deployment in commercial optical network infrastructure.

The following constrains and requirements were listed prior to work on the design:

- The controller should be small and compact so it can be installed with switch fabric in a single 1U or 2U enclosure.
- The device should have low power consumption and it should be able to be powered by a battery when the main power supply fails.
- It should not need any additional cooling mechanisms.
- The controller should operate autonomously and be able to boot up after a failure.
- The controller should be remotely controlled and configured.
- Uploading the configuration to the controller should be possible through the same optical link that carries the network traffic.
- The controller should be built from widely available components.

The development platform chosen for the controller prototype was Altera NIOS-II development board with a field programmable gateway array (FPGA) Stratix EP1S10F780C6 (Figure 131).

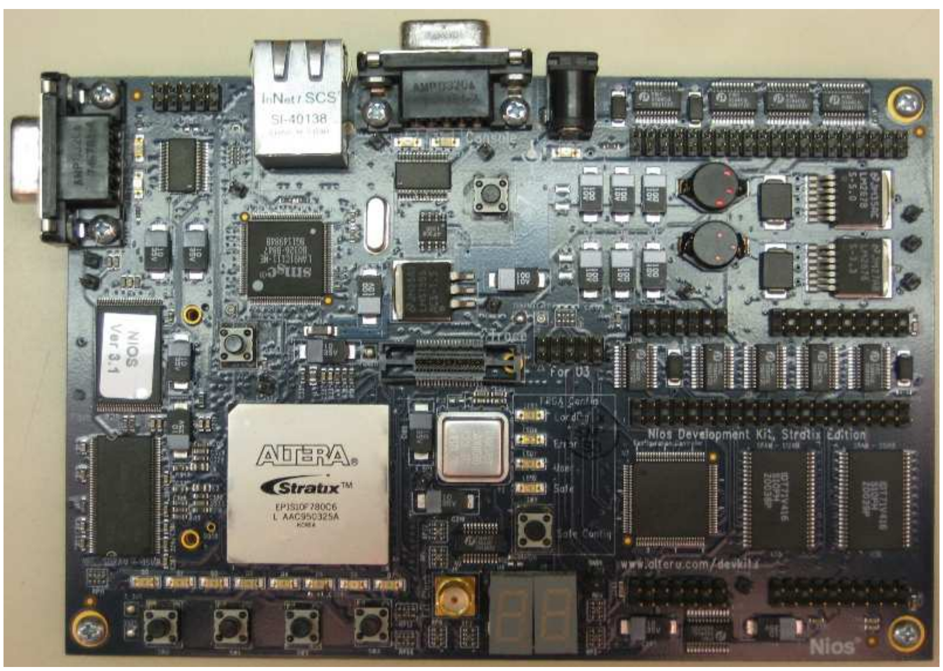

Figure 131: Altera NIOS-II development board with Stratix FPGA

The Stratix FPGA has 10570 logic elements (LEs), 6 DSP blocks and 426 user I/O pins. The board is equipped with a number of off-chip peripheral devices such as: 8 MB flash memory, 16 MB synchronous dynamic random access memory (SDRAM) and 1MB static random-access memory (SRAM). The board allows for design and implementation of customized signal processing and data processing systems that are crafted and optimized for user-specific applications.

The connection with the external world is provided through a 100 Mb/s Ethernet network interface, 9-pin console port, and number of I/O pins that can be custom configured. The board requires a 1A power supply at 9V DC and it can boot from a compact flash card without requiring uploading software from a PC. The physical dimensions of the board are 155 mm (L) x 105 mm (W) x 15 mm (H).

Features such as low power consumption, small dimensions, the capability of operation in autonomous fashion, a variety of on-board communication interfaces and high configuration flexibility make this board a very attractive candidate for the development platform.

The controller prototype has three-layer architecture (Figure 132) where the first layer is the hardware platform with FPGA, memory and communication ports. The second layer is the NIOS-II 32bit processor with a defined on-chip memory and drivers for all the on-board components located on the development board. The third layer is the software written in C/C++ code which provides all the functionality required to reconfigure the switch fabric.

User applications, ON/OFF signal modulation
NIOS CPU, on-chip RAM, device drivers, IRQs, memory addresses, timer
FPGA, SDRAM, SRAM, Ethernet NIC, I/O pins, Compact Flash, clock, RS232

Figure 132: The three-layer architecture of the switch controller.

The components of the NIOS are presented in figure 70. The processor was designed and built using the Altera System on a Programmable Chip (SOPC) Builder. The created processor is a complete and universal platform that can accommodate a variety of controlling applications. It has a 32bit CPU, timer, an interface for flash memory, Ethernet port, interface for LCD screen, DMA, SRAM, SDRAM, RS323, 8 LEDs and two 30-bit long parallel I/O interfaces with the option for two additional 12-bit long I/O interfaces.

The NIOS process chosen for this system was NIOS-II/f CPU with a performance 57 DMIPS at 50MHz clock [177]. This CPU consists of 64KB of on-chip memory and it occupies 1800 logic elements on the Stratix chip. This CPU provides the most universal and flexible processing unit available for this prototype.

The controller can address up to 84 switching components (SOAs), in parallel, in the switch fabric using TTL signals. This provides the ability to control the 9x9 optical switch with 81 SOAs.

Use	Co...	Module Name	Description	Clock	Base	End	Tags	IRQ
☑		⊞ pll	PLL	clk	0x032440c0	0x032440df		
☑		⊞ cpu	Nios II Processor	pll_c0	0x03243800	0x03243fff		
☑		⊞ sys_clk_timer	Interval Timer	pll_c0	0x03244040	0x0324405f		0
☑		⊞ sysid	System ID Peripheral	pll_c0	0x03244150	0x03244157		
☑		⊞ reconfig_request_pio	PIO (Parallel I/O)	pll_c0	0x032440e0	0x032440ef		
☑		⊞ jtag_uart	JTAG UART	pll_c0	0x03244158	0x0324415f		1
☑		⊞ ext_ram_bus	Avalon-MM Tristate Bridge	pll_c0				
☑		⊞ high_res_timer	Interval Timer	pll_c0	0x03244060	0x0324407f		2
☑		⊞ ext_flash	Flash Memory Interface (CFI)	pll_c0	0x02800000	0x02ffffff		
☑		⊞ ext_ram	IDT71V416 SRAM	pll_c0	0x03100000	0x031fffff		
☑		⊞ lan91c111	LAN91C111 Interface	pll_c0	0x03220000	0x0322ffff		3
☑		⊞ lcd_display	Character LCD	pll_c0	0x032440f0	0x032440ff		
☑		⊞ uart1	UART (RS-232 Serial Port)	pll_c0	0x03244080	0x0324409f		4
☑		⊞ button_pio	PIO (Parallel I/O)	pll_c0	0x03244100	0x0324410f		5
☑		⊞ led_pio	PIO (Parallel I/O)	pll_c0	0x03244110	0x0324411f		
☑		⊞ seven_seg_pio	PIO (Parallel I/O)	pll_c0	0x03244120	0x0324412f		
☑		⊞ tightly_coupled_instru...	On-Chip Memory (RAM or R...	*multiple*	*multiple*	*multiple*		
☑		⊞ tightly_coupled_data_...	On-Chip Memory (RAM or R...	*multiple*	*multiple*	*multiple*		
☑		⊞ performance_counter	Performance Counter Unit	pll_c0	0x03244000	0x0324403f		
☑		⊞ onchip_ram	On-Chip Memory (RAM or R...	pll_c0	0x03230000	0x0323ffff		
☑		⊞ sdram	SDRAM Controller	pll_c0	0x01000000	0x01ffffff		
☑		⊞ dma	DMA Controller	pll_c0	0x032440a0	0x032440bf		6
☑		⊞ pio_0	PIO (Parallel I/O)	clk	0x03244130	0x0324413f		
☑		⊞ pio_1	PIO (Parallel I/O)	clk	0x03244140	0x0324414f		

Figure 133: Detailed configuration of the NIOS processor

The software application that controls output modulating signals was written in NIOS II 9.0 (Figure 133) Integrated Development Environment. Since the application was written in high level programming language it may face difficulties in proper timing of the generated control signal. To ensure accuracy in the timing of the generated signal, a custom function was created to generate time intervals based on the time required by the CPU to perform a single instruction.

The function was characterized using the DSOX91604A scope (Figure 120). The accuracy of the generated signal was measured for a wide number of instructions from 0 to 1000, and the linearity of the characteristics were evaluated. Figure 134 presents the measured characteristics of the timing function in the controller; the length of the HI and LO states of the generated signal were measured for a different number of processor instructions.

The timing function exhibits a near-linear characteristic dependency between a number of instructions and lengths of HI/LO state of the generated signal from 3 µs to 300 µs. When the length of time slot is further reduced below 3 µs the linear characteristics become slightly disturbed and lengths of the HI and LO states are not equal. Below a length of 3 µs the LO state becomes approximately 65 ns longer than the length of the HI state.

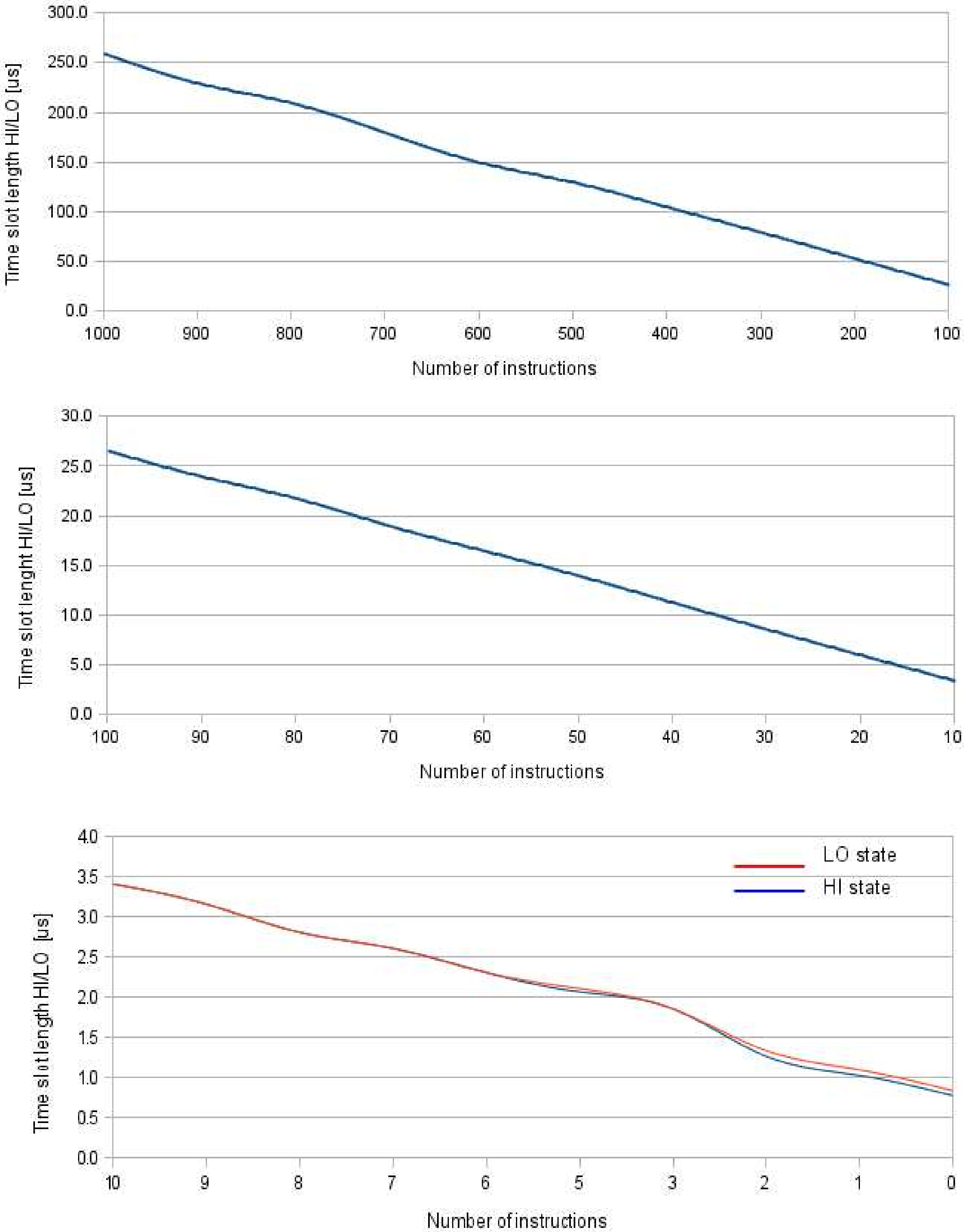

Figure 134: Accuracy of the timing function in the FPGA-based controller

The speed benchmark of the modulating signal is presented in figure 135. The result indicates that the highest available speed for this particular prototype is 1.785 MHz with a HI state length of 258.9 ns and a LO state length of 298.9 ns.

Figure 135: Speed benchmark of the FPGA-based controller

The difference exhibited in the lengths of the HI and LO states confirm the results of the timing function characterization. In addition, the measured rising and falling edges of the control signal were approximately 3 ns and 4 ns, respectively.

If the length of the optical Ethernet frame is 1526B, including the preamble and SFD (Figure 66), and the 258 ns long HI state represents the length of the time slot, than this switch controller prototype can support a network at a 47 Gb/s data rate with the frame-by-frame optical switching fashion.

The configuration of the controller can be loaded from a Compact Flash card, RS232 port or Ethernet port. The Ethernet port may be used for remote configuration and monitoring of the controller. The configuration data can be sent via the same optical link that transports data in PON. In this case, configuration data is sent through an additional wavelength that is separated at the remote node by a DWDM filter and directed to an opto-electrical signal converter (Figure 136).

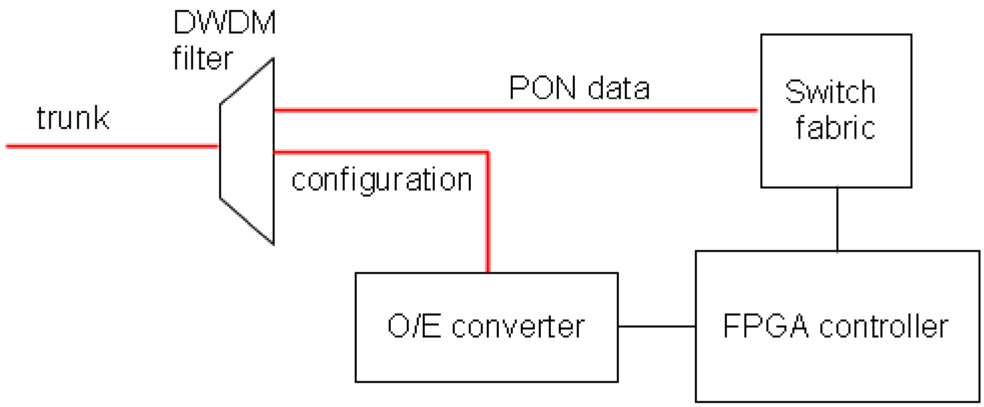

Figure 136: Controller configuration through the optical trunk. Controller can be collocated with optical switch in the remote node.

The switch fabric, controller and O/E converter can be collocated with DWDM filter in a single 1U size enclosure that has a size compatible with a standard telecommunication rack. If the control signal is not collocated within the data transmission band (1500 nm) than the DWDM can be replaced by a low cost 1500/1300 multiplexer such as the commercial CUBO-1659 (Figure 137). This solution would allow the sending of a 1300 nm control signal through the same trunk that accommodates the 1500 nm data signal.

Figure 137: Commercial grade MUX/DEMUX (1500nm and 1300nm) CUBO-1659

The total power supply for the optical switch would be the sum of the power supplies required by the switch fabric (dependent on the number of SOA elements), FPGA controller, TEC and O/E media converter.

To further reduce the power consumption of the controller, the Stratix FPGA development board may be replaced by the new generation energy efficient development board that implements Cyclone IV FPGA (Figure 138).

Figure 138: Small factor Cyclone IV FPGA development board MicroSDK

The *BeMicroSDK* [178] is an example of the new generation small size development boards with Cyclone IV EP4CE22 FPGA that consists of 22000 logic elements, 64MB DDR RAM, 16MB serial flash memory, a Micro SD card reader, 100Mb Ethernet NIC and a temperature sensor. The board consists of an interface with 80 I/O pins that allow the control of an 8x8 switch with 64 SOA elements. The total power supply requirement for this device is less than 500mA at 5V. The dimensions of the board do not exceed 130 mm (L) x 30 mm (W) x 20 mm (H). The significant reduction in physical size and power consumption make this board a very attractive candidate to be applied as an autonomous controller of the optical switch.

The dimensions of the controlling system and its power consumption can be further improved if an optical Ethernet port is integrated with the development board and unused components such as certain memory chips, LEDs and DIP switches are removed from the board.

SOA as an amplifier

Power budget considerations in CWDM/TDM-PON

To better understand the importance of proper positioning of the optical amplifiers within the network infrastructure there should be an analyzed power budget in the optical network and its evolution when the semiconductor optical amplifier is implemented.

As presented in previous chapters, GPON is one of the most popular standards in North America while EPON and GEPON standards are very popular in Asia and Europe. The 10-GEPON standard has already attracted a large number of network vendors due to its planned support of DWDM transmission. The reviewed standards carry several limitations;

- A limited number of ONUs (32× in EPON, 64× in BPON and 128× in GPON).
- The transmission distance without any additional amplification systems is limited to 20 km.
- The significant lack of compatibility between IEEE and ITU standards such as different transmission speeds (1Gbit/s GEPON vs. 2.488 Gbit/s GPON) and different encapsulation of the transmitted data (modified Ethernet in EPON vs. GEM in GPON).

Several improvements have been developed by device vendors. Huawei Technologies Ltd. provides APONs with a split ratio of 64x [179] (in comparison to the standard 16x); AD-net Technology Co. offers 1Gb/s EPONs with a split ratio of 64x (in comparison to the standard 32x) [180]; Flexlight and Infinera offer GPONs over 130 km with the DWDM extension (in comparison to the standard GPON limited to 20 km) [181]. Although number of commercial modification has been implemented to overcome PONs limitations most of those improvements are not properly standardized and they represent proprietary solutions.

Several transmission impairments have to be considered for the PON link design in order to ensure that the received signal power is large enough to maintain a required BER performance under all conditions. Power budget calculations are made to quantify such impairments.

A general PON link includes a transmitter, fiber, splitter and receiver for both down and upstream transmissions between the Optical Line Terminal (OLT) and the Optical Network Units (ONUs). Some of the main issues regarding the different link subsystems are:

- Transmitter: output power, bit rate, modulation format (binary or multilevel, phase or amplitude), extinction ratio, signal modulation method (direct modulation at the ONU or with an external modulator at the OLT), suppression ratio (if single mode source is used), wavelength, chirp, forward error correction (FEC), laser line width (to reduce the phase noise), relative intensity noise (RIN) and jitter.
- Fiber impacts: attenuation, return loss, polarization mode dispersion, chromatic dispersion, scattering and other nonlinear effects.
- The technology used to assemble an optical link also brings several sources of loss such as: bends, splices and connectors.
- Long reach links usually require amplification devices. Optical amplifiers have several limitations that can affect the overall performance of the optical path: output/input power, gain per channel, gain flatness, noise figure (NF).
- Optical splitters have a number of limitations that decrease the network overall performance. The most common are insertion loss, cross talk, jitter and polarization dependency loss.
- Receiver: the type of detector used (PIN or APD) determines the bit error rate (BER), sensitivity, jitter, preamplifier noise, bandwidth, jitter and signal to noise ratio (SNR).
- A margin for each subsystem should be considered in order to allow for ageing of sources and other components, extra splices (cable repair), upgrades in the bit rate or advances in multiplexing.

The link design in this analysis is based on the following parameters:

1. 5 CWDM wavelengths are used: 1270, 1290, 1310, 1330, and 1350 nm
2. One wavelength for upstream and four wavelengths for downstream
3. Average downstream bit rate: 100 Mbit/s,
4. Average upstream bit rate: 25 Mbit/s
5. Transmitter launch power: 7 dBm
6. Extinction ratio: 8 dB
7. Receiver sensitivity: -32 dBm
8. BER: 10^{-10}
9. Fibre type: SMF-28

10. Average OLT-ONU distance: 50km.
11. Connector pairs: 2
12. Splices: 1
13. Splitter insertion loss: -13 dB
14. Modulation type : NRZ-ASK
15. Mux/Demux insertion loss: 2 dB
16. Amplifier (BW): 100nm, G: 10, PDG: 0.5, NF: 6 dB)
17. Number of ONUs: 100
18. PON topology: star (Figure 139)

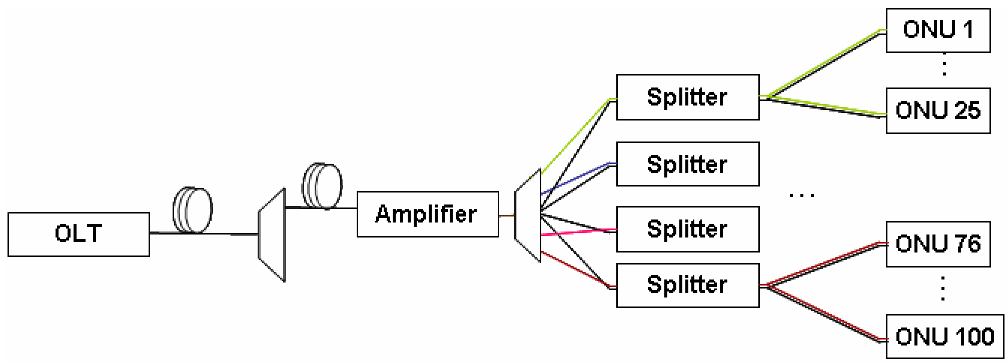

Figure 139: Topology of the analyzed PON

The estimated (calculated) power penalty in respect to the each impairment can be considered as following:

- Transmitter power margin (dB):
  - chirp margin: 0.5
  - extinction ratio margin: 1.4
  - ageing margin: 0.25
  - electrical response: 0.5
- Multiplexer/demultiplexer power margin (dB):
  - polarization dependency: 0.1
  - cross talk: 0.3
  - insertion loss: 2
  - ageing: 0.2
- Fiber power margin (dB):
  - dispersion: 2
  - self phase modulation: 0.5
  - cross phase modulation: 0.5
  - polarisation mode dispersion: 0.5
  - Raman effects: 0.5
- Amplifier power margin (dB):
  - gain tilt: 3
  - polarization dependency gain: 0.5
  - input loss: 0.1
  - ageing margin: 0.5

- Receiver power margin (dB):
  - input loss: 0.1
  - electrical response: 1
  - sensitivity tilt: 0.5
  - ageing: 0.5

In total, the link power penalty is around 17 dB. Figure 140 illustrates the corresponding link power budget. Adding new ONUs to the network will increase the total splitting loss. This table shows that there is a trade-off between fiber loss (fiber length) and splitting ratio (number of ONUs).

Parameter	Value [dB]	Power budget [dB]
Transmitter power	7	+7
Receiver sensitivity	-32	+32
Margin	17	-17
Fiber loss (50km)	17	-17
Splitter loss (32 ONUs)	15	-15
SOA gain	10	+10

Figure 140: PON power budget

The CWDM wavelengths used suffered different attenuation and dispersion in the fiber. Figure 141 presents the dispersion and attenuation of the SMF-28 fiber. As shown in this figure, the first CWDM channel (1.27 μm) has 0.084 dB/km more loss than the fifth channel (1.35 μm). In other words, for a fixed length of fiber (50 km) and the same transmitter power, the fifth CWDM channel can serve twice the number of ONUs than the first channel (50 km×0.084 (dB/km) = 10log(2)).

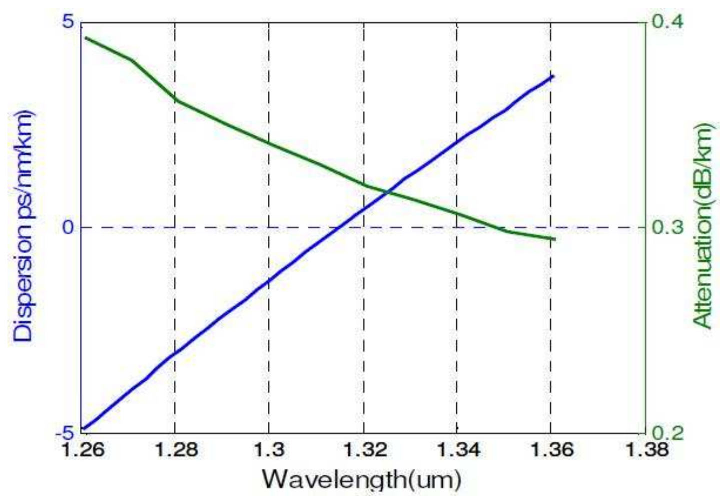

Figure 141: SMF-28 fiber characteristics [182]

The network topology consists of a remote node (RN) that contains several cascaded splitters, multiplexers and possibly an amplifier. The optical link between the remote node and each of the

ONUs is called an “optical arm”. Each arm has a certain power budget that can be distributed over all the elements of the arm.

For a typical optical path length (e.g. 50 km) and number of ONUs per wavelength (e.g. 32), the assigned power budget for loss and splitter is 32 dB. For a constant power budget in the PON, the impact of the optical path length on the maximum number of ONUs (from the power budget point of view only) is presented in figure 142. The graph was obtained using VPI simulation software and network assumptions that are listed earlier.

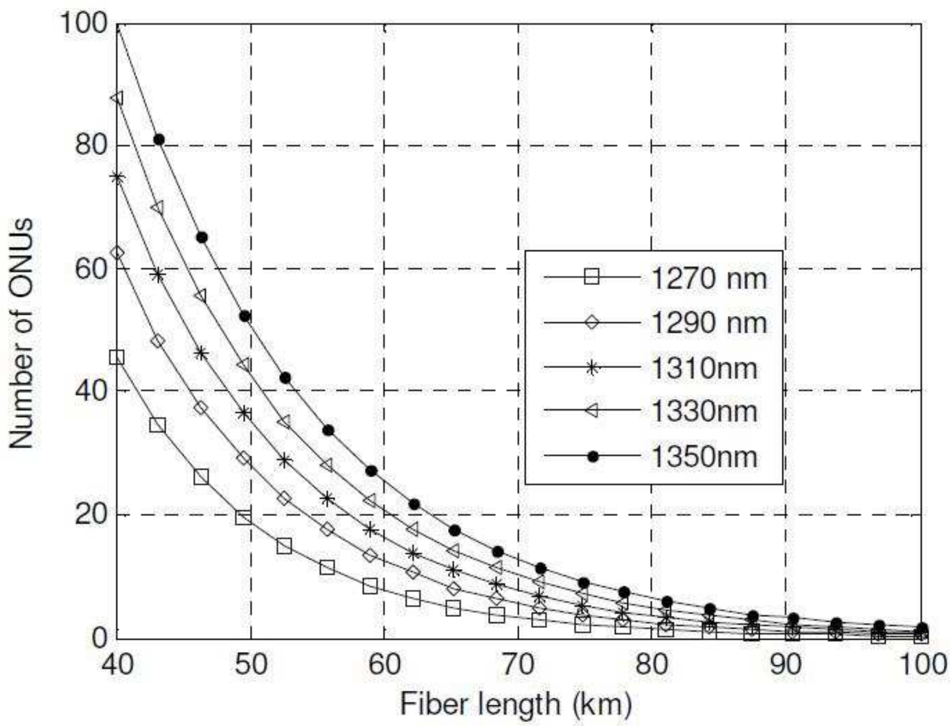

Figure 142: Limit of ONUs based on available power margin

A real network deployment usually does not have fibers of equal length between the OLT and the ONUs. The variable length of the fibers leads to different signal losses and power levels for both the upstream and the downstream signals. The most common solution to this problem is to use power equalization (via attenuator or amplifier). In order to reduce the loss, the wavelengths with lower attenuation should be assigned to the ONUs located far from the OLT while the wavelengths with higher attenuation are assigned to the shorter distances.

More efficient management in terms of power and capacity is needed to optimize the available power margins. As indicated in figure 142, a shorter fiber length transfers part of the power budget towards a larger number of end users. Figure 143 illustrates the BER variation as a function of fiber length for a splitting ratio of 32.

ITU recommendations define the maximum acceptable delay for VoIP services as 75 ms in one way

[183]. The maximum acceptable delay for IPTV is defined as the *delay factor* (DF) and it is one of the components of the *media delivery index* (MDI) [184]. A typical value of DF is between 9 ms and 50 ms. The discrepancy between these two values is attributed to a wide variation in the quality of available IPTV receivers (the recommendations are for different receiver buffer sizes).

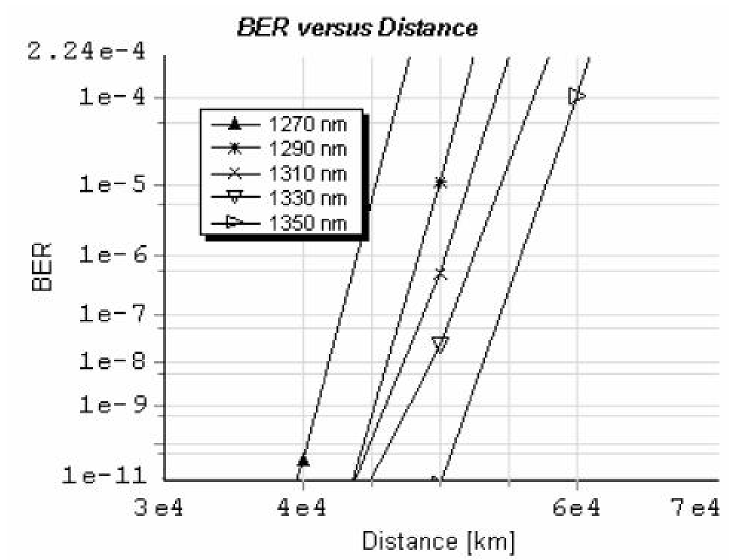

Figure 143: BER as function of fiber length for different CWDM wavelengths (splitting ratio of 32)

EPON provides a timeslot of 2 ms for each ONU. If only one wavelength per one way is used, the maximum number of ONUs is limited to 37 (75 ms/ 2 ms) for VoIP and 25 (50 ms/ 2 ms) for IPTV. By implementing 4 wavelengths for downstream transmission, the maximum number of ONUs is increased to 148 and 100 for VoIP and IPTV, respectively.

It is apparent that the EPON frame-length places a stronger limitation on the number of ONUs than on the power budget. To take advantage of the available generous power budget, the bit-rate has to be increased so that each data frame will take a shorter time to be transmitted and therefore more timeslots will fit within the maximum acceptable delay interval.

This chapter presented analysis of several impairments in PONs, with an emphasis on power budget issues. A PON design for 100 ONUs (each with average bit rates of 100 Mbit/s and 25 Mbit/s for downstream and upstream transmission, respectively) based on a 5-channel CWDM/TDM technique at a bit rate of 2.5 Gbit/s is presented. The impact of the link length on the maximum number of ONUs is shown, as well as the dependency between the number of end users and the number wavelengths used for data transmission. The link power budget analysis illustrates that the number of ONUs is limited when the TDM time-slots are large. Increasing the number of CWDM channels as well as the bit rate (in order to decrease the length of the TDM time-slots) will also allow an increase in the number of ONUs in the PON design presented.

Power booster in gigabit Ethernet infrastructure (IEEE 802.3z)

Operators and maintenance staff in commercial optical networks frequently deal with the deterioration of the transmitted signal due to number of imperfections along the optical line such as: interconnections and splices, too long optical fibre and low radius fibre bends. These imperfections may introduce an excess of optical loss and leading users to complain about low quality, slow and erroneous transmission.

In certain circumstances the elimination of those imperfections may require very expensive and complex modifications of the existing network infrastructure. Although those modifications usually are technically possible, their cost could be unbearable for the network operator. In such situations, there is a need for a low cost solution that can be implemented in the network infrastructure without expensive modifications. A possible solution would be the deployment of optical amplifiers at both ends of the optical link that exhibits excessive loss. In this configuration amplifiers will work as power boosters located near optical transmitters.

The commercially available amplifiers are based on EDFA. It was presented in previous chapters that EDFAs are relatively large sized devices and they require significant power supply. EDFA may be a sufficient solution from the technical perspective but its implementation may not be economically justifiable due to its high power consumption and poor integration with existing optical components.

Network operators may seek out a small size, low-cost, energy efficient alternative to EDFA that will be able to counterbalance the excessive loses in the optical link. The semiconductor optical amplifier (SOA) may be a good candidate when such characteristics as small size, low energy consumption and low cost of implementation are considered.

An experimental setup was built to evaluate SOA as a power booster deployed in optical gigabit Ethernet infrastructure. The experimental configuration consisted of a laptop with the Linux operating system that was custom configured to work as a portable network monitoring workstation and the source of the Ethernet frames. The JDS SFP OC48 telecommunication grade transceiver (output power: 0.7dBm at 1551 nm) was chosen as the source of optical signal and it was implemented in the media converter Omnitron iConverter GX/TM (Figure 144a).

The laptop was generating traffic in the form of ICMP packets and raw Ethernet 802.3 frames and sending it through the media converter along the optical loop with a date rate of approximately 1Gb/s. The returning signal was analyzed on the Agilent DCA86100B oscilloscope and network monitoring software installed in the laptop. The optical power was measured using a JDS power meter.

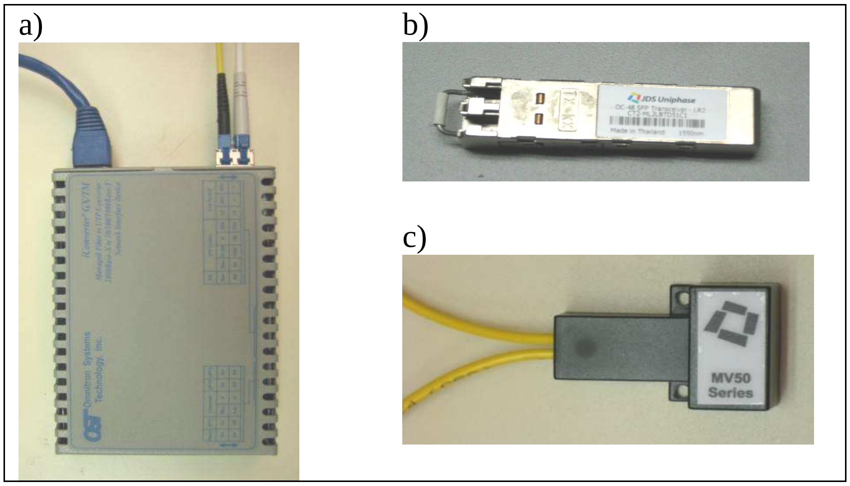

Figure 144: Media converter (a) and SFP OC-48 (b) tunable attenuator JDS MV50 (c)

The optical loop deployed a splitter 60/40 and optical tunable attenuators JDS MV50 (models MH6182 and MH6187) to create a near realistic environment of the network infrastructure with a significant optical loss (Figure 144c).

The figure 145 presents the configuration of the experimental test bed. The laptop was sending data through the media converter and 40% arm of the splitter. The returning packets and frames were analyzed for any data loss. The output power of the SFP was 0.7 dBm and the output power from 40% splitter arm was -11.755 dBm. The introduced optical loss (about 11 dB) represented approximately 22 km commercial SFM.

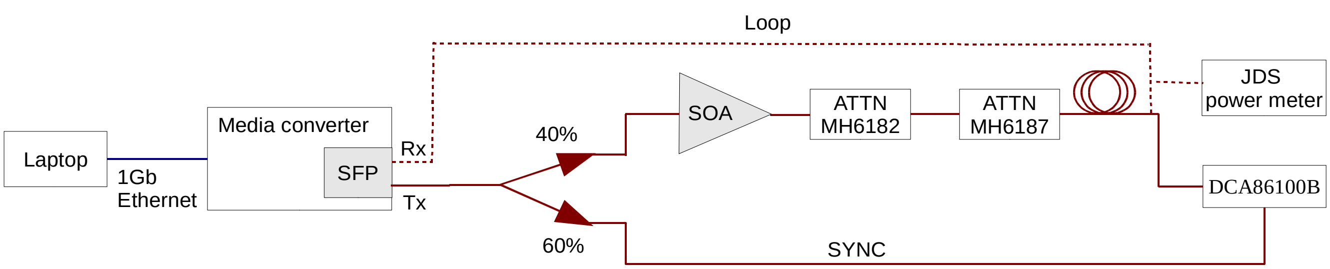

Figure 145: Test system for evaluation of SOA-based power booster

After the MH6182 was added to the loop, the measured optical output power was -17.890 dBm and the eye diagram was examined (Figure 146). The ICMP signal was received with no data loss. The added attenuator introduced 6.1 dB of additional optical loss that represents approximately 12 km commercial SMF.

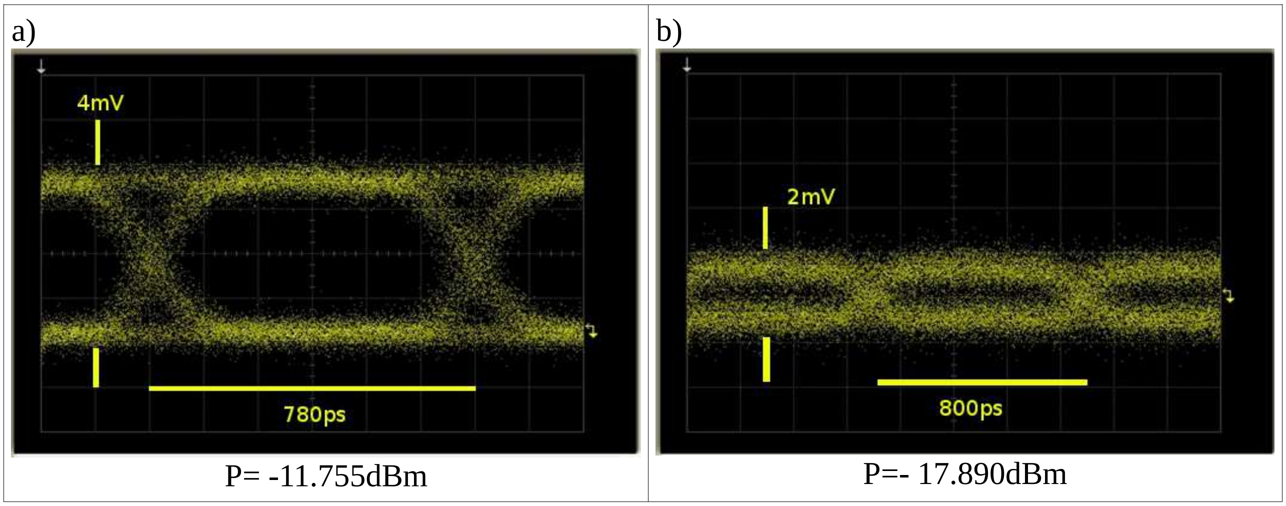

Figure 146: Eye diagram of the optical output signal measured after the splitter (a) and after MH6182 (b)

Although significant loss of the signal was observed the data was received from the loop with no disruptions. The second attenuator, MH6187, was added to the loop and its loss was tuned until the eye diagram became deteriorated beyond the sensitivity of the scope. The eye diagram was lost when the optical output power at the MH6187 decreased to -26.510 dBm, but the ICMP signal was received successfully. This result shows that the implemented SFP transceiver is sensitive enough to successfully detect an optical signal traveling along path with over 26 dB loss (approximately 50 km distance).

The SMF spool (-11 dB loss) was inserted into the optical loop after the MH6187 to introduce additional optical loss. The ICMP signal was lost when the optical output power decreased to -37 dBm. After the loss of the ICMP signal occurred the commercial grade SOA OPB1010NCFA was deployed in the test system between the optical splitter and the attenuator MH6182. The supply current of the SOA was tuned until recovery of the eye diagram and ICMP signal was observed.

Although the ICMP signal was recovered when the supply current reached 70 mA and the output power was -34dBm, the eye diagram was not yet recovered. The low level of optical output power can be explained by SOA characteristics of output power vs. input power that was presented in figure 109. Further increasing the SOA current to 150 mA allowed for the recovery of the eye diagram (Figure 147). The eye diagram became quite visible when the current approached 190 mA which was close to the saturation level.

The result of this test confirmed that SOA can be implemented as a low cost power booster in optical gigabit optical Ethernet infrastructure (EPON). The small physical dimensions and low power consumption makes SOA an attractive candidate to become an amplifier that is easy to deploy and maintain.

a) b)

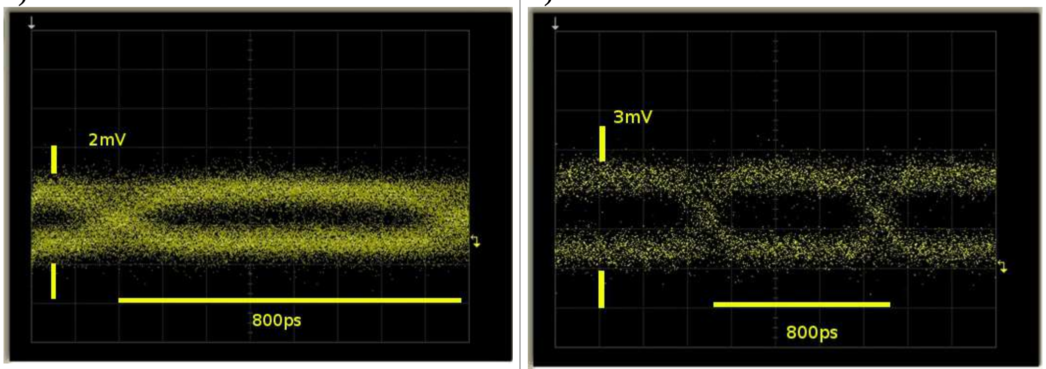

I(SOA)=150mA I(SOA)=190mA

Figure 147: Recovered eye diagram of the optical signal after implementation SOA in the test system

The results also exhibited a certain drawback of the SOA. The recovered eye diagram is not as clean and wide open as the original diagram measured after the splitter arm. This indicates that SOA injects to the optical link a certain amount of noise that has a negative impact on the transmitted data.

Power booster in OC-48 infrastructure

The previous chapter presented the successful application of the SOA as power booster in optical gigabit Ethernet infrastructure that was compatible with GE-PON. Although SOA provided counterbalance for the optical losses that the transmission link suffered from, it also showed that SOA injects a limited amount of noise which becomes strongly pronounced when the supply current for SOA approaches the saturation level.

OC-48 connections are used as the backbone of many regional Internet Service Providers (ISPs). This chapter examines the performance of the same commercial grade SOA when it was implemented as a power booster in OC-48 infrastructure at a 2.488 Gb/s data rate. The experimental test bed consisted of a continuous wave (CW) JDS LD with an optical output power of 0.5 dBm at 1551 nm, an external electro-optical modulator and two spools with commercial grade Lucent 20 km length SMF (Figure 148).

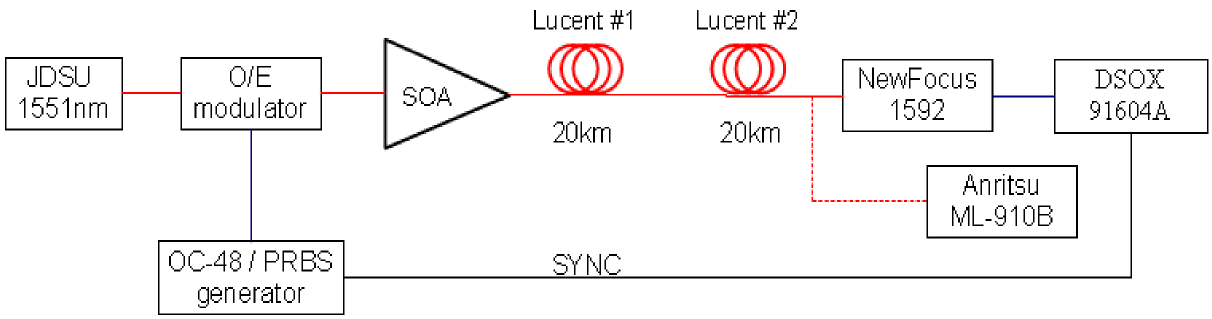

Figure 148: Test system for evaluation of the power booster SOA in OC-48 network

Figure 148 presents a test system with the implemented OC-48 transmission. The Agilent 4906B was used as a OC-48 source of optical Ethernet frames generated at a 2.488 Gb/s data rate. Fiber spools Lucent #1 and Lucent #2 have a measured loss of 8.9 dB and 9.7 dB respectively at 1551 nm. Both spools when connected together provided a 19 dB loss in total that included the loss at the SC/SC inter-connector between spools.

There were two O/E modulators used in the test system (one at the time): JDS 10020447 and Lucent 2623NA with measured insertion losses of 9.5 dB and 12 dB respectively. The eye diagram of the optical signal was analyzed in different locations of the optical link using the oscilloscope Agilent DSOX. The optical power of the transmitted signal was measured with the power meter Anritsu ML-910B.

Before SOA was deployed in the optical link, the output power of the optical signal and its eye diagram were analyzed to evaluate the loss and distortion. Figure 149 presents a comparison of the optical output signal measured after spool #2 with the original OC-48 modulating signal.

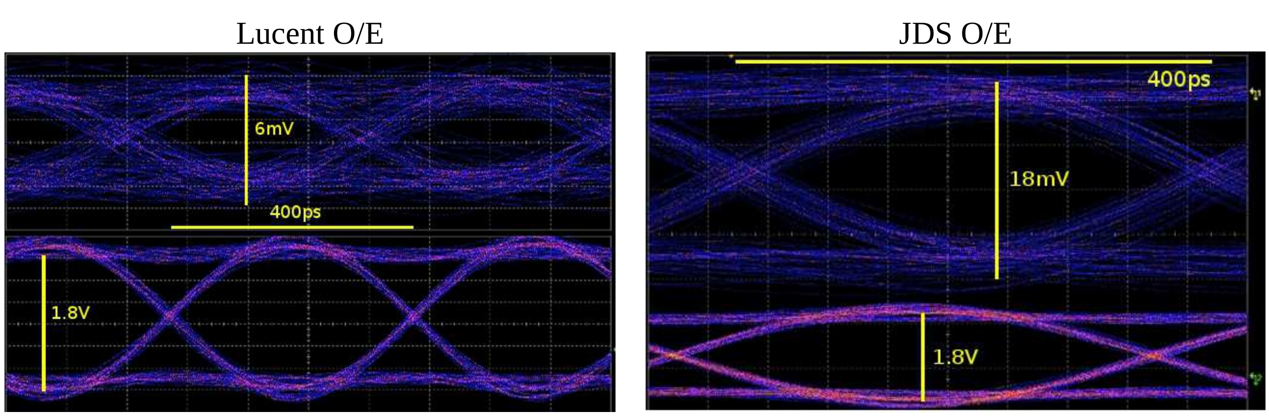

Figure 149: Comparison of the eye diagram OC-48 modulating signal (1.8V) with output optical signal after the spool #2 (top). No amplifier applied.

Visible signal distortion occurred when the Lucent modulator was implemented. This negative effect was caused by the temporary fiber adapter used in the input port of the modulator to replace the original FC adapter that had been damaged.

After SOA was implemented in the optical link between the modulator and spool #1, optical power was measured at the end of the link and the eye diagrams were compared with the original OC-48 modulating signal. Figure 150 presents a comparison of the eye diagrams for different values of the SOA supply current.

I(SOA)	Lucent O/E	JDS O/E
40mA	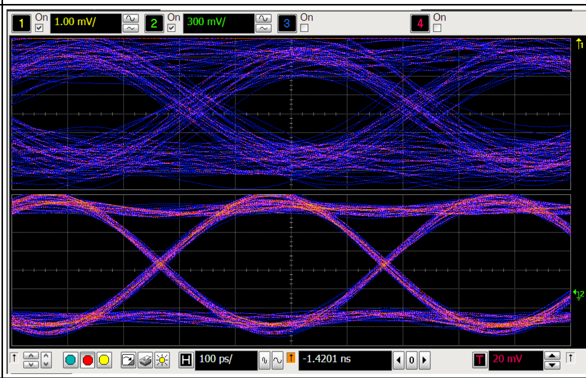	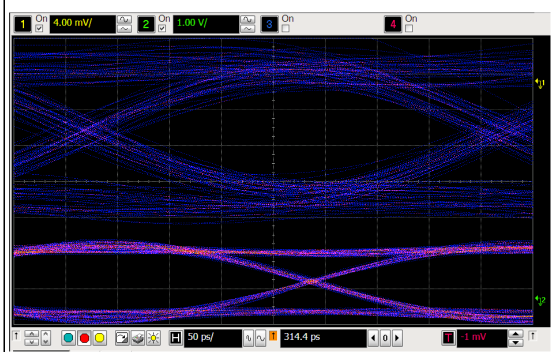
60mA	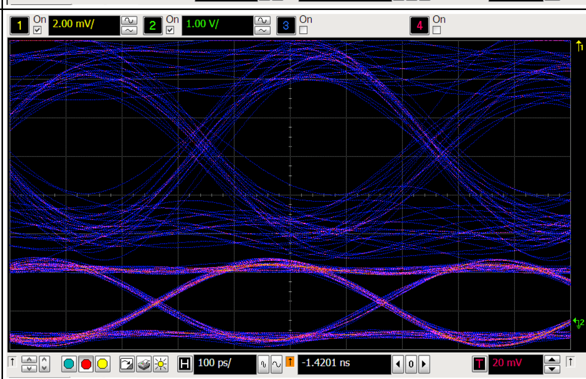	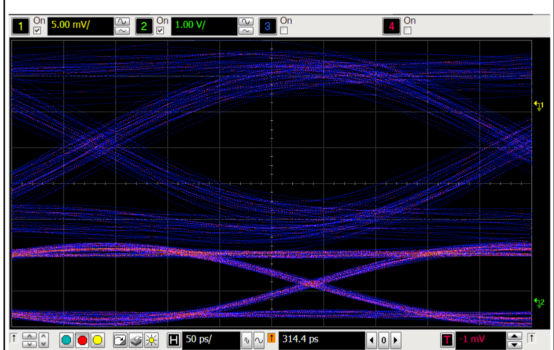
80mA	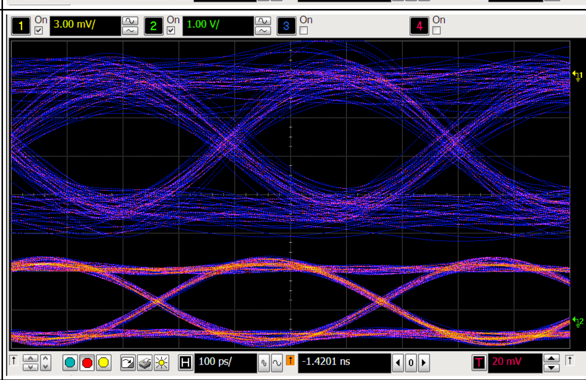	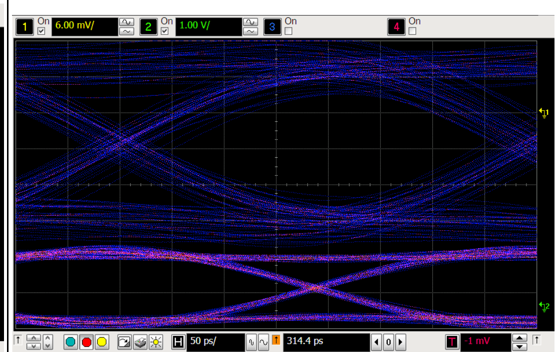

100mA	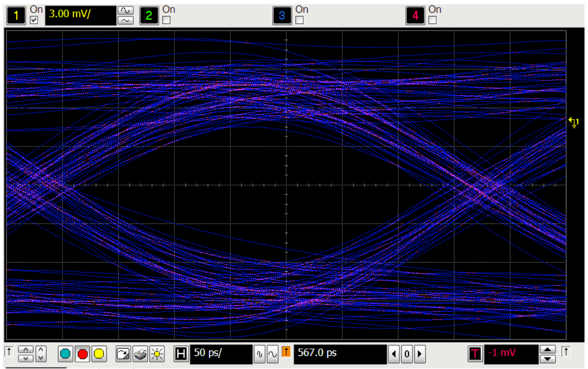 *output signal only*	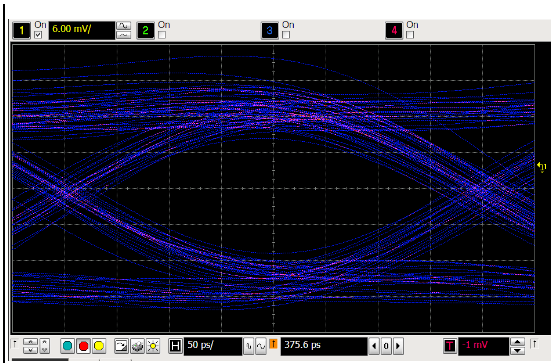 *output signal only*

Figure 150 Comparison of the eye diagrams OC-48 modulating signal (bottom) with output optical signal after the spool #2 (top) for different values of SOA supply current.

Results presented in figure 150 exhibit the presence of noise in optical signal in both configurations: with Lucent modulator as well as with JDS modulator. The main sources of the noise were imperfections of signal modulators used in the test system. The Lucent modulator had applied a temporary fiber termination that replaced the damaged FC connector in one of the optical ports. This modification caused additional optical noise and it increased insertion loss from 6 dB (guaranteed by manufacturer) to 12 dB. The JDS modulator is a 7 year unit that was intensively used in the laboratory. This device exhibited certain aging effects such as signal response deterioration that was strongly exhibited at modulating frequencies above 2.3 GHz.

An interesting effect was observed when the Lucent modulator was implemented; the signal noise was more intensive at lower values of the SOA supply current than at higher current values. It is also easy to notice that this noise was much higher at any SOA current than the noise exhibited when the JDS modulator was applied.

Figure 151 presents the changes in the optical output power of the modulated signal (measured after the spool #2) when the SOA supply current was tuned. The starting point of the graph is marked as 0 mA which indicated the status of the output power when no amplifier was implemented.

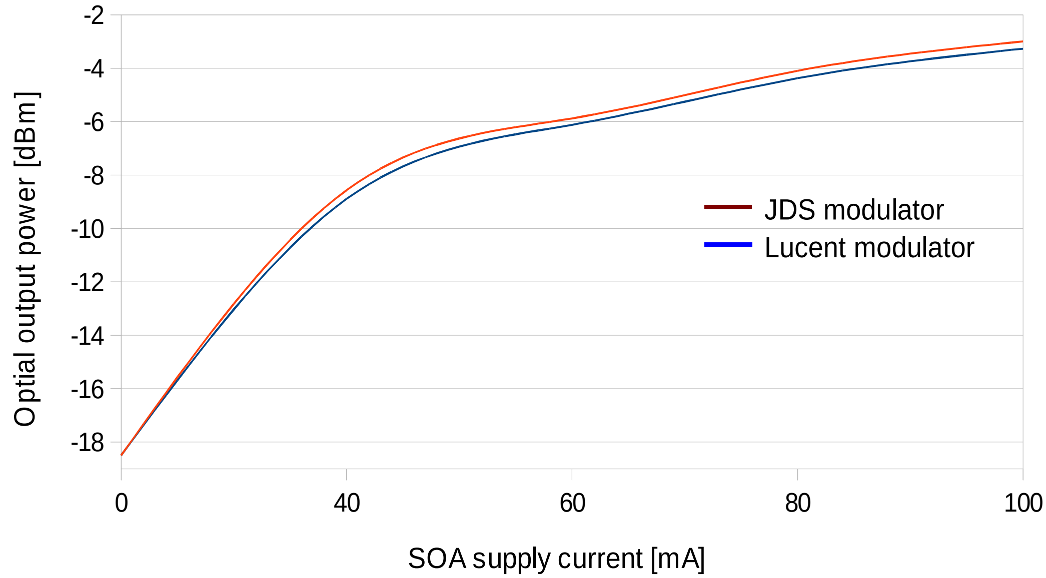

Figure 151: Changes in the optical output power when SOA supply current was tuned.
For I = 0mA, an amplifier was not present.

This graph indicates that the characteristics of the optical signal for both modulators follow the same path except the Lucent device which introduces a higher loss than the JDS device. There are visible two sections where both characteristics exhibit near-linear behavior: below 40 mA and above 50 mA of the supply current.

Although significant noise was observed in the received optical signal caused by imperfections of the signal sources amplified by SOA, the eye diagram was open for certain values of the SOA current. This result indicates that SOA can be successfully implemented as a power booster in OC-48 infrastructure under two conditions:

- The sources and modulators of the optical signal should not generate additional distortions or noise that would be amplified by SOA and then transmitted over the whole optical link.
- SOA should not work in its maximal amplification region because this causes significant increase of ASE.

Inline amplifier in OC-48 PON

Previous chapters presented results of implementation SOA in optical network as power booster. Those results proved that SOA is a good candidate for implementation in power booster devices under two conditions: SOA supply current does not reach values that could cause an extensive optical noise and the technique of light modulation does not insert additional signal distortion to the optical system.

Another configuration, where optical amplifier can be deployed is a middle of the optical path where. In this configuration SOA works as an inline amplifier and it amplifies optical signal that has been already partially deteriorated. It was discussed in previous chapters that SOA has tendency to emit a significant amount of noise when supply current is increased beyond certain threshold. This threshold depends on number factors such as: how SOA was designed and manufactured, what materials were used.

To evaluate influence of the SOA noise on the optical signal a test system was built with SOA OPB1010NCFA implemented as an inline amplifier. The figure 152 presents architecture of the test system that is very similar to the one described in the chapter 7.7.2, except the SOA is located between two spools of the SMF.

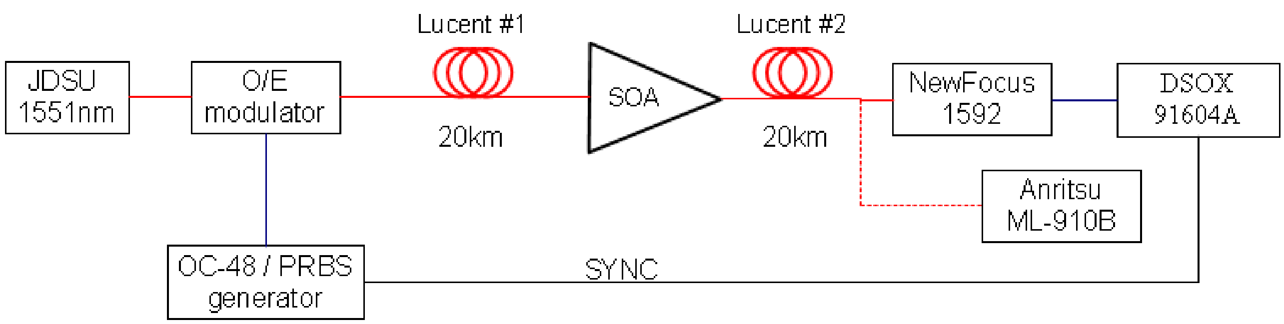

Figure 152 Test system for evaluation inline SOA in OC-48 network

The experimental test bed consisted of continuous wave (CW) JDS LD with optical output power 0.5dBm at 1551nm, external electro-optical modulator and two spools with commercial grade Lucent 20km length SMF. The Agilent 4906B was generating OC-48 optical Ethernet frames at 2.488Gb/s data rate. Fiber spools Lucent #1 and Lucent #2 had measured loss 8.9dB and 9.7dB respectively at 1551nm.

There was Lucent 2623NA O/E modulator used in the test system with measured insertion loss 12dB. Eye diagram of the optical signal was analyzed in using oscilloscope Agilent DSOX.

Figure 153 presents comparison of the original modulating signal generated by Agilent 4906B and optical signal at the output of the O/E modulator and signal at the out of the second fibre spool when no amplifier was implemented.

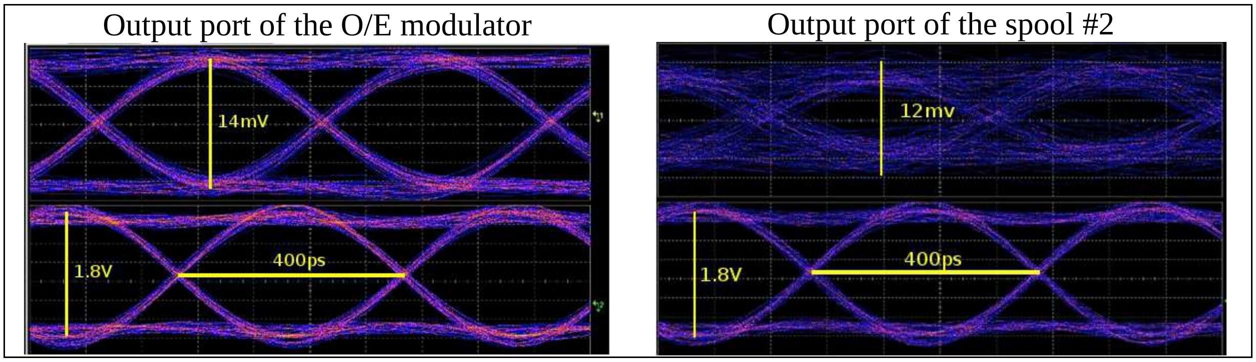

Figure 153 Comparison of eye diagrams in OC-48 modulating signal (1.8Vpp) with output optical signal. No amplifier applied.

The comparison exhibits significant deterioration of the eye diagram after optical signal travels two fibre spools that represent over 40 km of optical path.

After SOA was implemented in the optical link between two fibre spools optical power was measured at the end of the link and the eye diagrams were compared with original the OC-48 modulating signal. Figure 154 presents comparison of eye diagrams for different values of the SOA supply current.

I(SOA)	Eye diagrams
40mA	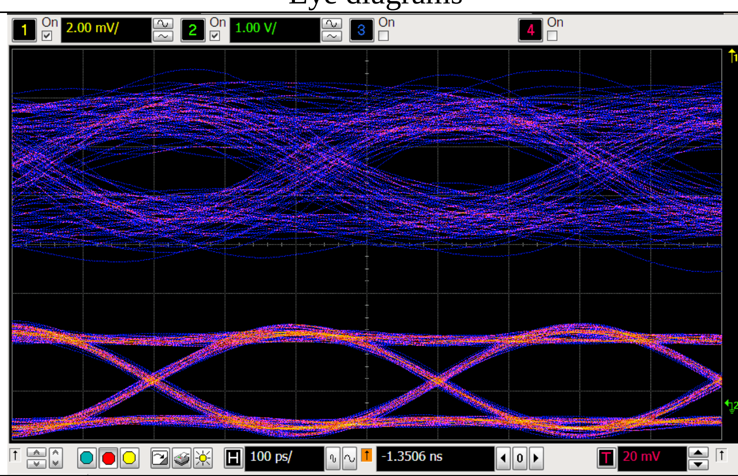

60mA	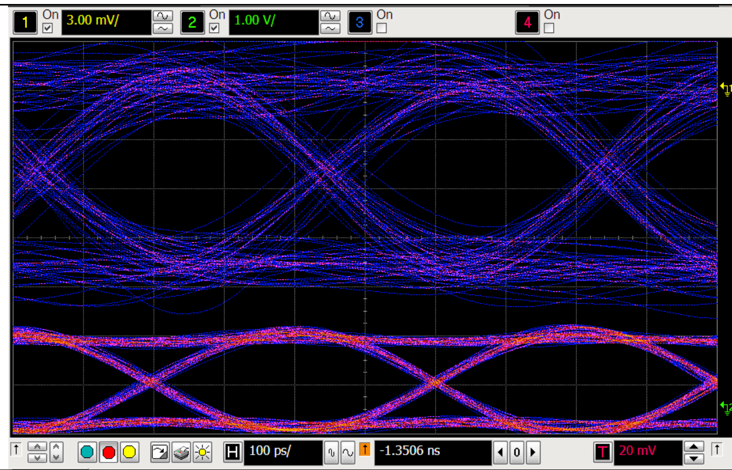
80mA	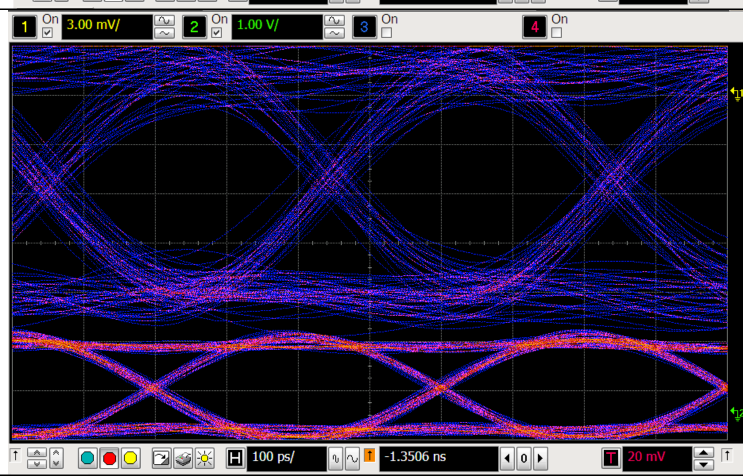
100mA	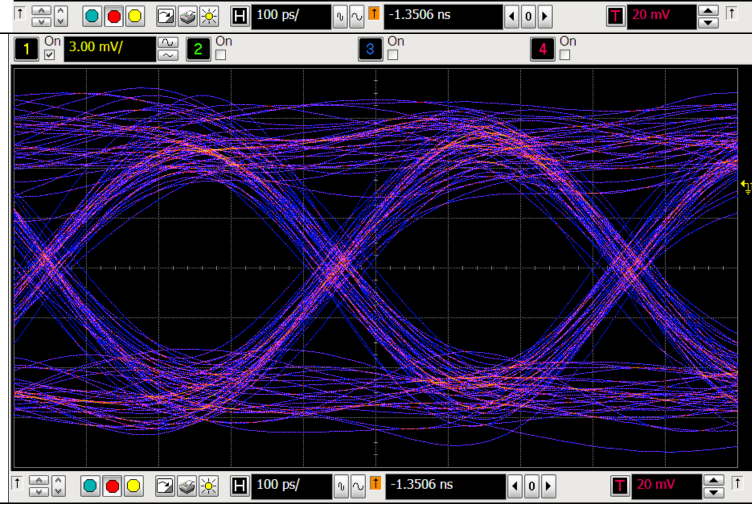

Figure 154 Comparison of eye diagrams OC-48 modulating signal (bottom) and output optical signal after the spool #2 (top) for different values of SOA supply current.

Presented results indicate that SOA working in inline amplifier configuration does not disrupt optical signal with spontaneous emitted noise in degree as high as when it works in power booster configuration. The captured eye diagrams are open at all values of the applied supply current.

The lack of significant noise and distortions in observed eye diagram of the amplified optical signal suggests that SOA is a good candidate for implementation in inline amplifiers. In addition to that, comparison with eye diagrams from bower booster configuration indicates that for higher levels of the optical gain (higher SOA supply current) shows that inline configuration is less prone to signal distortion caused by SOA spontaneous emission noise.

Preamplifier in OC-48 PON

The test presented in previous chapter proved that SOA is a good candidate for implementation as inline amplifier and in addition to this the inline configuration exhibits far less impact of spontaneous emitted noise on amplified signal than configuration with SOA working as a power booster.

To have better overview of possible SOA configurations an additional test was done to evaluate SOA performance in preamplifier configuration where amplifier is located just before photo receiver. The test system had similar configuration to the one presented in chapter 7.7.4 except the SOA was located after the second spool (fig 155).

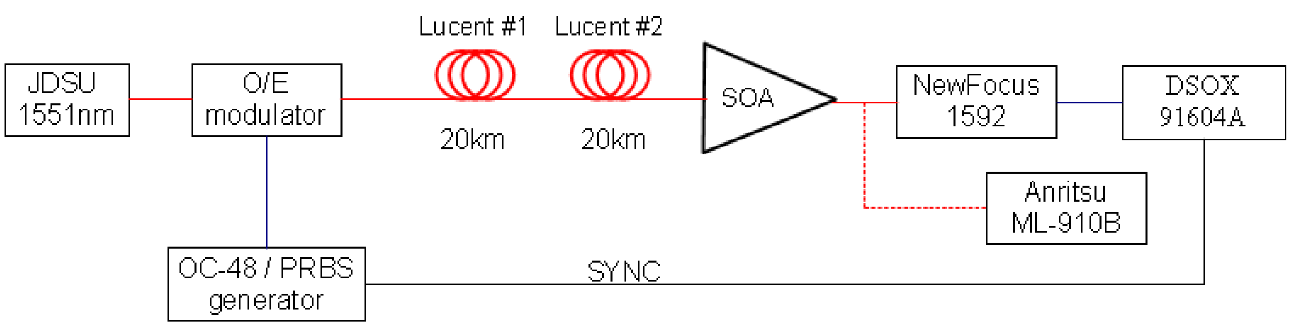

Figure 155 Test system for evaluation preamplifier SOA in OC-48 network

The experimental test bed consisted of continuous wave (CW) JDS LD with optical output power 0.5dBm at 1551nm, external electro-optical modulator Lucent 2623NA and two spools with commercial grade Lucent SMF with 20km length. The Agilent 4906B was generating OC-48 optical Ethernet frames at 2.488 Gb/s data rate. The modulator had measured insertion loss 12 dB and fiber spools Lucent #1 and Lucent #2 had measured loss 8.9 dB and 9.7 dB respectively at 155 1nm.

After SOA was implemented in the optical link between spool #2 and photo receiver New Focus 1592, optical power was measured at the end of the link and the eye diagrams were compared with original the OC-48 modulating signal. Figure 156 presents comparison of eye diagrams for different values of the SOA supply current.

I(SOA)	Eye diagram
40mA	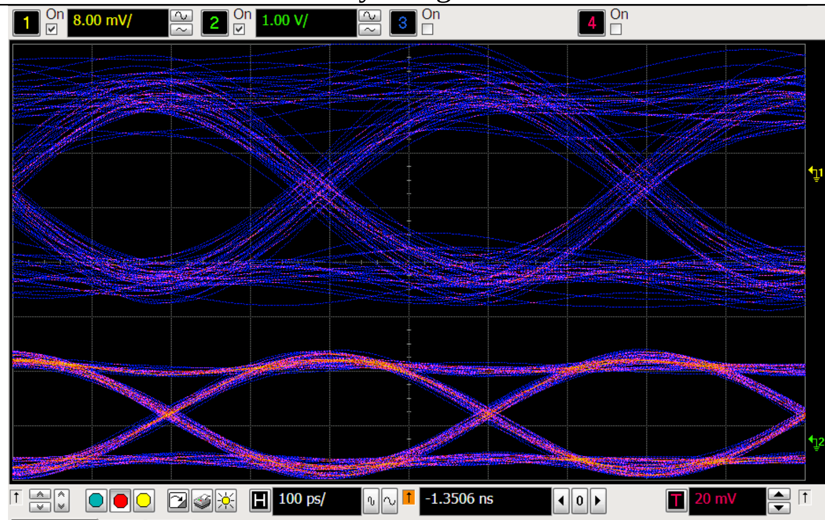
60mA	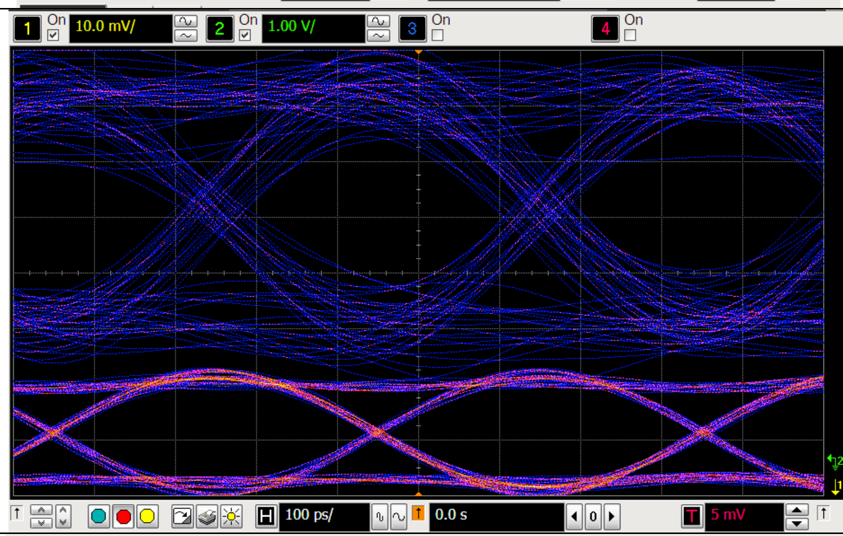
80mA	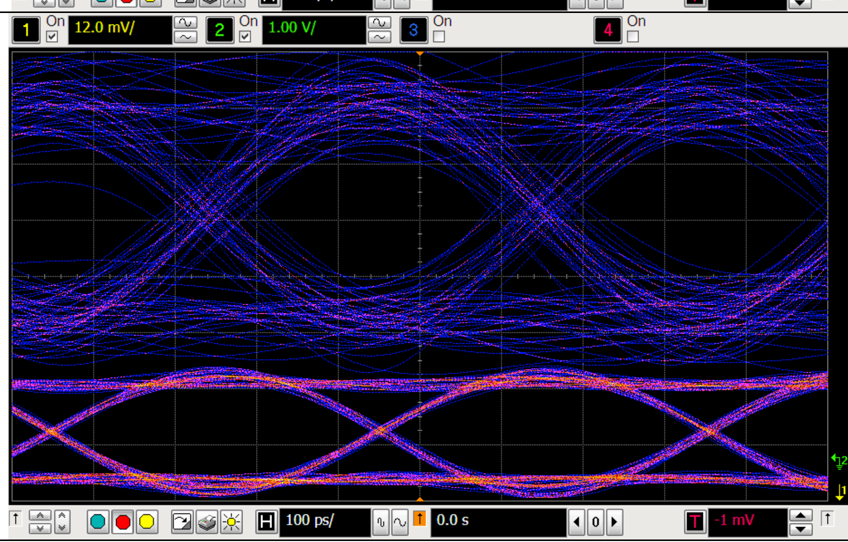

100mA	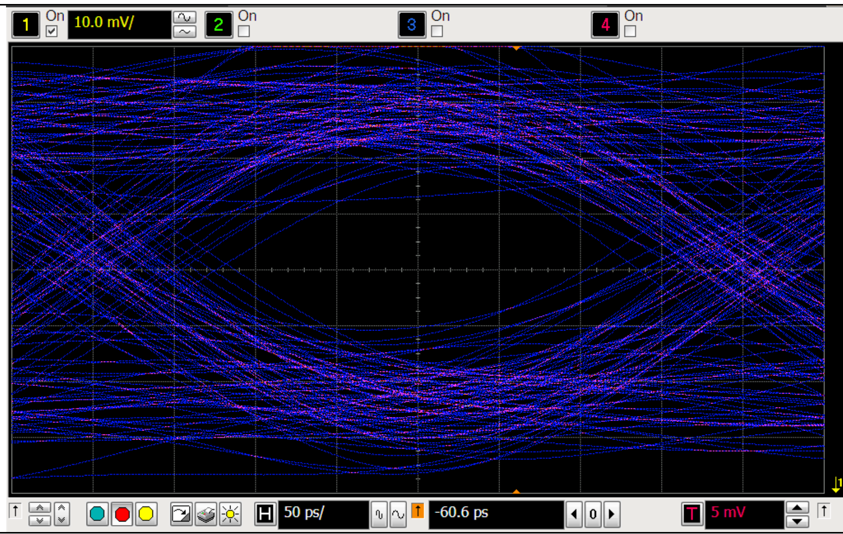

Figure 156 Comparison of eye diagrams OC-48 modulating signal (bottom) and output optical signal after the spool #2 (top) for different values of SOA supply current.

The observed eye diagram of the amplified signal was higher quality than non-amplified signal observed in figure 91. In addition, when eye diagrams in this configuration are compared to the eye diagrams that were obtained in configuration with inline amplifier across different values of the SOA current supply it becomes visible that preamplifier configuration in more fragile to noise and signal distortions coming along the optical line than inline configuration especially for higher values of supply current. The noise and signal distortions are amplified by the SOA and enter photo receiver.

This effect may result with difficulties in optical signal demodulation and data processing on the receiver side. The receiver my encounter more difficulties in signal processing if SOA introduces its own spontaneous amplification noise on the top of amplified noise that already existed in the optical signal.

The above problem may be solved in two different ways:

- The preamplifier configuration should have implemented an additional optical filter to limit noise that enters the photo receiver
- Digital signal processing unit that works in electrical domain should have implemented additional module to filter out noise from the demodulated data

Both methods will certainly increase cost of the ONU. To limit this additional cost the optical filter can be integrated with SOA during fabrication process. In case of filter that works in electrical domain, it can be implemented in the form of software processing unit embedded in low-cost FPGA. This would allow for dynamic tuning of the filer depending on type of noise that is dominating in decoded signal.

SOA in OC-48 DWDM PON

Previous sections provided results of implementing commercial grade SOA as an amplification device in different configuration of the optical transmission line. The configurations where SOA works as power booster were evaluated as well as configurations with SOA working as inline amplifier and preamplifier for photo receiver were presented.

All above results exhibits that SOA has ability to emit optical noise especially at higher values of supply current. The way how spontaneous emitted noise impacts the optical signal that carriers data depends on location of the SOA within optical path. Before an effective method of limiting the noise generated by SOA is developed, the characteristic of the noise has to be analyzed.

The SOA spontaneous emission noise was measured and presented in chapter 7.4. The total measured output power of the optical signal emitted by the SOA was -0.5 dBm at supply current 150 mA and near 0 dBm at supply current 180 mA.

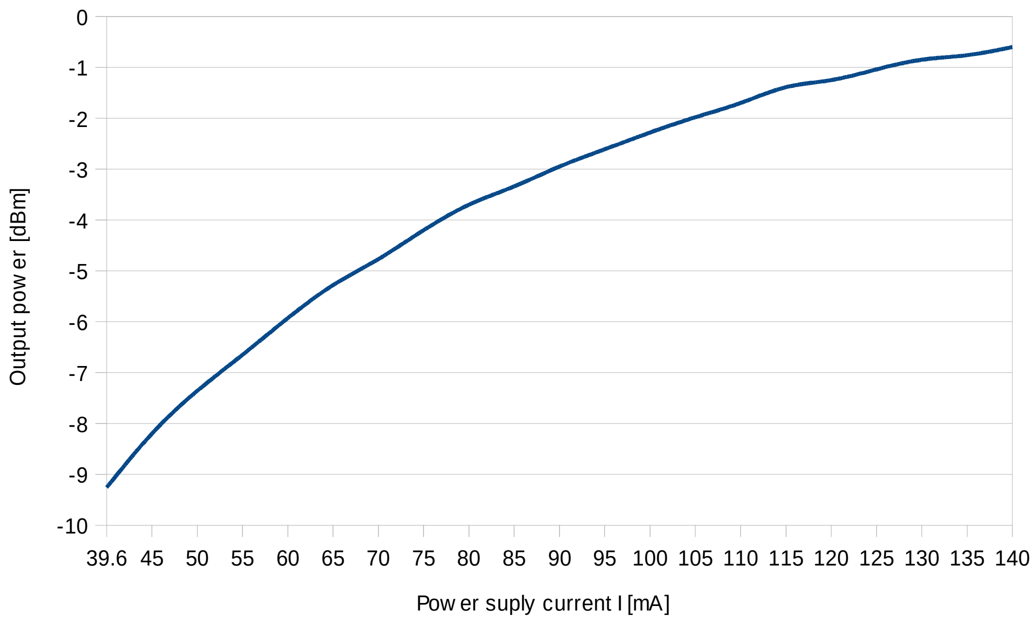

Figure 157; Total optical output power versus injection current when optical input power is not present (SOA OPB1010NCFA)

The figure 157 presents evolution of the SOA optical output power when value of the supply current changes. The graph shows that optical noise has nonlinear characteristics with rising tendency until supply current introduces SOA to the saturation state. Measurement of the noise characteristics provides explanation of the eye diagram distortions that were observed when SOA was implemented as amplifier in optical transmission line.

The observed optical power at the output port of SOA (with no optical input signal present) has level high enough to be compared to commercial grade SFP 0 dBm transceivers used in commercial optical infrastructure. Such high level of emitted noise creates obstacle in proper decoding data from the received optical signal.

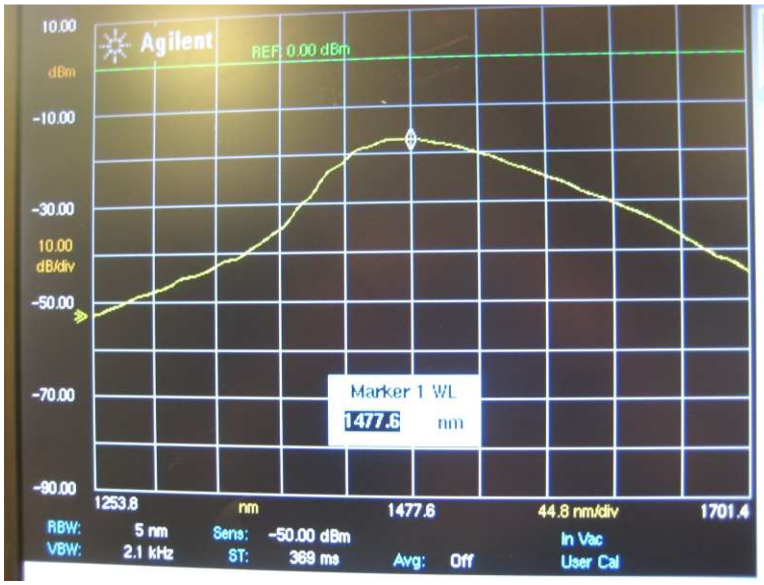

Figure 158; Spectrum of the optical signal emitted by SOA OPB1010NCFA when supply current is 100 mA. (No input optical power present).

When spectrum of the emitted noise is analyzed it becomes visible that the observed noise is spread across wide spectrum of wavelengths (Figure 158). The emitted optical noise is significantly stretched from 1300nm to 1700nm with the peak power exhibited around 1477 nm. The measured total output power of the noise consists of a sum of partial noises that are associated with all wavelengths that are spontaneously emitted by SOA.

The observation of the SOA spectrum unveils the fact that optical signal detected by photo receiver (after it is amplified by SOA) does not carry only the wavelength that was originally send by transmitter but also consists of a large number of wavelengths that does not carry any useful data but they are heavily polluted with optical noise.

The possible method of discrimination of the optical noise before it reaches photo receiver is to filter out, as many as possible, unused wavelengths that that carry the noise. This method may be a good candidate for the two following reasons:

- DWDM transmission uses optical channels that have narrow width channels with ITU-T standardized 100GHz spacing. Implementing an optical filter after the SOA would allow only the specific amplified wavelength to pass through and surrounding wavelengths would be extinguished
- Optical filter can be integrated with SOA during manufacturing process and this would allow for low cost mass production of the low noise amplification devices

To evaluate wavelength filtering as the method for SOA noise reduction a test system was designed and build. The system configuration is presented in figure 159.

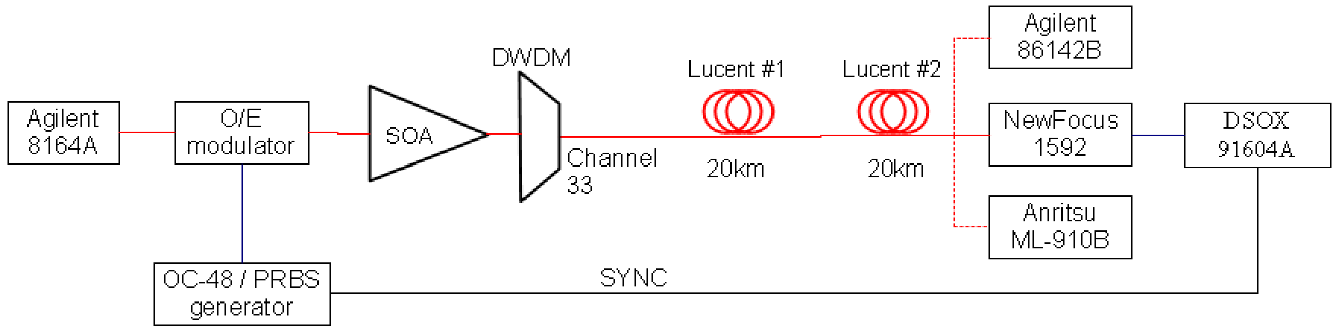

Figure 159; Tests system for evaluation of DWDM as SOA noise discriminator

The test system consists of tunable source Agilent 8164A that was set to 1550.918nm with output power 0dBm. The optical signal was externally modulated by electro optical modulator JDS 10020447 (insertion loss 9.5dB) that was driven by the generator Agilent 4906B. The driving signal had a random bit pattern OC-48 (2.488Gb/s). Modulated optical signal is amplified by SOA and then inserted to trunk port in DWDM IgnisPhotonyx M014007761. The DWDM had measured insertion loss 4.26 dB when channel 33 (1550.918 nm) was used. The optical signal exits DWDM through port 20 that carries ITU-T channel 33 (1550.918 nm, 193.3 GHz).

The optical signal was analyzed after it travels two spools of SMF that represent 40km transmission link with 20dB loss. The eye diagram of the output signal was analyzed in scope DSOX 91604A, its spectrum was analyzed in optical signal analyzer 86142B and its total optical power was measured in power meter ML-910B. Since DSOX scope does not have optical front end the fast photo detector New Focus 1592 with 100ps signal response was used to provide opto-electrical conversion of the incoming signal.

The eye diagram of the output optical signal was captured at different configurations of the test system and spectrum of the signal was compared. Before amplifier and filter were together implemented in the system an eye diagram and spectrum of the raw optical output signal raw optical signal was captured to have baseline for the later comparison.

Figure 160 presents comparison of the optical signal spectrum generated by 8164A source with and without applied DWDM filter. It is visible the total spectrum generated by the source is stretched over the 0.4 nm width (from 1550.7 nm to 1551.1 nm) if all detected wavelengths are included. After the DWDM filter was applied wavelengths above 1551 nm were significantly extinguished.

The interesting effect was observed in filtered signal at shorter wavelengths. The wavelengths below 1550.848nm experience visible attenuation and wavelengths below 1550.782 nm experience stronger attenuation (Figure 160b). This uneven extinguishing of shorter wavelengths created step-like shape of the filtered spectrum.

a) b)

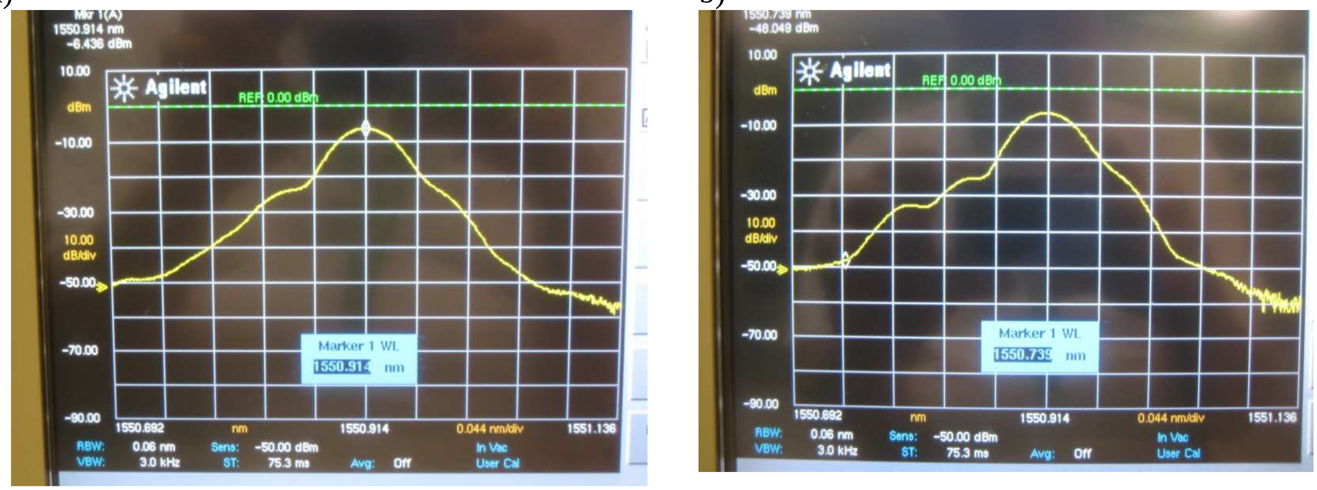

Figure 160; Optical spectrum of the signal generated by the source 8164A (a) and the same signal filtered by DWDM channel 33 in M014007761

After spectra of the raw and filtered optical signals were captured, electro-optical modulator JDS 10020447 was implemented between the light source and DWDM filter. The modulator was supplied with the OC-48 modulating signal and spectrum of the output optical signal was captured at different configurations of the optical link.

Figure 161 presents optical spectrum captured at the system with implemented JDS modulator (driven with OC-48 signal), DWDM filter and 40km optical fibre. Spectrum (a) was captured at the output port of the DWDM and spectrum (b) was captured after 40km optical fibre.

a) b)

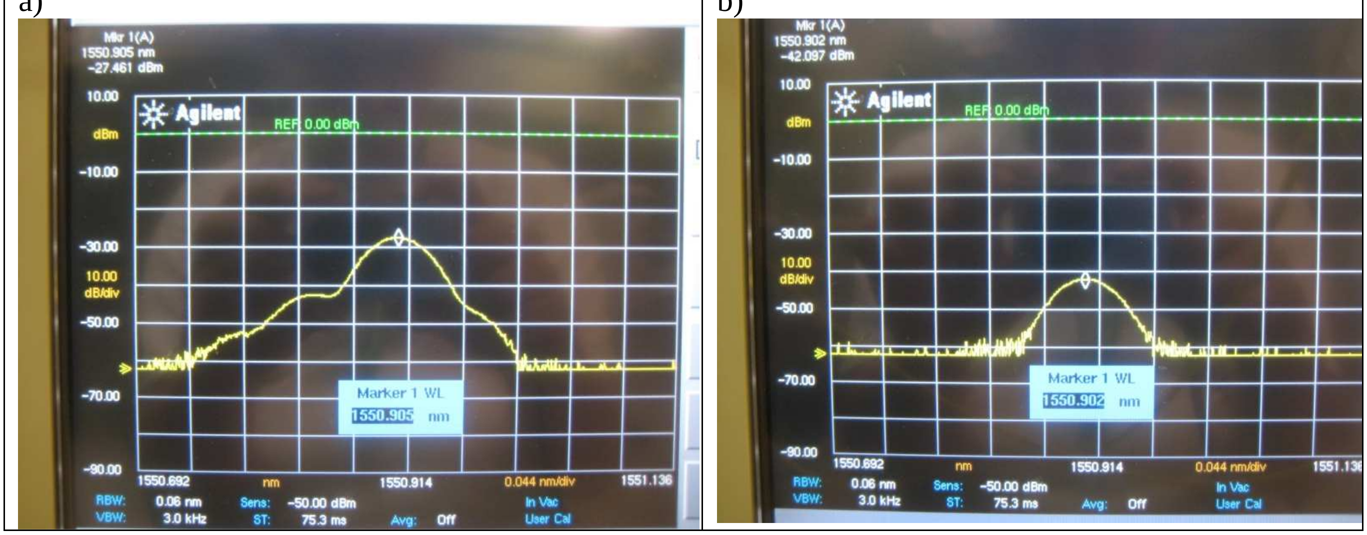

Figure 161; Optical spectrum after the modulator and DWDM filter (a) and after 40km SMF (b)

The comparison shows that the filtered signal after traveling 40km does not exhibits any wavelengths below 1550.848nm and above 1550.958 nm. When spectrum presented at figure 98b is compared with unfiltered spectrum that was captured after traveling 40km link (Figure 162) it becomes clear that those missing wavelengths were filtered out before optical signal entered the 40 km fiber link.

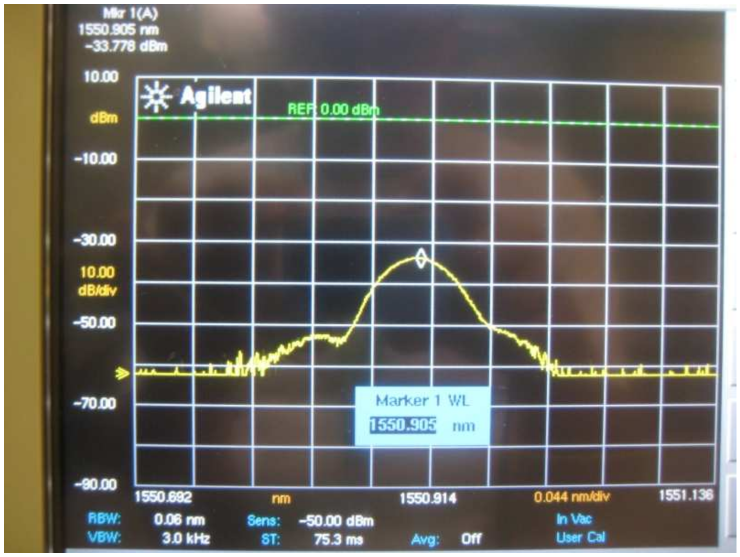

Figure 162; Optical spectrum of the non filtered signal captured after the 40km link.

Although implementation of the DWDM filter allowed for significant extinguishing a large number of wavelength that were not used around channel 33, it also introduced an additional optical noise due to high insertion loss of the DWDM filter. The total output power of the optical signal measured after the 40km link was less than -30 dBm (with applied filter).

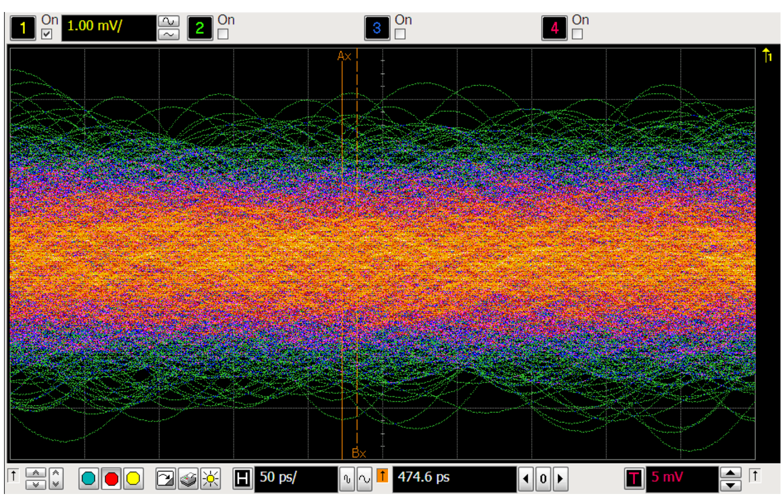

Figure 163; Eye diagram of the filtered optical signal captured after the 40km fibre.

The figure 163 shows eye diagram of the filtered optical signal captured after traveling 40km fibre. The very low power of the optical signal mad it impossible to recover eye diagram with available equipment. This result indicates that applying a DWDM filter does require also implementing amplification device to counterbalance optical power loses.

After the SOA was implemented in the test system, series of measurements were done for different values of the SOA supply current to evaluate performance of the amplifier in the optical system that has already implemented a filtering device. Eye diagram was capture for each value of the current supply and its Q-factor has been measured for parameters: 40% of edge window start and 60% edge window stop. Values of the output optical power of the signal were measured and their spectrum pictures have been captured.

For comparison purpose eye diagrams of the optical signal was captured at the output port of the JDS modulator and at the end of the second fiber spool when no amplifier and or filter was applied (Figure 164). The figure 164a exhibits distortions such as undershoot, shunt capacitance and signal loss. Those distortions were caused by aging effects of the implemented electro optical modulator that was very intensively used by researchers in the past. The output eye diagram (Figure 164b) showed low quality opening due significant losses caused by multiple fiber connectors along the light path. The electro-optical modulator was working nearby its bandwidth limit (2.5 GHz) and in addition it may had some aging effects that had negative impact on the modulated optical signal.

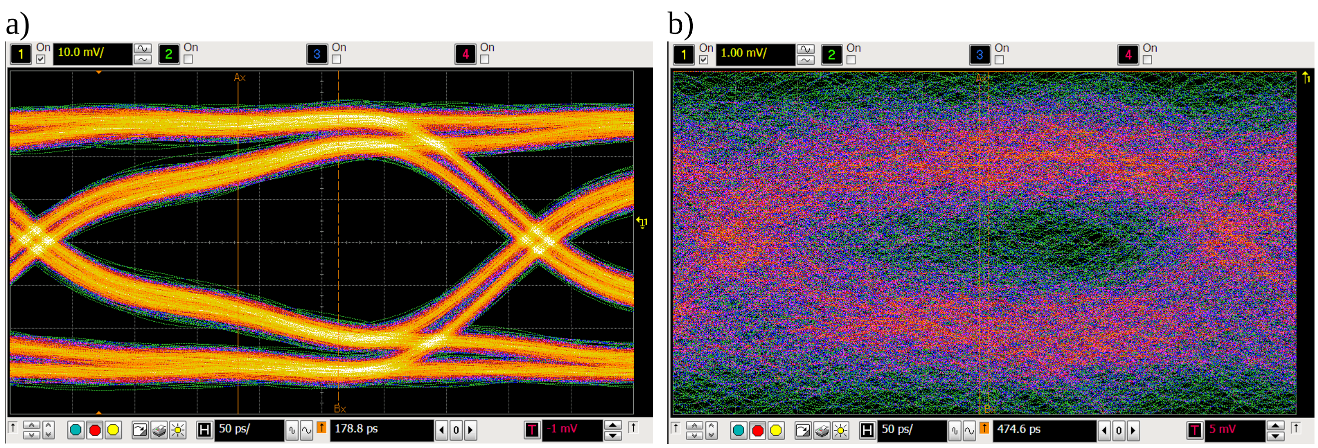

Figure 164; Eye diagram captured at the output port of the JDS modulator (a) and output port of the second fiber spool with no amplifier and filter was implemented (b).

The eye diagrams and optical spectra of the output signal captured by the test system in its full configuration (Figure 159) are presented in figure 165 for different values of the SOA supply current.

I(SOA)	Eye diagram	Spectrum
40mA	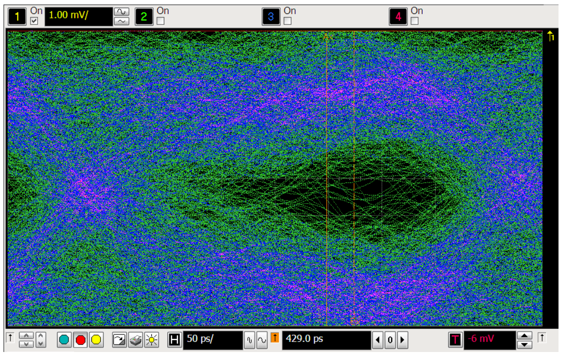	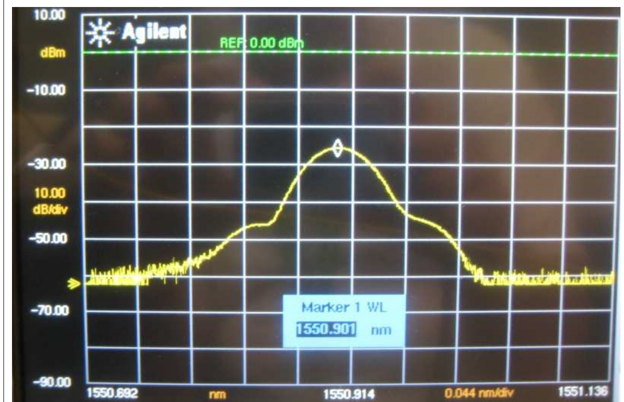
60mA	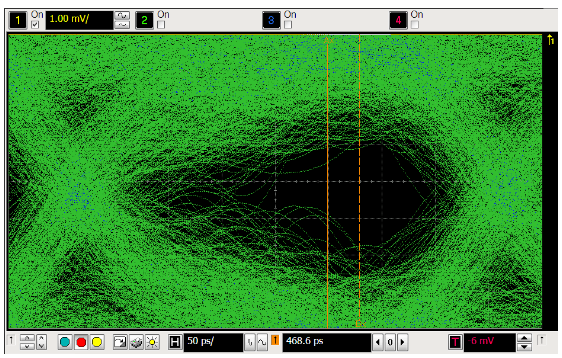	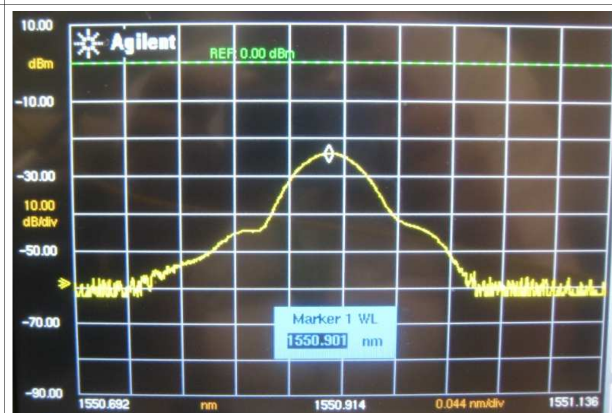
80mA	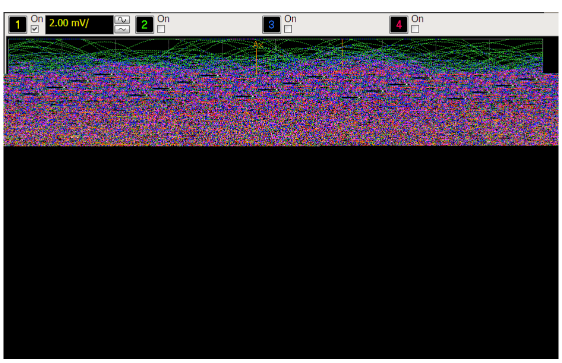	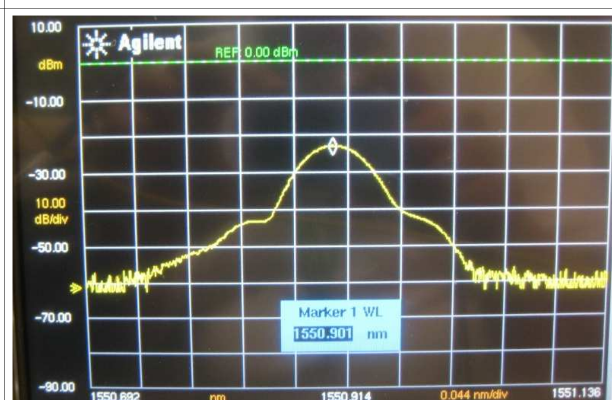

100mA

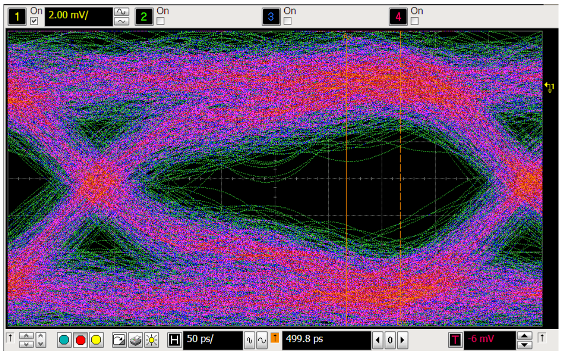

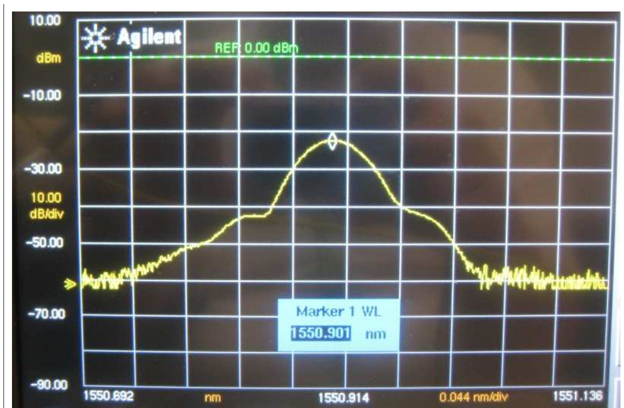

120mA

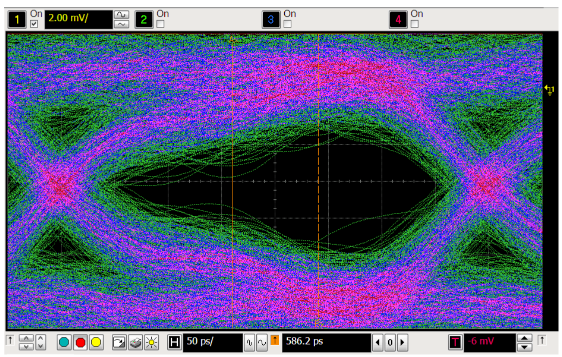

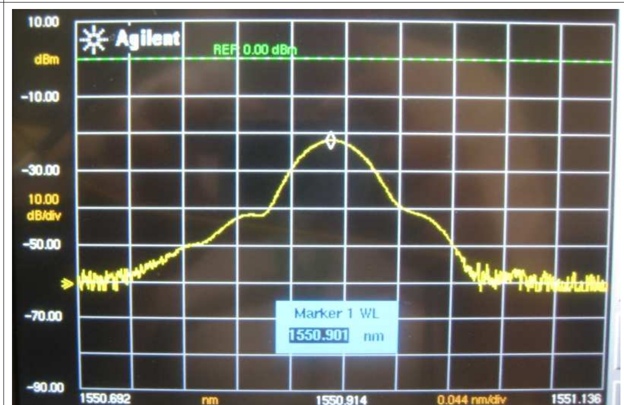

150mA

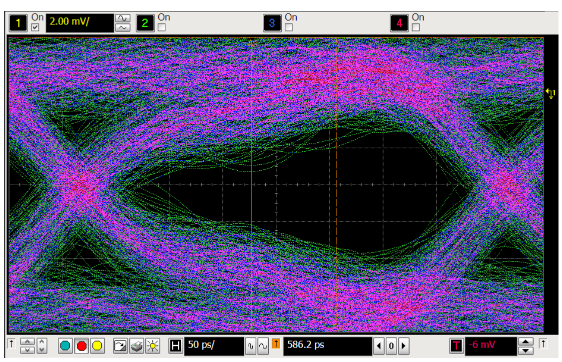

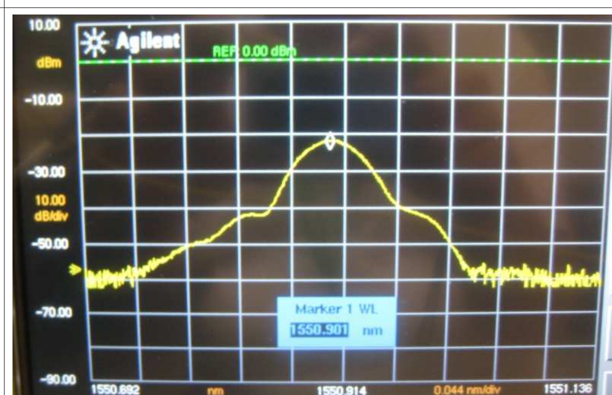

Figure 165; Evolution of 2.488Gb/s eye diagram and spectrum of the output optical signal for different values of the SOA current supply

Figure 165 presents that after the optical signal is filtered its spectrum shape does not exhibit significant changes when value of the SOA current supply is modified. This indicates ASE noise injected by SOA does not change significantly in range 80 mA-150 mA supply current.

The eye diagrams presented in figure 165 exhibit an evolutionary change when SOA current increases.

Although the eye opening at the low current values is very weak it presents higher quality then eye diagram of the unfiltered and non amplified signal presented in figure 100b. The quality of the eye diagram was significantly improved when SOA current increased. Although certain amount of noise was still present I the signal implementation of SOA and DWDM filter allowed for significant signal quality improvement in comparison to unfiltered and non amplified optical signal.

The optical output power of the modulated signal was measured for across changing values of SOA current. The characteristic of the optical output signal (measured after the second spool) as function of the SOA current is presented in figure 166. When no amplifier was implemented in the system the measured output optical power was -30.3dBm

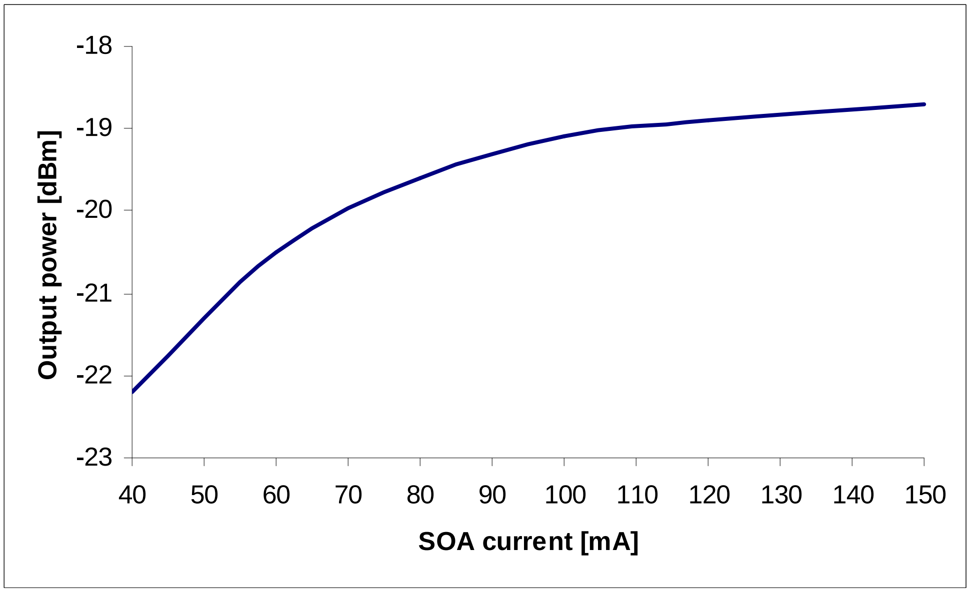

Figure 166; Optical output power (measured after the second spool) vs. SOA current.

The graph presented in figure 166 exhibits near linear characteristics below 60 mA and nonlinear above 60 mA. In addition to this, the graph indicates that characteristics may reach the saturation point above 150 mA.

In addition to measurements of the output power a Quality factor (Q factor) was measured for each captured eye diagram. The Q factor is a measure of the digital signal eye aperture; it adopts the concept of signal-to-noise ratio in a digital signal and is an evaluation method that assumes a normal noise distribution (Figure 167).

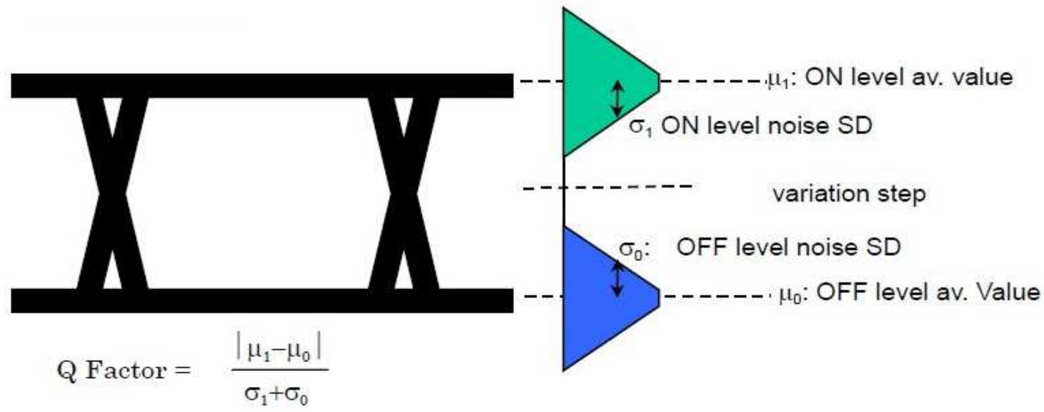

Figure 167; Quality factor (Q factor) [185]

The Q factor in this experiment was measured in automated process by DSOX 91604A with the 1ps measurement accuracy and assumption of 40% eye window start and 60% eye window stop according to standard ITU-T G.976/OSFTP-9 [186]. The results of the measurement are presented on figure 168. The Q-factor was measured for data rates 2.488 Gb/s and 1.25 Gb/s.

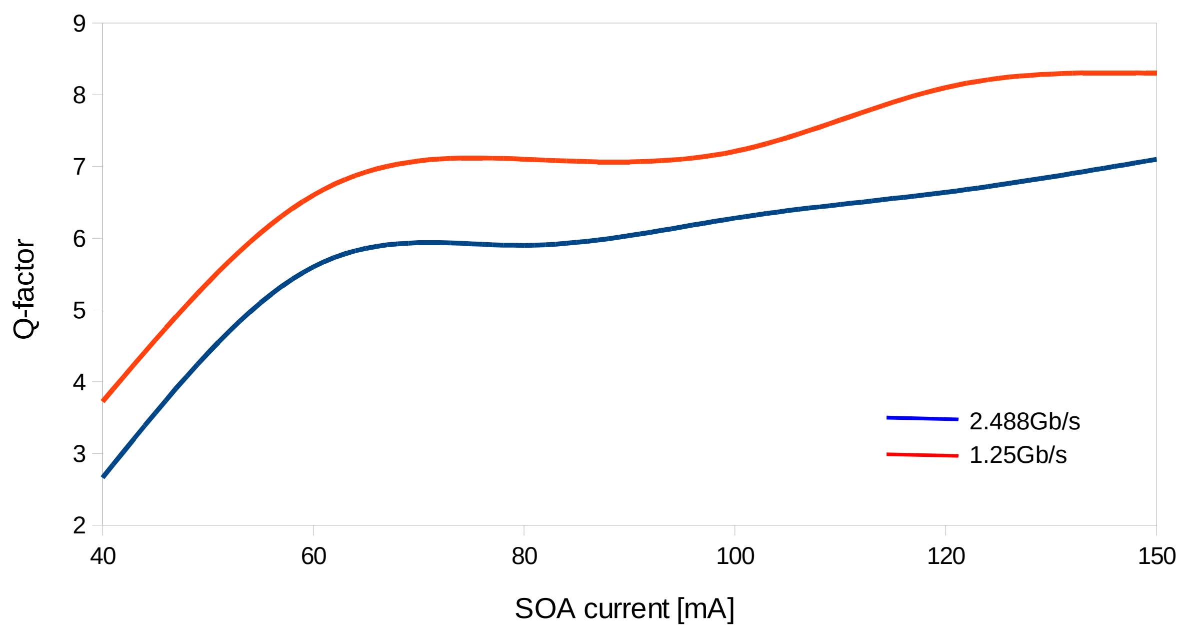

Figure 168; Measured Q factor for different values of the SOA current.

The figure 168 shows significant improving in Q-factor, when SOA current increased from 40 mA to 60 mA. Above 60 mA there is visible region where Q factor has near constant value until supply current reaches 95 mA and 100 mA for 2.488 Gb/s and 1.25 Gb/s respectively. Further increase in supply current leadt do significant improvement in Q factor for 1.25 Gb/s while 2.488 Gb/s experiences very slow increase. When supply current was further increased beyond 130 mA the Q-factor entered flat region for 1.25 Gb/s while 2.488 Gb/s data rate keeps tendency of slow growth.

For the comparison purposes Q factor was measured also for number of incomplete configurations of the test system and it was compared to the original modulating signals 2.488Gb/s and 1.25Gb/s. The comparison chart is presented in figure 169.

The presented chart shows a dramatic difference in Q factor values between modulating electrical signal (measured at the output port of the generator) and modulated optical signal (O/E) that was measured at the output port of the JDS modulator. This effect may be caused by applying modulating signal with frequency close to bandwidth limit (2.5 GHz) of the modulator. In addition, this particular modulator may exhibit some aging effects and physical material fatigue that introduce noticeable instability to the modulated optical signal.

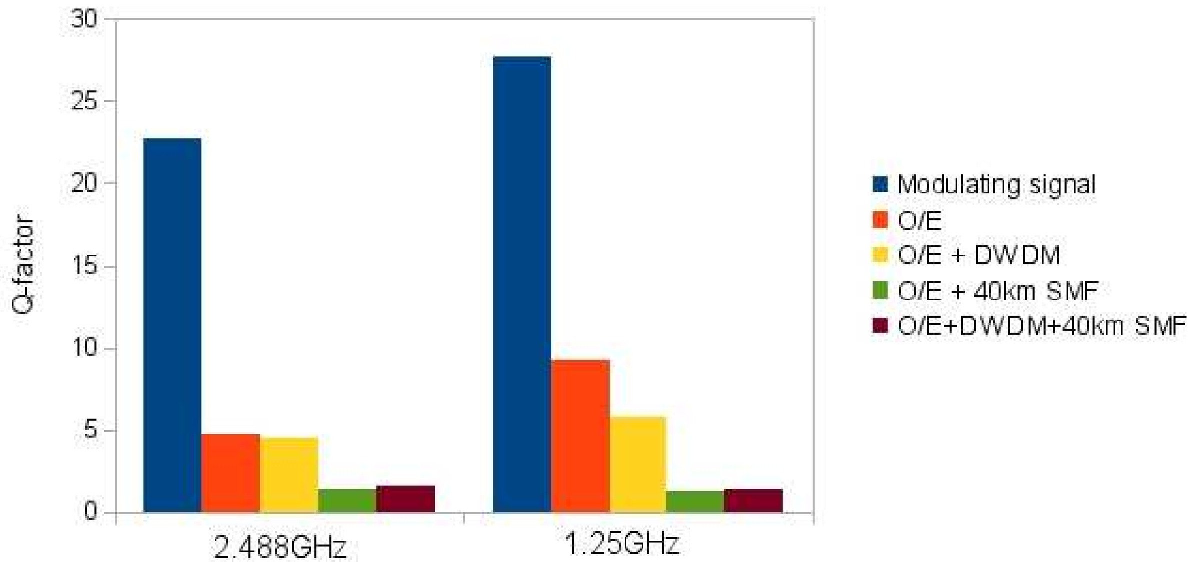

Figure 169; Measured Q-factor for the incomplete test system

The empirically measured Q factor can be used to evaluate the bit error ratio (BER) in the optical system through the following equation:

$$BER = \frac{1}{\sqrt{2\pi}} \frac{Exp(-Q^2/2)}{Q} \quad (7.7.6.1)$$

Based on measured Q factor for different values of the SOA current number of BER values were estimated for both bit rates of the optical signal: 1.25 Gb/s and 2.488Gb/s. The results of the estimation are presented in figure 170. The mathematically evaluated BER reaches 10^{-12} at current value 100mA and 10^{-17} at current value 150mA for data rate 1.25 Gb/s. The BER for data rate 2.488 Gb/s reaches 10^{-11} at current value 120 mA and 10^{-13} at current value 150 mA.

The low bit error ratio that was achieved in the test system confirms that implementing DWDM filter in optical system with SOA working as modulated signal amplifier provides improvement in quality of the optical signal.

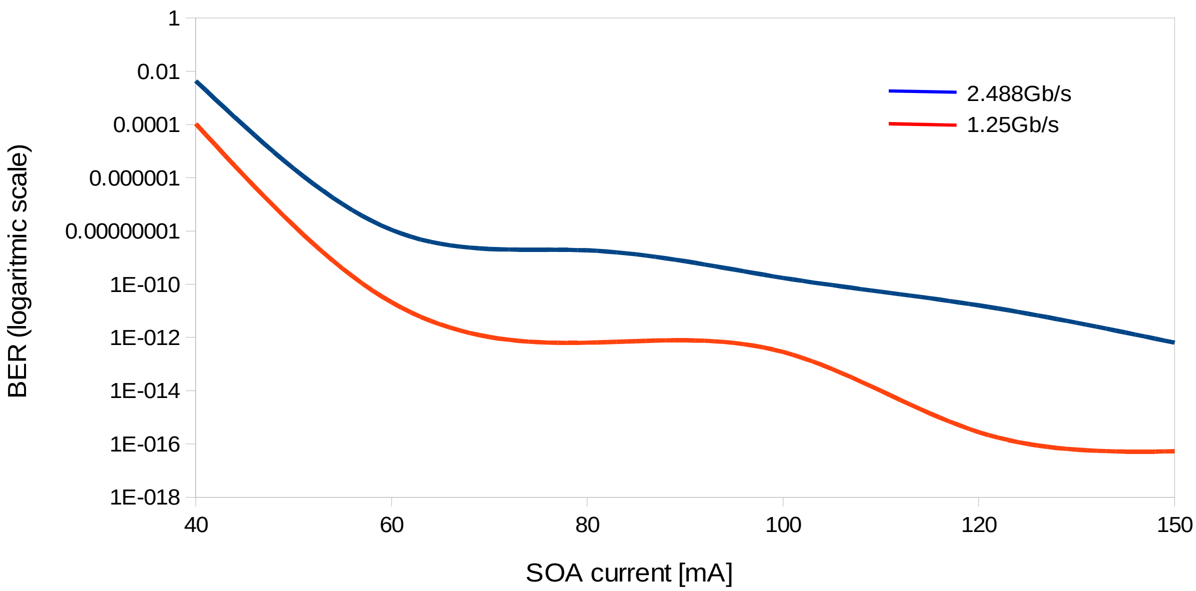

Figure 170; Values of BER estimated based on the measured Q factor.

The DWDM filter removed from the signal a large number of unused wavelengths that carry noise generated by SOA. Although the wavelength filter introduces significant insertion loss into the transmission system it does improve quality of the transmitted signal by filtering large amount of noise. The additional loss has to be counter-balanced by optical gain introduced by the optical amplifier.

The results of the test system proved concept of implementing SOA and DWDM filter as effective amplification device. Although spontaneously emitted noise is not totally removed from the optical line large part of the noise is successfully extinguished at the filter. The collocating DWDM and SOA in one enclosure may be achieved at the manufacturing process where amplifier and filter are integrated in one optical chip. In this way production cost of the device can be reduced and physical dimensions of the integrated chip will allow it to be implemented as a part of larger optical devices.

Multilevel signal modulation in PON

This chapter presents a study on technological progress in advanced signal modulation techniques and their potential availability to be implemented in access networks. The most probable future changes in signal modulation systems are discussed and paths for their evolutionary development are listed.

An innovative platform for testing and evaluation advanced signal modulation techniques for PON extensions was designed. The platform consists of commercially available test and measurement components that offer multi-wavelength intensity, phase and polarization modulation at 10GHz and possibility of upgrade to 40 GHz. The estimated capacity of the designed platform exceeds 450Gb/s data rate over 24 DWDM channels.

The previous chapters discussed number of PON extensions that were based on amplitude modulation technologies, optical switching systems and optical signal amplification techniques. Presented extensions addressed issues related to compatibility new devices with existing commercial network infrastructure and issues related to costs of manufacturing, implementation and maintenance.

Another method of enhancing PON infrastructure is implementing innovative signal modulation methods to increase effective data rate available to customers. The data rate provided by standard ON/OFF amplitude keying (OOK) has significant limitations related to modulation frequency. This limitation can be significantly pushed if other characteristics of the optical signal are considered. Optical signal modulation can be applied not only to intensity but also to its frequency and phase.

Progress in development of advanced modulation techniques

Mutilevel signal modulation and detection has been drawing attention as a technology that allows for increase transmission data rate without physical increase frequency of the intensity modulation. Although advanced modulation formats offers data rates transmission beyond the limits of binary systems, their implementation was not justified economically in access networks due to high complexity and cost of the detection and decoding systems on the receiver end. The multilevel transmission technologies were considered as good candidate for implementation in high bandwidth long distance transmission systems.

There are number of advanced modulation formats that have reached successful prototyping stage of development in optical domain [187]. One of them is the differential quadrature phase shift keying (DQPSK) format. With DQPSK the data is encoded into one out of four different symbols, thus enabling simultaneous transmission of two bits per symbol. The main benefit of DQPSK is the reduced spectral width, which is about half that of a binary format at the same bit rate. The successful prototype of 25 Gb/s long distance transmission system with implemented Return-to-Zero DQPSK modulation was presented in [188]. The prototype had implemented 1000 km loop with EDFA amplifiers deployed every 100km. Although the system reached 0.8 b/s/Hz spectral efficiency its BER was 10^{-3} high. To achieve low BER (below 10^{-9}) a Forward Error Correction methods should be applied if the prototype is implemented in commercial infrastructure.

There are number of more advanced modulation formats that provide improved spectral efficiency beyond what DQPSK can offer. One of the improved optical systems is combination of phase and amplitude shift keying (DQPSK-ASK). By adding binary amplitude modulation (amplitude shift keying - ASK) to a DQPSK signal, the bit rate can be increased by 50% [187]. This is obtained by only small modifications to the transmitter and receiver of a standard DQPSK setup. In the transmitter an extra modulator is added to impose the amplitude modulation, and in the receiver an extra photodiode detects the amplitude information. The proposition of DQPSK-ASK system that offers data rate beyond 200 Gb/s was presented in [189]. The successful prototype of DQPSK-ASK 120 Gb/s transmission system over 50km SMF was presented and its extension that reached 240 Gb/s was also presented. The extended prototype had implemented polarization multiplexing and it achieved 10^{-9} BER. The interesting feature of this prototype was implementing commercial components that were rated at 40 Gb/s. This proves that it is possible to build advanced modulation system using lower data rate components.

Another method of improving DQPSK-ASK system is implementing inverse return-to-zero (inverse RZ) modulation instead of normal RZ. This modification allows the separation of the phase and amplitude modulation in such a way that the phase modulation is stored in the part of the waveform that has high and constant power. Thanks to this, the amplitude modulation is allowed to use high extinction ratio at the same time as the phase modulation is hardly affected. The prototype of the inverse RZ DQPSK-ASK was presented in [190]. The presented system was capable of transmitting 31 Gb/s data rate with 10^{-9} BER over 75 km fibre.

DQPSK-ASK can be also improved if amplitude modulation is replaced by higher number of phase levels. This technique is called differential 8-ary phase shift keying (D8PSK) and it requires very little modification on transmitter side: a phase modulator should be added after the DQPSK transmitter. The D8PSK receiver is more complex than DQPSK because it requires four sets of delay demodulators and balanced photodiodes plus an XOR gate [191]. The D8PSK was presented in [187] where 30 Gb/s data rate was achieved with 10^{-9} BER over 80km SMF.

Above examples indicates that advanced modulation techniques appear increasingly attractive in perspective of potential improvement network capacity. Although multilevel modulation technique improves density of the information that can be carried along optical fiber it does have significant drawback of a very high implementation cost. Receiver systems for detecting and demodulating such advanced optical signal have much higher complexity then receivers that have implemented binary-only techniques.

To make deployment of advanced modulation schemes commercially justifiable there have to be developed low cost detecting and receiving systems. The cost of receivers manufacturing, deployment and maintenance has to be on acceptable level to successfully compete with existing commercial binary-only technologies. One of the first prototypes of commercial ready coherent transmission systems was developed by Siemens AG in October 1991 and published in January 1992 [192]. The prototype was a fully functional transmitter and receiver pair enclosed in standard telecommunication racks. The system was capable of transmitting 140 Mb/s data rate with implemented frequency shift keying (FSK). Transmitter had implemented DFB tunable lasers operating at 1560nm with 30MHz line widths over tunable range. The Manchester coding was used to overcome the nonuniform FM response. The observed frequency deviation was 1.2 GHz The laser modules were highly stable which was confirmed by a beat frequency drift of only 150 MHz during 1 hour.

Although the prototype made by Siemens was a significant achievement that would satisfy bandwidth requirements in early 1990s it would certainly not survive competition with modern commercial telecommunication systems. In 1996 Lucent Technologies presented prototype of monolithic integrated coherent transceiver that was capable of reaching data rate 108 Mb/s [193]. The device consisted of a tunable distributed-Bragg-reflector (DBR) laser as a local oscillator (LO) and an integrated detector.

The fabrication process of this device was similar to process of manufacturing a DBR laser. The incoming signals were mixed with the LO light in the DBR laser cavity itself. The heterodyne intermediate frequency (IF) signals are taken out from the detector section through a bias-T.

The device had implemented FSK-NRZ transmission and detection with sensitivity -43 dBm. The BER of 10^{-9} was achieved at 108 Mb/s. The device had high sensitivity because of design of the laser structure that allowed only one Fabry-Perot (FP) cavity mode inside the grating stop band. This design reached high side mode suppression ratio and narrow line width and to contribute to the lower intensity noise and phase noise.

Although Lucent prototype presented a significant progress in manufacturing process and device integration (and therefore lower production costs) it did not offer data rate significantly higher than first generation optical devices developed in early 1990s. The later works focused mainly on simplification receiver part of the coherent transmission systems. With new fabrication process becoming available a new integrated devices were possible to design to further decrease production costs. In 2007 a new integrated chip was presented [194] that consisted of innovative coherent receiver for phase demodulation. The device provided linear conversion of optical phase modulation into electrical current through the feedback receiver model (fig 171).

The concept proposes mixing the received optical phase with an optical reference, to produce a sinusoidal response to optical phase. The detected photocurrent is amplified and fed back to a reference phase modulator. The received phase is now given by standard control theory 8.1:

$$\varphi_S - \varphi_{LO} = \frac{\varphi_S}{1+T} \qquad 8.1$$

Where φ_S and φ_{LO} are signal and reference optical phase, and T is the loop transmission gain. For the high loop gain, the reference phase follows the received signal phase. The net detected phase gain will fall within the linear range of the sine transfer function of the optical mixing process, and the driving signal is linearly related to the received optical phase. In addition this feedback concept reduces receiver noise sources just as much as net detected signal, such that the SNR remains unchanged when the loop is closed.

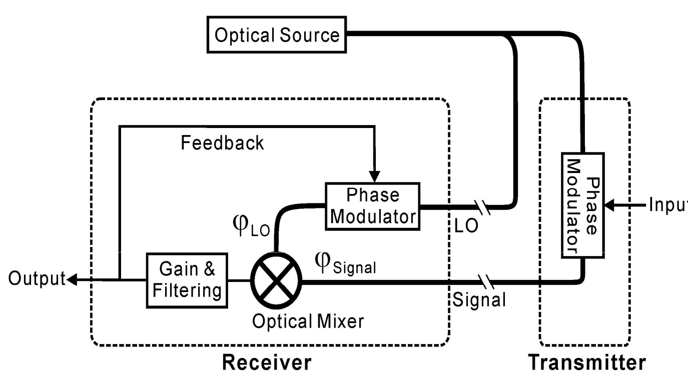

Figure 171; Concept of the coherent receiver with feedback [194]

To reach linear operation at 1 GHz, the loop bandwidth must approach 10 GHz, which require the loop delay to be in the 10-20 ps range. Such short latency can not be delivered by fibre coupled components or $LiNbO_3$ therefore very compact optical components material base, such as InP has to be implemented.

The prototype device was presented in [194] to provide proof of this concept. The prototype setup consisted of phase modulators, balanced photodetector, polarisation beam splitter and electrical spectrum analyzer. Then communication between transmitter and receiver were provided by polarization mianaining fiber. The output from the optical source was split into a signal and reference path using a polarization beam splitter and polarization maintaining fiber (Figure 172). A two-tone RF probe signal (140 and 160 kHz) was applied to the signal path using separate phase modulators. In the receiver signal and reference was mixed and photodetected. The output from the balanced detector pair was then directly connected to the reference modulator to provide the feedback path. The feedback gain and filter function was regulated by the detector load, converting photocurrent to modulator drive voltage.

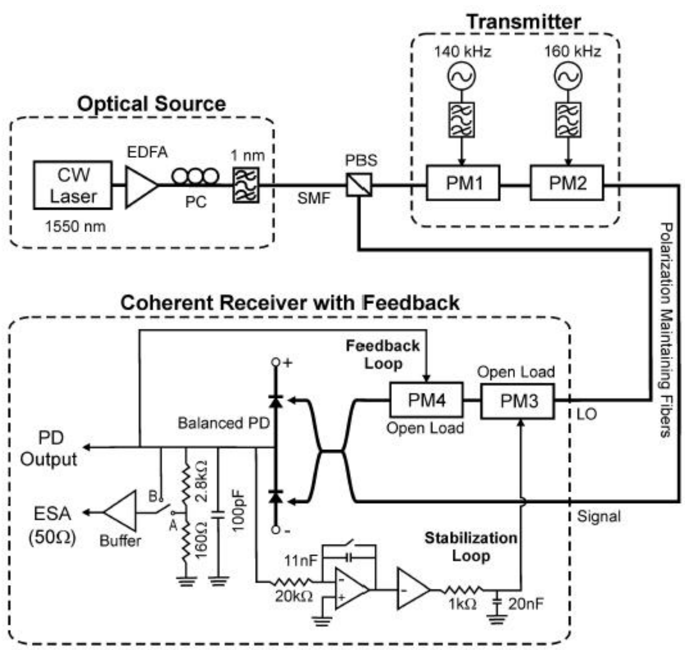

Figure 172; Prototype coherent system with feedback. PC - polarization controller, SMF - single-mode fiber, PBS - polarization beam splitter, PM# - phase modulator, PD - photodetector, ESA - electrical spectrum analyzer [194]

The prototype reached Spurious-Free Dynamic Range (SFDR) in range of 104.5 dBHz. In addition detected power at the signal frequency was reduced as a result of the reduced net phase difference between signal and local oscillator (LO).

The above example indicates that it is possible to implement linear optical phase modulators to generate highly linear optical links. The prototype proved also that this concept it also supports optical links where the available signal to noise ratio exceeds what is possible using standard intensity modulation links.

Although number of works was published on multilevel modulation techniques, most of proposals consisted of fairly complex hardware configurations that were not suitable to be implemented in existing commercial infrastructure. The high manufacturing and maintenance cost of proposed systems pushed their potential commercialization onto unspecified far future.

With the recent decrease in the cost of optoelectronic hardware components the research of advanced modulation techniques and their implementation in PON entered new level. The focus of the research seems to be slowly drifting towards cost efficient techniques that remove a number of potholes on then road to commercialization. In April 2010 there was a published proposal of implementing low cost coherent optical code-division multiple access (OCDMA) in PON [195]. OCDMA is perceived as one of promising candidates for advanced signal modulation in PON because it offer various system benefits including asynchronous operation, protocol transparency, simplified network control, and enhanced security [196].

The proposed OCDMA implementation in PON consisted of gain-switched FP (GS-FP) laser with external injection, which is considered as a simple, low-cost but high-quality short-pulse source (fig 173). The prototype of 1.25 Gb/s OCDMA-PON with 20km length was published.

a)

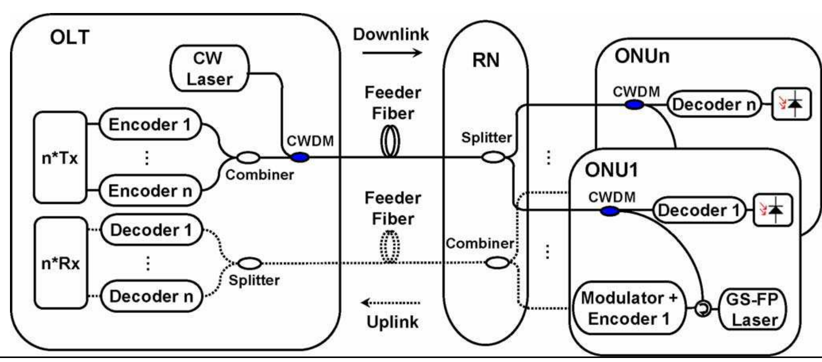

b)

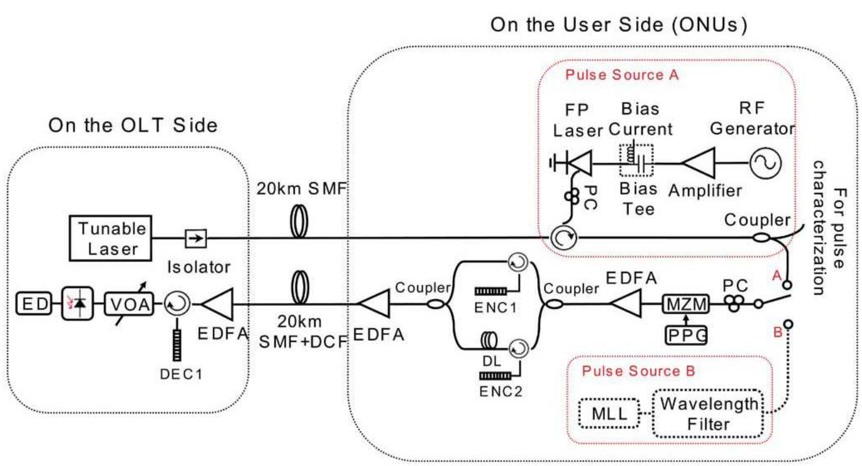

Figure 173; OCDMA-PON with GS-FP lasers at the ONUs [195].
Architecture (a) and experimental prototype (b)

The FP laser used in a prototype was a commercial 1550 nm multiple quantum-well (MQW) laser module with cooled package. Its threshold current of was 13 mA and a longitudinal mode spacing was of 1.5nm at 25ºC. To realize the gain-switching operation, a dc bias current in conjunction with an amplified sinusoidal signal was applied to the laser. The external injection seed was provided by a tunable CW laser in order to tune the central wavelength of the GS-FP laser. Two polarization controllers (PCs) were implemented on the ONU side: one was located before the GS-FP laser for controlling the polarization state of the injection light from OLT, and the other was used before the Mach–Zehnder modulator (MZM).

The amplified optical signal was split 50/50 into two paths and encoded by two 127-chip, 320-Gchip/s superstructured fiber Bragg gratings (SSFBGs). An optical delay line
(DL)was used to decorrelate the two encoded signals. The encoded signals were recombined, amplified, and launched into another 20-km SMF followed by a dispersion-compensation fiber (DCF). On the OLT side, the uplink channels are decoded by the matched SSFBG and direct detection was used for signals reception.

The PON prototype with two ONUs achieved BERR 10^{-9} and 10^{-11} at received optical power -22dBm and -20dBm. The side mode suppression ratio (SMSR) of the FP laser exceeded 28dB. Although the prototype had low data rate (1.25 Gb/s) in comparison to existing commercial 10Gb/s GEPON it provided prove of concept that OCDMA-PON is possible to implement using widely available low cost commercial components.

The rapidly increasing bandwidth demand observed in commercial access networks pushed commercial and academic research and development groups to intensify seek for cost efficient high bandwidth solutions that implement advanced modulation techniques.
In September 2010 there was published prototype of coherent wavelength division multiplexed (CoWDM) system capable of reaching 70 Gb/s data rate [197].

The CoWDM prototype is presented on figure 174. The prototype consisted of cost efficient optical frequency comb source based on a sine wave driven discrete mode (DM) laser. Comb source is a source where generated sinusoidal electrical signal is amplified by RF amplifier and then directly applied to discrete mode laser in conjunction with a bias current. This particular configuration consisted of 10.6GHz signal generator and 60.4 mA bias current. The optical output signal was filtered to improve the comb flatness to approximately 2 dB and optically amplified in order to maintain an adequate optical signal to noise ratio (OSNR).

Although in a commercial prototype, the generated comb lines would be separated by an AWG, and each individual channel would be modulated independently, whilst preserving the phase relationship between the adjacent channels, in this particular experimental prototype the comb was passed through a set of cascaded dis-interleavers based on asymmetric Mach Zehnder interferometers (AMZI), with a free spectral range (FSR) of 21.33 GHz. The dis-interleaver separated the seven sub-carrier optical comb into four odd and three even sub channels.

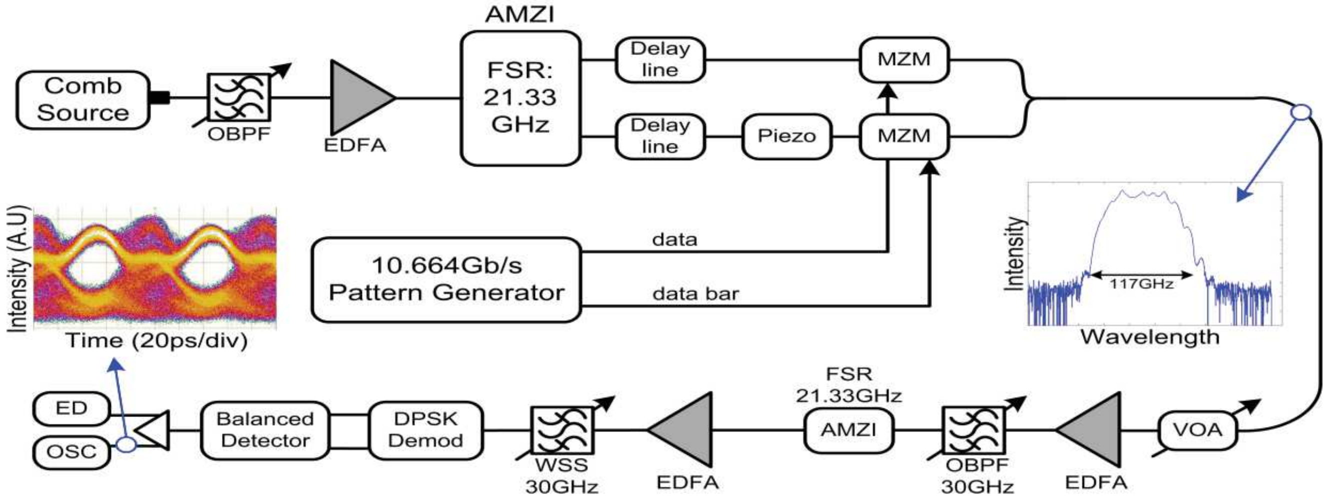

Figure 174; CoWDM prototype [197]

Both the odd and even sub-carriers were passed through separate polarization controllers, optical delay lines (ODL), piezo electric fibre stretchers and a DPSK modulator before being combined with the aid of a polarisation maintaining 3 dB fibre coupler. Two 10.664 Gb/s NRZ electrical streams with a pseudo random bit sequence (PRBS) de-correlated with a 26 bit differential delay were used to drive the two DPSK modulators. This configuration provided 74.648 Gb/s (7×10.664) DPSK CoWDM signal with of 117 GHz.

The receiver module had implemented, a variable optical attenuator (VOA) to vary the input power falling on an optically pre-amplified receiver. The first stage of the receiver consisted of an erbium doped fibre amplifier (EDFA), a 0.3nm tunable optical bandpass filter (OBPF) and an AMZI with an FSR of 21.33 GHz. The second amplification stage of the receiver consisted of a booster EDFA, a wavelength selective switch (WSS) and a 10.664 GHz DPSK demodulator (1 bit delay AMZI). The demodulated signal was detected using a balanced photodiode and amplified using a limiting differential amplifier, before being fed into an error detector (ED) and a high speed sampling oscilloscope (OSC).

The CoWDM prototype achieved BER 10^{-9} and 10^{-11} at -24dBm at received optical power -24 dBm. The achieved spectral efficiency was 0.64 bit/s/Hz. The 3 dB bandwidth of the system allowed for a spectral efficiency of 1 b/s/Hz therefore this model is a good optimal candidate for high-speed multi-carrier transmission systems.

Above example proved that high bandwidth advanced modulation systems become increasingly feasible for commercial implementation in near future. The number of published works address issues related to low cost coherent transmission systems where receiving module in prototype was frequently represented by Vector Signal Analyzer (VSA). Wide availability of low cost opto-electronic components allowed researchers recently to be more focused on development receiving modules. In February 2010 there was published a prototype of coherent optical receiver for 53.3-Gb/s sub-banded OFDM [198]. Soon after this achievement in November 2010 there was published prototype of DQPSK optical coherent receivers that were capable of reaching 100 Gb/s data rate [199].

The homodyne coherent optical receiver that implements optical injection phase-lock loop (OI-PLL) was presented in April 2011 [200]. The functional model of OI-PLL that was used in is presented on figure 175. The small fraction of the master signal power is tapped off and used to optically injection lock the slave laser.

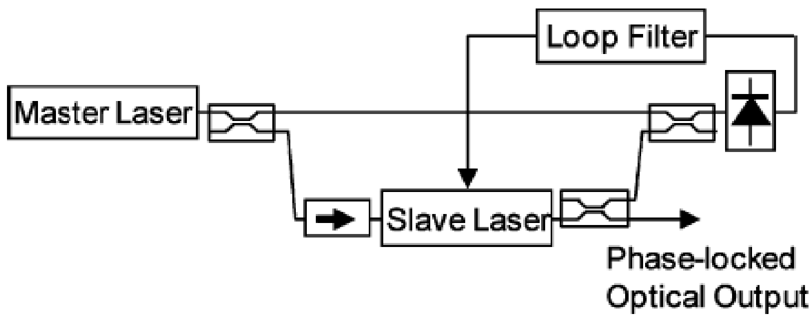

Figure 175; Optical injection PLL [200]

The output of the slave laser is combined with the remaining master signal and detected to give an error signal, which is passed through a loop filter and fed back to control the frequency of the slave laser. Thus, the OIPLL combines optical injection locking to give low phase noise with an OPLL to give a wide tracking range. In principle, the tracking range is limited only by the tuning range of the slave laser. From the application perspective OIPLL has very important characteristics: it can lock to the data carrier. The slave laser gives a continuous-wave (CW) output that is phase locked to the carrier. This feature can be used as the local oscillator (LO) for homodyne coherent demodulation of the data signal, by combining the LO with the data signal.

Because the OIPLL will lock with the LO in quadrature with the data-signal carrier at the input to the control loop photodetector (PD), any quadrature modulation components will be demodulated to baseband after this PD, provided it has sufficient bandwidth (only low-bandwidth detection is required for the control loop).

The configuration of coherent receiver prototype with implemented OIPLL is presented on figure 176. The optical input signal used to test the receiver was derived from a transmitter which consisted of a laser operating at a wavelength of approximately 1566 nm (to match the wavelength of the slave laser) and externally modulated with a pseudorandom binary sequence (PRBS) at 10 Gb/s using a Mach–Zehnder modulator.

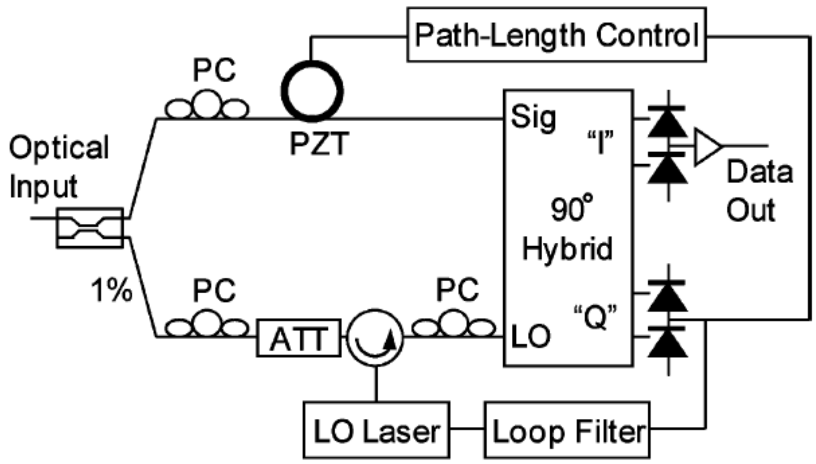

Figure 176; Coherent receiver prototype with implemented OIPLL [200]

At the receiver input, 1% of the input signal power was redirected to injection lock the LO (slave) laser. The LO and the other branch of the input signal were combined in a lithium niobate integrated optics optical hybrid, to give separate data and phase-error signal outputs. The splitting ratio of the input and output couplers in the optical hybrid and the relative phase of the signals combined on the PDs were electrically adjustable. The phase error signal was fed back through a loop filter to control the frequency of the LO laser, thus forming an OPLL, which ensured that the LO laser remained locked to the incoming signal.

The LO laser was a three-section DBR laser operated above the threshold current, giving an output power of approximately 9dBm. Fine control of the LO laser wavelength and OPLL frequency tuning were performed by controlling the current to the gain section. The PD in the control path is the phase detector for the OPLL; its output depends sinusoidal on the difference in the phase between the LO and the master at its input. To control slow phase variations, a low-amplitude current dither was applied to the LO laser, resulting in a phase dither on the injection-locked LO output.

The 10-Gb/s amplitude-shift-keying (ASK) and phase-shift-keying (PSK) over 40km long optical link was applied and the prototype performance was examined for its BER, optical signal to nose ratio (OSNR) and phase noise. The observed phase noise spectrum was around -100dB/Hz. The observed BER at ASK modulation reached 10^{-9} at OSNR 18 dB/nm and 10^{-10} at OSNR 21 dB/nm. The observed BER at PSK modulation reached 10^{-9} at OSNR 15 dB/nm and 10^{-12} at OSNR 17 dB/nm. The observed phase-error variance for optical injection locking was proportional to the combined laser line width and inversely proportional to the optical injection-locking range.

The published results indicate that OIPLL can be considered as a good candidate for implementation in conjunction with the orthogonal polarization pilot scheme to demodulate arbitrary modulation formats, such as multilevel amplitude and phase-modulated signals (e.g., QPSK, 8PSK, or QAM), or analog modulation.

Although the receiver prototype has a fairly complex architecture it can be successfully assembled using widely available commercial components. In this particular case commercial GaAs modulators, manufactured by the u^{2}t Photonics UK Ltd, were implemented.

In parallel to research on advanced modulation formats there is intensive research on demodulation techniques that limit use of optical components and move demodulation and decoding workload towards electronic domain. Significant decrease in manufacturing costs of computing devices together with unprecedented increase in computing power of modern computers opened door for innovative application digital signal processing systems (DSP) in advanced signal modulation and demodulation.

Replacing expensive all-optical components in coherent receiver with low cost electronic elements will not only decrease overall manufacturing costs but also it will limit costs of deployment and maintenance. Those cost effective modifications will certainly make coherent systems more attractive for commercial implementation.

In March 2010 NEC Corp. and AT&T Corp. published research results on low-cost prototype of coherent transmission system with implemented electronic DSP components in the receiver module [201] . The presented prototype had implemented polarization-division-multiplexed (PDM) eight-level coding (8PSK and 8QAM),

The digital coherent receiver mixed the incoming optical field with a local oscillator (LO) through a polarization- and phase-diverse 90° hybrid. This hybrid separated the in-phase and quadrature components of the received optical field in both X- and Y-polarizations, which were detected by four balanced photodetectors (four single-ended photodetectors were also possible for this prototype). The detected analog electrical signals were digitized by four analog-to-digital converters (ADCs) and then directed to a digital signal processing (DSP) unit, which was the heart of a digital coherent receiver.

The DSP module consisted of receiver distortion mitigation device, slowly adaptable digital equalization for chromatic dispersion (CD) compensation, 2x2 MIMO-based adaptive equalization for polarization recovery and PMD compensation. It had also implemented carrier-frequency- and phase recovery. Clock recovery and soft decision were also implemented within DSP module.

The RZ-shaped PDM-8PSK version of the prototype system reached effective data rate 17 Tb/s (161 DWDM channels, 114 Gb/s each) over 662 km of ultra-low-loss (ULL) SMF-28 fiber with deployed C-band EDFA amplifiers. The optical link had at an average span length of 82.75 km, channel spacing of 25 GHz and spectral efficiency of 4.2 bit/s/Hz.

The RZ-shaped PDM-8QAM version of the prototype system reached data rate 32 Tb/s (320 DWDM channels, 114-Gb/s each) over 580km of ULL SM-28 fiber with C+L-band EDFA amplifies deployed every 82km of optical fiber.

The optical system had average launch power of -5 dB per single DWDM channel. The observed BER was between 10^{-4} and 10^{-3}. It is important to notice that BER level that was reached in this particular prototype system was much higher than the level accepted in existing commercial telecommunication systems (10^{-9}).

Although the observed BER was much higher than BER in already existing telecommunication systems, this prototype presents a very important step towards high bandwidth and cost efficient advanced modulation systems. It also exhibits a potential capability of coherent detection systems with signal decoding functionality embedded in high-end DSP modules. Computing power of DSP systems that are already commercially available will certainly steer the research on advanced modulation systems towards hybrid electro-optical technologies that open door for cost effective commercialization process.

Universal platform for development and testing advanced modulation techniques in PON

As it was presented in previous chapter there are number of working prototype systems, developed in academic and commercial institutions that implement advanced modulation techniques. Unfortunately presented prototypes do not find easily their way to commercialization process because of drawbacks such as very complex architecture, high cost of implementing optical components and high bit error ratio. Significant differences in costs of all-optical components and electronic components make DSP-based architectures more attractive in perspective of future commercialization. Chapters 6.6.4 and 7.6 presented innovative applications of commercial low-cost electronic components with computing power that is sufficient to be part of hybrid electro-optical devices.

To develop and test innovative advanced modulation techniques and to evaluate hybrid electro-optical systems with implemented DSP functionality a universal test platform was designed (Figure 177).

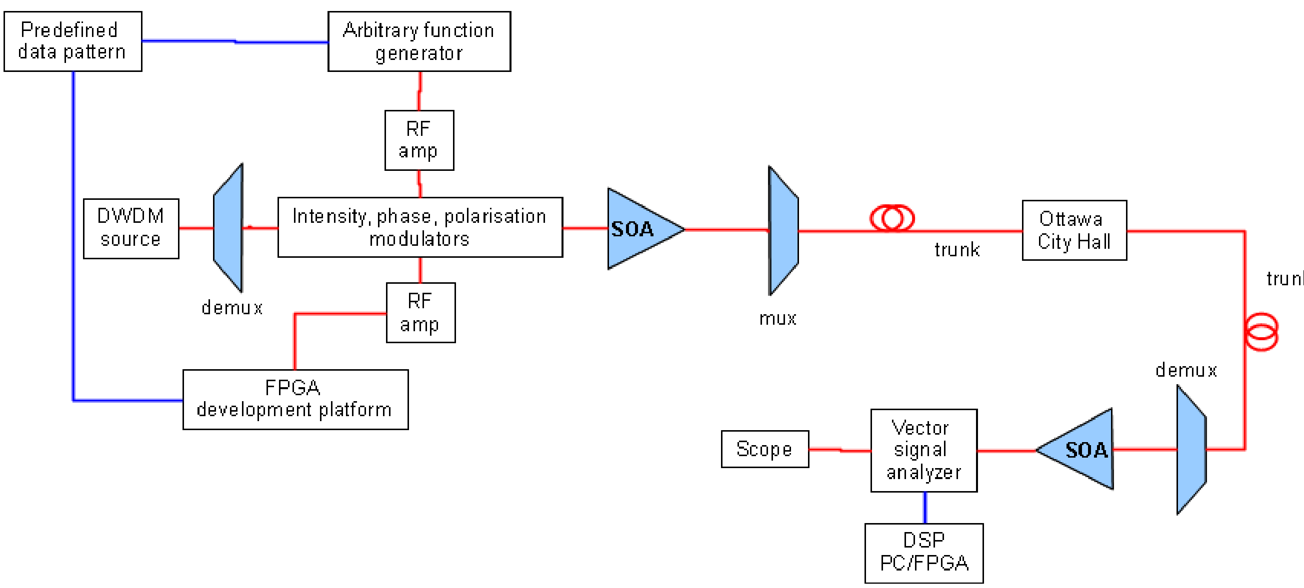

Figure 177; Architecture of universal test bed for advanced modulation development and techniques evaluation

The test platform is designed to be assembled from commercially available electrical and optical components and it has two main purposes: prototyping and testing low-cost advanced modulation and demodulation techniques and development and evaluation innovative cost-efficient optical amplifiers such as SOA. The test platform will support research and development extensions for PON as well as it will support development innovative radio-over-fiber systems.

The source of the continuous optical wave is DWDM laser, such as ThorLabs PRO8000-DWDM. To separate each wavelength a demultiplexer should be applied after the source, such as 32-channel IgnisPhotonyx M014007761. The light is externally modulated by intensity-, phase- and polarization modulators that can work in two-level fashion (ON/OFF) or multilevel fashion. The examples of external modulators that can be implemented are 40 Gb/s ThorLabs LN05S (intensity modulation), 40 Gb/s ThorLabs LN66S (phase modulation) and 10 GHz ThorLabs LN58S (analog modulation).

The source of the modulating signal is arbitrary wave form generator Tektronix AWG7122C that supports coherent signals (IQ/IF/RF): DPSK, QPSK, OFDM, QAM with a data rate 24GS/s. The prototype of low cost signal generator can be also implemented in FPGA development board. The NIOS FPGA platform designed and developed in chapter 7.6 provides 84 parallel modulating signals. This platform supports 42 DWDM channels with intensity and phase modulation. This particular Stratix platform supports 1.7MHz modulating ON/OFF signals that allows effective data rate of the DWDM system to reach 71 GS/s (142 Mb/s).

If energy-efficient Cyclone IV platform is implemented with 64 parallel modulating signals 50MHz each, the coherent system will have aggregated capacity 1.6 GS/s (3.2 Gb/s) over 32 DWDM channels. Further upgrade of the FPGA platform to new technology and energy efficient Stratix IV that supports 48 parallel modulating signals at 8.5 GHz each, will increase the total data rate to 204 GS/s (408 Gb/s) over 24 DWDM channels. Upgrading the system to Stratix V FPGA that supports 10 GHz modulating signals will increase overall system capacity to 240 GS/s (480 Gb/s).

Since DWDM demultiplexers and electro-optical modulators do have high insertion loss an effective optical amplifier should be implemented to counter balance the signal loss. This creates opportunity to design and evaluate innovative SOA devices that can be tested in the setup that reflects near realistic commercial telecommunication infrastructure. The polarization modulation of the optical signal will provide opportunity to develop and test polarization-insensitive SOA prototypes.

Since modulating signal generated by FPGA platforms and wave form generators may be too low for effective driving electro-optical modulators, number of low-noise RF/microwave amplifiers should be also implemented in the transmitter section of the test system.

Modulated DWDM wavelengths are aggregated in multiplexer and launched into optical fiber that connects School of Information Technology and Engineering and Ottawa City Hall located in downtown at corner of Elgin Street and Laurier Avenue. This optical fiber is a part of the commercial public telecommunication infrastructure deployed in City of Ottawa. Beside of the fiber link to the Ottawa City Hall (about 15 km length) there is also access to long haul optical link that connects University of Ottawa to Queens University in Kingston (over 200km length). This particular link is a part of Ontario Research and Innovation Optical Network (ORION).

The optical signal that comes back to the receiver may be significantly attenuated as well as it can carry some amount of noise therefore an optical amplifier is implemented (before of after the DWDM demultiplexer) before signal enters receiver.

For the detailed test and measurements purposes the receiver part is built form vector signal analyzer (VSA) Agilent N4391A that supports modulating formats FSK, QPSK, BPSK, DQPSK, QAM at data rate 60GS/s. The vector signal analyzer is a front end for optical signal detection and demodulation. The demodulated signal is analyzed in the scope Agilent DSO-X 91604A. The scope together with vector signal analyzer is a complex system for detailed analysis of the advanced modulated signals.

Demodulated signal from VSA can be also redirected to custom DSP system that is built on the FPGA platform. VSA can be also replaced by simplified optical front end that provides optical phase detection such as DPSK Kylia Mint-1X2. This flexibility at the receiver end creates an opportunity to design and develop innovative low cost hybrid electro-optical demodulation systems.

The predefined data pattern for the optical transmission can be stored in a form of Matlab code, Excel sheet, binary data file or any other format that is acceptable for wave for generator or FPGA platform.

The designed test system has number of important advantages that significantly enhances the research on advanced signal modulation techniques in PON. The first advantage is its integration with commercial telecommunication infrastructure that allows for configuration testing scenarios that reflects realistic environment of commercial systems. The second advantage is opportunity to test innovative photonic integrated devices such as SOA to evaluate their performance in optical systems with implemented advanced signal modulation techniques.

Third important feature is its flexibility of applying variety of modulation techniques such as QAM, SFK, DPSK, QPSK. The system works with commercial laboratory instruments such as scopes and analyzers to provide data measurements that later become the reference point for evaluating performance of custom designed coherent systems with implemented DSP modules.

This universal test platform will allow for having effective and efficient research on design and development of advanced modulation systems that implement cost effective components and bring them closer to the commercialization process.

Future work

The presented results of this thesis create a solid foundation on which to further expand the study of PON extensions, to continue improvement of developed prototypes and to address new issues that were presented in this work.

The software based system for traffic aggregation and encapsulation represents a successful proof of concept that low cost PC-based architecture can be used to create a low cost network access node. The software implementation of traffic processing functionality provides the advantage of flexibility and adaptability in node configuration and maintenance. The promising results of the benchmark tests that were performed on singe-core CPU architecture do not fully evaluate implementation of parallel processing in the prototype. Today's wide availability of new generation multi-core CPUs provides countless opportunities to continue working on improvement of the node scalability through implementing parallel processing techniques within frameworks of the new generation CPU architecture.

The innovative prototype of the electro-optical switch that is based on a Linux platform represents a promising architecture that can be used as a transparent intermediate node to provide interconnection between access networks that are deployed in both the electrical domain and the optical domain. The switch prototype also explores a unique opportunity to develop low cost technologies to facilitate a smooth transition from hybrid electro-optical network infrastructure to all-optical access networks in the future. Although the prototype has already successfully proved its capability to work in optical gigabit Ethernet LAN and a number of technologies that offer an upgrade to higher data rates are commercially available, the issue of increased power consumption may need to be addressed. Because the switch prototype relies heavily on traffic flow processing in the electrical domain, it may require further study into issues such as energy efficiency. Scaling the device up to higher data rate (40 Gb/s and beyond), will certainly require higher processing power and this may lead to an increase in overall power consumption. Further research will undoubtedly be required to develop switch configurations that offer energy efficiency without compromising their performance.

The semiconductor optical amplifier (SOA) was implemented as an innovative optical switching component that offers valuable features such low energy consumption and a simplified reconfiguration process through an external control unit. Although the SOA successfully proved its performance as a switch fabric it did exhibit unusual behaviour at specific operational frequencies. Although the possible explanation of this occurrence may be due to the patterning effect, this issue must be studied further to understand the effect of operational frequencies on performance and to develop technology that can limit impact of this effect on switch performance at higher switching ratios.

The SOA was also successfully implemented in an energy efficient optical amplification system that supports multiwavelength transmission. The main difficulty in implementation within an optical amplification system lay in the SOA's tendency to emit significant amounts of spontaneous noise. Although the successful solution for this problem was implemented using DWDM filters, considerable optical loss was observed. There is much work to be done still on noise reduction techniques as well as a need for decreasing the overall physical dimensions of the device without introducing significant optical losses.

Advanced modulation techniques are becoming the focus of research and development centers in both academia and industry. The goal of increasing the data rate without increasing physical modulation frequency is a very promising endeavour for next generation optical transmission infrastructure. The universal system for developing and evaluating components of optical networks that support innovative modulation techniques provides an excellent tool for continuing research on PON extensions. It also allows for a focus on development of new signal modulation techniques to be incorporated in the next generation of telecommunication infrastructure.

Conclusions

The presented work has focused on researching and proposing new methods to implement low cost hardware and software components in new system solutions to address the need for passive optical network (PON) extension. Particular emphasis is placed on incorporating commercially available components that offer low costs of production, implementation and maintenance to allow the prototype system to be deployed in existing network infrastructure.

A low-cost network traffic analyzer was designed and built using PC-based components and a Linux operating system. The analyzer was used to study traffic structure in commercial access networks. This task relates closely to study of the expansion of PONs as it improved knowledge and understanding of the nature of real traffic characteristics and fluctuation over extended time periods.

The novel application of a universal PC platform was successfully evaluated. It was proven that modern multipurpose computer architecture used in consumer electronics offers a level of processing power that satisfies computing tasks related to data flow processing. The benchmark test of traffic aggregation and data encapsulation was performed and the results indicated that PC architecture can successfully be implemented as components in 10G EPON network devices.

The innovative optical switch was also designed and built using low-cost PC based components. Its performance was sufficient to satisfy 1G Ethernet optical infrastructure, and its flexibility allows it to work with IP packets, Ethernet IEEE 802.3z frames and MPLS labels. Its routing and filtering capability enables it to be deployed as inter-network bridge or firewall. Evaluation of PC architecture as a candidate for switch fabric devices in 10G and 40G infrastructures was explored, and future paths of migration towards 100G were presented.

An energy efficient controller for SOA-based switch fabric was designed, built and tested. The controller allows for parallel reconfiguration multiple SOA components and its small size allows it to be incorporated with switch fabric in the same enclosure. The controller performance was evaluated and available methods of further limiting its power consumption and its physical dimensions were presented.

Comparison of PON and Agile All-Photonic Network (AAPN) infrastructures was made and novel methods of PON analysis were demonstrated based on similarities to the AAPN.

Application of SOA as an energy efficient amplification device was presented. Power budget analysis was made where SOA was incorporated as an amplifier in CWDM infrastructure. Detailed analysis of commercial SOA device implementation as power booster, inline amplifier and preamplifier in optical gigabit Ethernet network was given. Available methods of SOA performance improvement were explored from perspective of commercial applications. SOA impairments and drawbacks were also described and potential methods of improvements were listed.

Leading-edge analysis of commercial SOA device that worked as component of optical switch fabric was shown. The study focused on SOA performance and its signal responsiveness for different switching ratios. The patterning effects were exhibited in the form that has not been reported before. The observed effects helped in evaluation of data rate and time slot length that can be supported by SOA based optical switch in PON.

Additionally, this work investigated the progress to date of the development of advanced signal modulation techniques and their potential with regards to application in present and future PON extension and enhancement strategies. The development of coherent transmission and detection systems has the potential to be one such solution.

Finally, research was presented on the design of a universal platform for evaluation and advanced signal modulation techniques. A platform of this kind would allow for the creation of groundbreaking energy efficient devices built from low cost, off-the-shelf components. These devices will offer advanced signal processing and decoding in an electrical domain as an alternative to expensive all-optical receiver systems. The aggregated data rate able to be supported by the platform was evaluated to be in range of 240GS/s if a DWDM transmission system is applied.

This platform is designed to continue research on PON extension techniques with an emphasis on simplification of data processing, implementation of embedded systems and migration from all-optical coherent receiver systems to alternative low-cost DSP based systems that are becoming the technology of choice for future advanced modulation systems in optical access networks.

The results of this work were presented in the following publications:

R. Radziwilowicz, T.J.Hall, “Energy efficient photonic devices in Radio Over Fibre systems”, GROWAN 2011, Brest, France, 15-17 June 2011

R. Radziwilowicz, J. Gama Benitez,. T.J.Hall, “Energy-efficient Extensions in Passive Optical Networks”, Proc. SPIE Photonics North 2011, Ottawa, Canada, 16-18 May 2011

R. Radziwilowicz, “Innovative applications of Semiconductor Optical Amplifiers in commercial Passive Optical Networks”, CMC Texpo 2010, 4-5 October 2010

R. Radziwilowicz, H. Teimoori, P. Dicorato, V. Eslamdoost, T. Hall, “Optical Ethernet Time-Division Switched Access Network”, CMC Texpo 2009, 4-5 October 2009

R. Radziwilowicz, H. Teimoori, S. A. Paredes, V. Tolstikhin, K. Hinzer, T. Hall, "Power budget considerations in CWDM/TDM based passive optical networks", Proc. IEEE 1st Microsystems and Nanoelectronics Research Conference (MNRC 2008), Ottawa, Ontario, 15 October, 2008

R. Radziwilowicz, M. G. Khair, S. A. Paredes, T. J. Hall, "Design issues for edge nodes in agile all-photonic networks", Proc. IEEE Workshop on High Performance Switching and Routing, Poznan, Poland, June 2006

S. Parveen, **R. Radziwilowicz**, S. A. Paredes, T. J. Hall, ,"Evaluation of Burst Aggregation Method in an Optical Burst Switched Agile All-Photonic Network" Proc. SPIE (Vol.5970-85) Photonics North 2005, Toronto, Canada, 12-14 September 2005

References

[1] S. J. Lukasik, "Why the Arpanet Was Built," *Annals of the History of Computing, IEEE,* vol. 33, pp. 4-21, 2011.

[2] H. P. C. J. P. Moschovitis, T. Schuyler, T. M. Senft, "History of the Internet: A Chronology, 1843 to the Present," *The Moschovitis Group, Inc* pp. 79-80, 1999 1999.

[3] ITU-T, "History of X.25, CCITT Plenary Assemblies and Book Colors," 1976 1976.

[4] T. O. R. Ed Ravin, Dale Doughtery, and Grace Todino, "Using & Managing UUCP," *O'Reilly & Associates, Inc,* 1996.

[5] P. Borsook. (1996, April 1996). The Anarchist. *Weird.com 4(04)*. Available: http://www.wired.com/wired/archive/4.04/jennings_pr.html

[6] Y. D. Vinton Cerf, Carl Sunshine, "Specification of Internet Transmission Control Protocol," December 1974 1974.

[7] TIAA, "Wireless Fidelity (WiFi) Technology," ed, 2004.

[8] R. Marks, "IEEE 802.16 Wireless MAN Standard: Myths and Facts," *IEEE Proceedings on Wireless Communications,* vol. C802, June 2006 2006.

[9] V. Tipparaju, "Local Multipoint Distribution Service (LMDS)," *Ohio State University,* 2000.

[10] M. K. W. S. M. Redl, M. W. Oliphant, "An Introduction to GSM," *Artech House,* March 1995 1995.

[11] A. J. Viterbi, *CDMA: Principles of Spread Spectrum Communication*: Prentice Hall PTR, 1995.

[12] E. S. Agency. (2006). *Project ARTEMIS*. Available: http://www.esa.int/esaTE/SEMN6HQJNVE_index_0.html

[13] ANSI, "Synchronous Optical Network (SONET) - Sub-STS-1 Interface Rates and Formats Specificatio," *[Standard],* vol. ANSI T1.105.07-1996 (R2005), 2005.

[14] ITU-T, "Network node interface for the synchronous digital hierarchy (SDH)," in *Recommendation G.707,* ed, 2007.

[15] J. W. Lechleider, "High bit rate digital subscriber lines: a review of HDSL progress," *Selected Areas in Communications, IEEE Journal on,* vol. 9, pp. 769-784, 1991.

[16] ITU-T, "Enhancements to Recommendation V.90," ed, 2000.

[17] ITU-T, "Data compression procedures," ed, 2000.

[18] CCT, "Red Book." vol. 4, ed, 1996, pp. 320 - 325

[19] J. H. Green, *The Irwin handbook of telecommunications*, 2005.

[20] N. I. o. S. a. Technology, "IEEE Standard for Local and Metropolitan Area Networks," in *Approval Notification* vol. 802.16g-2007, ed, 2001.

[21] IEEE-SA, "IEEE 802.11: Wireless LAN Medium Access Control (MAC) and Physical Layer (PHY) Specifications," vol. IEEESTD 2007.373646, ed, 2007.

[22] IEEE-SA, "802.11a-1999 High-speed Physical Layer in the 5 GHz band," in *ISO/IEC* vol. 8802-11:1999, ed, 1999.

[23] IEEE-SA, "802.11b-1999 Higher Speed Physical Layer Extension in the 2.4 GHz band," in *[Online]*, ed, 1999.

[24] IEEE-SA, "Further Higher Data Rate Extension in the 2.4 GHz Band," vol. IEEE 802.11g-2003, ed, 2003.

[25] IEEE-SA, " Enhancements for Higher Throughput," in *Amendment 5* vol. IEEE 802.11n-2009,

ed, 2009.
[26] M. K. Ohlhausen, "Municipal provision of wireless internet," *Office of Policy Planning, Federal Trade Commission*, September 2006 2006.
[27] 3GPP. (2011). *3rd Generation Partnership Project (3GPP)*. Available: http://www.3gpp.org/
[28] G. M. S. Association, "GSA - The Global mobile Suppliers Association EDGE Databank," *EDGE Fact Sheet*, 2011.
[29] J. S. L. Jhong Sam Lee, "CDMA Systems Engineering Handbook," *Artech House Publishers (January 1998)*, 1998.
[30] ITU-T, "G.983.1: Broadband optical access systems based on Passive Optical Networks (PON), ," in *[Recommendation G.983.1]*, ed, 2006.
[31] P. Kyung-Seok, Y. Zhi-bin, C. Jeong-hyun, and K. Sung-ho, "An Intra-ONU Scheduling Method in 10G EPON Supporting IEEE 802.1 AVB," in *Complex, Intelligent and Software Intensive Systems (CISIS), 2010 International Conference on*, 2010, pp. 631-636.
[32] ITU-T, "G.984.1: Gigabit-capable Passive Optical Networks (GPON): General characteristics," in *[Recommendation G.984.1]*, ed, 2009.
[33] E. W. GROUP, "Ethernet in the First Mile," in *Standards for Ethernet based LAN* vol. IEEE 802.3, ed, 2004.
[34] C. P. Michael J. O'Mahony, Dimitrios Klonidis, Reza Nejabati, Dimitra Simeonidou "Future Optical Networks," *Journal of Lightwave Technology*, vol. 24, pp. 4684-4696, 2006.
[35] Z. X. Yong-Kee Yeo, Dawei Wang, Jianguo Liu, Yixin Wang, and Tee-Hiang Cheng, "High-speed optical switch fabrics with large port count," *OPTICS EXPRESS*, vol. 17, June 2009 2009.
[36] G. Kramer, "10G-EPON: Drivers, challenges, and solutions," in *Optical Communication, 2009. ECOC '09. 35th European Conference on*, 2009, pp. 1-3.
[37] M. Hajduczenia, H. J. A. da Silva, and P. P. Monteiro, "On Efficiency of Ethernet Passive Optical Networks (EPONs)," in *Computers and Communications, 2006. ISCC '06. Proceedings. 11th IEEE Symposium on*, 2006, pp. 566-571.
[38] I. Cale, A. Salihovic, and M. Ivekovic, "Gigabit Passive Optical Network - GPON," in *Information Technology Interfaces, 2007. ITI 2007. 29th International Conference on*, 2007, pp. 679-684.
[39] C. Assi, Y. Yinghua, and D. Sudhir, "Support of QoS in IP-based Ethernet-PON," in *Global Telecommunications Conference, 2003. GLOBECOM '03. IEEE*, 2003, pp. 3737-3741 vol.7.
[40] L. Editorial. (2011, China Telecom chooses Alcatel-Lucent PON for Fibre Cities project. *Lightware Online*. Available: http://www.lightwaveonline.com/articles/2011/07/china-telecom-chooses-alcatel-lucent-pon-for-fibre-cities-project-125008099.html
[41] ITU. (2011). *ITU Statistics*. Available: http://www.itu.int
[42] I. C. M. Federation. (2011). *ICF News*. Available: http://www.icf.at
[43] C. J, "HDTV penetration," *Washington Business Journal*, vol. May 6, May 6, 2010 2010.
[44] J. Nakagawa, N. Suzuki, C. Man, and T. Uo, "Development of optical interfaces for GE-PON PX-20 supporting a 64x split ratio and 20 km transmission range," in *Optical Communication, 2005. ECOC 2005. 31st European Conference on*, 2005, pp. 143-144 vol.2.
[45] E. Skaljo and A. Mujcic, "Measurement of optical power in the upstream of PON signal from a single ONU at the side of the central office by optical power meter," in *Ultra Modern Telecommunications and Control Systems and Workshops (ICUMT), 2010 International Congress on*, 2010, pp. 998-1002.
[46] T. An Vu, C. Chang-Joon, and R. S. Tucker, "Ethernet PON or WDM PON: A Comparison of Cost and Reliability," in *TENCON 2005 2005 IEEE Region 10*, 2005, pp. 1-6.

[47] U. S. C. Bureau, "Apportionment Data 2010," in *2010 Census*, ed, 2010.
[48] U. S. C. Bureau, "New Jersey State Stats," *Quick Facts,* 2010.
[49] D. Heo, J. S. Lee, I. K. Yun, H. C. Shin, S. W. Kim, D. K. Jung, D. J. Shin, H. S. Kim, H. S. Shin, S. B. Park, S. T. Hwang, Y. J. Oh, Y. K. Oh, D. H. Jang, and C. S. Shim, "Polarization-independent, high-power, and angle-flared superluminescent diode for WDM-PON applications," in *Lasers and Electro-Optics Society, 2005. LEOS 2005. The 18th Annual Meeting of the IEEE*, 2005, pp. 627-628.
[50] N. I. Gorlov and I. V. Bogachkov, "Estimation of nonlinear effects in the optical fiber," in *Actual Problems of Electronic Instrument Engineering (APEIE), 2010 10th International Scientific-Technical Conference on*, 2010, pp. 142-144.
[51] M. Nakamura, Y. Imai, Y. Umeda, J. Endo, and Y. Akatsu, "A burst-mode optical receiver with high sensitivity using a PIN-PD for a 1.25 Gbit/s PON system," in *Optical Fiber Communication Conference, 2005. Technical Digest. OFC/NFOEC*, 2005, p. 3 pp. Vol. 6.
[52] S. Nishihara, S. Kimura, T. Yoshida, M. Nakamura, J. Terada, K. Nishimura, K. Kishine, K. Kato, Y. Ohtomo, N. Yoshimoto, T. Imai, and M. Tsubokawa, "A Burst-Mode 3R Receiver for 10-Gbit/s PON Systems With High Sensitivity, Wide Dynamic Range, and Fast Response," *Lightwave Technology, Journal of,* vol. 26, pp. 99-107, 2008.
[53] A. Borghesani, "Optoelectronic Components for WDM-PON," in *Transparent Optical Networks, 2007. ICTON '07. 9th International Conference on*, 2007, pp. 305-308.
[54] B. Schrenk, G. de Valicourt, M. Omella, J. A. Lazaro, R. Brenot, and J. Prat, "Direct 10-Gb/s Modulation of a Single-Section RSOA in PONs With High Optical Budget," *Photonics Technology Letters, IEEE,* vol. 22, pp. 392-394, 2010.
[55] U. R. E. Asociation, "Buying Townhouse or Semi-attached House," 2007.
[56] S. Canada, "Report on House Prices Change," ed, 2011.
[57] TIA, "Transmission Performance Specifications," *TIA Standards News and Reports,* vol. TIA-568-B.3, 2002.
[58] I. O. f. Standardization, "Generic cabling for customer premises, ISO/IEC 11801:2002," *Information Technology,* vol. 11801:2002, 2002.
[59] B. W. Kim, "R&D and first commercial service of WDM-PON," in *Optical Fiber Communication & Optoelectronic Exposition & Conference, 2008. AOE 2008. Asia*, 2008, pp. 1-2.
[60] H. Ishii, M. Kohtoku, and Y. Yoshikuni, "Semiconductor arrayed-waveguide-grating (AWG) and its applications," in *Lasers and Electro-Optics, 2001. CLEO/Pacific Rim 2001. The 4th Pacific Rim Conference on*, 2001, pp. I-262-I-263 vol.1.
[61] Y. P. A. Banerjee, F. Clarke and H. Song, S. Yang, G. Kramer, K. Kim, B. Mukherjee "Wavelength-division-multiplexed passive optical network (WDM-PON) technologies for broadband access: a review," *JOURNAL OF OPTICAL NETWORKING* vol. 4, November 2005 2005.
[62] H. Yu-Li, S. Wei-Tao, L. G. Kazovsky, A. Agata, and Y. Shu, "Success pon demonstrator: experimental exploration of next-generation optical access networks," *Communications Magazine, IEEE,* vol. 43, pp. s26-s33, 2005.
[63] P. D. T. G. Talli, "Feasibility demonstration of 100 km reach DWDM Super-PON with upstream bit rates of 2.5 Gb/s and 10 Gb/s," *Proceedings, Optical Fiber Communication Conference, Anaheim, California,* March 2005 2005.
[64] G. Maier, M. Martinelli, A. Pattavina, and E. Salvadori, "Design and cost performance of the multistage WDM-PON access networks," *Lightwave Technology, Journal of,* vol. 18, pp. 125-143, 2000.

[65] N. J. Frigo, P. P. Iannone, P. D. Magill, T. E. Darcie, M. M. Downs, B. N. Desai, U. Koren, T. L. Koch, C. Dragone, H. M. Presby, and G. E. Bodeep, "A wavelength-division multiplexed passive optical network with cost-shared components," *Photonics Technology Letters, IEEE,* vol. 6, pp. 1365-1367, 1994.

[66] M. Zirngibl, C. H. Joyner, L. W. Stulz, C. Dragone, H. M. Presby, and I. P. Kaminow, "LARnet, a local access router network," *Photonics Technology Letters, IEEE,* vol. 7, pp. 215-217, 1995.

[67] N. FABIO, "Optical Networks: Towards Bandwidth Manageability and Cost Efficiency, E-PHOTON/ONE+ " *Politecnico di Torino* 2008.

[68] C. B. Jose A. Lazaro, Victor Polo, Reynaldo I. Martinez, and Josep Prat, "Remotely amplified combined ring-tree dense access network architecture using reflective RSOA-based ONU," *JOURNAL OF OPTICAL NETWORKING* vol. 6, June 2007 2007.

[69] S. Smolorz, H. Rohde, P. Ossieur, C. Antony, P. D. Townsend, T. De Ridder, B. Baekelandt, X. Z. Qiu, S. Appathurai, H. G. Krimmel, D. Smith, and A. Poustie, "Next generation access networks: PIEMAN and beyond," in *Photonics in Switching, 2009. PS '09. International Conference on*, 2009, pp. 1-4.

[70] K. Grobe and J. P. Elbers, "PON in adolescence: from TDMA to WDM-PON," *Communications Magazine, IEEE,* vol. 46, pp. 26-34, 2008.

[71] A. Eung-Suk and C. Sung-Gon, "QoS mechanism with E-PON scheduling scheme between access networks and optical backbone networks," in *Advanced Communication Technology, 2005, ICACT 2005. The 7th International Conference on*, 2005, pp. 1347-1348.

[72] H. Yu-Li, M. S. Rogge, S. Wei-Tao, S. Yamamoto, and L. G. Kazovsky, "Quality of service support over SUCCESS-DWA: a highly evolutional and cost-effective optical access network," in *Optical Fiber Communication Conference, 2005. Technical Digest. OFC/NFOEC*, 2005, p. 3 pp. Vol. 4.

[73] F. Y., "Application of Ethernet Technologies to FTTH Access Systems," *IEICE Transactions on Communications,* vol. E89-B, pp. 661-667, March 2006 2006.

[74] M. Lau, S. Shieh, W. Pei-Feng, B. Smith, Y. Min-Shueh, D. Lee, J. Gaba, J. Chao, B. Shung, and S. Cheng-Chung, "A packet-memory-integrated 44Gb/s switching processor with a 10Gb port and 12Gb ports," in *Solid-State Circuits Conference, 2002. Digest of Technical Papers. ISSCC. 2002 IEEE International*, 2002, pp. 34-388.

[75] J. L. Shin, H. Dawei, B. Petrick, H. Changku, A. S. Leon, and A. Strong, "A 40nm 16-core 128-thread SPARC processor," in *Solid State Circuits Conference (A-SSCC), 2010 IEEE Asian*, 2010, pp. 1-4.

[76] V. Pandit, "The American economy: The great debt drag," *The Economist,* vol. Sept. 16, 2010 2010.

[77] T. Economist, "Withdrawal symptoms: After the stimulus, the hangover " *The Economist,* vol. October 7, 2010, 2010.

[78] P. Regnier, "It Ain't Heavy... It's My Debt," *The Time Magazine,* vol. April 16, 2001 2001.

[79] IEEE-SA, "Carrier Sense Multiple Access with Collision Detection (CSMA/CD) Access Method and Physical Layer Specifications-Amendment," in *Physical Layers Specifications and Management Parameters for 10 Gb/s Passive Optical Networks* vol. IEEE 802.3av, ed, 2009.

[80] J. i. Kani, "Enabling Technologies for Future Scalable and Flexible WDM-PON and WDM/TDM-PON Systems," *Selected Topics in Quantum Electronics, IEEE Journal of,* vol. 16, pp. 1290-1297, 2010.

[81] H. Yu-Li, M. S. Rogge, S. Yamamoto, and L. G. Kazovsky, "A highly flexible and efficient passive optical network employing dynamic wavelength allocation," *Lightwave Technology, Journal of,* vol. 23, pp. 277-286, 2005.

[82] P. Kun-Youl and L. Chang-Hee, "Noise Characteristics of a Wavelength-Locked Fabry–Perot Laser Diode," *Quantum Electronics, IEEE Journal of*, vol. 44, pp. 995-1002, 2008.

[83] F. Payoux, P. Chanclou, and R. Brenot, "WDM PON with a single SLED seeding colorless RSOA-based OLT and ONUs," in *Optical Communications, 2006. ECOC 2006. European Conference on*, 2006, pp. 1-2.

[84] N. Genay, P. Chanciou, R. Brenot, M. Moignard, and F. Payoux, "Colourless ONU modules in TDM-PON and WDM-PON architectures optical carrier remote modulation," in *Optical Communication, 2005. ECOC 2005. 31st European Conference on*, 2005, pp. 147-148 vol.2.

[85] K. Jun-ichi and K. Iwatsuki, "A wavelength-tunable optical transmitter using semiconductor optical amplifiers and an optical tunable filter for metro/access DWDM applications," *Lightwave Technology, Journal of*, vol. 23, pp. 1164-1169, 2005.

[86] J. S. Lee, Y. C. Chung, and D. J. DiGiovanni, "Spectrum-sliced fiber amplifier light source for multichannel WDM applications," *Photonics Technology Letters, IEEE*, vol. 5, pp. 1458-1461, 1993.

[87] P. Kun-Youl, M. Sil-Gu, C. Ki-Man, and L. Chang-Hee, "A theoretical model of a wavelength-locked Fabry-Perot laser diode to the externally injected narrow-band ASE," *Photonics Technology Letters, IEEE*, vol. 17, pp. 1797-1799, 2005.

[88] C. Ki-Man, B. Jin-Serk, and L. Chang-Hee, "Color-free operation of dense WDM-PON based on the wavelength-locked fabry-Pe/spl acute/rot laser diodes injecting a low-noise BLS," *Photonics Technology Letters, IEEE*, vol. 18, pp. 1167-1169, 2006.

[89] L. Gong-Ru, L. Yu-Sheng, C. Yu-Chieh, K. Hao-Chung, L. Gong-Cheng, W. Hai-Lin, and C. Yung-Jui, "Long-Cavity Fabry-Perot Laser Amplifier Transmitter With Enhanced Injection-Locking Bandwidth for WDM-PON Application," *Lightwave Technology, Journal of*, vol. 28, pp. 2925-2932, 2010.

[90] H. Takesue and T. Sugie, "Wavelength channel data rewrite using saturated SOA modulator for WDM networks with centralized light sources," *Lightwave Technology, Journal of*, vol. 21, pp. 2546-2556, 2003.

[91] N. Genay, P. Chanclou, T. Duong, N. Brochier, and E. Pincemin, "Bidirectional WDM/TDM-PON access networks integrating downstream 10 Gbit/s DPSK and upstream 2.5 Gbit/s OOK on the same wavelength," in *Optical Communications, 2006. ECOC 2006. European Conference on*, 2006, pp. 1-2.

[92] P. Chanclou, F. Payoux, T. Soret, N. Genay, R. Brenot, F. Blache, M. Goix, J. Landreau, O. Legouezigou, and F. Mallecot, "Demonstration of RSOA-based remote modulation at 2.5 and 5 Gbit/s for WDM PON," in *Optical Fiber Communication and the National Fiber Optic Engineers Conference, 2007. OFC/NFOEC 2007. Conference on*, 2007, pp. 1-3.

[93] M. Fujiwara, K. Jun-ichi, H. Suzuki, and K. Iwatsuki, "Impact of backreflection on upstream transmission in WDM single-fiber loopback access networks," *Lightwave Technology, Journal of*, vol. 24, pp. 740-746, 2006.

[94] H. Suzuki, M. Fujiwara, T. Suzuki, N. Yoshimoto, H. Kimura, and M. Tsubokawa, "Demonstration and Performance of Colorless ONU for Coexistence-Type WDM-PON Using a Wavelength-Tunable <formula formulatype="inline"> <img src="/images/tex/236.gif" alt="L"> </formula>-Band DWDM-SFP Transceiver," *Photonics Technology Letters, IEEE*, vol. 20, pp. 1603-1605, 2008.

[95] S. Kaneko, K. Jun-ichi, K. Iwatsuki, A. Ohki, M. Sugo, and S. Kamei, "Scalability of spectrum-sliced DWDM transmission and its expansion using forward error correction," *Lightwave Technology, Journal of*, vol. 24, pp. 1295-1301, 2006.

[96] A. D. McCoy, P. Horak, B. C. Thomsen, M. Ibsen, and D. J. Richardson, "Noise suppression of incoherent light using a gain-saturated SOA: implications for spectrum-sliced WDM systems," *Lightwave Technology, Journal of,* vol. 23, pp. 2399-2409, 2005.
[97] Y. Katagiri, K. Suzuki, and K. Aida, "Intensity stabilisation of spectrum-sliced Gaussian radiation based on amplitude squeezing using semiconductor optical amplifiers with gain saturation," *Electronics Letters,* vol. 35, pp. 1362-1364, 1999.
[98] H. H. Lee, M. Y. Park, S. H. Cho, J. H. Lee, J. H. Yu, and B. W. Kim, "Filtering effects in a spectrum-sliced WDM-PON system using a gain-saturated reflected-SOA," in *Optical Fiber Communication - incudes post deadline papers, 2009. OFC 2009. Conference on*, 2009, pp. 1-3.
[99] L. Han Hyub, C. Seung-Hyun, and L. Sang Soo, "Efficient Excess Intensity Noise Suppression of 100-GHz Spectrum-Sliced WDM-PON With a Narrow-Bandwidth Seed Light Source," *Photonics Technology Letters, IEEE,* vol. 22, pp. 1542-1544, 2010.
[100] S. Kamei, "Recent progress on athermal AWG wavelength multiplexer," in *Optical Fiber Communication - incudes post deadline papers, 2009. OFC 2009. Conference on*, 2009, pp. 1-3.
[101] H. Nakamura, H. Suzuki, K. Jun-ichi, and K. Iwatsuki, "Reliable wide-area wavelength division multiplexing passive optical network accommodating gigabit ethernet and 10-Gb ethernet services," *Lightwave Technology, Journal of,* vol. 24, pp. 2045-2051, 2006.
[102] J. Nakagawa, M. Noda, N. Suzuki, S. Yoshima, K. Nakura, and M. Nogami, "First demonstration of 10G-EPON and GE-PON co-existing system employing dual-rate burst-mode 3R transceiver," in *Optical Fiber Communication (OFC), collocated National Fiber Optic Engineers Conference, 2010 Conference on (OFC/NFOEC)*, 2010, pp. 1-3.
[103] A. Shawky, H. Bergheim, O. Ragnarsson, A. Wratny, and J. Pedersen, "Characterization and modeling of network traffic," in *Computer Engineering Conference (ICENCO), 2010 International*, 2010, pp. 72-76.
[104] A. Nogueira, P. Salvador, and R. Valadas, "Modeling network traffic with multifractal behavior," in *Telecommunications, 2003. ICT 2003. 10th International Conference on,* 2003, pp. 1071-1077 vol.2.
[105] D. Radev and I. Lokshina, "Modeling and simulation of self-similar wireless IP network traffic," in *Wireless Telecommunications Symposium, 2009. WTS 2009*, 2009, pp. 1-6.
[106] M. Schlosser, H. Woesner, and A. Schroth, "Simulation model for an optical burst switched network," in *Local and Metropolitan Area Networks, 2004. LANMAN 2004. The 13th IEEE Workshop on*, 2004, pp. 103-108.
[107] K. G., *Ethernet Passive Optical Networks*, 2005.
[108] Y. Liu, G. Zhang, and Q. Li, "A bandwidth allocation algorithm for reducing the average delay in GPON," in *Future Computer and Communication (ICFCC), 2010 2nd International Conference on*, 2010, pp. V1-600-V1-603.
[109] I. F. Akyildiz, S. Hrastar, H. Uzunalioglu, and W. Yen, "Comparison and evaluation of packing schemes for MPEG-2 over ATM using AAL5," in *Communications, 1996. ICC 96, Conference Record, Converging Technologies for Tomorrow's Applications. 1996 IEEE International Conference on*, 1996, pp. 1411-1415 vol.3.
[110] M. Noda, N. Suzuki, S. Yoshima, E. Igawa, K. Ishii, M. Nogami, and J. Nakagawa, "Burst-mode transceiver technology for 10G-EPON systems," in *Optical Internet (COIN), 2010 9th International Conference on*, 2010, pp. 1-3.
[111] J. Sugawa, D. Mashimo, and H. Ikeda, "10.3 Gbps burst-mode receiver capable of upstream transmission with short overhead for 10G-EPON," in *Optical Communication (ECOC), 2010 36th European Conference and Exhibition on*, 2010, pp. 1-3.
[112] G. Kramer, B. Mukherjee, and G. Pesavento, "IPACT a dynamic protocol for an Ethernet PON

(EPON)," *Communications Magazine, IEEE,* vol. 40, pp. 74-80, 2002.

[113] M. Ma, Y. Zhu, and T. H. Cheng, "A bandwidth guaranteed polling MAC protocol for Ethernet passive optical networks," in *INFOCOM 2003. Twenty-Second Annual Joint Conference of the IEEE Computer and Communications. IEEE Societies*, 2003, pp. 22-31 vol.1.

[114] C. M. Assi, Y. Yinghua, D. Sudhir, and M. A. Ali, "Dynamic bandwidth allocation for quality-of-service over Ethernet PONs," *Selected Areas in Communications, IEEE Journal on,* vol. 21, pp. 1467-1477, 2003.

[115] Y. Wei and T. Shih-Wei, "Delay Sensitive EPON Dynamic Bandwidth Allocation Mechanism," in *Systems, Man and Cybernetics, 2006. SMC '06. IEEE International Conference on*, 2006, pp. 489-494.

[116] B. Huiszoon, J. A. Hernandez, H. Waardt, G. D. Khoe, J. Aracil, and A. M. J. Koonen, "Performance evaluation of an optical transparent access tier based on PON and spectral codes," *Selected Areas in Communications, IEEE Journal on,* vol. 27, pp. 143-155, 2009.

[117] T. H. S. Paredes, "An Agile All-Photonic Network," *Proceeedings, The International Conference on Optical Communications and Networks, ICOCN 2005,* December 2005 2005.

[118] R. V. M. Beshai, "Petaweb Architecture, Networks 2000, Towards Natural Networks," *9th International Telecommunication Network Planning Symposium*, 2000.

[119] R. Radziwilowicz, M. G. Khair, S. A. Paredes, and T. J. Hall, "Design issues for edge nodes in agile all-photonic networks," in *High Performance Switching and Routing, 2006 Workshop on*, 2006, p. 7 pp.

[120] A. V. Lorne Mason, Ning Zhao, David Plant, "Topological design and dimensioning of Agile All- Photonic Networks," *Journal of Computer Networks,* vol. 50, pp. 268--287, 2006.

[121] N. S. T. Ahmed, M.J. Coates, "Time-slot reservation in all-photonic networks based on flow prediction," *Proceedings, 2nd Workshop on Optimization of Optical Networks,* 2005.

[122] S. P. R. R. S. A. P. T. J. Hall, "Evaluation of Burst Aggregation Method in an Optical Burst Switched Agile All-Photonic Network," *Photonic Applications in Devices and Communication Systems, Proceedings SPIE* vol. 5970, 13 October 2005 2005.

[123] J. Faucher, R. Adams, L. R. Chen, and D. V. Plant, "Multiuser OCDMA system demonstrator with full CDR using a novel OCDMA receiver," *Photonics Technology Letters, IEEE,* vol. 17, pp. 1115-1117, 2005.

[124] E. S. Inc. (2011). *NPA-1 / NPA-2 / NPA-3 Network Processor Family* Available: http://www.ezchip.com/

[125] S. Y. Ji, B. Loop, P. D. James, and V. Paranjape, "An empirical study of performance and power scaling of low voltage DDR3," in *Electrical Performance of Electronic Packaging and Systems (EPEPS), 2010 IEEE 19th Conference on*, 2010, pp. 9-12.

[126] P. Shivam, P. Wyckoff, and D. Panda, "Can user-level protocols take advantage of multi-CPU NICs?," in *Parallel and Distributed Processing Symposium., Proceedings International, IPDPS 2002, Abstracts and CD-ROM*, 2002, pp. 8-13.

[127] M. Yuffe, E. Knoll, M. Mehalel, J. Shor, and T. Kurts, "A fully integrated multi-CPU, GPU and memory controller 32nm processor," in *Solid-State Circuits Conference Digest of Technical Papers (ISSCC), 2011 IEEE International*, 2011, pp. 264-266.

[128] L. Gopalakrishnan. (2005, November 2005). DDR2 controller using Virtex-4 devices. *Xilinx Application Notes XAPP702*. Available: http://www.xilinx.com/bvdocs/appnotes/xapp702.pdf

[129] T. Corp., "Thunder K8QW (S4881) Technical Specification," *[Online]*, 2010.

[130] A. M. D. Corp. (2004, AMD Opteron Product Data sheet. Rev. 3.11. *AMD White Papers 23932*. Available: http://www.amd.com/us-en/assets/content_type/white_papers_and_tech_docs/23932.pdf

[131] H. Consortium, "HyperTransport Technology Specifications 2.0 revB " *White Papers*, 2005.
[132] K. Technology. (2010). *2GB 400 MHz DDR ECC Registered CL3 DIMM Dual Rank, KVR400D4R3A/2G* Available: http://www.kingston.com/us/
[133] X. Yijun, M. Vandenhoute, and H. C. Cankaya, "Control architecture in optical burst-switched WDM networks," *Selected Areas in Communications, IEEE Journal on,* vol. 18, pp. 1838-1851, 2000.
[134] V. M. Vokkarane and J. P. Jue, "Prioritized burst segmentation and composite burst-assembly techniques for QoS support in optical burst-switched networks," *Selected Areas in Communications, IEEE Journal on,* vol. 21, pp. 1198-1209, 2003.
[135] Z. Tairan, L. Xinwan, W. Guiling, and C. Jianping, "Design and implementation of high-speed BCP processor for OBS core node based on FPGA," in *Wireless and Optical Communications Conference (WOCC), 2010 19th Annual*, 2010, pp. 1-3.
[136] D. Klonidis, C. T. Politi, R. Nejabati, M. J. O'Mahony, and D. Simeonidou, "OPSnet: design and demonstration of an asynchronous high-speed optical packet switch," *Lightwave Technology, Journal of*, vol. 23, pp. 2914-2925, 2005.
[137] R. Varrazza, T. Bricheno, and Y. Siyuan, "A fully packaged 4x4 integrated optical switch matrix," *Selected Topics in Quantum Electronics, IEEE Journal of,* vol. 11, pp. 1248-1254, 2005.
[138] S. M. C. Abdulla, L. J. Kauppinen, M. Dijkstra, E. Berenschot, M. J. de Boer, R. M. de Ridder, and G. J. M. Krijnen, "Mechano-optical switching in a MEMS integrated photonic crystal slab waveguide," in *Micro Electro Mechanical Systems (MEMS), 2011 IEEE 24th International Conference on*, 2011, pp. 9-12.
[139] H. Choi, H. Higuchi, and H. Kikuchi, "Fast electro-optic switching in liquid crystal blue phase II," *Applied Physics Letters,* vol. 98, pp. 131905-131905-3, 2011.
[140] L. X. Mu, W. S. Shi, T. P. Zhang, H. Y. Zhang, Y. Wang, G. W. She, Y. H. Gao, P. F. Wang, J. C. Chang, and S. T. Lee, "ZnO nanowire-based all-optical switch with Reset-Set flip-flop function," *Applied Physics Letters,* vol. 98, pp. 163101-163101-3, 2011.
[141] A. Al Amin, K. Nishimura, K. Shimizu, M. Takenaka, T. Tanemura, H. Onaka, T. Hatta, A. Kasukawa, S. Tsuji, Y. Kondo, Y. Urino, H. Uetsuka, and Y. Nakano, "Development of an Optical-Burst Switching Node Testbed and Demonstration of Multibit Rate Optical Burst Forwarding," *Lightwave Technology, Journal of,* vol. 27, pp. 3466-3475, 2009.
[142] H. Frazier, "The 802.3z Gigabit Ethernet Standard," *Network, IEEE,* vol. 12, pp. 6-7, 1998.
[143] IEEE-SA, "10Gb/s Ethernet Task Force Blue book.," in *IEEE Std. 802.3ae-2002*, ed, 2002.
[144] D. Siracusa, D. Careglio, G. Maier, A. Pattavina, Sole, x, and J. Pareta, "Multi-layer design of an MPLS-TP based Carrier Ethernet network," in *Optical Network Design and Modeling (ONDM), 2011 15th International Conference on,* 2011, pp. 1-6.
[145] P. S. I. Group, "PCI-X 2.0," ed, 2010.
[146] P. S. I. Group, "PCI-Express 2.0," ed, 2010.
[147] I. Corp. (2008). *Intel Core i7*. Available: http://www.intel.com/products/processor/corei7ee/index.htm
[148] M. Aiki, T. Tsuchiya, and M. Amemiya, "446 Mbit/s integrated optical repeater," *Lightwave Technology, Journal of,* vol. 3, pp. 392-399, 1985.
[149] G. Bourret, A. Doll, G. Bassier, G. Raffin, and M. Jurczyszyn, "81 km submarine optical repeater trial," *Electronics Letters,* vol. 19, pp. 1053-1055, 1983.
[150] E. Desurvire, "Erbium-Doped Fiber Amplifiers: Principles and Applications," *Wiley Series in Telecommunications and Signal Processing*, 1994.
[151] P. Urquhart, O. G. Lopez, G. Boyen, and A. Bruckmann, "Optical Amplifiers for

Telecommunications," in *Intelligent Signal Processing, 2007. WISP 2007. IEEE International Symposium on*, 2007, pp. 1-6.

[152] C. L. T. J. L. Philipsen, L. Leick, Y. Shen, P. C. Nielsen, C. Laurent-Lund, M. G. Dyndgaard, T. Feuchter, "Erbium-Doped Waveguide Amplifier (EDWA) Technology and Components," *ECOC*, 2003.

[153] K. Ennser, G. D. Valle, M. Ibsen, J. Shmulovich, and S. Taccheo, "Erbium-doped waveguide amplifier for reconfigurable WDM metro networks," *Photonics Technology Letters, IEEE,* vol. 17, pp. 1468-1470, 2005.

[154] D. Barbier, "The present and future of EDWA technology," in *Optical Fiber Communication Conference and Exhibit, 2002. OFC 2002*, 2002, p. 11.

[155] S. Taebi and S. S. Saini, "L-Band Polarization-Independent Reflective SOA for WDM-PON Applications," *Photonics Technology Letters, IEEE,* vol. 21, pp. 334-336, 2009.

[156] X. Z. J. Dong, F. Wang, W. Hong, and D. Huang, "Experimental study of SOA-based NRZ-to-PRZ conversion and distortion elimination of amplified NRZ signal using spectral filtering," *Optical Communications,* vol. 281, pp. 5618–5624, Nov. 2008 2008.

[157] K. E. Zoiros, C. O'Riordan, and M. J. Connelly, "Semiconductor Optical Amplifier Pattern Effect Suppression Using a Birefringent Fiber Loop," *Photonics Technology Letters, IEEE,* vol. 22, pp. 221-223, 2010.

[158] M. Xiaohua and K. Geng-Sheng, "Optical switching technology comparison: optical MEMS vs. other technologies," *Communications Magazine, IEEE,* vol. 41, pp. S16-S23, 2003.

[159] E. Ollier, "Optical MEMS devices based on moving waveguides," *Selected Topics in Quantum Electronics, IEEE Journal of,* vol. 8, pp. 155-162, 2002.

[160] P. De Dobbelaere, K. Falta, S. Gloeckner, and S. Patra, "Digital MEMS for optical switching," *Communications Magazine, IEEE,* vol. 40, pp. 88-95, 2002.

[161] R. Kasahara, M. Yanagisawa, T. Goh, A. Sugita, A. Himeno, M. Yasu, and S. Matsui, "New structure of silica-based planar lightwave circuits for low-power thermooptic switch and its application to 8 × 8 optical matrix switch," *Lightwave Technology, Journal of,* vol. 20, pp. 993-1000, 2002.

[162] T. Sakata, H. Togo, M. Makihara, F. Shimokawa, and K. Kaneko, "Improvement of switching time in a thermocapillarity optical switch," *Lightwave Technology, Journal of,* vol. 19, pp. 1023-1027, 2001.

[163] H. C. Tapalian, J. P. Laine, and P. A. Lane, "Thermooptical switches using coated microsphere resonators," *Photonics Technology Letters, IEEE,* vol. 14, pp. 1118-1120, 2002.

[164] R. Krahenbuhl, M. M. Howerton, J. Dubinger, and A. S. Greenblatt, "Performance and modeling of advanced Ti:LiNbO₃ digital optical switches," *Lightwave Technology, Journal of,* vol. 20, pp. 92-99, 2002.

[165] N. A. Riza and S. Yuan, "Low optical interchannel crosstalk, fast switching speed, polarisation independent 2×2 fibre optic switch using ferroelectric liquid crystals," *Electronics Letters*, vol. 34, pp. 1341-1342, 1998.

[166] A. J. Agranat, "Electroholographic wavelength selective crossconnect," in *Nanostructures and Quantum Dots/WDM Components/VCSELs and Microcavaties/RF Photonics for CATV and HFC Systems, 1999 Digest of the LEOS Summer Topical Meetings*, 1999, pp. II61-II62.

[167] L. H. Domash, C. Yong-Ming, P. Haugsjaa, and M. Oren, "Electronically switchable waveguide Bragg gratings for WDM routing," in *Vertical-Cavity Lasers, Technologies for a Global Information Infrastructure, WDM Components Technology, Advanced Semiconductor Lasers and Applications, Gallium Nitride Materials, Processing, and Devi*, 1997, pp. 34-35.

[168] M. J. Potasek and Y. Yang, "Multiterabit-per-second all-optical switching in a nonlinear

directional coupler," *Selected Topics in Quantum Electronics, IEEE Journal of,* vol. 8, pp. 714-721, 2002.
[169] K. Nashimoto, H. Moriyama, S. Nakamura, M. Watanabe, T. Morikawa, E. Osakabe, and K. Haga, "PLZT electro-optic waveguides and switches," in *Optical Fiber Communication Conference and Exhibit, 2001. OFC 2001*, 2001, pp. PD10-PD10.
[170] M. P. Earnshaw and D. W. E. Allsopp, "Semiconductor space switches based on multimode interference couplers," *Lightwave Technology, Journal of,* vol. 20, pp. 643-650, 2002.
[171] J. Gibong and J. W. Goodman, "Gain optimization in switches based on semiconductor optical amplifiers," *Lightwave Technology, Journal of,* vol. 13, pp. 598-605, 1995.
[172] C. P. Larsen and M. Gustavsson, "Comprehensive investigation of linear cross talk in 4×4 semiconductor optical amplifier gate switch matrix," in *Optical Fiber Communication. OFC 97., Conference on*, 1997, pp. 6-7.
[173] H. Wang, E. T. Aw, K. A. Williams, A. Wonfor, R. V. Penty, and I. H. White, "Lossless multistage SOA switch fabric using high capacity monolithic 4×4 SOA circuits," in *Optical Fiber Communication - incudes post deadline papers, 2009. OFC 2009. Conference on*, 2009, pp. 1-3.
[174] W. E. Inc. (2009, WTC3243 Thermoelectric Temperature Controller Board with Display. *White Papers*. Available: http://www.teamwavelength.com/products/product.asp?part=120
[175] N. Inc. (2011, New Focus 1592NF. *Technical data sheet*. Available: http://www.newport.com
[176] C. F. Lam, *Passive Optical Networks. Principles and practice*: Elsevier Inc., 2007.
[177] A. Inc. (2011). *Nios II Reference Handbook*. Available: http://www.altera.com/literature/hb/nios2/n2cpu_nii5v1.pdf
[178] A. Inc. (2011). *BeMicroSDK, Reference manual*. Available: http://www.altera.com/b/bemicro-sdk-design.html
[179] H. T. Co. (2011). *Corporate information*. Available: http://www.huawei.com/
[180] A.-n. T. Co. (2011). *Corporate information*. Available: http://www.ad-net.com.tw
[181] R. P. Davey, P. Healey, I. Hope, P. Watkinson, D. B. Payne, O. Marmur, J. Ruhmann, and Y. Zuiderveld, "DWDM reach extension of a GPON to 135 km," *Lightwave Technology, Journal of,* vol. 24, pp. 29-31, 2006.
[182] R. Radziwilowicz, H. Teimoori, S. A. Paredes, V. Tolstikhin, K. Hinzer, and T. Hall, "Power budget considerations in CWDM/TDM based Passive Optical Networks," in *Microsystems and Nanoelectronics Research Conference, 2008. MNRC 2008. 1st*, 2008, pp. 173-176.
[183] L. Bin Hong, C. Guan Yan, G. Yu, and W. K. G. Seah, "VoIP Capacity over Wireless Mesh Networks," in *Local Computer Networks, Proceedings 2006 31st IEEE Conference on*, 2006, pp. 551-552.
[184] A. Technologies. (2006). *IPTV QoE: Understanding and interpreting MDI values*. Available: http://cp.literature.agilent.com/litweb/pdf/5989-5088EN.pdf
[185] Anritsu. (2003, Q Factor Measurement/Eye Diagram Measurement, SDH/SONET Pattern Editing. *Application Note dwl1491*. Available: http://www.anritsu.com/en-us/downloads/application-notes/application-note/dwl1491.aspx
[186] ITU-T, "TRANSMISSION SYSTEMS AND MEDIA, DIGITAL SYSTEMS AND NETWORKS," in *Test methods applicable to optical fibre submarine cable systems* vol. Recommendation G.976, ed: TELECOMMUNICATION STANDARDIZATION SECTOR OF ITU, 2004.
[187] T. Tokle, M. Serbay, J. B. Jensen, W. Rosenkranz, and P. Jeppesen, "Advanced Modulation Formats for Transmission Systems," in *Optical Fiber communication/National Fiber Optic Engineers Conference, 2008. OFC/NFOEC 2008. Conference on*, 2008, pp. 1-3.

[188] P. S. Cho, V. S. Grigoryan, Y. A. Godin, A. Salamon, and Y. Achiam, "Transmission of 25-Gb/s RZ-DQPSK signals with 25-GHz channel spacing over 1000 km of SMF-28 fiber," *Photonics Technology Letters, IEEE,* vol. 15, pp. 473-475, 2003.

[189] T. Tokle, M. Serbay, J. B. Jensen, G. Yan, W. Rosenkranz, and P. Jeppesen, "Investigation of Multilevel Phase and Amplitude Modulation Formats in Combination With Polarization Multiplexing up to 240 Gb/s," *Photonics Technology Letters, IEEE,* vol. 18, pp. 2090-2092, 2006.

[190] T. Torger, S. Murat, R. Werner, and J. Palle, "32.1 Gbit/s InverseRZ-ASK-DQPSK Modulation with Low Implementation Penalty," in *Lasers and Electro-Optics Society, 2006. LEOS 2006. 19th Annual Meeting of the IEEE*, 2006, pp. 490-491.

[191] M. Serbay, C. Wree, and W. Rosenkranz, "Experimental investigation of RZ-8DPSK at 3x10.7 Gb/s," in *Lasers and Electro-Optics Society, 2005. LEOS 2005. The 18th Annual Meeting of the IEEE*, 2005, pp. 483-484.

[192] R. Noe, H. Rodler, A. Ebberg, E. Meissner, V. Bodlaj, K. Drogemuller, and J. Wittmann, "Fully engineered coherent multichannel transmitters and receivers with low-cost potential," *Electronics Letters,* vol. 28, pp. 14-16, 1992.

[193] M. H. Shih, F. S. Choa, T. Tanbun-Ek, R. A. Logan, W. T. Tsang, and C. A. Burrus, "High performance integrated coherent transceivers for optical access networks," in *Lasers and Electro-Optics Society Annual Meeting, 1996. LEOS 96., IEEE*, 1996, pp. 288-289 vol.1.

[194] L. A. Johansson, C. Hsu-Feng, A. Ramaswamy, J. Klamkin, L. A. Coldren, M. Rodwell, and J. E. Bowers, "Coherent Optical Receiver for Linear Optical Phase Demodulation," in *Microwave Symposium, 2007. IEEE/MTT-S International*, 2007, pp. 47-50.

[195] L. Jie, L. Yang, G. Changjian, H. Xuezhi, X. Lei, and H. Sailing, "Demonstration of Low-Cost Uplink Transmission in a Coherent OCDMA PON Using Gain-Switched Fabry–Pérot Lasers With External Injection," *Photonics Technology Letters, IEEE,* vol. 22, pp. 583-585, 2010.

[196] P. R. Prucnal, *Optical Code Division Multiple Access: Fundamentals and Applications*: CRC Press, 2005.

[197] R. Maher, P. M. Anandarajah, S. K. Ibrahim, L. P. Barry, A. D. Ellis, P. Perry, R. Phelan, B. Kelly, and J. O'Gorman, "Low cost comb source in a coherent wavelength division multiplexed system," in *Optical Communication (ECOC), 2010 36th European Conference and Exhibition on*, 2010, pp. 1-3.

[198] N. Kaneda, Y. Qi, L. Xiang, S. Chandrasekhar, W. Shieh, and C. Young-Kai, "Real-Time 2.5 GS/s Coherent Optical Receiver for 53.3-Gb/s Sub-Banded OFDM," *Lightwave Technology, Journal of,* vol. 28, pp. 494-501, 2010.

[199] Z. Xian, C. Xue, Z. Weiqing, F. Yangyang, Z. Hai, and L. Zhiyu, "All-Digital Timing Recovery and Adaptive Equalization for 112 Gbit∕s POLMUX-NRZ-DQPSK Optical Coherent Receivers," *Optical Communications and Networking, IEEE/OSA Journal of,* vol. 2, pp. 984-990, 2010.

[200] M. J. Fice, A. Chiuchiarelli, E. Ciaramella, and A. J. Seeds, "Homodyne Coherent Optical Receiver Using an Optical Injection Phase-Lock Loop," *Lightwave Technology, Journal of,* vol. 29, pp. 1152-1164, 2011.

[201] Z. Xiang and Y. Jianjun, "Advanced coherent modulation formats and algorithms: Higher-order multi-level coding for high-capacity system based on 100Gbps channel," in *Optical Fiber Communication (OFC), collocated National Fiber Optic Engineers Conference, 2010 Conference on (OFC/NFOEC)*, 2010, pp. 1-3.